

Stolonifera from shallow waters in the north-western Pacific: a description of a new genus and two new species within the Arulidae (Anthozoa, Octocorallia)

Yee Wah Lau¹, Frank Robert Stokvis²,
Leendert Pieter van Ofwegen², James Davis Reimer^{1,3}

1 Molecular Invertebrate Systematics and Ecology Laboratory, Graduate School of Engineering and Science, University of the Ryukyus, 1 Senbaru, Nishihara, Okinawa 903-0123, Japan **2** Naturalis Biodiversity Center, Darwinweg 2, 2333 CR Leiden, The Netherlands **3** Tropical Biosphere Research Center, University of the Ryukyus, 1 Senbaru, Nishihara, Okinawa 903-0123, Japan

Corresponding author: James Davis Reimer (jreimer@sci.u-ryukyu.ac.jp)

Academic editor: B. W. Hoeksema | Received 4 August 2018 | Accepted 10 September 2018 | Published 15 October 2018

<http://zoobank.org/EA626489-DE6A-496A-A788-290A36F127BC>

Citation: Lau YW, Stokvis FR, van Ofwegen LP, Reimer JD (2018) Stolonifera from shallow waters in the north-western Pacific: a description of a new genus and two new species within the Arulidae (Anthozoa, Octocorallia). ZooKeys 790: 1–19. <https://doi.org/10.3897/zookeys.790.28875>

Abstract

A new genus and two new species of stoloniferous octocorals (Alcyonacea) within the family Arulidae are described based on specimens collected from Okinawa (Japan), Palau and Dongsha Atoll (Taiwan). *Hana* **gen. n.** is erected within Arulidae. *Hana hanagasa* **sp. n.** is characterised by large spindle-like table-radiates and *Hana hanataba* **sp. n.** is characterised by having ornamented rods. The distinction of these new taxa is also supported by molecular phylogenetic analyses. The support values resulting from maximum likelihood and Bayesian inference analyses for the genus *Hana* and new species *H. hanagasa* and *H. hanataba* are 82/1.0, 97/1.0 and 61/0.98, respectively. *Hana hanagasa* **sp. n.** and *Hana hanataba* **sp. n.** are the first arulid records for Okinawa, Palau, and Dongsha Atoll, and represent species of the second genus within the family Arulidae.

Keywords

Arulidae, COI, molecular phylogeny, mtMutS, north-western Pacific, octocoral, 28S rDNA, Stolonifera, taxonomy

Introduction

Stolonifera is a subordinal group within Octocorallia, consisting of octocoral families that have been grouped together based mainly on the character of having polyps that arise separately from an encrusting horizontal, branching, ribbon-like stolon, or with polyps arising from broad, encrusting membranes. Stoloniferans are therefore morphologically different from other octocorals, which have their polyps embedded within common coenenchymal tissue. Like soft corals, stoloniferan octocorals are found in various marine ecosystems, such as coral reefs in shallow tropical and temperate seas (Fabricius and Alderslade 2001; Daly et al. 2007, McFadden and Ofwegen 2012). Relative to some other octocoral groups (soft corals and gorgonians) little is known about stoloniferan octocorals, and this is especially true concerning molecular studies. Most Stolonifera studies involve the formal description of new species based on historical alpha-taxonomy methodology (Ofwegen et al. 2006, Alderslade and McFadden 2007, Williams 2013, Churashima Foundation and Biological Institute on Kuroshio 2016). The most comprehensive study on stoloniferan phylogenetic relationships to date was conducted by McFadden and Ofwegen (2012). Their results demonstrated that there is still much work to be done for this taxonomic group and confirmed the polyphyletic distribution of Stolonifera within Alcyonacea.

Until 2012, there were six families of Alcyonacea considered to belong to the Stolonifera; Acrossotidae Bourne, 1914, Coelogorgiidae Bourne, 1900, Cornulariidae Dana, 1846, Clavulariidae Hickson, 1894, Pseudogorgiidae Utinomi & Harada, 1973, and Tubiporidae Ehrenberg, 1828. Of these, the family Clavulariidae is the most speciose and most studied, comprising 27 genera and over 60 species (Cordeiro et al. 2018). The other five families are all either monospecific or monogeneric; having no more than a few described species. A seventh monotypic family, Arulidae, was erected in 2012 (McFadden and Ofwegen 2012), describing the single genus *Arula* and the single species *Arula petunia*, collected from subtropical South African waters. Arulidae is characterised by having polyps with tentacles that are fused together proximally, forming an expanded and broad circular oral membrane. Arulidae also has ‘table-radiate’ sclerites that are altar-like shaped, which had never been recorded before in any other octocoral species. The known distribution of *Arula petunia* is from the east coast of South Africa from Tanskei to northern Natal, and there are additional photographic records of similar species or relatives from Bali, Indonesia (McFadden and Ofwegen 2012), Oman (Weinberg 2017) and Sabah, Malaysia (Lau pers. obs.).

Recent observations and collections in the north-western Pacific have revealed a similar abundance of stoloniferous octocoral species in coral reefs that are either unrecorded or even undescribed (Churashima Foundation and Biological Institute on Kuroshio 2016). Many stoloniferan octocorals have small and inconspicuous polyps that are usually only ~2–3 mm in diameter and are often overlooked. These octocorals could potentially fill up important knowledge gaps concerning phylogenetic relationships within the subordinal group Stolonifera, as this group is polyphyletic within the Octocorallia. Thus, there is a need to investigate and identify Stolonifera in this region.

Here, we describe a new genus and two new species within the family Arulidae from recent collections in Okinawa (Japan), Palau, and Dongsha Atoll (Taiwan), which are situated in the north-western Pacific.

Methods

Specimen collection

A total of 16 arulid specimens were collected, at Okinawa Island, Japan (n=12) from June to August 2017, at Palau (n=2) from December 2017 to January 2018, and at Dongsha Atoll, Taiwan (n=2) from April to May 2018. All specimens were collected at depths between 5–30 m by means of SCUBA. Material was preserved in 99% ethanol. In total eight localities were visited for sampling, Okinawa Island (n = 4), Palau (n = 2), and Dongsha Atoll (n = 2) (Figure 1). An overview with collection data of the specimens is presented in Table 1. Vouchers and type material have been deposited at the National Museum of Nature and Science, Tokyo, Japan.

Morphological study

Sclerites were isolated by dissolving entire polyps and stolons in 4% hypochlorite (household bleach). Sclerites were rinsed at least seven times with de-ionised water, dried, and initially studied by embedding the sclerites in Euparal on glass slides. In addition, for more detailed morphological studies, sclerites were mounted on scanning electron microscope (SEM) stubs and coated with Pd/Au for imaging on a JEOL JSM6490LV SEM operated at high vacuum at 15kV.

DNA extraction, amplification, and sequencing

DNA was extracted from polyps, using a DNeasy Blood and Tissue kit (Qiagen, Tokyo). PCR was performed for two mitochondrial markers, cytochrome c oxidase subunit I (COI) and the MSH homologue mtMutS. The nuclear ribosomal marker, 28S rDNA, was amplified as well. The ~900 bp fragment of COI was amplified using the primers COII8068xF 5'-CCATAACAGGACTAGCAGCATC-3' and COIOCTr 5'-TCATAGCATAGACCATACC-3' (McFadden et al. 2011) in 20 µL PCR reaction mixes, containing 10 µL of HotStarTaq master mix, 7 µL of RNase-free water, 1 µL of each primer, and 1 µL DNA template. The amplification protocol consisted of 3 min of initial denaturation at 95 °C followed by 39 cycles of 10 sec at 95 °C, annealing at 58 °C for 1 min, extension at 72 °C for 1 min and a final extension at 72 °C for 5 min. An ~800 bp fragment of mtMutS was amplified using the primers ND42599F 5'-GCCATTATGGTTAACTATTAC-3' (France and Hoover 2002), and MUT3458R

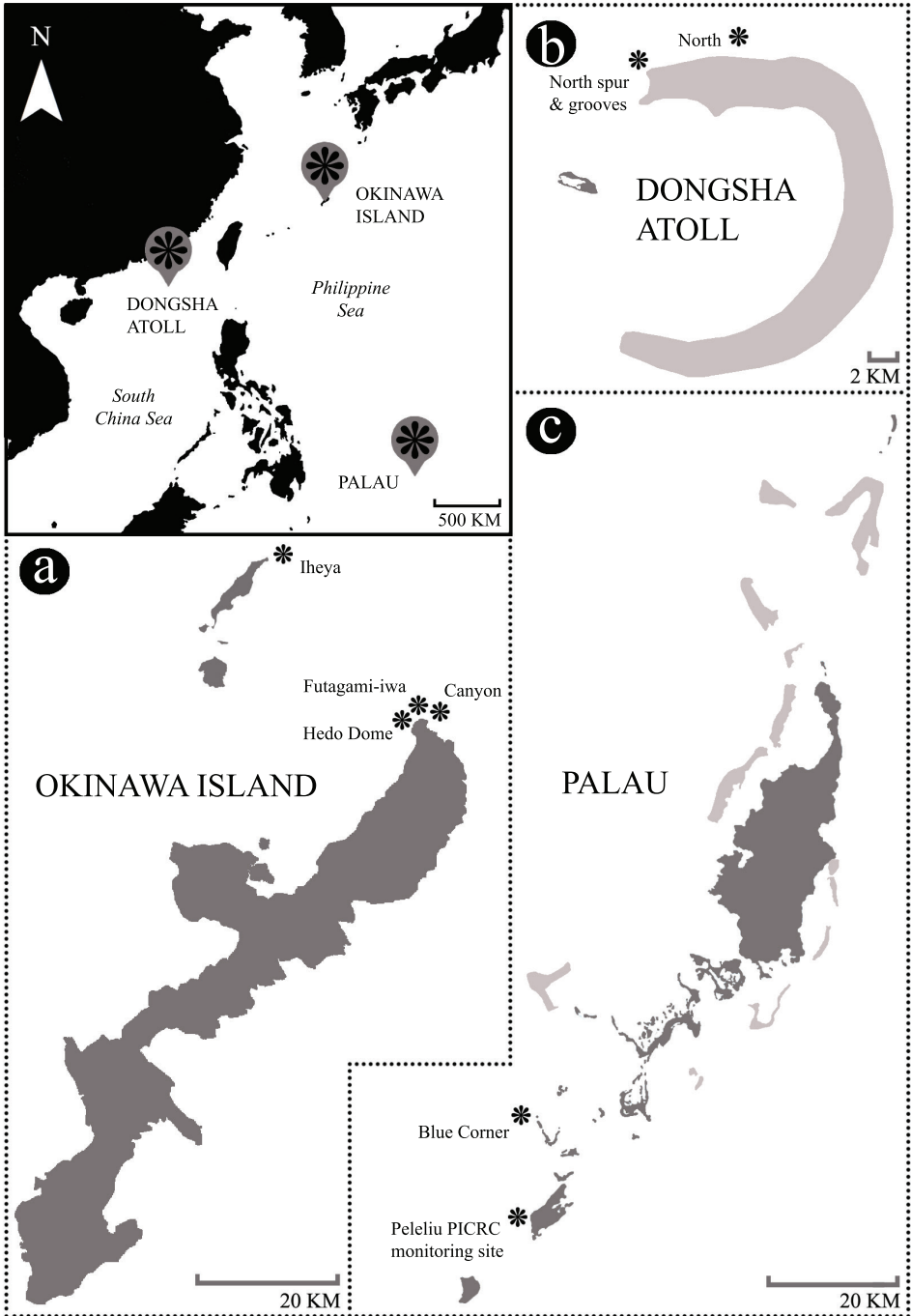


Figure 1. Map of sampling sites at three locations in the north western Pacific; **a** Okinawa Island (Japan) **b** Dongsha Atoll (Taiwan); and **c** Palau.

5'-TSGAGCAAAGCCACTCC-3' (Sánchez et al. 2003). Reactions for mtMutS were carried out in 25 μ L reaction mixes, containing 0.25 μ L Taq DNA polymerase, 0.5 μ L dNTP's, 1 μ L BSA, 2.5 μ L Coral Load Buffer, 1 μ L MgCl₂, 16.8 μ L RNase-free water, 1 μ L of each primer, and 1 μ L DNA template. PCR conditions were similar to COI, with the exception of the 48 °C annealing temperature. The ~900 bp 28S rDNA fragment was amplified using the primers 28S-Far 5'-CACGAGACCGATAGCGAACAA-GTA-3' and 28S-Rar 5'-TCATTTCGACCCTAAGACCTC-3' (McFadden and Ofwegen 2013). An annealing temperature of 50 °C was used for 28S. Amplified PCR fragments were purified using the standard ExoSAP protocol and sent for bidirectional sequencing on an ABI 3730XL (Fasmac, Kanagawa, Japan). Sequences were assembled and edited using Geneious R11 (Kearse et al. 2012) and BioEdit (Hall 1999). COI and mtMutS were checked for stop-codons in AliView (Larsson 2014).

Molecular phylogenetic analyses

Multiple sequence alignments were performed using MAFFT 7 (Katoh and Standley 2013) under default parameters. Consensus sequences for each marker were aligned to a reference dataset of four octocoral taxa (McFadden and Ofwegen 2012), including two stoloniferan specimens of the family Arulidae, *Arula petunia*. The nearest sister taxa, *Paratelesto* sp. and *Rhodelinda* sp., were used as outgroup taxa in the alignments. Subsequently, alignments of 909 bp for COI, 714 bp for mtMutS and 825 bp for 28S rDNA were obtained. Each dataset was separately run for maximum likelihood (ML) analyses, to check for contamination [Suppl. material 1]. All new sequences generated in this study were deposited in GenBank (Table 1). Maximum likelihood and Bayesian inference were performed on the Naturalis OpenStack computing cloud using PhyloStack (Doorenweerd 2016). Alignments of different markers were concatenated using SequenceMatrix 1.8 (Gaurav et al. 2011), resulting in a 2448 bp dataset of 17 taxa. Maximum likelihood analyses were run with RAxML 8 (Stamatakis 2014) using the GTRCAT model. The best maximum likelihood tree was calculated using the $-D$ parameter. A multi-parametric bootstrap search was performed, which automatically stopped based on the extended majority rule criterion. The resulting RaxML bootstrap tree was analysed with RogueNaRok (Aberer et al. 2013). The Bayesian inference was performed with ExaBayes 1.5 (Aberer et al. 2014) using the GTR substitution model. Four independent runs with each four Monte Carlo Markov Chains were run for 1,000,000 generations during which convergence, with a standard deviation of split frequencies <2%, had been reached. The effective sample size was confirmed using Tracer 1.6.0 (Rambaut et al. 2014). Bootstrap supports and posterior probabilities were depicted on the branches of the best maximum likelihood tree using P4 (Foster 2004). The resulting tree was visualized in FigTree 1.4.2 (Rambaut 2014). Additionally, average distance estimations within species and within genera were computed using MEGA7 (Kumar et al. 2016) by analysing pairwise measures of genetic distances (uncorrected P) among sequences.

Table 1. Information on voucher specimens and GenBank accession numbers of stoloniferan octocoral taxa and reference taxa used in phylogenetic analyses in this study. Collection numbers: NTM=National Museum and Art Gallery of the Northern Territory; RMNH=Naturalis Biodiversity Center; USNM=Natural Museum of Natural History (Smithsonian Inst.). Voucher numbers: OKA=Okinawa Island; ROR=Palau; DSX=Dongsha Atoll. Genbank accession number (AN), n.a.=not available.

Family	Genus/species	Specimen voucher	Location	GPS (DDM)		COI	Genbank AN	
				Mcfadden and Ofwegen 2012	Mcfadden and Ofwegen 2012		mtMuntS	28S rDNA
Arulidae	<i>Arula petunia</i>	RMNH Coel. 40188	South Africa	Mcfadden and Ofwegen 2012		JX203827	JX203773	JX203670
		USNM 1178392	South Africa	Mcfadden and Ofwegen 2012		JX203828	JX203774	JX203671
			OKA170629-01	Iheya – Iheya Island, Okinawa Island, Japan	27°5.710'N, 128°1.828'E	MH845559	n.a.	MH844382
			OKA170711-06	Hedo Dome – Cape Hedo, Okinawa Island, Japan	26°51.125'N, 128°15.027'E	MH845552	n.a.	n.a.
			OKA170711-07	Hedo Dome – Cape Hedo, Okinawa Island, Japan	26°51.125'N, 128°15.027'E	n.a.	n.a.	n.a.
			OKA170711-08	Hedo Dome – Cape Hedo, Okinawa Island, Japan	26°51.125'N, 128°15.027'E	MH845553	n.a.	n.a.
			OKA170711-10	Hedo Dome – Cape Hedo, Okinawa Island, Japan	26°51.125'N, 128°15.027'E	MH845554	MH845544	n.a.
			OKA170711-16	Hedo Dome – Cape Hedo, Okinawa Island, Japan	26°51.125'N, 128°15.027'E	n.a.	n.a.	n.a.
			OKA170711-15	Canyon – Cape Hedo, Okinawa Island, Japan	26°52.326'N, 128°15.995'E	MH845555	MH845545	n.a.
			OKA170711-17	Canyon – Cape Hedo, Okinawa Island, Japan	26°52.326'N, 128°15.995'E	n.a.	MH845546	n.a.
		<i>Hana hanagasa</i>	OKA170711-20	Hedo Dome – Cape Hedo, Okinawa Island, Japan	26°51.125'N, 128°15.027'E	MH845556	MH845547	MH844383
		gen. n., sp. n.	OKA170818-03	Furugami-iwa – Cape Hedo, Okinawa Island, Japan	26°52.177'N, 128°14.847'E	MH845557	n.a.	MH844384
			OKA170818-05	Furugami-iwa – Cape Hedo, Okinawa Island, Japan	26°52.177'N, 128°14.847'E	n.a.	n.a.	n.a.
			OKA170818-11	Canyon – Cape Hedo, Okinawa Island, Japan	26°52.326'N, 128°15.995'E	MH845558	n.a.	n.a.
			ROR171225-01	Blue Corner – Ngemelis Island, Palau	7°8.400'N, 134°13.200'E	MH845550	n.a.	MH844386
			ROR171226-03	Peleliu PICRC monitoring site – Peleliu, Palau	7°0.400'N, 134°13.060'E	MH845551	MH845543	MH844387
			DSX180420-1-01	North spur & grooves – Dongsha Atoll, Taiwan	20°46.291'N, 116°46.057'E	MH845548	n.a.	n.a.
			DSX180424-3-15	North – Dongsha Atoll, Taiwan	20°46.677'N, 116°50.090'E	MH845549	MH845542	MH844385
	Clavulariidae	<i>Paratelecto</i> sp.	RMNH Coel. 40019	Mcfadden & Ofwegen, 2012	Mcfadden and Ofwegen 2012		GQ342411	GQ342489
<i>Rhodolinda</i> sp.		NTM C12792	Mcfadden & Ofwegen, 2012	Mcfadden and Ofwegen 2012		JX203845	n.a.	JX203695

Systematics

Class Anthozoa Ehrenberg, 1831

Subclass Octocorallia Haeckel, 1866

Order Alcyonacea Lamouroux, 1812

Family Arulidae McFadden & Ofwegen, 2012

Type genus. *Arula* McFadden & Ofwegen, 2012

Diagnosis (after McFadden and Ofwegen 2012). Alcyonacea with polyps that have tentacles that are fused proximally into a broad, circular oral membrane. Sclerites in the form of table-radiates.

Genus *Hana* gen. n.

<http://zoobank.org/E1625D14-C9E7-4106-8B5E-1518D6C9F81B>

Type species. *Hana hanagasa*, sp. n., by original designation.

Diagnosis. Colony with polyps connected through flat and thin ribbon-like stolons. Anthocodiae (retractile portion of polyp) retract into cylindrical to clavate calyces. Tentacles are fused proximally, forming a broad, circular oral membrane. The oral membrane has eight deep furrows, which run from the intertentacular margin to the mouth of the polyp, giving it a plump appearance. Sclerites of anthocodia are rods. Sclerites of calyx are 6-radiates and table-radiates. The main difference between *Hana* and *Arula* is in sclerites found in the type species *Hana hanagasa* sp. n. and *Arula petunia* in the stolon. Sclerites of the stolon are fused sheets that form a flattened network of table-radiates in *H. hanagasa*, while in *A. petunia* they are similar to the separate table-radiates found in the calyx. Additionally, there is a difference in sizes of the table-radiates, being longer in *H. hanagasa* than in *A. petunia*. Sclerites colourless. Zooxanthellate.

Etymology. From the Japanese language 'hana' (花), meaning flower; denoting the shape of the polyps, which resemble flowers. Gender: feminine.

***Hana hanagasa* sp. n.**

<http://zoobank.org/698530D5-AD0B-4406-BB66-49547647E629>

Figures 2a, 3

Material examined. All specimens are from Okinawa Island, Okinawa, Japan. Holotype: OKA170711-15, Canyon, Cape Hedo (26°52.326'N, 128°15.995'E), 17 m depth, coll. YW Lau, 11 July 2017 (MH845555; MH845545). Paratype 1: OKA170629-01, Iheya, Iheya Island (27°5.710'N, 128° 1.828'E), coll. R Janssen, 29 June 2017 (MH845559; MH844382). Paratype 2: OKA170711-06, Hedo Dome, Cape Hedo (26°51.125'N, 128°15.027'E), 6 m depth, coll. YW Lau, 11 July 2017 (MH845552). Paratype 3: OKA170711-07, Hedo Dome, Cape Hedo (26°51.125'N,

128°15.027'E), 6 m depth, coll. YW Lau, 11 July 2017. Paratype 4: OKA170711-08, Hedo Dome, Cape Hedo (26°51.125'N, 128°15.027'E), 10 m depth, coll. YW Lau, 11 July 2017 (MH845553). Paratype 5: OKA170711-10, Hedo Dome, Cape Hedo (26°51.125'N, 128°15.027'E), 11 m depth, coll. YW Lau, 11 July 2017 (MH845554; MH845544). Paratype 6: OKA170711-16, Hedo Dome, Cape Hedo (26°51.125'N, 128°15.027'E), 7 m depth, coll. FR Stokvis, 11 July 2017. Paratype 7: OKA170711-17, Canyon, Cape Hedo (26°52.326'N, 128°15.995'E), 16 m depth, coll. FR Stokvis, 11 July 2017 (MH845546). Paratype 8: OKA170711-20, Hedo Dome, Cape Hedo (26°51.125'N, 128°15.027'E), coll. JD Reimer, 11 July 2017 (MH845556; MH845547; MH844383). Paratype 9: OKA170818-11, Canyon, Cape Hedo (26°52.326'N, 128°15.995'E), collected by JD Reimer, 18 August 2017 (MH845558). Paratype 10: OKA170818-03, Futagami-iwa, Cape Hedo (26°52.177'N, 128°14.847'E), 22 m depth, coll. YW Lau, 18 August 2017 (MH845557; MH844384). Paratype 11: OKA170818-05, Futagami-iwa, Cape Hedo (26°52.177'N, 128°14.847'E), 11 m depth, coll. JD Reimer, 18 August 2017.

Description. The colony consists of numerous small polyps (~50) growing on hard coral rock. Polyps are spaced apart irregularly (0.3–2.5 mm), connected by stolons that are 0.5 mm in diameter and flat thin ribbon-like in cross-section. Polyps have anthocodia fully retracted into calyces of 2.5–3 mm tall and up to 1.0 mm diameter at the widest point; calyces are slightly club-shaped or barrel shaped, wider near the distal end than at the proximal point of attachment to the stolon.

The oral disk expands into a broad circular membrane by fusion of the proximal regions of the adjacent tentacles. The margin of the oral membrane has eight broad lobes, with eight deep furrows, which run from the intertentacular margin to the mouth of the polyp, giving a plump appearance (Figure 2a). The distal two-thirds of the tentacles extend from fused margins of the oral membrane. Tentacles are long and thin, with 10 pairs of widely spaced pinnules, which are arranged in a single row on either side of the rachis.

Anthocodial sclerites are small rods with simple tubercles around margins 0.10–0.18 mm long (Figure 3a). Calyx containing small 6-radiates 0.05–0.06 mm long (Figure 3b) and table-radiates ranging 0.03–0.17 mm, giving the largest table-radiates a spindle- and sometimes club-like appearance (Figure 3c). Stolons with fused table-radiates form a flat network (Figure 3d).

The oral disk is white and the tentacles are brown in life (Figure 2a), yellowish-white in ethanol (Figure 2h). Zooxanthellate.

Morphological variation. Paratypes are colonies consisting of 50–100 polyps, growing on hard substrates and sponges. Colonies show variations in number of pinnules, having 8–10 pairs lining either side of the rachis.

Distribution. Northwest coast of Okinawa Island and southeast coast of Iheya Island in the East China Sea.

Remarks. *Arula* and *Hana* are the only two genera within the family Arulidae. *Arula petunia* and *H. hanagasa* have very similar polyp morphologies with only a clear difference in polyp colour. Oral disk and tentacles of *A. petunia* are blue in life and

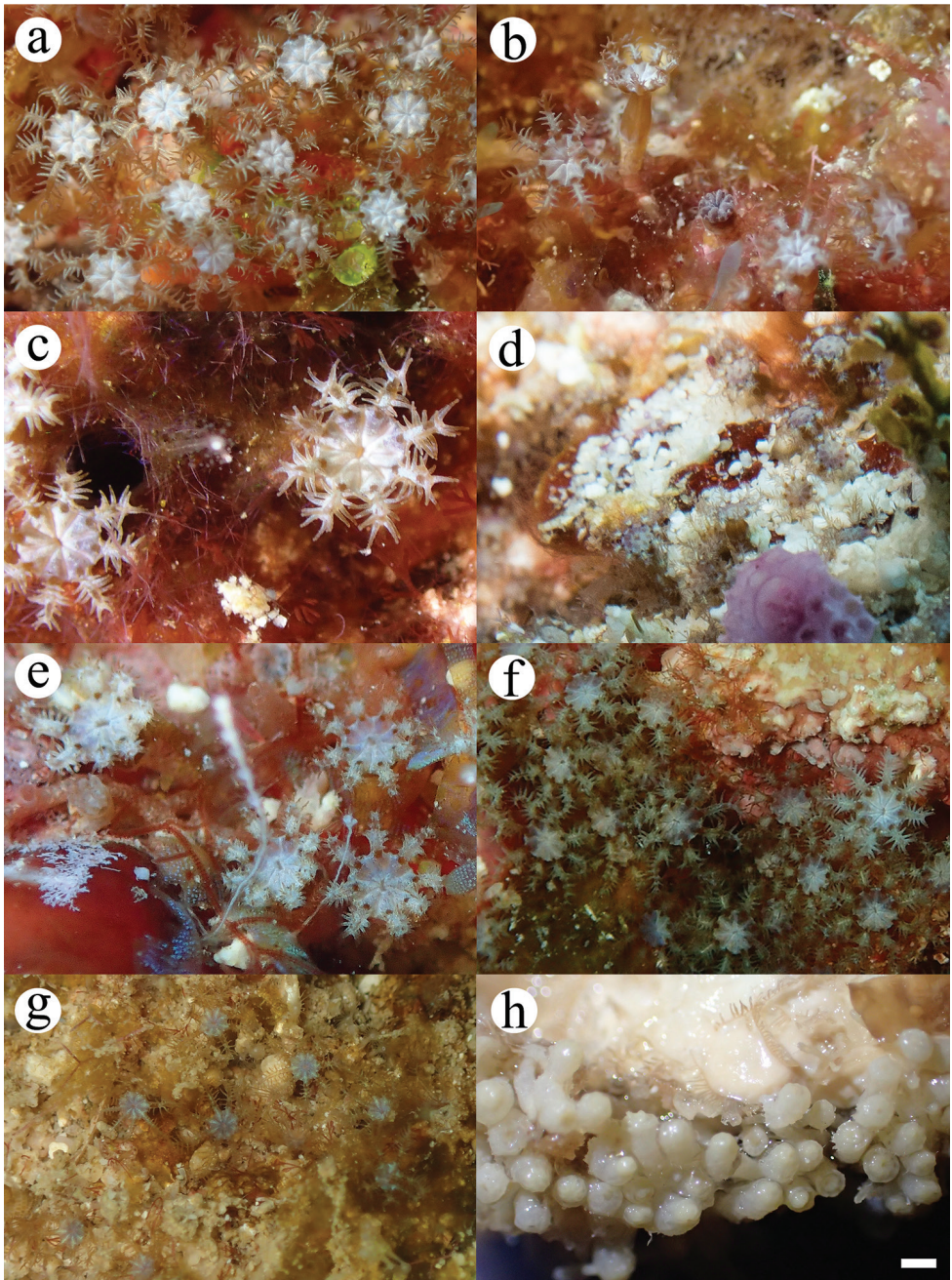


Figure 2. In situ photographs of examined *Hana* specimens from Okinawa, **a** *Hana hanagasa*, holotype, OKA170711-15 and **b** *Hana hanagasa*, paratype, OKA170711-06; Palau **c** *Hana hanataba* holotype, ROR171225-01 and **d** *Hana hanataba*, paratype, ROR171226-03; Dongsha **e** *Hana hanataba*, paratype, DSX180320-1-01 and **f** *Hana hanataba*, paratype, DSX180324-3-15 **g** specimen BK1180320-2-10, an arulid photographed in Tunku Abdul Rahman Park, Sabah, Malaysia **h** *Hana hanagasa*, holotype, OKA170711-15, colony preserved in ethanol. Scale bar: 1 mm.

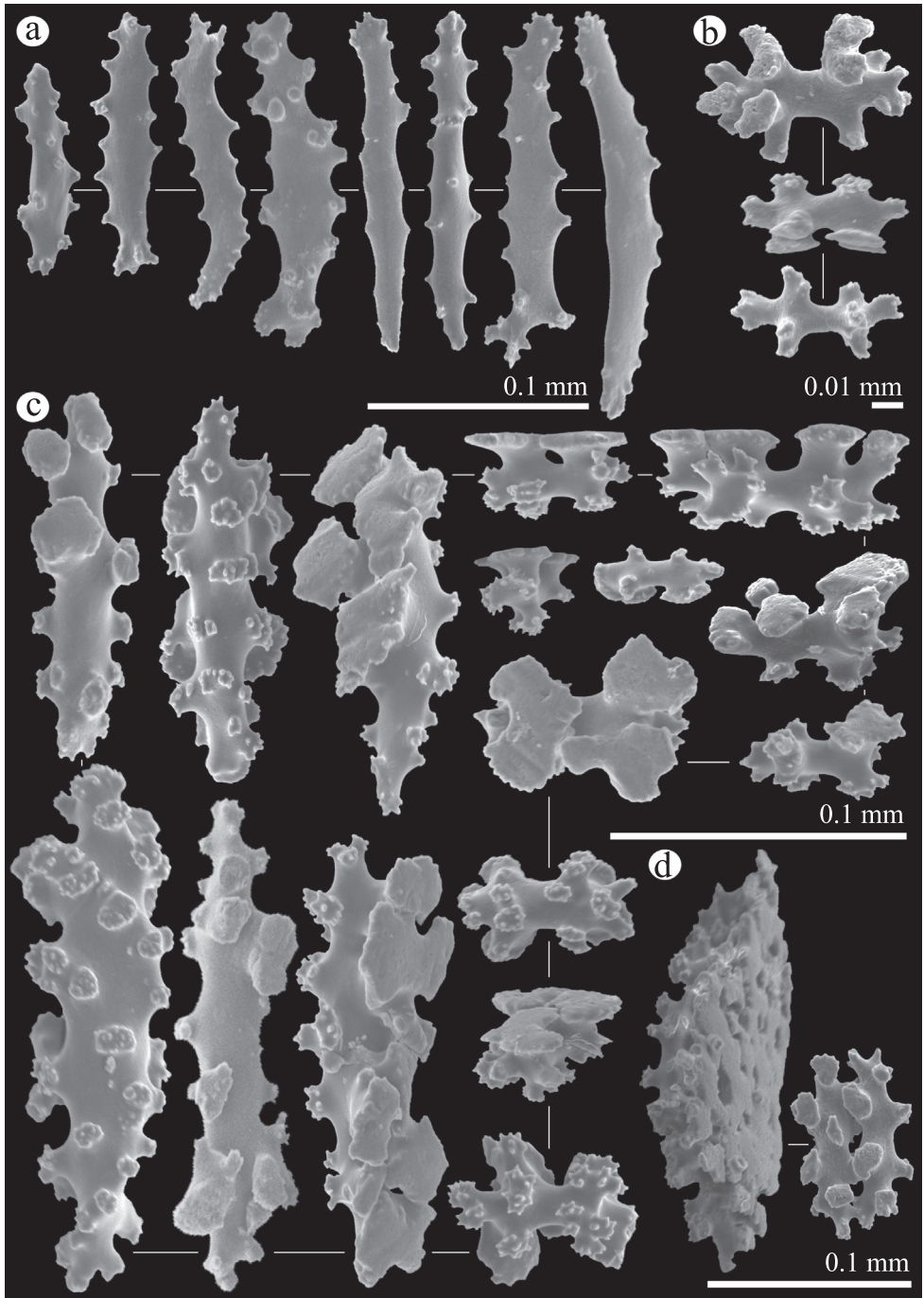


Figure 3. *Hana hanagasa*, holotype, OKA170711-15: **a** anthocodial rods **b** 6-radiates of calyx **c** table-radiates of calyx **d** pieces of fused table-radiates of stolon.

white and brown in *H. hanagasa*, respectively. This would suggest assignment to the same genus, however, the combination of differences in genetic data and sclerite morphology indicate that they should be separate from each other at the generic level. The possibility that there are similar species or previous descriptions and reports on arulid species has previously been discussed (McFadden and Ofwegen 2012) and so far, no reports have been made on possible congeners.

Etymology. From the Japanese language 'hanagasa' (花笠), the traditional Okinawan ceremonial dance headpiece worn by female performers; denoting the shape of the polyps, which resembles the flower headpiece.

***Hana hanataba* sp. n.**

<http://zoobank.org/578DEA2C-046E-498C-B0FE-0777A213209D>

Figures 2c, 4

Material examined. Holotype: ROR171225-01, Blue Corner, Ngemelis Island, Palau (7°8.400'N, 134°13.200'E), 23 m depth, coll. YW Lau, 25 July 2017 (MH845550; MH844386). Paratype 1: ROR171226-03, Peleliu PICRC monitoring site, Peleliu, Palau (7°0.400'N, 134°13.060'E), 28 m depth, coll. GY Soong, 26 December 2017 (MH845551; MH845543; MH844387). Paratype 2: DXS180420-1-01, North spur & grooves, Dongsha Atoll, Taiwan (20°46.291'N, 116°46.057'E), 7 m depth, coll. YW Lau, 20 April 2018 (MH845548). Paratype 3: DSX180424-3-15, North, Dongsha Atoll, Taiwan (20°46.677'N, 116°50.090'E), 8 m depth, coll. JD Reimer, 24 April 2018 (MH845549; MH845542; MH844385).

Description. The colony consists of small polyps (~30) growing on rock. Polyps are spaced apart irregularly (0.5–2.5 mm), connected by stolons that are 0.5 mm in diameter and flat thin ribbon-like in cross-section. Polyps have anthocodia retracted into calyces of 2.5–3.0 mm tall and up to 1.0 mm diameter at the widest point; calyces are slightly club-shaped or barrel shaped, wider near the distal end than at the proximal point of attachment to the stolon.

The oral disk expands into a broad circular membrane by fusion of the proximal regions of the adjacent tentacles (Figure 2c). The margin of the oral membrane has eight broad lobes, with eight deep furrows, which run from the intertentacular margin to the mouth of the polyp, giving a plump appearance. The distal two-thirds of the tentacles extend from fused margins of the oral membrane. Tentacles are long and thin, with eight pairs of widely spaced pinnules, which are arranged in a single row on either side of the rachis.

Anthocodial sclerites are rods with sparse simple tubercles around margins 0.07–0.24 mm long and rods ornamented with clustered tubercles on one end, giving it a club-shaped appearance, size 0.10–0.18 mm (Figure 4a). Calyx containing small capstans 0.02–0.05 mm long (Figure 4b) and table-radiates ranging 0.03–0.09 mm (Figure 4d). Sclerites of stolon are fused table-radiates forming a flat network (Figure 4c).

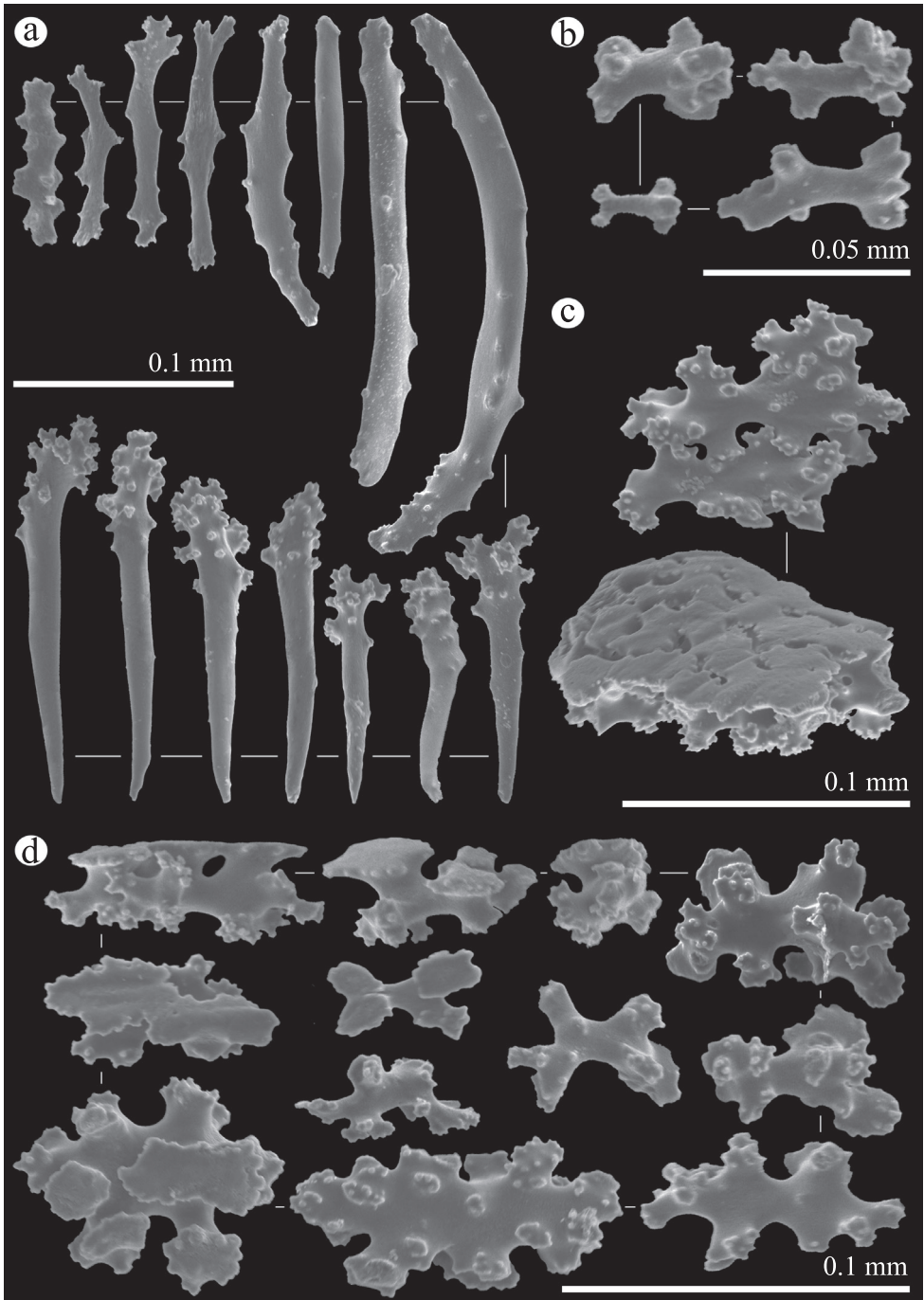


Figure 4. *Hana hanataba*, holotype, ROR171225-01: **a** anthocodial rods **b** capstans of calyx **c** pieces of fused table-radiates of stolon **d** table-radiates of calyx.

The oral disk and tentacles are white in life with brown in the proximal part of tentacle (Figure 2c), yellowish-white in ethanol. Zooxanthellate.

Morphological variation. Paratypes consist of colonies with 30–100 polyps, growing on hard substrates. Colonies show variations in the tentacles, sometimes having ten pairs of pinnules.

Distribution. The south-east of Palau in the Philippine Sea and the north to north-east reef of Dongsha Atoll, Taiwan in the South China Sea.

Remarks. *Hana hanagasa* and *Hana hanataba* have very similar polyp morphology, with minor colour differences, which could be due to differing abundances of zooxanthellae. Genetic data and sclerite morphology indicate that *H. hanagasa* and *H. hanataba* should be separated from each other at the species level. Sclerites found in *H. hanataba* are different from those in *H. hanagasa* in the presence of ornamented rods, which are lacking in *H. hanagasa*. It is noteworthy that both *H. hanagasa* and *H. hanataba* were found in environments with the presence of a comparatively strong current.

Etymology. From the Japanese language ‘hanataba’ (花束), meaning bouquet; denoting the multitude of polyps resembling arranged flowers.

Molecular phylogenetic analyses

This study has added 24 sequences to the reference database, representing two species for which no barcodes have been sequenced before. The phylograms resulting from the ML analyses of the separate markers were highly congruent with those from the analysis of the combined markers (Figure 5). ML and Bayesian analyses of the combined dataset yielded almost identical tree topologies.

Hana hanagasa and *Hana hanataba* from the north-western Pacific

Sequences of *H. hanagasa*, gen. n., sp. n., from Okinawa Island and *H. hanataba*, gen. n., sp. n., from Palau and Dongsha Atoll, Taiwan, grouped together in a well-supported clade within the Arulidae. The sequences formed a separate clade from sequences of *Arula petunia* (Figure 5). Molecular phylogenetic analyses support the distinctiveness of the genera *Hana* and *Arula*. The genetic distances (uncorrected p , expressed as percentage) between *Arula* and *Hana* taxa were 3.54% and 5.36% for COI and mtMutS, respectively [Suppl. material 2]. This is on the far upper end of the range typical of differences among congeneric octocoral species (McFadden et al. 2011). The major ramification and distances indicate a separation of *H. hanagasa*, gen. n., sp. n., and *H. hanataba*, gen. n., sp. n., from *Arula petunia* at the generic level. Morphological features support this division; comparing sclerite characteristics between *Arula* and *Hana* specimens, there are several differences that stand out. The main morphological

difference are the table-radiates of the stolon in genus *Hana*, which are fused together into a flattened network. The table-radiates of *Arula petunia* are of a smaller size range and lack two shapes of table-radiates that are seen in *Hana hanagasa* specimens, somewhat spindle and club shaped table-radiates. Additionally, there are differences in anthocodial rods; differing in size range, larger in *Hana* specimens. Additionally *Arula* specimens lack ornamented rods that are seen in *Hana hanataba* specimens (Figs 3–5).

The separation of *H. hanagasa* and *H. hanataba* was confirmed by molecular analyses and through the investigation of the sclerites. The genetic distances (uncorrected *p*, expressed as percentage) within the genus *Hana* between *H. hanagasa* and *H. hanataba* were 0.8% and 0.67% for COI and mtMutS, respectively [Suppl. material 2]. These percentages are far above margins typical of differences among intraspecific octocorals (McFadden et al. 2011). Specimens of the two species do not differ much in polyp morphology (Figure 2); however, investigation of the sclerites demonstrated differences between characters of sclerite morphology (Figs 3–4). Next to anthocodial rods with sparse tubercles arranged on the margins, a second type of rod was seen in *H. hanataba*; rods that are ornamented with lumps of tubercles on one end, giving the rods a club-like shape. Additionally, the table-radiates of the calyx seen in *H. hanataba* are of a smaller size range than of those in *H. hanagasa*, being much more similar to the table-radiates seen in *Arula petunia*. These morphological characters unique to *H. hanagasa* and *H. hanataba* are projected on the phylogenetic tree (Figure 5).

Accession numbers

MH844382	MH845552	MH845558	MH845544
MH844383	MH845553	MH845559	MH845545
MH844384	MH845554	MH845548	MH845546
MH844385	MH845555	MH845549	MH845547
MH844386	MH845556	MH845550	MH845542
MH844387	MH845557	MH845551	MH845543

Discussion

The new species *H. hanagasa* and *H. hanataba* bring the total number of species within the Arulidae to three and represent the first confirmed records of arulids for the north-western Pacific. Arulids so far have been recorded only in South Africa with informal reports of other possible congeners occurring in Sabah, Malaysia (Figure 2g) and a photographic record of a congener in Bali, Indonesia (McFadden and Ofwegen 2012). Even though it is still unknown what genus the photographed specimens from Bali and Sabah belong to, the current study expands the zoogeographical distribution of members of family Arulidae from the type locality (South Africa) to the north-western Pacific.

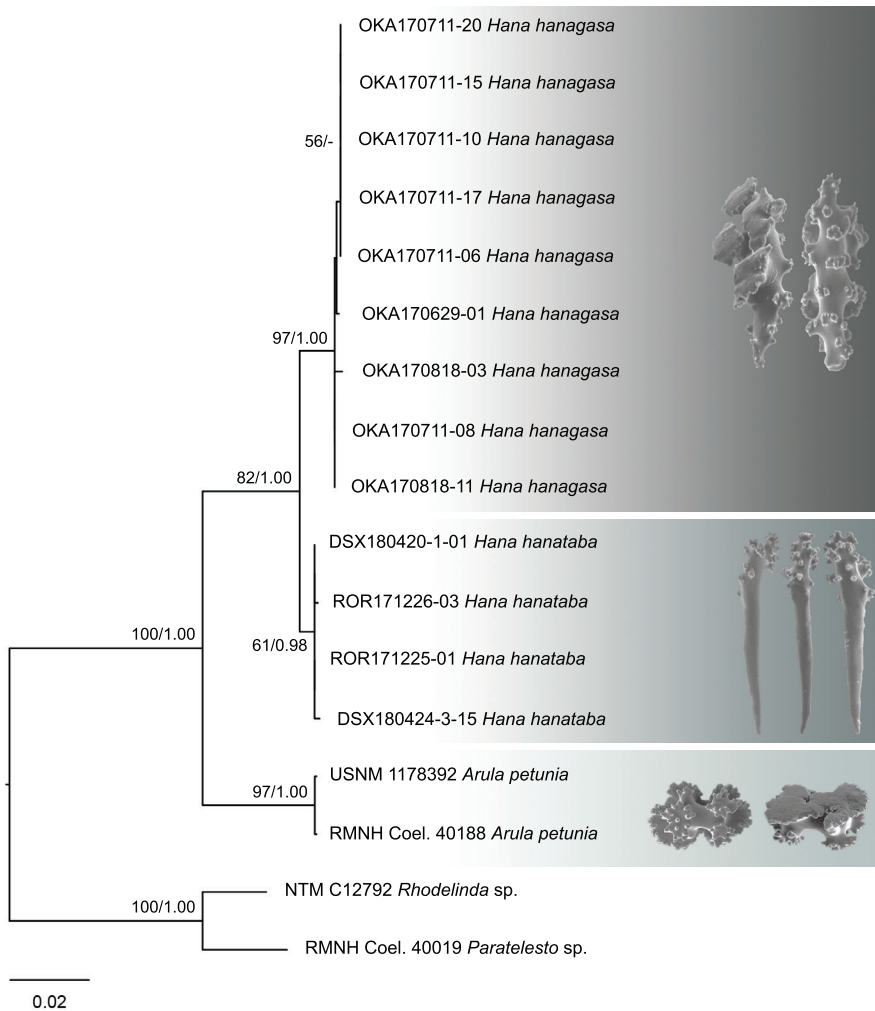


Figure 5. Phylogenetic reconstruction for arulid specimens from Okinawa Island (OKA), Palau (ROR), Dongsha Atoll (DSX), arulid reference taxa (*Arula petunia*) and outgroup sister taxa (*Paratelesto* sp. and *Rhodelinda* sp.) using the combined COI+mtMutS+28S rDNA dataset. The best maximum likelihood tree is shown, with values at branches representing bootstrap probabilities (>50%) and posterior probabilities from the Bayesian inference analysis (>0.50), respectively. Sclerites unique to *Hana hanagasa* and *Hana hanataba* are shown and typical table radiates found in the family Arulidae are shown for the genus *Arula*.

Even though all new arulid specimens were amplified for four markers, here we used only three of the gene regions, 28S rDNA, COI and mtMutS, in the analyses. ND6 was excluded from the analyses, as the outgroup sequences lacked available ND6 sequences. There were no differences in results when including or excluding this region when performing analyses with concatenated datasets. However, utilising four region sequences resulted in better resolution. Therefore, for future analyses, it is recommended to include ND6 to obtain better resolution.

It has been made clear in previous studies that the subordinal group Stolonifera is polyphyletic (McFadden et al. 2006, McFadden and Ofwegen 2012, Conti-Jerpe and Freshwater 2017). There is still much work needed, with families in need of formal description in order to reflect adequately the phylogenetic distribution of stoloniferous genera. The addition of the genus *Hana* and its two species to the recently erected family Arulidae is a small step in the process to fully interpret the morphological and molecular distinctions amongst clades of Stolonifera and ultimately the Octocorallia. It is clear that many new records of Stolonifera still await discovery and that this group still has morphological surprises, such as previously discovered pinnuleless tentacles, sclerite-free clavulariids, and new sclerite types (Bayer et al. 1983, Williams 2000, Alderslade and McFadden 2007, 2011, McFadden and Ofwegen 2012).

Acknowledgements

Fieldwork in Palau was part of the SATREPS P-CoRIE Project “Sustainable management of coral reef and island ecosystem: responding to the threat of climate change”, funded by the Japan Science and Technology Agency (JST) and the Japan International Cooperation Agency (JICA) in cooperation with Palau International Coral Reef Center and Palau Community College. We thank H Kise and J Oruetamor for logistics in Palau. We thank GY Soong for providing a specimen and corresponding photograph (Palau; ROR171226-03 *Hana hanataba*; Figure 2d). Around Dongsha Atoll, fieldwork was supported by a collaborative grant from Dongsha Atoll Research Station (DARS) to JD Reimer. We thank Prof. K Soong and the DARS staff: Captain Muchi Wang, Arthur Chang, Oscar Kanmin Ng, Jenny Liu, Jia-Kun Chen, and the Marine Park staff for their help in fieldwork and logistics. In Okinawa we thank MISE members for fieldwork help, R Janssen for providing a specimen and images (Okinawa; OKA170629-01 *Hana hanagasa*). Prof. E Hirose is thanked for providing a scanning electron microscope (SEM). Win Island Diving is thanked for the boat at Cape Hedo. Finally, we would like to thank the reviewers for their insightful suggestions and comments. All material included in this manuscript was collected under approved collection permits and ethics guidelines. The first author was supported by Japan Student Services Organization (JASSO).

References

- Aberer AJ, Krompass D, Stamatakis A (2013) Pruning rogue taxa improves phylogenetic accuracy: an efficient algorithm and webservice. *Systematic Biology* 62: 162–166. <https://doi.org/10.1093/sysbio/sys078>
- Aberer AJ, Kobert K, Stamatakis A (2014) ExaBayes: massively parallel Bayesian tree inference for the whole-genome era. *Molecular Biology and Evolution* 31: 2553–2556. <https://doi.org/10.1093/molbev/msu236>

- Alderslade P, McFadden CS (2007) Pinnule-less polyps: a new genus and new species of Indo-Pacific Clavulariidae and validation of the soft coral genus *Acrossota* and the family Acrossotidae (Coelenterata: Octocorallia). *Zootaxa* 1400: 27–44. <https://doi.org/10.11646/zootaxa.1400.2>
- Alderslade P, McFadden CS (2011) A new sclerite-free genus and species of Clavulariidae (Coelenterata: Octocorallia). *Zootaxa* 3104: 64–68. <http://www.mapress.com/zootaxa/2011/f/z03104p068f.pdf>
- Bayer FM, Grasshoff M, Verseveldt J (1983) Illustrated trilingual glossary of morphological and anatomical terms applied to octocorallia. EJ Brill/Dr W Backhuys, Leiden, 75 pp. http://www.cap-recifal.com/ccs_files/articles/octo1_denisio/guide-bayer.pdf
- Conti-Jerpe IE, Freshwater DW (2017) *Hedera caeruleascens* (Alcyonacea: Alcyoniidae), a new genus and species of soft coral from the temperate North Atlantic: invasive in its known range? *Invertebrate Systematics* 31: 723–33. <https://doi.org/10.1071/IS16069>
- Churashima Foundation, Biological Institute on Kuroshio (2016) Soft corals of Okinawa – catalogue of the collection of the Churashima Research Center. [In Japanese]
- Cordeiro R, Ofwegen LP, Williams G (2018) World List of Octocorallia. Clavulariidae Hickson, 1894. <http://www.marinespecies.org/aphia.php?p=taxdetails&id=125270>
- Daly M, Brugler MR, Cartwright P, Collins AG, Dawson MN, Fautin DG, France SC, McFadden CS, Opresko DM, Rodriguez E, Romano SL, Stake JL (2007) The phylum Cnidaria: A review of phylogenetic patterns and diversity 300 years after Linnaeus. *Zootaxa* 1668: 127–182. <http://hdl.handle.net/1808/13641>
- Doorenweerd C (2016) PhyloStack: a phylogenetic analyses pipeline in Linux Ubuntu 14.04 using OpenStack cloud computing. <https://github.com/naturalis/openstack-docs/wiki>
- Fabricius K, Alderslade P (2001) Soft corals and sea fans: A comprehensive guide to the shallow-water genera of the central-west Pacific, the Indian Ocean and the Red Sea. Australian Institute of Marine Science, Townsville, 264 pp. <http://epubs.aims.gov.au/11068/5817>
- Foster PG (2004) Modeling compositional heterogeneity. *Systematic Biology* 53: 485–495. <https://doi.org/10.1080/10635150490445779>
- France SC, Hoover LL (2002) DNA sequences of the mitochondrial *COI* gene have low levels of divergence among deep-sea octocorals (Cnidaria: Anthozoa). *Hydrobiologia* 471: 149–155. <https://link.springer.com/article/10.1023/A:1016517724749>
- Gaurav V, Lohman DJ, Meier R (2011) SequenceMatrix: concatenation software for the fast assembly of multi-gene datasets with character set and codon information. *Cladistics* 27: 171–180. <https://doi.org/10.1111/j.1096-0031.2010.00329.x>
- Hall TA (1999) BioEdit: a user-friendly biological sequence alignment editor and analysis program for Windows 95/98/NT. *Nucleic Acids Symposium Series* 41: 95–98. <http://jwbrown.mbio.ncsu.edu/JWB/papers/1999Hall1.pdf>
- Katoh K, Standley DM (2013) MAFFT multiple sequence alignment software version 7: improvements in performance and usability. *Molecular Biology and Evolution* 30(4): 772–780. <https://doi.org/10.1093/molbev/mst010>
- Kearse M, Moir M, Wilson A, Stones-havas S, Cheung M, Sturrock S, Buxton S, Cooper A, Markowitz S, Duran C, Thierer T, Ashton B, Meintjes P, Drummond A (2012) Geneious Basic: An integrated and extendable desktop software platform for the organization and

- analysis of sequence data. *Bioinformatics* 28: 1647–1649. <https://doi.org/10.1093/bioinformatics/bts199>
- Kumar S, Stecher G, Tamura K (2016) MEGA7: Molecular Evolutionary Genetics Analysis Version 7.0 for bigger datasets. *Molecular Biology and Evolution* 33(7): 1870–1874. <https://doi.org/10.1093/molbev/msw054>
- Larsson A (2014) AliView: a fast and lightweight alignment viewer and editor for large datasets. *Bioinformatics* 30: 3276–3278. <https://doi.org/10.1093/bioinformatics/btu531>
- McFadden CS, France SC, Sánchez JA, Alderslade P (2006) A molecular phylogenetic analysis of the Octocorallia (Coelenterata: Anthozoa) based on mitochondrial protein-coding sequences. *Molecular Phylogenetics and Evolution* 41: 513–527. <https://doi.org/10.1016/j.ympev.2006.06.010>
- McFadden CS, Benayahu Y, Pante E, Thoma JN, Nevarez PA, France SC (2011) Limitations of mitochondrial gene barcoding in Octocorallia, *Molecular Ecology Resources* 11: 19–31. <https://doi.org/10.1111/j.1755-0998.2010.02875.x>
- McFadden CS, van Ofwegen LP (2012) Stoloniferous octocorals (Anthozoa, Octocorallia) from South Africa, with descriptions of a new family of Alcyonacea, a new genus of Clavulariidae, and a new species of *Cornularia* (Cornulariidae). *Invertebrate Systematics* 26: 331–356. <http://dx.doi.org/10.1071/IS12035>
- McFadden CS, van Ofwegen LP (2013) A second, cryptic species of the soft coral genus *Incrustatus* (Anthozoa: Octocorallia: Clavulariidae) from Tierra del Fuego, Argentina, revealed by DNA barcoding. *Helgoland Marine Research* 67: 137–147. <https://doi.org/10.1007/s10152-012-0310-7>
- van Ofwegen LP, Häussermann V, Försterra G (2006) A new genus of soft coral (Octocorallia: Alcyonacea: Clavulariidae) from Chile. *Zootaxa* 1219: 47–57. <http://citeseerx.ist.psu.edu/viewdoc/download?doi=10.1.1.439.2939&rep=rep1&type=pdf>
- Rambaut A (2014) FigTree. <http://tree.bio.ed.ac.uk/software/figtree/>
- Rambaut A, Suchard MA, Xie D, Drummond AJ (2014) Tracer v1.6. <http://beast.bio.ed.ac.uk/Tracer>
- Sánchez JA, McFadden CS, France SC, Lasker HR (2003) Molecular phylogenetic analyses of shallow-water Caribbean octocorals. *Marine Biology* 142: 975–987. <http://dx.doi.org/10.1007/s00227-003-1018-7>
- Stamatakis A (2014) RAxML version 8: a tool for phylogenetic analyses and post-analysis of large phylogenies. *Bioinformatics* 30(9): 1312–1313. <https://doi.org/10.1093/bioinformatics/btu033>
- Weinberg S (2017) Découvrir la vie sous-marine, Mer Rouge, océan Indien, océan Pacifique. Guide d'identification, 1001 espèces de faune et flore. Tome 1: 1–261.
- Williams GC (2000) A new genus and species of stoloniferous octocoral (Anthozoa: Clavulariidae) from the Pacific coast of North America. *Zoologische Mededelingen Leiden* 73: 333–344. <http://citeseerx.ist.psu.edu/viewdoc/download?doi=10.1.1.844.3643&rep=rep1&type=pdf>
- Williams GC (2013) New taxa and revisionary systematics of alcyonacean octocorals from the Pacific coast of North America (Cnidaria, Anthozoa). *Zookeys* 283: 15–42. <https://doi.org/10.3897/zookeys.283.4803>

Supplementary material 1

Supplemental figures 1–3

Authors: Yee Wah Lau, Frank Robert Stokvis, Leendert Pieter van Ofwegen, James Davis Reimer

Data type: multimedia

Explanation note: Figure 1: Maximum likelihood phylogenetic reconstruction of gene region 28S rDNA of arulid specimen from Okinawa (OKA), Palau (ROR), Dongsha Atoll (DSX), reference taxa *Arula petunia* and outgroup sister taxa (*Paratelesto* sp. and *Rhodelinda* sp.). Figure 2: Maximum likelihood phylogenetic reconstruction of gene region COI of arulid specimen from Okinawa (OKA), Palau (ROR), Dongsha Atoll (DSX), reference taxa *Arula petunia* and outgroup sister taxa (*Paratelesto* sp. and *Rhodelinda* sp.). Figure 3: Maximum likelihood phylogenetic reconstruction of gene region mtMutS of arulid specimen from Okinawa (OKA), Palau (ROR), Dongsha Atoll (DSX), reference taxa *Arula petunia* and outgroup sister taxa (*Paratelesto* sp.).

Copyright notice: This dataset is made available under the Open Database License (<http://opendatacommons.org/licenses/odbl/1.0/>). The Open Database License (ODbL) is a license agreement intended to allow users to freely share, modify, and use this Dataset while maintaining this same freedom for others, provided that the original source and author(s) are credited.

Link: <https://doi.org/10.3897/zookeys.790.28875.suppl1>

Supplementary material 2

Supplemental tables 1, 2

Authors: Yee Wah Lau, Frank Robert Stokvis, Leendert Pieter van Ofwegen, James Davis Reimer

Data type: measurement

Explanation note: Table 1. Numbers of base differences per site from averaging over all sequence pairs between groups (d) shown for gene regions COI and mtMutS (uncorrected p , expressed as percentage). Table 2. Estimates of average evolutionary divergence over sequence pairs within groups for gene regions COI and mtMutS.

Copyright notice: This dataset is made available under the Open Database License (<http://opendatacommons.org/licenses/odbl/1.0/>). The Open Database License (ODbL) is a license agreement intended to allow users to freely share, modify, and use this Dataset while maintaining this same freedom for others, provided that the original source and author(s) are credited.

Link: <https://doi.org/10.3897/zookeys.790.28875.suppl2>

A new species of *Procamallanus* Baylis, 1923 (Nematoda, Camallanidae) from *Astronotus ocellatus* (Agassiz, 1831) (Perciformes, Cichlidae) in Brazil

Raul Henrique da Silva Pinheiro^{1,2}, Francisco Tiago de Vasconcelos Melo^{1,3},
Scott Monks⁴, Jeannie Nascimento dos Santos^{1,3}, Elane Guerreiro Giese^{1,2}

1 Programa de Pós-Graduação em Biologia de Agentes Infeciosos e Parasitários – Instituto de Ciências Biológicas, Universidade Federal do Pará, Belém, Pará 66075-110, Brazil **2** Laboratório de Histologia e Embriologia Animal – Instituto da Saúde e Produção Animal – Universidade Federal Rural da Amazônia – UFRA, Belém, Pará, 66.077-830, Brazil **3** Laboratório de Biologia Celular e Helmintologia “Profa Dra Reinalda Marisa Lanfredi” Instituto de Ciências Biológicas, Universidade Federal do Pará, Belém, Pará 66075-110, Brazil **4** Laboratorio de Morfología Animal, Centro de Investigaciones Biológicas, Universidad Autónoma del Estado de Hidalgo, Pachuca, Hidalgo, 42001, México

Corresponding author: Elane Guerreiro Giese (elane.giese@ufra.edu.br)

Academic editor: Y. Mutafchiev | Received 1 March 2018 | Accepted 8 August 2018 | Published 15 October 2018

<http://zoobank.org/D4FB203D-9735-4759-94A6-B460DC9F0B2A>

Citation: Pinheiro RHS, Melo FTV, Monks S, Santos JN, Giese EG (2018) A new species of *Procamallanus* Baylis, 1923 (Nematoda, Camallanidae) from *Astronotus ocellatus* (Agassiz, 1831) (Perciformes, Cichlidae) in Brazil. ZooKeys 790: 21–33. <https://doi.org/10.3897/zookeys.790.24745>

Abstract

A new species of *Procamallanus* Baylis, 1923 was found as a parasite of the fish *Astronotus ocellatus* (Agassiz, 1831) from a lake in the Jardim Botânico Bosque Rodrigues Alves, Belém, Brazil. *Procamallanus spiculastratus* **sp. n.** has a smooth buccal capsule and a well-developed basal ring that is armed with four sclerotized tooth-like structures. The male of the new species is similar to the two species that are known from Brazilian fish, *P. peraccuratus* Pinto, Fábio, Noronha & Rolas, 1976, and *P. annipetterae* Kohn & Fernandes, 1988, by the absence of the gubernaculum. It differs from these two by the morphology of the buccal capsule, the number and arrangement of the caudal papillae in males, the size and morphology of the spicules and the shape of the tail of both sexes. *Procamallanus spiculastratus* **sp. n.** is the third species discovered in fish from Brazil. This finding extends the geographical distribution of the genus into the Brazilian Amazon.

Keywords

Amazon, fish, helminth, nematode

Introduction

The genus *Astronotus* is comprised of two species, *A. crassipinnis* (Heckel, 1840) and *A. ocellatus* (Agassiz, 1831) (Perciformes: Cichlidae) (Kullander 2003; Froese and Pauly 2017). *Astronotus ocellatus* (known as Acaraú-açu; Apaiari; Oscar) is popular among aquarists, but it is not as popular for aquaculture because of its slow growth rate. Early attempts at cultivation were encouraged by the government in the early 1970s, but they were not successful they only succeeded in the introduction of the species into almost all of Brazil (Fontenele and Nepomuceno 1983). Because it is an introduced species, there has been little interest on studies of its parasites; to date, only three studies (Azevedo et al. 2007; Malta 1984; Neves et al. 2013) have included this species of fish.

Nematodes of the genus *Procamallanus* Baylis, 1923 (Camallanida, Procamallaninae) are predominately parasites of freshwater fish that are distributed over several zoogeographical regions (Moravec 1998; Hoffman 1999). Members of the genus are easily recognized by the presence of a buccal capsule that is strongly sclerotized, but without ridges (Baylis 1923; Moravec and Scholz 1991; Moravec and Thatcher 1997). Despite the importance of introduced species of fish as mechanisms of co-introduction of parasites into native populations (Bautista-Hernández et al. 2014), helminths of most of introduced species have not been studied. As part of an ongoing study of the helminths of vertebrates of eastern Brazil, samples of *A. ocellatus* were collected and necropsied. Procamallanin nematodes were found as parasites of these fish, but they could not be assigned to a known species; therefore, the new species is described herein.

Materials and methods

Forty specimens of *A. ocellatus* were collected from Iara Lake, at the Jardim Botânico Bosque Rodrigues Alves (1°25'49"S, 48°27'22"W), located in an urban area of the city of Belém, state of Pará, eastern Brazilian Amazon. Fish were collected during March to July 2015 with the aid of a casting net. Fish were transported alive to the Laboratório de Biologia Celular e Helmintologia “Profa. Dra. Reinalda Marisa Lanfredi”, Instituto de Ciências Biológicas, Universidade Federal do Pará-UFPA, for necropsy. Nematodes were collected, washed in phosphate-buffered saline, fixed in AFA solution (93 parts 70% ethanol, 5 parts formalin, and 2 parts glacial acetic acid) (Pritchard and Kruse 1982), and stored in 70% ethanol. For light microscopy, helminths were cleared in Amman’s lactophenol solution (Giese et al. 2009) and examined under an Olympus BX41 microscope with a drawing tube. Measurements are given in micrometers unless otherwise noted and are presented as the range (minimum and maximum values) followed by the mean in parentheses. For scanning electron microscopy (SEM), helminths were washed in phosphate-buffered saline with a pH of 7.0 (Sodium Phosphate Monobasic 3.12 g, Sodium Phosphate Dibasic 2.83 g, and 17 g Sodium Chloride in 200 ml of distilled water), post-fixed in 1% osmium tetroxide, dehydrated to the critical point using CO₂, coated with gold+palladium, and studied using a scanning

electron microscope (VEGA 3 LMU/TESCAN) in the Laboratório de Histologia e Embriologia Animal – Instituto da Saúde e Produção Animal – Universidade Federal Rural da Amazônia – UFRA, campus Belém, state of Pará, Brazil. Type material was deposited in the Coleção de Invertebrados of the Museu Paraense Emílio Goeldi (MPEG), Belém, Pará, Brazil. Other material examined included specimens of *Procamallanus peraccuratus* Pinto, Fábio, Noronha & Rolas, 1976, Coleção Helminológica do Instituto Oswaldo Cruz (CHIOC): females-16.747A-C, 16.759A-C, 31.082A, 31.083A-C; males-16.753B-D, 16.757A-B, 16.769A-C, 16.773B, 31.083A-B); *Spirocamallanus inopinatus* Travassos, Artigas & Pereira, 1928, CHIOC 31.315A-B, CHIOC 31.323A-B, CHIOC 31.324, CHIOC 31.325A-B, CHIOC 31.326A-B, CHIOC 31.327, CHIOC 31.328 and CHIOC 31.329; *S. rarus* Travassos, Artigas & Pereira, 1928, CHIOC 31.027A-B, CHIOC 31.328A-C; *S. pexatus* Pinto, Fabio, Noronha & Rolas, 1974, CHIOC 31.086A-D, CHIOC 31.087, CHIOC 31.088A-B, CHIOC 31.089A-B and 32.504A-B; *S. paraensis* Pinto, Fabio, Noronha & Rolas, 1976, CHIOC 31.342A-E; and *S. saofranciscensis* Moreira, Oliveira & Costa, 1994, CHIOC 37.857, CHIOC 37.858 and CHIOC 38.042.

Systematics

Family Camallanidae Railliet & Henry, 1915

Subfamily Camallaninae Railliet & Henry, 1915

Genus *Procamallanus* Baylis, 1923

Procamallanus spiculastratus sp. n.

<http://zoobank.org/AD83ABF3-9B63-455C-8AC6-3B3795CD6156>

Figures 1, 2, 3

Material. Type specimens. Holotype male (MPEG 195), allotype female (MPEG 196), and four paratypes (MPEG 197; MPEG 198; MPEG 199; MPEG 200) were deposited in the Coleção de Invertebrados of the Museu Paraense Emílio Goeldi (MPEG), Belém, Pará, Brazil.

Type host. *Astronotus ocellatus* (Agassiz) (Perciformes: Cichlidae). Average length = 24.7±2.6 cm; average weight = 331.8±96.3 g.

Type locality. Iará Lake, Jardim Botânico Bosque Rodrigues Alves (1°25'49"S, 48°27'22"W), Belém, Pará, Amazon Biome, Brazil.

Site in host. Mid-intestine.

Host-parasite data. Prevalence 55% (22 infected, 40 examined); Mean intensity = 14.8; Mean abundance = 8.5; Range = 1–59.

Etymology. The species name refers to the unique morphology of the spicules, which membranous alae that are supported by rays, giving them a striated appearance.

Description. [Based on 10 males, 11 females, 20 eggs (from allotype female), and 20 intrauterine larvae (from allotype female)] Medium-sized nematodes, red while

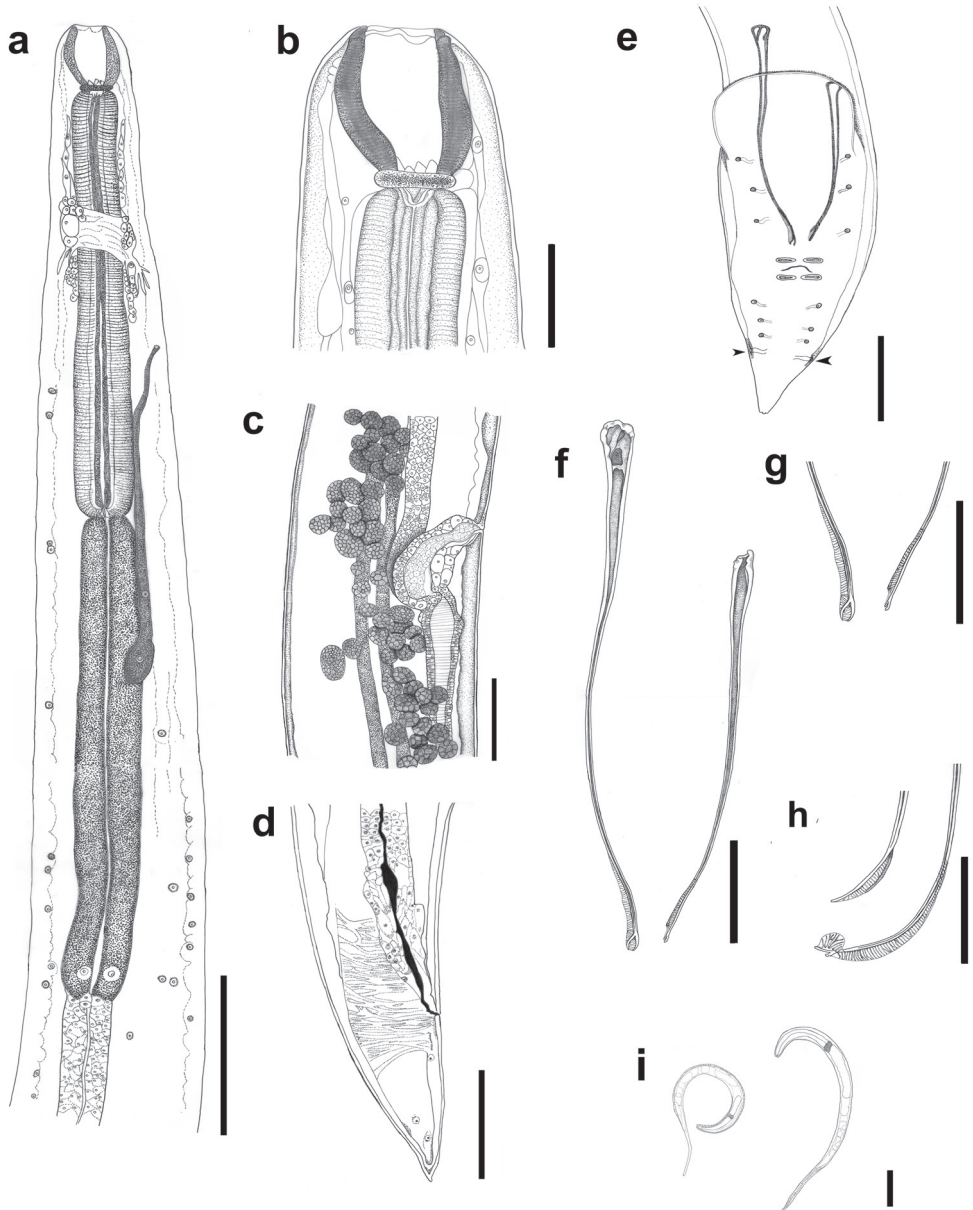


Figure 1. *Procammallanus spiculastratus* sp. n., line drawings **a** adult male, anterior part of the body, lateral view **b** buccal capsule, lateral view **c** vulvar opening and vagina **d** tail of a female worm, lateral view **e** posterior end of a male worm and phasmids (arrowheads), ventral view **f** spicules, ventral view **g** distal part of spicules, ventral view **h** distal end of spicules, lateral view **i** larvae. Scale bars: 150 μm (**a**); 40 μm (**b**); 100 μm (**c**, **d**); 20 μm (**e**); 50 μm (**f**); 50 μm (**g**, **h**, **i**).

alive and white after fixation. Cuticle with fine transverse striations. Oral opening circular, surrounded by three concentric circles with four papillae each, inner circle with six small pores at base proximal to oral opening, pair of small lateral amphids present

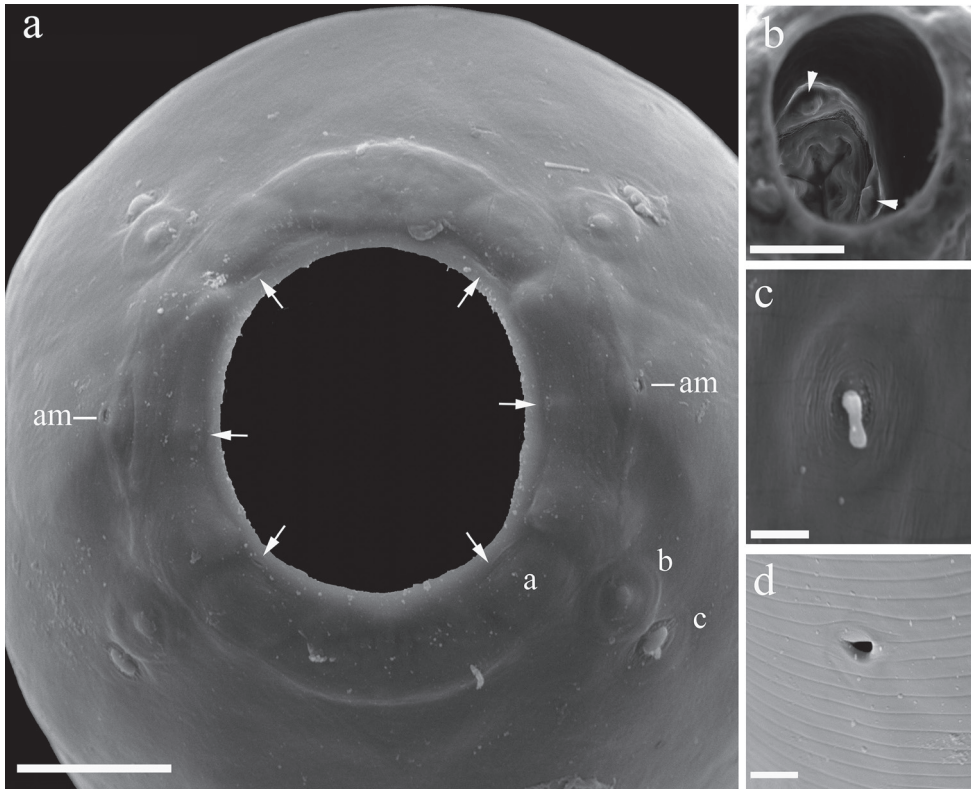


Figure 2. *Procamallanus spiculastratus* sp. n., female, scanning electron microscopy. **a** oral opening, frontal view, three circles of cephalic papillae (a, b, c), amphid (am, arrowhead), pore-like structures (arrows) **b** oral opening, view of buccal capsule, two teeth are visible at the base of the basal ring (arrows) **c** deirid **d** excretory pore. Scale bars: 10 μm (**a**, **b**); 2 μm (**c**); 5 μm (**d**).

(Figure 2a). Buccal capsule, orange-brown, barrel-shaped with a well-developed basal ring armed with four sclerotized tooth-like structures (Figs 1a, b, 2b). Inner surface of capsule smooth (Figure 1a, b) without ridges. Muscular esophagus somewhat shorter than glandular esophagus. Deirids minute, simple with rounded tip, situated between the buccal capsule and nerve ring (Figure 2c).

Males (based on holotype and 9 paratypes): body 8–11 (9) mm long; maximum width at esophageal/intestinal junction 105–147 (130). Buccal capsule including basal ring 57–74 (65) long and 32–39 (36) wide, basal ring 5–8 (6.5) long, 22–29 (26) wide. Maximum length/width ratio of buccal capsule 1:0.55. Deirids, nerve-ring and excretory pore at 91–119 (104), 156–188 (171) and 248–292 (263), respectively, from anterior extremity. Muscular portion of esophagus 316–395 (353) long and 42–53 (48) wide; glandular portion of esophagus 421–558 (470) long and 42–63 (51) wide. Muscular/glandular esophagus length ratio 1:1.3. Length of entire esophagus and buccal capsule 9–12% of body length. Posterior end of body ventrally curved, provided with wide caudal alae bearing six pairs of pedunculated papillae: three precloacal pairs and three postcloacal pairs (Figs 1e, 3a). Two pairs of adcloacal papillae. (Figs 1e, 3a).

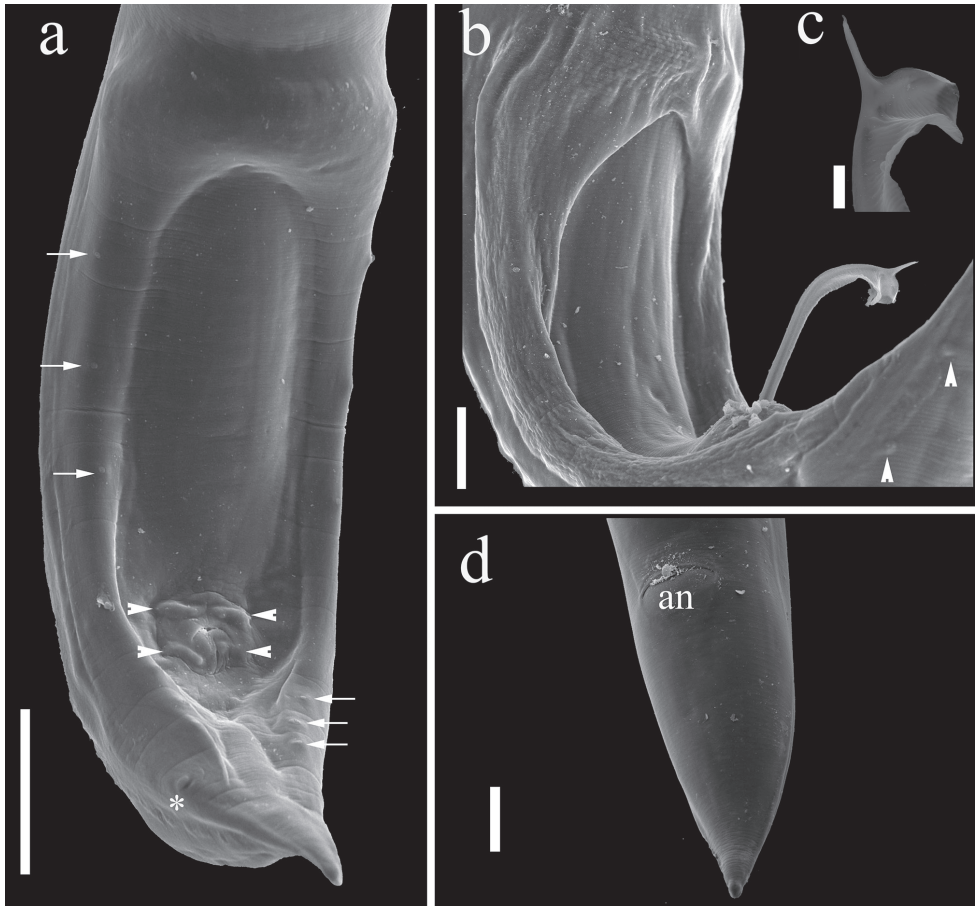


Figure 3. *Procamallanus spiculastratus* sp. n., scanning electron microscopy. **a** tail of a male worm, ventral view, three preanal pairs (arrows) and three postanal pairs (arrows), four adcloacal papillae (arrowheads) and a lateral phasmid (*) are visible **b** tail of a male worm, lateral view with the spicule partially extroverted, and two pairs of sessile papillae are located along lateral margin (arrowhead); inset **c** detail of the tip of a spicule **d** tail of a female worm, ventral view, anus (an). Scale bars: 25 μm (**a**); 50 μm (**b**); 5 μm (**c**); 50 μm (**d**).

Two pairs of dorso-lateral sessile papillae, between cloaca and tip of tail present (Figure 3b). Caudal alae anteriorly interconnected, forming a pseudosucker, and not reaching tip of tail; a pair of phasmids located immediately posterior to the 6th pair of pedunculated papillae (Figs 1e, 3a). Spicules elongate and ventrally curved, with slightly sclerotized core; distal end of spicules with membranous alae supported by sclerotized rays (Figs 1e–h, 3b, c). Spicules with terminal bifurcation, similar in form, bifurcation of right spicule always larger than that of left spicule. Spicules dissimilar in length; left spicule shorter, 229–284 (247) long and right spicule 312–355 (332) long (Figure 1e–h). Gubernaculum absent. Length of tail 156–205 (184).

Females with larvae (based on 4 specimens): body 17–20 mm (18 mm) long; maximum width at esophageal/intestinal junction 160–173 (167). Buccal capsule including

basal ring 78–83 (81) long and 47–52 (50) wide, basal ring 12–13 (12) long, 32–43 (36) wide. Maximum length/width ratio of buccal capsule 1:0.62. Deirids, nerve-ring, and excretory pore at 147–167 (156), 220–233 (225), and 330–397 (371), respectively, from the anterior extremity (Figure 1c). Muscular portion of esophagus 413–453 (433) long and 53–60 (58) wide; glandular portion of esophagus 600–693 (633) long and 67–80 (70) wide. Muscular/glandular esophagus length ratio 1:1.5. Length of entire esophagus and buccal capsule representing 6–7% of body length. Vulva situated at, 8–11 (9) mm from anterior end, at about 50% of body length; vulval lips not elevated. Muscular vagina directed posteriorly (Figure 1c); uterus filled with larvae 210–280 (245±22 long) (Figure 1i) and eggs 17–29 (24) long by 14–26 (22) wide. Tail conical, 190–220 (208) long, without cuticular projections (Figs 1d, 3d).

Females with eggs (based on 7 specimens): body 11–13 mm (12 mm) long; maximum width at esophageal/intestinal junction 100–133 (124). Buccal capsule including basal ring 80–87 (82) long and 50–60 (53) wide, basal ring 10–12 (10) long, 33–38 (35) wide. Maximum length/width ratio of buccal capsule 1:0.64. Deirids, nerve-ring, and excretory pore at 127–163 (144), 183–227 (208), and 283–357 (308), respectively, from the anterior extremity. Muscular portion of esophagus 387–460 (427) long and 47–60 (52) wide; glandular portion of esophagus 447–527 (489) long and 60–67 (61) wide. Muscular/glandular esophagus length ratio 1:1.5. Length of entire esophagus and buccal capsule representing 8–9% of body length. Vulva situated at 6–7 mm (6 mm) from anterior end, at 52% of body length; vulval lips not elevated. Muscular vagina directed posteriorly; uterus filled with eggs 28–32 (29) long by 25–30 (26) wide. Tail conical, 140–180 (166) long, without cuticular projections.

Discussion

The family Camallanidae was established for species with a prominent, sclerotized buccal capsule (Railliet and Henry 1915). Yeh (1960) divided the family into two subfamilies, Camallaninae Railliet & Henry, 1915, for species with the buccal capsule divided into two halves, and Procamallaninae Yeh, 1960, for those with a single, cup-like buccal capsule. The new species with its cup-like buccal capsule composed of two lateral halves is identified as a member of Procamallaninae. Six genera have been assigned to Procamallaninae: *Procamallanus*, *Spirocamallanus* Olsen, 1952, *Malayocamallanus* Jothy & Fernando, 1970, *Punctocamallanus* Moravec & Scholz, 1991, *Spirocamallanoides* Moravec & Sey, 1988 and *Denticamallanus* Moravec & Thatcher, 1997 (Baylis 1923; Olsen 1952; Jothy and Fernando 1970; Moravec and Scholz 1991; Moravec and Thatcher 1997; Rigby and Rigby 2014). The genus *Procamallanus* consists of approximately 40 known species distributed worldwide, but only two species have been reported from Brazil, *P. peraccuratus* and *P. annipetterae* Kohn & Fernandes, 1988, both from southern Brazil (Pinto et al. 1976; Petter and Dlouhy 1985; Kohn and Fernandes 1988). The new species is assigned to *Procamallanus* because its cup-like buccal capsule with smooth walls (without striations); according to Moravec and

Thatcher (1997) the main characteristic of this genus is the presence of a smooth buccal capsule in both sexes.

The new species can be distinguished from all known members of the genus outside of Brazil in having tooth-like structures on the basal ring of the buccal capsule. In addition to the above characteristic, it differs from *P. annulatus* Yamaguti, 1955 (Indonesia), *P. elatensis* Fusco & Overstreet, 1979 (Israel), *P. laeviconchus* Wedl, 1861 (Egypt), *P. planoratus* Kulkarni, 1935 (India) and *P. pseudolaeviconchus* Moravec & Van As, 2015 (Botswana) by the absence of a sclerotized gubernaculum, present in the other five species (Wedl 1861; Kulkarni 1935; Yamaguti 1955; Fusco and Overstreet 1979; Moravec and Van As 2015). *P. spiculastriatum* can be distinguished from *P. pacificus* Moravec, Justine, Würtz, Taraschewski & Sasal, 2006 (New Caledonia) also not found in Brazil, by the absence of the small processes (mucrons) (*sensu* Moravec et al. 2006) on the tip of the tail.

Two species of *Procamallanus* have been found in Brazil: *P. peraccuratus* Pinto, Fábio, Noronha & Rolas, 1976, from *Geophagus brasiliensis* (Quoy & Gaimard) and *Australoheros facetus* (Jenyns) (both Cichlidae) in the State of Espírito Santo (Southern Region of Brazil) and *P. annipetterae* Kohn & Fernandes, 1988 (= *P. petterae* Kohn & Fernandes, 1988), from *Corydoras paleatus* (Jenyns) in the Iguaçú River, State of Paraná (south of Brazil) (Pinto et al. 1976; Kohn and Fernandes 1988). Pinto et al. (1976) suggested that the characteristics of the buccal capsule and the morphological and morphometric data of each taxon should be considered for the differentiation of species, a view shared by Moravec (1998).

Procamallanus spiculastriatum sp. n. has tooth-like structures on the basal ring of the buccal capsule similar to these in *P. annipetterae* although the new species has four distinct tooth-like structures, whereas these are six in *P. annipetterae* as described by Petter (1990; see also her fig. 5A) in addition the latter species is distinct. Kohn and Fernandes (1988) provide no info on the number of cephalic papillae in females; only in the holotype male *P. spiculastriatum* sp. n. can be distinguished from *P. annipetterae* by the tail shape (conical in female of the new species vs. pointed in both sexes with a marked long and narrow posterior part); number of caudal papillae (three precloacal, two adcloacal, and five postcloacal vs. four precloacal and four postcloacal), shape of oral opening (circular in *P. spiculastriatum* vs. oval in *P. annipetterae*) and morphometric parameters such as spicule length (smaller spicule 229–284 µm, larger spicule 312–355 µm vs. 150–160 µm and 180–210 µm, respectively) and length of the tail (184 µm in males and 208 µm in females vs. 336 µm in males and 281 µm in females), comparisons made based on the description of Kohn and Fernandes (1988).

Procamallanus spiculastriatum sp. n. resembles *P. peraccuratus* in the morphology of the buccal capsule, oral opening circular and presence of caudal alae of males, but differs by the presence of four internal sclerotized tooth-like structures on the basal ring, the presence of two postcloacal dorsal papillae, and the presence of spicules with alate distal end supported by sclerotized rays of *P. spiculastriatum* and those characters are absent in *P. peraccuratus* (Moravec et al. 1993; Moravec 1998). Despite sharing hosts from the same family (Cichlidae), the species differ with respect to species of host and

the biomes where they are found: *P. spiculastratus* sp. n. is a parasite of *A. ocellatus* (biome Amazonia), whereas *P. peraccuratus* is a parasite of *G. brasiliensis* and *Au. facetus* (biome Brazilian Atlantic Forest). This finding extends the geographical distribution of the genus into the Brazilian Amazon. Additional morphometric comparisons between *P. spiculastratus* sp. n. and the two species found in Brazil are presented in Table 1.

The six genera currently assigned to Procamallaninae were reduced to subgenera of *Procamallanus* by Moravec (1998). However, Moravec (1998) did not provide any arguments why the former genera should be demoted to a lower level. Rigby and Rigby (2014) noted the overlap in the diagnostic characteristics of the buccal capsules of these taxa. Two molecular phylogenetic studies (Černotíková et al. 2011; Choud-

Table 1. Comparison of morphometric characteristics of the known South American species of *Procamallanus* with those of *Procamallanus spiculastratus* n. sp. Except as noted for individual characteristics, all data for *P. peraccuratus*, and *P. annipetterae* were taken from the original descriptions.

Caracteres	<i>Procamallanus spiculastratus</i> n. sp.				<i>P. peraccuratus</i>		<i>P. annipetterae</i>	
	Holotype	Allotype	Male	Female	Male	Female	Male	Female
Length (mm)	10.76	17	8–11	17–20	9.42–9.75	12.78–22.34	9.69	21.8
Width	147.36	166	105–147	160–173	150–170	210–400	500	720
Buccal capsule (L)a	64.93	80	57–74	78–83	72–87	87–113	131	180
Buccal capsule (W)	38.96	51	32–39	47–52	49	52–66	123	187
Mouth opening	Circular		Circular		Circular		–	
Teeth	Present	Present	Present	Present	Absent	Absent	Present	Present
Deirids	107.79	150	91–119	147–167	–	–	–	–
Nerve ring	168.83	226.66	156–188	220–233	220	230–240	298	326
Excretory pore	280.51	330	248–292	330–397	–	260–330	–	–
Muscular esophagus (L)	352.63	420	316–395	413–453	410–440	560–660	625	644
Glandular esophagus (L)	557.89	600	421–558	600–693	450–520	580–660	868	887
Ratio L/Oc and esophagus	9%	6.5%	9–12%	6–7%	10.32% ^b	7.57% ^b	16.76% ^b	7.8% ^b
Vulva (mm)	–	8	–	8–11	–	6.7–10.90	–	–
Preanal papillae (pairs)	3	–	3	–	3	–	2	–
Additional papillae (pairs)	2	–	2	–	2	–	2	–
Postanal papillae (pairs)	3 + 2DL ^a	–	3 + 2DL ^a	–	4	–	1	–
Spicule large	342.17	–	312–355	–	270–290	–	210	–
Spicule small	230.8	–	229–284	–	180–200	–	160	–
Caudal alae	Present	–	Present	–	Present	–	Absent	–
Tail	166.23	190	156–205	190–220	140	220–310	336	281
Host	<i>Astronotus ocellatus</i>				<i>Geophagus brasiliensis</i> and <i>Australoheros facetus</i>		<i>Corydonas paleatus</i>	
Site	Intestine				Intestine		Intestine	
Locality	Belém, Pará, Brazil				Vale do Rio Itaúnas, Espírito Santo, Brazil		Rio Iguaçú, Paraná, Brazil	
Biome	Amazonia				Atlantic Forest		Atlantic Forest	
Author	In this study				Pinto et al. (1976)		Kohn and Fernandes (1988)	

^aAbbreviations: L = length; W = width, e = esophagus, DL = dorsolateral papillae; Ratio L/Oc and esophagus = Length of entire oesophagus and buccal capsule representing of body length.

^bDerived or calculated from the original publication of the species description.

hury and Nadler 2016), further revealed that *Procamallanus* and *Spirocamallanus* are paraphyletic. We find that phylogenetic relationships within Procamallaninae have not been evaluated in an objective analysis using both morphological and molecular data. There is no evidence that such different taxa should be assigned to the same genus-level group (i.e., that they should be recognized as sub-genera rather than distinct genera, which is an arbitrary decision). Therefore, based on the current knowledge of the studied group we follow the concept accepting the full generic status of all recognized genus-group names within Procamallaninae. Even in the absence of a rigorous test of the monophyly of the genera, all but *Procamallanus* have contain species with consistent features; all known species of *Procamallanus* have smooth-walled buccal capsules without tooth-like structures except for *P. spiculastratus* sp. n. and *P. annipetterae*, both of which have tooth-like structures on the basal ring. This suggests that these two species might represent a distinct genus. Currently, we do not feel confident in describing a new genus without the support of a formal phylogenetic analysis. Among the camallanid species parasitizing *A. ocellatus*, only *Spirocamallanus inopinatus* from northern Brazil (Moravec 1998; Thatcher 2006) and *Camallanus* sp. from Midwestern Brazil have been reported (Kohn et al. 1985; Vicente et al. 1985).

Acknowledgements

The authors are grateful to Dr. Marcelo Knoff, curator of the Helminthological collection of the Oswaldo Cruz for loan of specimens; Patrick Cardoso, Andréa Abreu and Yago Larrat for technical support; the Laboratório de Histologia e Embriologia Animal – Instituto da Saúde e Produção Animal – Universidade Federal Rural da Amazônia – UFRA, campus Belém, state of Pará, Brazil for the use of the scanning electron microscope; the managers of the Jardim Botânico Bosque Rodrigues Alves (Rodrigues Alves Botanical Garden) for encouragement and technical support for the collection of specimens of *A. ocellatus*. This study is part of the Ph.D. thesis of Raul Henrique da Silva Pinheiro, developed for the Programa de Pós-Graduação em Biologia de Agentes Infeciosos e Parasitários (Graduate Program in Biology of Infectious Agents and Parasites), Instituto de Ciências Biológicas (Biological Sciences Institute), Universidade Federal do Pará-UFPA. Part of this research was carried out by Raul Henrique da Silva Pinheiro during a visit to the Laboratorio de Morfología Animal, Universidad Autónoma del Estado de Hidalgo, Pachuca, Hidalgo, México.

References

- Agrawal V (1966) On a new nematode, *Procamallanus muelleri* n. sp. from the stomach of a freshwater fish, *Heteropneustes fossilis*. Proceedings of the Helminthological Society of Washington 33: 204–208.

- Azevedo RKD, Abdallah VD, Luque JL (2007) Ecologia da comunidade de metazoários parasitos do apaiari *Astronotus ocellatus* (Cope, 1872) (Perciformes: Cichlidae) do rio Guandu, Estado do Rio de Janeiro, Brasil. *Revista Brasileira de Parasitologia Veterinária* 16: 15–20.
- Bautista-Hernández CE, Violante-González J, Monks S, Pulido-Flores G (2014) Helminth communities of *Xiphophorus malinche* (Pisces: Poeciliidae), endemic freshwater fish from the Pánuco River drainage, México. *Revista Mexicana de Biodiversidad* 85: 838–844. <https://doi.org/10.7550/rmb.40560>
- Baylis HA (1923) Report on a collection of parasitic nematodes, mainly from Egypt. Part III. Camallanidae, etc. with a note on *Probstmatria* and an Appendix on Acanthocephala. *Parasitology* 15: 24–38. <https://doi.org/10.1017/S0031182000014475>
- Černotíková E, Horák A, Moravec F (2011) Phylogenetic relationships of some spirurine nematodes (Nematoda: Chromadorea: Rhabditida: Spirurina) parasitic in fishes inferred from SSU rRNA gene sequences. *Folia Parasitologica* 58: 135–148. <https://doi.org/10.14411/fp.2011.013>
- Choudhury A, Nadler SA (2016) Phylogenetic relationships of Cucullanidae (Nematoda), with observations on Seuratoidea and the monophyly of *Cucullanus*, *Dicbelyne* and *Truttaedacnitis*. *Journal of Parasitology* 102: 87–93. <https://doi.org/10.1645/15-806>
- Fontenele O, Nepomuceno FH (1983) Exame dos resultados da introdução do *Astronotus ocellatus* (Agassiz, 1849), em açudes do nordeste do Brasil. *Boletim Técnico do DNOCS* 41: 85–99.
- Froese R, Pauly D (Eds) (2017) FishBase. Version (02/2017). www.fishbase.org [Version (02/2018), last visited 7 May 2018]
- Fusco AC, Overstreet RM (1979) Two camallanid nematodes from Red Sea fishes including *Procamallanus elatensis* sp. nov. from siganids. *Journal of Natural History* 13: 35–40. <https://doi.org/10.1080/00222937900770041>
- Giese EG, Santos JN, Lanfredi RM (2009) A new species of Camallanidae from *Ageneiosus ucayalensis* (Pisces: Siluriformes) from Pará state, Brazil. *Journal of Parasitology* 95: 407–412. <https://doi.org/10.1645/GE-1680.1>
- Hoffman GL (1999) *Parasites of North American Freshwater Fishes*. Cornell University Press, New York, 539 pp.
- Jothy AA, Fernando CH (1970) A new camallanid nematode, *Malayocamallanus intermedius* gen. et. sp. nov., from a Malayan freshwater fish, *Fluta alba* (Zuiew) with a key to the genera of the subfamily Procamallaninae. *Helminthologia* 11: 87–91.
- Kohn A, Fernandes BMM (1988) *Procamallanus annipetterae* nom. nov. for *Procamallanus petterae* Kohn & Fernandes, 1988 preoccupied by *Procamallanus (Procamallanus) petterae* Moravec & Sey, 1988. *Memórias do Instituto Oswaldo Cruz* 83: 535. <https://doi.org/10.1590/S0074-02761988000400025>
- Kohn A, Fernandes BMM, Pipolo HV, Godoy MP (1988) Helminthos parasitos de peixes das Usinas Hidrelétricas Eletrosul (Brasil). II. Reservatórios de Salto Osório e de Salto Santiago. Bacia do Rio Iguaçu. *Memórias do Instituto Oswaldo Cruz* 83: 299–303. <https://doi.org/10.1590/S0074-02761988000300006>
- Kohn A, Fernandes BMM, Macedo B, Abramson B (1985) Helminths parasites of freshwater fishes from Pirassununga, SP, Brazil. *Memórias do Instituto Oswaldo Cruz* 80: 327–336. <https://doi.org/10.1590/S0074-02761985000300009>

- Kulkarni RB (1935) A second species of *Procamallanus* Baylis, 1923, from India. Proceedings of the Indian Academy of Sciences 2: 29–32.
- Kullander SO (2003) Cichlidae (Cichlids). In: Reis RE, Kullander SO, Ferraris Jr CJ (Eds) Checklist of the freshwater fishes of South and Central America. EDIPUCRS, Porto Alegre.
- Malta JCdO (1984) Os peixes de um lago de várzea da Amazônia Central (Lago Janauacá, Rio Solimões) e suas relações com os crustáceos ectoparasitas (Branchiura: Argulidae). Acta Amazonica 14: 355–372. <https://dx.doi.org/10.1590/1809-43921984143372>
- Moravec F, Van As LL (2015) *Procamallanus* (*Procamallanus*) spp. (Nematoda: Camallanidae) in fishes of the Okavango river, Botswana, including the description of *P. (P.) pseudolaeviconchus* n. sp. parasitic in *Clarias* spp. (Clariidae) from Botswana and Egypt. Systematic Parasitology 90: 137–149. <https://doi.org/10.1007/s11230-014-9541-0>
- Moravec F, Justine JL, Würtz J, Taraschewski H, Sasal P (2006) A new species of *Procamallanus* (Nematoda: Camallanidae) from pacific eels (*Anguilla* spp.). Journal of Parasitology 92: 130–137. <https://doi.org/10.1645/GE-3509.1>
- Moravec F (1998) Nematodes of freshwater fishes of the Neotropical region. Academia, Prague, 464 pp.
- Moravec F, Thatcher VE (1997) *Procamallanus* (*Denticamallanus* subgen. n.) *dentatus* n. sp. (Nematoda: Camallanidae) from the characid fish, *Bryconops alburnoides*, in the Brazilian Amazon. Parasite 4: 239–243. <https://doi.org/10.1051/parasite/1997043239>
- Moravec F, Scholz T (1991) Observations on some nematodes parasitic in freshwater fishes in Laos. Folia Parasitologica 38: 163–178.
- Moravec F, Kohn A, Fernandes BMM (1993) Nematode parasites of fishes of the Paraná River, Brazil. Part 3. Camallanoidea and Dracunculoidea. Folia Parasitologica 40: 211–229
- Neves LR, Pereira FB, Tavares-Dias M, Luque JL (2013) seasonal influence on the parasite fauna of a wild population of *Astronotus ocellatus* (Perciformes: Cichlidae) from the Brazilian Amazon. Journal of Parasitology 99: 718–721. <https://doi.org/10.1645/12-84.1>
- Olsen LS (1952) Some nematodes parasitic in marine fishes. Publications of the Institute of Marine Science, University of Texas. 2: 175–215.
- Petter AJ (1990) Nématodes de poissons du Paraguay. VI. Description de deux nouvelles espèces du genre *Spirocamallanus* et compléments à la description de *Procamallanus annipetterae* Kohn & Fernandes, 1988. Revue Suisse de Zoologie 97: 327–338. <https://doi.org/10.5962/bhl.part.82069>
- Petter AJ, Dlouhy C (1985) Nématodes de poissons du Paraguay. III Camallanina. Description d'une espèce et d'une sous-espèce nouvelles de la famille des Guyanemidae. Revue Suisse de Zoologie 92: 165–175. <https://doi.org/10.5962/bhl.part.81607>
- Pinto RM, Fábio SPde, Noronha D, Rolas FJT (1976) Novas considerações morfológicas e sistemáticas sobre os *Procamallanus* brasileiros (Nematoda, Camallanoidea). Memórias do Instituto Oswald Cruz 74: 77–84. <https://doi.org/10.1590/S0074-02761976000100008>
- Pritchard MH, Kruse GOW (1982) The collection and preservation of animal parasites. University of Nebraska Press, Lincoln, Nebraska, 141 pp.
- Railliet A, Henry A (1915) Sur les nématodes du genre *Camallanus* Raill. et Henry, 1915 (*Cucullanus* auct., non Mueller, 1777). Bulletin de la Societe de Pathologie Exotique 8: 446–452.

- Rigby MC, Rigby E (2014) 7.20 Order Camallanida: Superfamilies Anguilliculoidea and Camallanoidea. In: Schmidt-Rhaesa A (Ed.) Handbook of Zoology: Gastrotricha, Cycloneuralia and Gnathifera: Vol. 2, Nematoda. Walter De Gruyter, Berlin, 637–659.
- Thatcher VE (2006) Amazon fish parasites. Pensoft Publishers, Sofia, 508 pp.
- Vicente JJ, de Oliveira Rodrigues H, Correa Gomes D (1985) Nematóides do Brasil. I.: Nematóides de peixes. Atas da Sociedade de Biologia do Rio de Janeiro 25: 1–79.
- Wedl K (1861) Zur Helminthenfauna Aegyptens. 2. Abtheilung, III. Nematoda. Sitzungsberichte der Kaiserlichen Akademie der Wissenschaften, Mathematisch-Naturwissenschaftlichen Classe 44: 463–482.
- Yamaguti S (1955) Parasitic worms mainly from Celebes. Part 9. Nematodes of fishes. Acta Medicinæ Okayama 9: 122–133.
- Yeh L-S (1960) On a reconstruction of the genus *Camallanus* Railliet & Henry, 1915. Journal of Helminthology 34: 117–124. <https://doi.org/10.1017/S0022149X00020435>

A morphological re-evaluation of *Pachyseius humeralis* Berlese, 1910 (Acari, Mesostigmata, Pachylaelapidae)

Peter Mašán¹

¹ Institute of Zoology, Slovak Academy of Sciences, Dúbravská cesta 9, 845-06 Bratislava, Slovakia

Corresponding author: Peter Mašán (peter.masan@savba.sk; uzaepema@savba.sk)

Academic editor: Farid Faraji | Received 23 May 2018 | Accepted 26 September 2018 | Published 15 October 2018

<http://zoobank.org/EF3342CA-4E9C-4EF2-ACDD-4768026D1967>

Citation: Mašán P (2018) A morphological re-evaluation of *Pachyseius humeralis* Berlese, 1910 (Acari, Mesostigmata, Pachylaelapidae). ZooKeys 790: 35–44. <https://doi.org/10.3897/zookeys.790.26894>

Abstract

Based on features of the lectotype and newly collected specimens from Italy (Boboli Gardens, Florence), a morphological concept of *Pachyseius humeralis* Berlese, 1910 is revised and re-evaluated. New diagnostic character states important for recognition of the species are provided. A misidentified species, formerly widely published in Europe under the name *P. humeralis*, is established as a new species, *Pachyseius subhumeralis* sp. n.

Keywords

Description, morphology, soil mites, taxonomic revision, type species, systematics

Introduction

Pachyseius humeralis was quite briefly and insufficiently described by Berlese in 1910, as the type species of the genus *Pachyseius*, originally based on female specimens from the two collection sites in Italy (Rome, Mugello). Later in his next paper, Berlese (1913) supported his primary description of the species by adding of some illustrations (ventral idiosoma with gnathosoma, and tarsus II), based on the specimen from Rome (pers. obs.).

Several specimens of *Pachyseius humeralis* are present in the Berlese Collection, Florence, all from several localities of Central Italy (Maccarese close to Rome, Monte Giovi in Mugello Region, Filettino in Lazio Region, Vallombrosa in Regello Municipality, and

Boboli Gardens in Florence), but only two of them (numbered 83/5 and 83/6) belong to the original series of Berlese. In his original description of *P. humeralis*, Berlese (1910) did not designate a holotype, so his two specimens from “Roma” (83/5) and “Mugello” (83/6) must be considered as syntypes. Mašán (2007) based his revision of *P. humeralis* upon these two syntypes of which one of them, from Maccarese, Rome, is labelled “tipico” (83/5) by Berlese, and should be considered to be lectotype. Mašán (2007) found that the type specimens examined by him belong to two different species. The lectotype female mounted onto the slide 83/5 was incorrectly considered by him to be identical with the species which was redescribed and illustrated by several authors (Hyatt 1956, Karg 1971, Solomon 1982, Lapina 1988, Mašán 2007). Mašán (2007) overlooked specific morphological differences, described in present paper, between the lectotype and the specimens which were available for his comparative study from Slovakia and other countries in Europe. The paratype female in slide 83/6 was identified as *Pachyseius wideventris* Afifi & Nasr, 1984 originally described from Netherlands (Afifi and Nasr 1984). The concept of *P. humeralis* is therefore based on a single specimen, from Rome.

In the Boboli Gardens in Florence, Italy, fourteen specimens of a species which was putatively considered as a new and closely related with *Pachyseius humeralis*, were collected by me in leaf litter and soil detritus. In order to define the differences between the newly collected specimens and *P. humeralis*, the lectotype of the species was re-examined. The analysis indicated that my specimens from the Boboli Gardens in Florence were actually clearly conspecific with that on slide number 83/5 of Berlese. So now I can confirm my mistake, and reveal the true identity of *P. humeralis* sensu Berlese (1910).

The main aim of this study is to diagnose and redescribe the type species of *Pachyseius*, misinterpreted by the followers of Berlese (1910, 1913), and compare that species with similar but confused species widely reported from various European countries under the name *Pachyseius humeralis*.

Materials and methods

Collected mites were extracted from the litter and soil detritus by means of a modified Berlese-Tullgren funnel equipped with a 40-Watt bulb, and preserved in ethyl alcohol. Before identification, the mites were mounted onto permanent microscope slides, using Swan's chloral hydrate mounting medium. A Leica DM 1000 light microscope equipped with a Leica EC3 digital camera was used to obtain measurements and photos. Some multiple images were combined using the CombineZP software program (Hadley 2010). Measurements were made from slide-mounted specimens. Lengths of shields and legs were measured along their midlines, and widths at their widest point (if not otherwise specified in the description). Dorsal setae were measured from the bases of their insertions to their tips. Measurements are mostly presented as ranges (minimum to maximum). The terminology of dorsal and ventral chaetotaxy follows Lindquist and Evans (1965), and that for leg setae follows that of Evans (1963). Identification of pore-like structures on the idiosomal integument is based on the mor-

phological observations of Athias-Henriot (1969); notation for these structures such as adenotaxy and poroidotaxy follows Johnston and Moraza (1991).

For the purpose of this study, all the specimens from the large-scale collections so far reported from Slovakia under the confused name *Pachyseius humeralis* by the author (see Mašán 2007) were checked once again for their correct identity. If available, also specimens recently collected in various European countries were re-examined and listed below.

Systematics

Pachyseius humeralis Berlese, 1910

Figures 1A, 1B, 3A, 4A, 5A, 6A, 7A

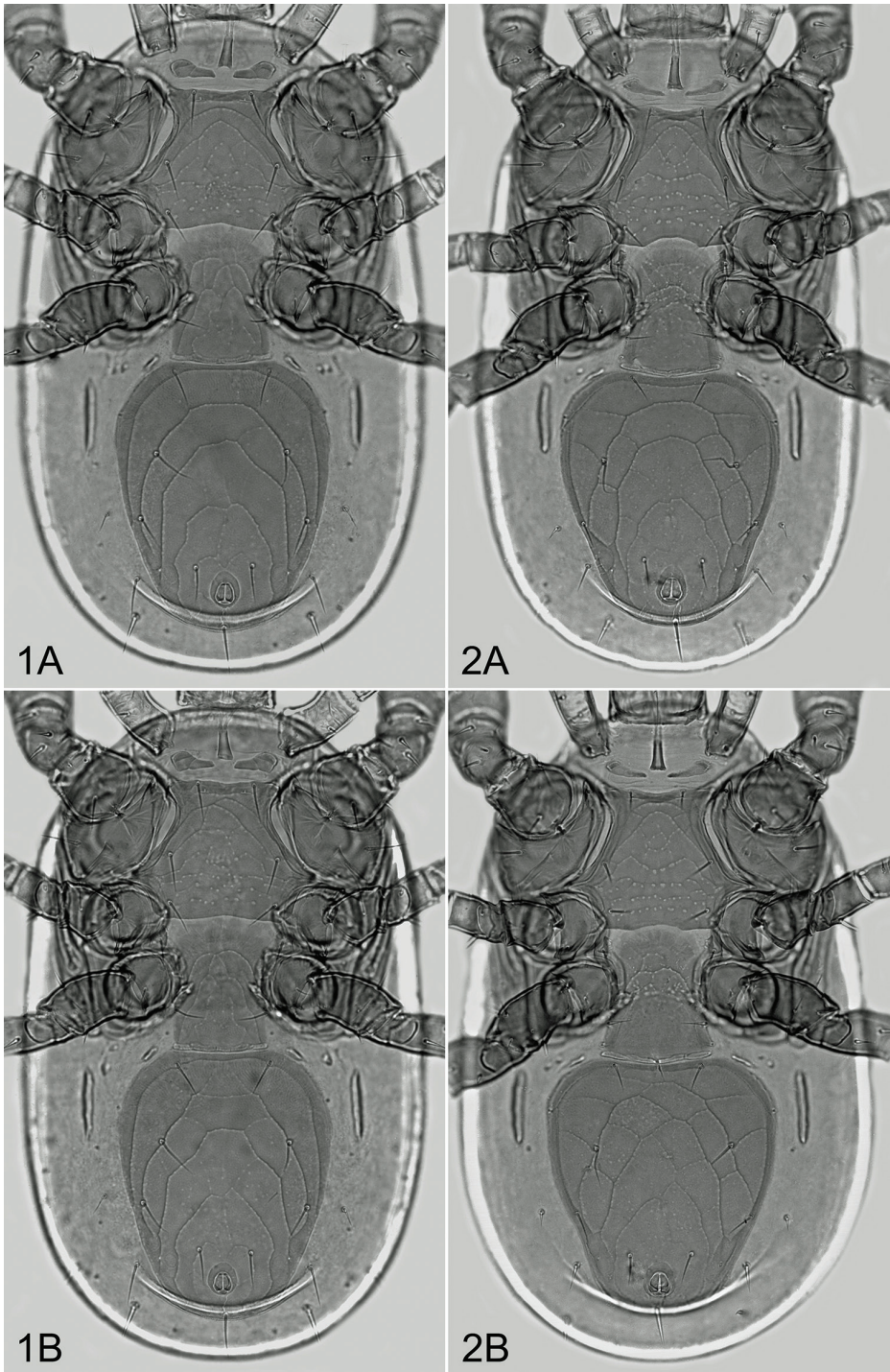
Pachyseius humeralis Berlese, 1910: 255; Berlese 1913: 81; Castagnoli and Pegazzano 1985: 187 (in part).

non *Pachyseius humeralis*: Nefedov 1966: 1098 (= *Pachyseius wideventris* Afifi & Nasr, 1984) (a newly introduced misidentification).

Material examined. Lectotype by present designation: female (slide number 83/5), **Italy**, Maccarese Village (Rome), humus, labelled as *Pachylaelaps humeralis*, deposited at the Research Centre for Agrobiological and Pedology, Florence; other specimens: 14 females, **Italy**, Florence City, Boboli Gardens, leaf litter and soil detritus, May 21, 2006, leg. P. Mašán, deposited at the Institute of Zoology, Slovak Academy of Sciences, Bratislava.

Diagnosis. The species may be distinguished from the other congeners especially by combination of the following female characters: (1) dorsal shield setae simple, needle-like; (2) dorsal shield between setae z1 and z2 and peritrematal shields close to stigma with enlarged and cavity-like poroid structure; (3) presternal platelets well sclerotized, with two striae, separate each other, and free from anterior margin of sternal shield; (4) exopodal platelets II–III and III–IV free, not fused to peritrematal shields; (5) ventrianal shield with three pairs of preanal setae (JV1–JV3); (6) lateral and opisthogastric soft integument with seven pairs of setae: r6, R2–R4, ZV2, JV4, and JV5; (7) tarsus II with two subdistal posterolateral setae thickened, spur-like; (8) tarsus IV with 17 setae.

Description. *Female. Dorsal idiosoma.* Dorsal shield 540–600 µm long (most frequently 565–595 µm), 320–380 µm wide, suboval, oblong (length/width: 1.6–1.75), widely rounded anteriorly and posteriorly, with almost parallel lateral margins, and delicate reticulation on posterior surface. Dorsal shield with 30 pairs of setae; the setae simple, smooth, needle-like and mostly similar in length; the length of some selected setae as follows: z1 7–10 µm, j1 15–19 µm, j5 19–25 µm, J1 24–28 µm, J2 and J3 27–32 µm, J4 30–36 µm, J5 31–39 µm; the longest dorsal setae 40–48 µm in length. A pair of gland pores gdj3 enlarged, cavity-like, well sclerotized, and situated between setae z1 and z2 close to anterior margin of dorsal shield. Anterior surface with two pairs of minute suboval sclerites situated between setae j2 and j3.



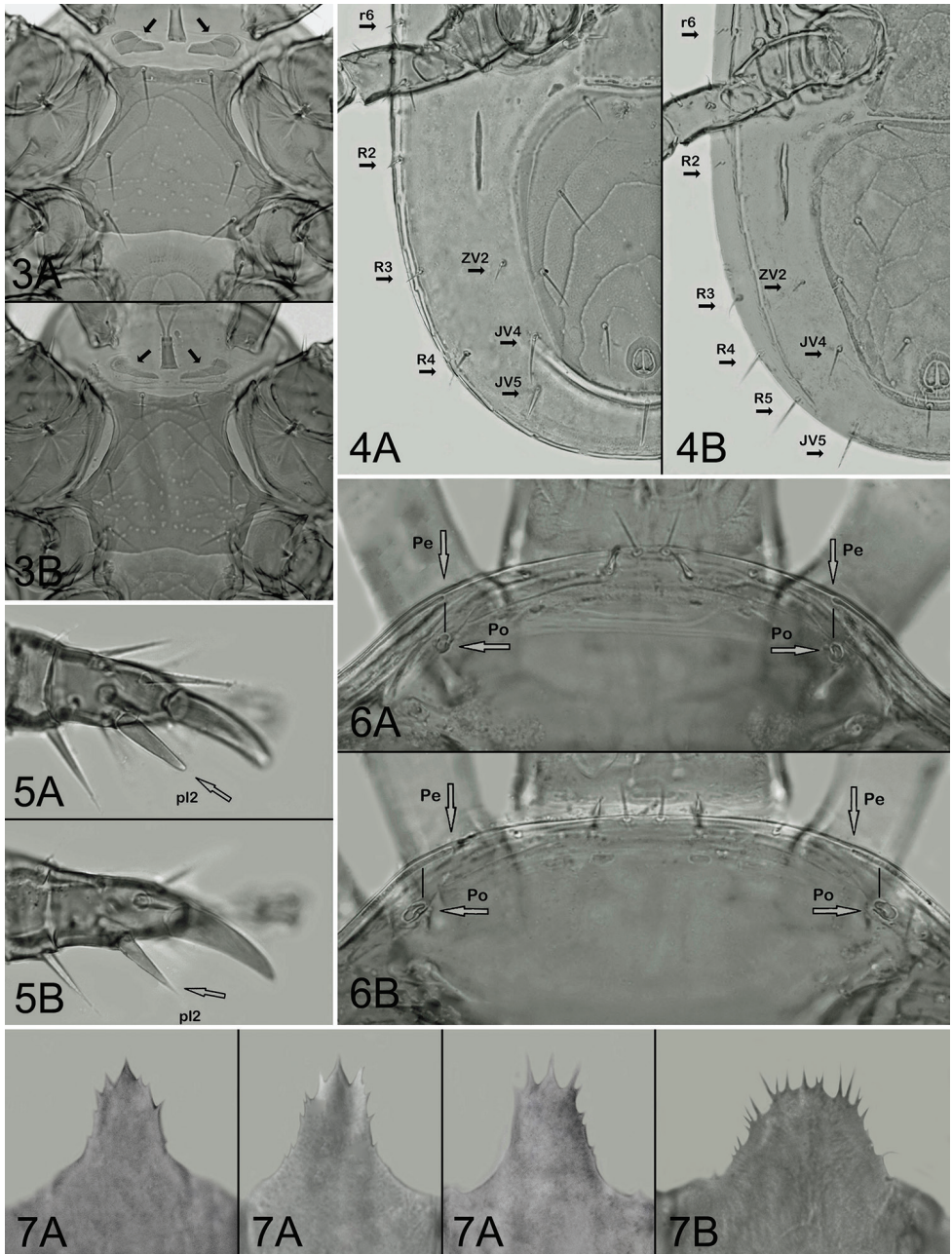
Figures 1–2. *Pachyseius* spp., ventral idiosoma of females. **1** *Pachyseius humeralis* **2** *Pachyseius subhumeralis* sp. n. Not to scale **A, B** variant specimens.

Ventral idiosoma (Figure 1A, B). Presternal area with two platelets (Figure 3A); the platelets free on soft integument, small, subtriangular, with two striae transversely or obliquely oriented on their well sclerotized surface. Sternal shield 112–125 μm long, 76–87 μm wide at the narrowest level of coxae II (120–140 μm at the level of setae st2), with three pairs of subequal setae (st1–st3 36–42 μm), and two pairs of lyrifissures; the shield with anterior and posterior margin almost straight or very slightly concave; sculptural ornamentation well developed, with curved punctate lines on anterior and lateral surface and polygonal or linear pattern of punctations on medial and posterior surface. Two metasternal platelets suboval, each with a seta and pore-like structure. Epigynal shield 110–130 μm long, 74–90 μm wide, oblong, with convex anterior margin, truncate posterior margin, two genital setae, and delicate punctate-reticulate pattern on surface; a row of four suboval and elongate postgenital sclerites along its posterior margin present; genital pore-like structures normally situated on soft integument, outside the shield. Ventrianal shield suboval, longer than wide (length: 218–252 μm , width: 168–198 μm , length/width: 1.2–1.37), with anterior portion moderately expanded, widest anterior to setae JV2, straight or mostly slightly concave anteriorly, widely rounded anterolaterally and posteriorly, bearing lineate-reticulate pattern on entire surface (parallel lines more expressively indicated), three pairs of preanal setae (JV1–JV3), and three circum-anal setae close to suboval anus. Peritrematal shields free from closely adjacent exopodal platelets II–III and III–IV; post-stigmatic sections of the shields narrowed posteriorly, rounded terminally, not reaching beyond the posterior margin of exopodals III–IV, and each bearing three small pore-like structures and one greatly enlarged cavity-like poroid close to stigma. Peritremes normal, with anterior tips reaching marginal dorsal surface between setae z1 and z2, close to enlarged gland pores gdj3 (Figure 6A). Exopodal platelets III–IV free but contiguous to exopodals II–III. Soft integument between peritrematal shields and anterolateral margins of ventrianal shield with two pairs of minute irregular sclerites and a pair of larger suboval platelets. Metapodal region with a pair of narrow, conspicuously elongated and longitudinally oriented platelets; the platelets 52–69 μm long and relatively well separated from anterolateral margins of ventri-anal shield. Lateral and opisthogastric soft integument with seven pairs of setae (Figure 4A): four pairs of dorsomarginal (r6, R2–R4) and three pairs of opisthogastric setae (ZV2, JV4, JV5). All ventrally inserted setae similar to those on dorsal shield.

Gnathosomal structures. Corniculi slender and horn-like; deutosternal groove with four or five transverse rows of denticles and two smooth transverse lines; internal malae reaching beyond the corniculi; gnathosomal setae smooth and needle-like. Palptibia without outgrowths, palptarsus with three-tined apotele. Epistome narrow, with anterior and lateral margin irregularly dentate, apex with larger and pointed central cusp (Figure 7A).

Legs. Leg setation as previously described in the genus (Mašán 2007), and for *Pachyseius humeralis* species group: tarsus IV bearing 17 setae (seta ad2 absent). Tarsus II with two obtuse spur-like distal setae pl1 and pl2 (Figure 5A).

Sperm induction system. Tubiform structures of sperm induction system detectable, weakly sclerotized, long and thin, and associated with posterior margin of coxae III.



Figures 3–7. *Pachyseius humeralis* (A) and *Pachyseius subhumeralis* sp. n. (B), females. **3** Sternal regions (arrows pointing to presternal platelets) **4** Opistogastric regions (arrows pointing to marginal and opistogastric setae placed on soft integument) **5** Tarsi II (arrows pointing to seta pl2) **6** Anteriormost portion of dorsal shields [arrows pointing to anterior tip of peritremes (Pe) and enlarged gland pores g_{dj}3 (Po)] **7** Epistomes (with three variant forms in *P. humeralis*). Not to scale.

***Pachyseius subhumeralis* sp. n.**

<http://zoobank.org/3B4BDFFF-BE84-4FF9-B2E0-91E053317BC8>

Figures 2A, 2B, 3B, 4B, 5B, 6B, 7B

Pachyseius humeralis: Hyatt 1956: 4; Karg 1971: 141; Solomon 1982: 102; Lapina 1988: 178; Karg 1993: 116; Mašán 2007: 32, 210.

Material examined. Type material. Holotype female: **Slovakia**, Trnavská Pahorkatina Highland, Štefanová Village, Dubník Forest, oak forest (with *Quercus* spp.), leaf litter and soil detritus, altitude 250 m, June 18, 1997, leg. P. Mašán. Paratypes: 2 females, with the same collection data as in holotype; seven females, **Slovakia**, Malé Karpaty Mts., Bratislava Capital, Železná Studienka Forest, beech forest (with *Fagus sylvatica*), leaf litter and soil detritus, altitude 370 m, April 27, 1993, leg. P. Mašán; 17 females, Bratislava Capital, Devín Settlement, Devínska Kobyla Mt., oak forest (with *Quercus* spp.), leaf litter and soil detritus; altitude 270 m, July 30, 1997, leg. P. Mašán. All these specimens were previously published as *Pachyseius humeralis* by Mašán (2007), and are deposited at the Institute of Zoology, Slovak Academy of Sciences, Bratislava.

Non-type material. Bulgaria: one female, Shumen Plateau Natural Park, Shumen City, Bukaka Reserve, old beech forest (*Fagus sylvatica*) with admixed hornbeam (*Carpinus betulus*), leaf litter and soil detritus, altitude 500 m, October 23, 2007, leg. I. Mihál. **Czech Republic:** two females, with unknown collection data. **France:** two females, Alpes Cottiennes Mts., Arvieux Village, Gorges du Guil Canyon, pine forest (*Pinus* sp.) on a slope with loose rock debris (limestone), humid needle litter with tussocks of grass and mushrooms, altitude 1,180 m, June 11, 2007, leg. P. Fenda. **Germany:** three females, Bavaria, Bavarian Prealps Mts., Flintsbach am Inn Village, St. Peter's Abbey on the Madron ("Peterskirchlein"), broadleaved deciduous forest predominated by beech (*Fagus sylvatica*), humid soil detritus under a deep layer of leaf-fall, altitude 600 m, April 25, 2007, leg. P. Mašán. **Hungary:** six females, with unknown collection data. **Italy:** four females, Lombardy Region, Bergamo Province, Bergamasque Alps and Prealps Mts., Zambla Alta Village, near to Zambla Pass, spruce forest (*Picea abies*) with admixed beech (*Fagus sylvatica*), needle litter and soil detritus with decomposed wood substrate, altitude 1,170 m, May 13, 2015, leg. P. Mašán; three females, Tuscany Region, Florence City, Villa Camerata Hostel, park, broadleaved deciduous wood, leaf litter, altitude 75 m, April 23, 2009, leg. P. Mašán; two females, Florence City, Parco delle Cascine Gardens, broad-leaved deciduous wood, leaf litter with soil and wood detritus, altitude 45 m, May 23, 2006, leg. P. Mašán. **Poland:** one female, with unknown collection data. **Romania:** one female, Transylvania Region, Apuseni Mts. (Gilău Mts. in Bihor Massif), Cluj County, Turda Town, Turda Gorge, near to Peștera Ungurească Cave, oak-hornbeam forest, leaf litter, altitude 530 m, July 13, 2006, leg. P. Fenda. **Serbia:** three females, Kučajske Planine Mts., Pomoravlje District, Troglan Bara Settlement, Velika Brezovica Forest, beech forest (*Fagus sylvatica*), leaf litter and soil detritus, altitude 900 m, April 23, 2009, leg. I. Mihál. **Switzerland:** four females, Basel-Stadt

Canton, Riehen Town, Wenken Settlement, old beech forest with limes (*Tilia* sp.) and maples (*Acer* sp.), leaf litter and soil detritus, altitude 380 m, June 1, 2016, leg. P. Mašán. **United Kingdom, Wales:** two females, Anglesey Island, Llangefni Town, The Dingle Forest, alluvium of Cefni River, mixed broadleaved deciduous forest, leaf litter and soil detritus, altitude 35 m, July 31, 2010, leg. P. Mašán; four females, Anglesey Island, Llandegfan Village, alluvium of Cadnant River, mixed broadleaved deciduous wood, leaf litter and soil detritus, altitude 50 m, July 25, 2010, leg. P. Mašán.

Diagnosis. The species may be distinguished from the other congeners especially by combination of the following female characters: (1) dorsal shield setae simple, needle-like; (2) dorsal shield between setae z1 and z2 and peritrematal shields close to stigma with enlarged and cavity-like poroid structure; (3) presternal platelets well sclerotized in anterior part, transversely striate, separate each other but connected to anterior margin of sternal shield; (4) exopodal platelets II-III and III-IV free, not fused to peritrematal shields; (5) ventrianal shield with three pairs of preanal setae (JV1–JV3); (6) lateral and opisthogastric soft integument with eight pairs of setae: r6, R2–R5, ZV2, JV4, and JV5; (7) tarsus II with two subdistal posterolateral setae thickened, of which pl1 with obtuse apex, spur-like, and pl2 terminally attenuate and sharply pointed (but the tip of pl2 is fragile and can be very often broken in slide-mounted specimens); (8) tarsus IV with 17 setae.

Description. The morphological attributes of the species were described and illustrated in detail by Mašán (2007), and the description does not need to be repeated here. The original illustrations given by the cited author are based on the type specimens from Štefanová Village (see above).

Etymology. Many epithets beginning with *sub-*, a Latin name-forming prefix meaning “approaching”, are intended to distinguish a species from that with which it was previously confused. The new epithet is proposed as an alternative name for *Pachyseius humeralis* in the broad sense understood to date.

Discussion. The re-evaluation of the lectotype and newly collected material of *Pachyseius humeralis* sensu Berlese, 1910 showed that there are several apparent and constant morphological differences between this species and its congener widely reported from Europe under the same name, and here established as *Pachyseius subhumeralis* sp. n. According to these findings, *P. humeralis* may be most reliably distinguished from *P. subhumeralis* by the following characters:

- (1) the placement of genital pores (placed outside the epigynal shield in *P. humeralis*, or on posterolateral corners of the shield in *P. subhumeralis*; Figs 1 and 2),
- (2) the form and placement of presternal platelets (the platelets evenly sclerotized and free on soft integument in *P. humeralis*, or separately connected to sternal shield with their weakly sclerotized posterior portions in *P. subhumeralis*; Figure 3),
- (3) the number of dorsomarginal setae on soft integument (four pairs in *P. humeralis* – setae R5 absent, or five pairs in *P. subhumeralis* – setae R5 present; Figure 4),

- (4) the form of posterolateral seta pl2 on tarsus II (pl2 robust, spur-like, and apically rounded in *P. humeralis*, or regularly tapered and apically pointed in *P. subhumeralis*; Figure 5),
- (5) the relative length of peritremes (the peritreme with anterior tip never reaching beyond the longitudinal axis of gland pore gdj3 in *P. humeralis*, or reaching slightly beyond this point in *P. subhumeralis*; Figure 6),
- (6) the form of epistome (the epistome with narrow base and large central cusp in *P. humeralis*, or with widened base and uniformly spinate anteriormost margin in *P. subhumeralis*; Figure 7).

There are also less serious differences recognizable between the two compared species, having partly transitional character, for instance in size and proportions of the dorsal and ventroanal shield, and relative length of some idiosomal setae. Generally, when compared with *Pachyseius subhumeralis* (based on metric data given by Mašán in 2007), *Pachyseius humeralis* is smaller species (optimum length: 565–595 μm versus 595–640 μm), possessing relatively narrower ventrianal shield (L/W ratio: 1.2–1.37 versus 1.08–1.28; Figs 1 and 2), relatively longer setae (j5: 19–25 μm versus 15–23 μm , J5: 31–39 μm versus 24–34 μm), and shallower medial concavity of posterior margin of sternal shield.

The specimens of *Pachyseius humeralis* available in the Berlese Collection in Florence from several localities of Central Italy (Monte Giovi, Filettino, Vallombrosa, and Florence), and those from other European regions widely published by various authors (especially from the Mediterranean areas), should be carefully re-examined in the next studies to define their correct identity, and to re-evaluate spatial distribution of the species treated in this paper.

Acknowledgements

I am deeply grateful to Kamila Hruzová (Comenius University, Bratislava, Slovakia) who helped me by providing many valuable photos of *Pachyseius humeralis* lectotype specimen taken during her stay in the Berlese Collection, Florence, and to Roberto Nannelli (Agriculture Research Council, Research Centre for Agrobiological and Pedology, Florence, Italy) for his kindness in providing access to the Berlese Acaroteca, and providing laboratory space and all-round assistance. I sincerely thank Ivan Mihál (Institute of Forest Ecology, Zvolen, Slovakia) and Peter Fenda (Comenius University, Bratislava, Slovakia) who collected some specimens of *Pachyseius* examined for this study which was fully supported by the Scientific Grant Agency of the Ministry of Education of Slovak Republic and the Academy of Sciences [VEGA Grant No. 2/0036/18: Systematics, ecological requirements and chorology of saproxylic mites (Acari: Mesostigmata) phoretically associated with woodboring insects in Europe].

References

- Affi AM, Nasr AK (1984) Description of *Pachyseius wideventris*, a new species from Holland (Acari – Gamasida – Pachylaelapidae). Zoological Society of Egypt Bulletin 34: 5–10.
- Atthias-Henriot C (1969) Les organes cuticulaires sensoriels et glandulaires des Gamasides. Poroidotaxie et adénotaxie. Bulletin de la Société Zoologique de France 94: 458–492.
- Berlese A (1910) Lista di nuove specie e nuovi generi di Acari. Redia 6: 242–271.
- Berlese A (1913) Acari nuovi. Manipoli VII–VIII. Redia 9: 77–111.
- Castagnoli M, Pegazzano F (1985) Catalogue of the Berlese Acaroteca. Istituto Sperimentale per la Zoologia Agraria, Firenze, 490 pp.
- Evans GO (1963) Observations on the chaetotaxy of the legs in the free-living Gamasina (Acari: Mesostigmata). Bulletin of the British Museum (Natural History), Zoology 10: 277–303.
- Hadley A (2010) CombineZP. Image Stacking Software. <http://www.hadleyweb.pwp.blueyonder.co.uk/>
- Hyatt KH (1956) British mites of the genus *Pachyseius* Berlese, 1910 (Gamasina – Neoparasitidae). Annals and Magazine of Natural History (Series 12)9: 1–6. <https://doi.org/10.1080/00222935608655716>
- Johnston DE, Moraza ML (1991) The idiosomal adenotaxy and poroidotaxy of Zerconidae (Mesostigmata: Zerconina). In: Dusbábek F, Bukva V (Eds) Modern Acarology. Academia Press, Prague, 349–356.
- Karg W (1971) Acari (Acarina), Milben, Unterordnung Anactinochaeta (Parasitiformes). Die freilebenden Gamasina (Gamasides), Raubmilben. Die Tierwelt Deutschlands 59: 1–475.
- Karg W (1993) Acari (Acarina), Milben. Parasitiformes (Anactinochaeta). Cohors Gamasina Leach. Raubmilben. 2. Überarbeitete Auflage. Die Tierwelt Deutschlands 59: 1–523.
- Lapina IM (1988) Gamasina mites of Latvia. Zinātne Publishing House, Riga, 197 pp. [In Russian]
- Lindquist EE, Evans GO (1965) Taxonomic concepts in the Ascidae, with a modified setal nomenclature for the idiosoma of the Gamasina (Acarina: Mesostigmata). Memoirs of the Entomological Society of Canada 47: 1–64. <https://doi.org/10.4039/entm9747fv>
- Mašán P (2007) A Review of the family Pachylaelapidae in Slovakia, with systematics and ecology of European species (Acari: Mesostigmata: Eviphidoidea). NOI Press, Bratislava, 247 pp.
- Nefedov VN (1966) The mites *Pachyseius humeralis* Berlese, 1910 (Gamasoidea, Neoparasitidae) in the USSR fauna. Zoologicheskyy Zhurnal 45: 1098–1099. [In Russian]
- Solomon L (1982) A new *Pachyseius* species (Acari: Mesostigmata) and a new one for the Romanian fauna. Revue Roumaine de Biologie, Serie de Biologie Animale 27: 99–102.

A review of the spider genus *Sinanapis*, with the description of a new species from Tibet (Araneae, Anapidae)

Qiqi Zhang¹, Yucheng Lin¹

¹ Key Laboratory of Bio-resources and Eco-environment (Ministry of Education), College of Life Sciences, Sichuan University, Chengdu, Sichuan 610064, China

Corresponding author: Yucheng Lin (linyucheng@scu.edu.cn)

Academic editor: Y. Marusik | Received 13 April 2018 | Accepted 17 August 2018 | Published 15 October 2018

<http://zoobank.org/4B74B0E4-3945-4858-AFCA-F02F38445308>

Citation: Zhang Q, Lin Y (2018) A review of the spider genus *Sinanapis*, with the description of a new species from Tibet (Araneae, Anapidae). ZooKeys 790: 45–61. <https://doi.org/10.3897/zookeys.790.25793>

Abstract

The genus *Sinanapis* Wunderlich & Song, 1995 is reviewed in this paper. The material of all three known species was reexamined and photographed resulting in a new species, *Sinanapis medogense* sp. n. (♂, ♀) being described from Tibet, China. A key is provided for the genus, as well as species diagnoses, illustrations, and distribution maps for all four species of *Sinanapis*.

Keywords

Araneoidea, anapids, Asia, key, revision, Xizang

Introduction

According to the World Spider Catalog (2018), 223 extant species in 58 genera are documented in the family Anapidae Simon, 1895, including eleven species in seven genera from China. This family is chiefly distributed in the tropical and southern temperate regions (Lin and Li 2012).

The *Sinanapis* was originally erected by Wunderlich and Song (1995) as a monotypic genus based on *S. crassitarsa* Wunderlich & Song, 1995 from Xishuangbanna in Yunnan

of China. Currently *Sinanapis* comprises three valid species distributed in southern China, Vietnam and Laos: *S. crassitarsa* Wunderlich & Song, 1995, *S. longituba* Lin & Li, 2012, and *S. wuyi* Jin & Zhang, 2013, making *Sinanapis* the genus with the highest number of species within the family Anapidae in China. The genus was previously known in China from Yunnan to Fujian Provinces only.

While studying material from Tibet, we recognized several specimens belonging to Anapidae. Detailed study of these specimens reveals that they belong to an undescribed species of *Sinanapis*, a genus previously unknown in Tibet. The goal of this paper is to provide detailed description of the new species and to conduct a comprehensive review of the genus *Sinanapis*.

Materials and methods

Specimens were examined and measured with a Leica M205 C stereomicroscope. Further details were studied with an Olympus BX43 compound microscope. Male and female copulatory organs were examined after they were dissected and detached from the bodies. Epigyne were removed and treated with lactic acid before photographed. All type specimens were preserved in 95% ethanol. Photos were taken with a Canon EOS 60D wide zoom digital camera (8.5 megapixels) mounted on an Olympus BX43 stereomicroscope. The images were montaged using Helicon Focus 3.10 (Khmelik et al. 2006) image stacking software.

All measurements are in millimeters. Leg measurements are given in the following sequence: total length (femur, patella, tibia, metatarsus, and tarsus). Abbreviations in figures or text are as follows:

ALE	anterior lateral eyes;	FD	fertilization ducts;
AME	anterior median eyes;	Fe	femur;
BA	basal patellar apophysis on palp;	LA	lateral patellar apophysis on palp;
BC	book lung covers;	LS	labral spur;
CD	copulatory ducts;	Pa	patella;
Cu	cusps on leg I;	PLE	posterior lateral eyes;
Cy	cymbium;	PME	posterior median eyes;
CO	copulatory opening;	S	spermathecae;
DA	dorsal patellar apophysis on palp;	TA	tibial apophysis on palp;
DP	dentigerous patellar process on palp;	Ti	tibia;
Em	embolus;	Te	tegulum.

All examined materials are deposited in the following institutions:

SMF	Senchenberg Research Institute, Frankfurt, Germany
IZCAS	Institute of Zoology, Chinese Academy of Sciences in Beijing, China

NHMSU Natural History Museum of Sichuan University in Chengdu, China
 HNU School of Life Sciences, Hunan Normal University in Changsha, China
 MHBU Museum of Hebei University in Baoding, China

Taxonomy

Family Anapidae Simon, 1895

Genus *Sinanapis* Wunderlich & Song, 1995

Type species. *Sinanapis crassitarsa* Wunderlich & Song, 1995 from Xishuangbanna, Yunnan.

Diagnosis. The males of *Sinanapis* can be distinguished from other male anapids by the palp with at least 3 patellar apophyses (Figs 2C, 4A, 6H, 9D), the ventrally flat bulb lacking conductor (Figs 2E, 4B, 6E, 9C), the embolus coiling around the bulb margin in at least one loop (Figs 2E, 4B, 6E, 9C), and having ventral cusps on metatarsus and tarsus I (Figs 1A, 4D, 6D). Females of *Sinanapis* can be distinguished from other Chinese anapids by the globular spermathecae spaced by less than 1.5 diameters (Figs 4H, 7I, 9F), and the copulatory ducts with at least one loop (Figs 4H, 7I, 9F).

Composition. *Sinanapis crassitarsa* Wunderlich & Song, 1995 (♂), *S. longituba* Lin & Li, 2012 (♂, ♀), *S. medogense* sp. n. (♂, ♀), and *S. wuyi* Jin & Zhang, 2013 (♂, ♀).

Distribution. China (Tibet, Yunnan, Hunan, Jiangxi, Fujian, Hainan), Laos, Vietnam.

Remarks. This genus gender is considered as masculine at its establishment by Wunderlich and Song (1995). But it was later corrected to feminine by World Spider Catalog (2018).

Key to species of *Sinanapis* Wunderlich & Song, 1995

- 1 Males..... 2
- Females..... 5
- 2 Anterior median eyes present (Fig. 3G); palp without a rasper-like dentigerous patellar process (Figs 4A, 9D) 3
- Anterior median eyes absent (Figs 1D, 5G); palp with a rasper-like dentigerous patellar process (Figs 1C, 6H–I) 4
- 3 Leg I robust (Fig. 4C–D); basal patellar apophysis of palp very long, more than 3 times longer than patella; dorsal patellar apophysis long, narrow (Fig. 4A–B)..... *S. longituba*
- Leg I normal (Fig. 8A, D); basal patellar apophysis of palp not longer than patella; dorsal patellar apophysis short, wide (Fig. 9B, D) *S. wuyi*

- 4 A rasper-like dentigerous patellar process as large as dorsal patellar apophysis (Fig. 2B–D); basal patellar apophysis short, laminar (Fig. 2F) ***S. crassitarsa***
- A rasper-like dentigerous patellar process shorter than dorsal patellar apophysis (Fig. 6H–I); basal patellar apophysis long, tubular (Fig. 6B, G).....
..... ***S. medogense* sp. n.**
- 5 Anterior median eyes present (Fig. 3G)..... **6**
- Anterior median eyes absent (Figs 1D, 5G)..... ***S. medogense* sp. n.**
- 6 Abdomen with white pattern dorsally and laterally (Fig. 3C, F); copulatory duct wide, with 2 loops, coiled around the entire spermatheca (Fig. 4H)
..... ***S. longituba***
- Abdomen without white pattern dorsally and laterally (Fig. 8D, F); copulatory duct narrow, with one loop, coiled around the base of spermatheca (Fig. 9F) ***S. wuyi***

***Sinanapis crassitarsa* Wunderlich & Song, 1995**

Figs 1, 2

Syn. *Sinanapis thaleri* Ono, 2009 (see Lin et al. 2013).

Type material. Holotype ♂ (IZCAS), CHINA: Yunnan Province, Xishuangbanna Dai Autonomous Prefecture, Mengla County, Menglun Town, tropical botanical garden near rainforest, in leaf litter, 2.X.1987, L.M. Yu leg. (not examined).

Other material examined. 1♂ (SMF), LAOS: Champasak Province, Muang Bachieng, Ban Lak 35, That Etu, secondary forest, sieved leaf litter near waterfall, 15°11.628'N, 106°06.105'E; 595 m, 26-XI-2009, P. Jäger leg.

Diagnosis. *Sinanapis crassitarsa* may be distinguished from the other two species except *S. medogense* sp. n. by having a rasper-like dentigerous patellar process and the absence of anterior median eyes (Figs 1D, 2C, D). In contrast, the other two species lack the dentigerous patellar process, and the anterior median eyes are present (Figs 3G, 4A, 9D). It may be distinguished from *S. medogense* sp. n. by the wide, laminar basal patellar apophysis, and the dentigerous patellar process is as large as the dorsal patellar apophysis (Figure 2B–D, F). In contrast, *S. medogense* sp. n. has a narrow, tubular basal patellar apophysis, and its dentigerous patellar process is smaller than dorsal patellar apophysis (Figure 6A, B, F–I).

Description. See Figs 1A–E, 2A–F and Wunderlich and Song (1995), see also Song et al. (1999) and Lin et al. (2013).

Distribution. China (Yunnan), Laos, and Vietnam.

***Sinanapis longituba* Lin & Li, 2012**

Figs 3, 4

Type material. Holotype: ♂ (IZCAS), CHINA: Hainan Province, Qiongzong City, Mt. Limushan Nature Reserve, in leaf litter, 19°11.000'N, 109°44.000'E; 655 m,

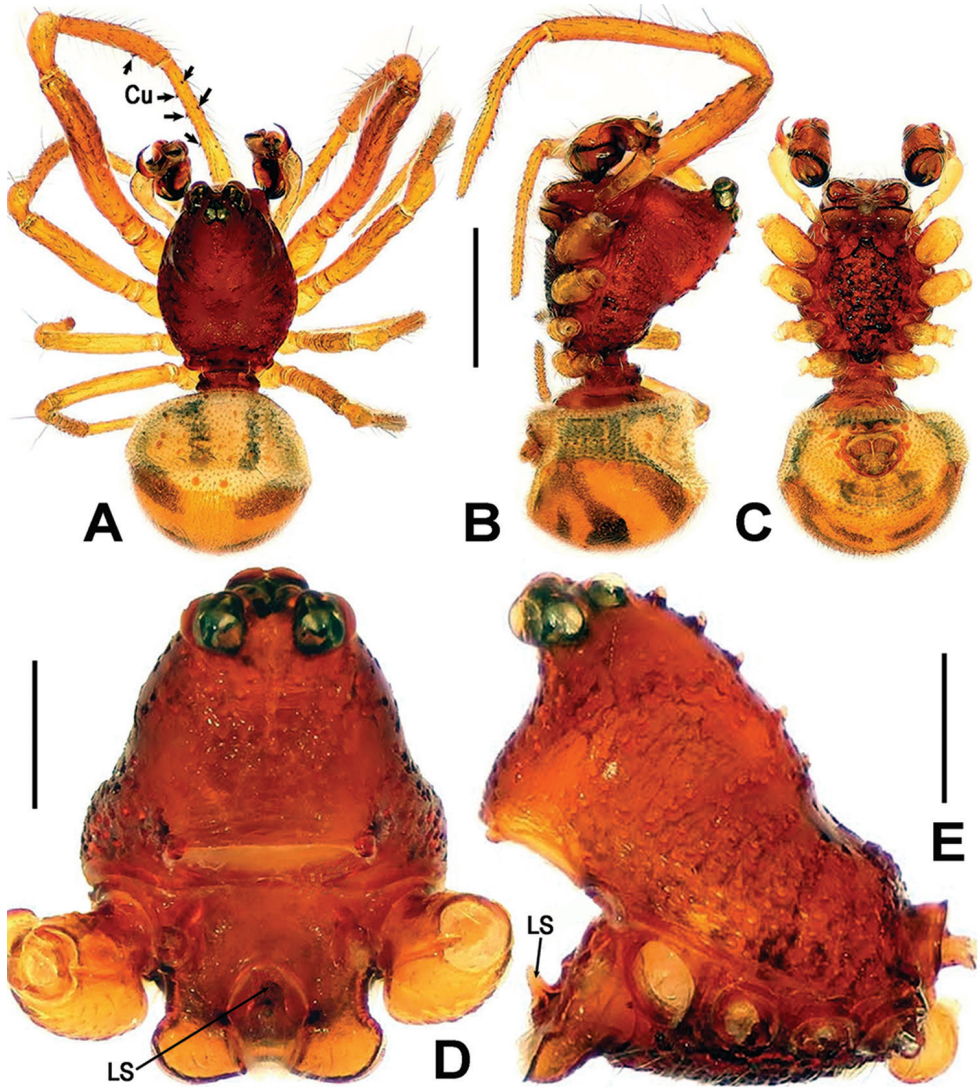


Figure 1. *Sinanapis crassitarsa* Wunderlich & Song, 1995, **A–C** Male habitus **D, E** Prosoma (chelicerae and appendages omitted) **A** dorsal **B, E** lateral **C** ventral **D** anterior. Abbreviations: **Cu** cusps on leg I; **LS** labial spur. Scale bars: 0.50 (**A–C**); 0.20 (**D, E**).

12.VIII.2007, S.Q. Li & C.X. Wang leg. *Paratypes*: 3♂, 11♀ (IZCAS), same data as holotype (examined).

Other material examined. 4♂, 2♀ (NHMSU), CHINA: Hainan Province, Qiongzong City, Yinggeling National Natural Reserve, Yinggezui Management Station, 19°03.037'N, 109°44.899'E; 622 m, 8–9.V.2011, Y.Y. Zhou leg.; 1♀ (NHMSU), CHINA: Hainan Province, Baisha County, Yuanmen Town, Hongxin Village, Yinggeling, 19°03.643'N, 109°31.329'E; 598±11 m, 27.III.2013, Z.G. Chen leg.

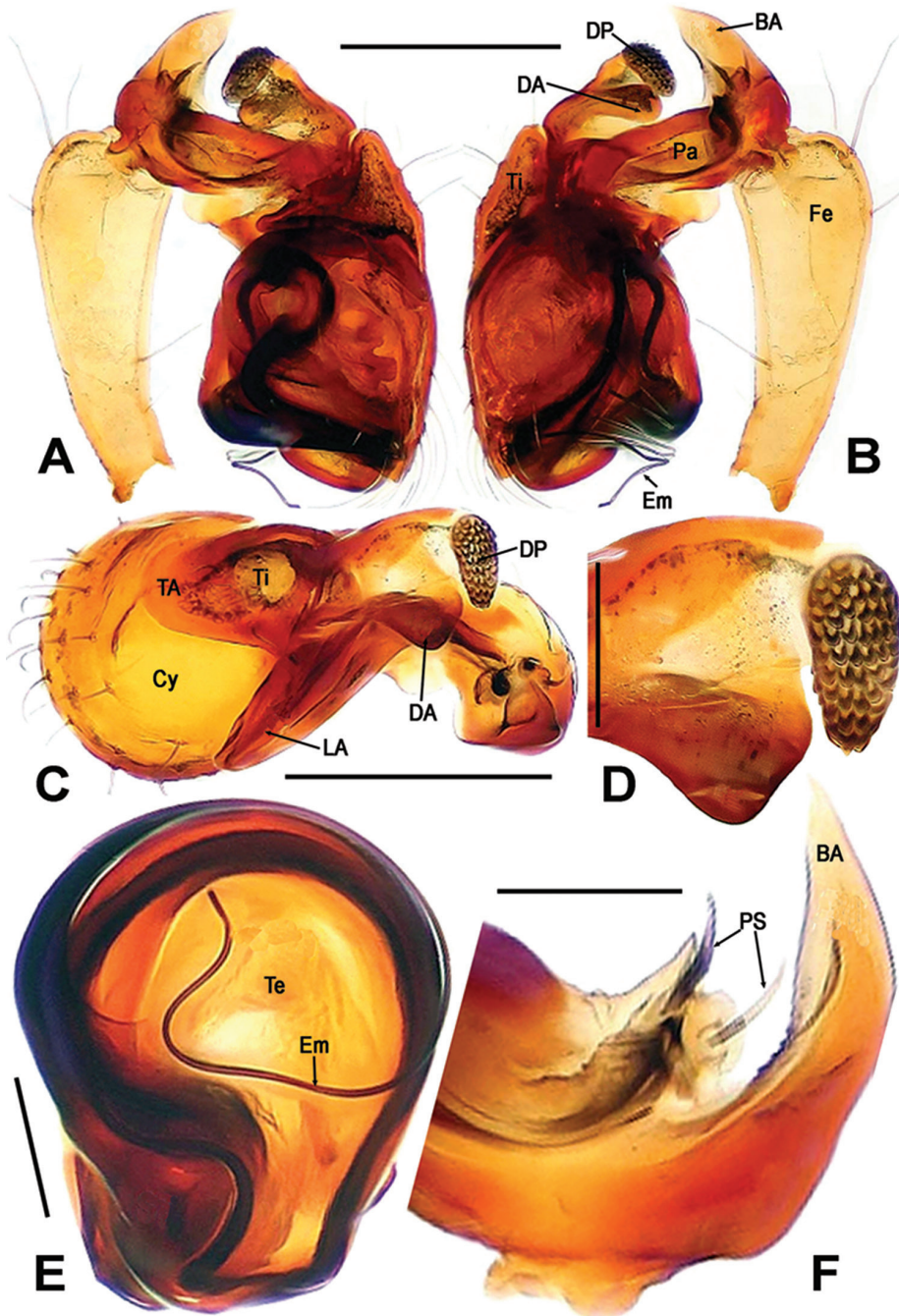


Figure 2. *Sinanapis crassitarsa* Wunderlich & Song, 1995, **A–C** Male left palp **D** Dorsal patellar apophyses on palp **E** Bulb **F** Basal patellar apophysis **A** prolateral **B, F** reterolateral **C, D** dorsal **E** ventral. Abbreviations: **BA** basal patellar apophysis; **Cy** cymbium; **DA** dorsal patellar apophysis; **DP** dentigerous patellar process; **Em** embolus; **Fe** femur; **LA** lateral patellar apophysis; **Pa** patella; **PS** patellar spine; **TA** tibial apophysis; **Te** tegulum; **Ti** tibia. Scale bars: 0.20 (**A–C**); 0.10 (**D, E**); 0.05 (**F**).

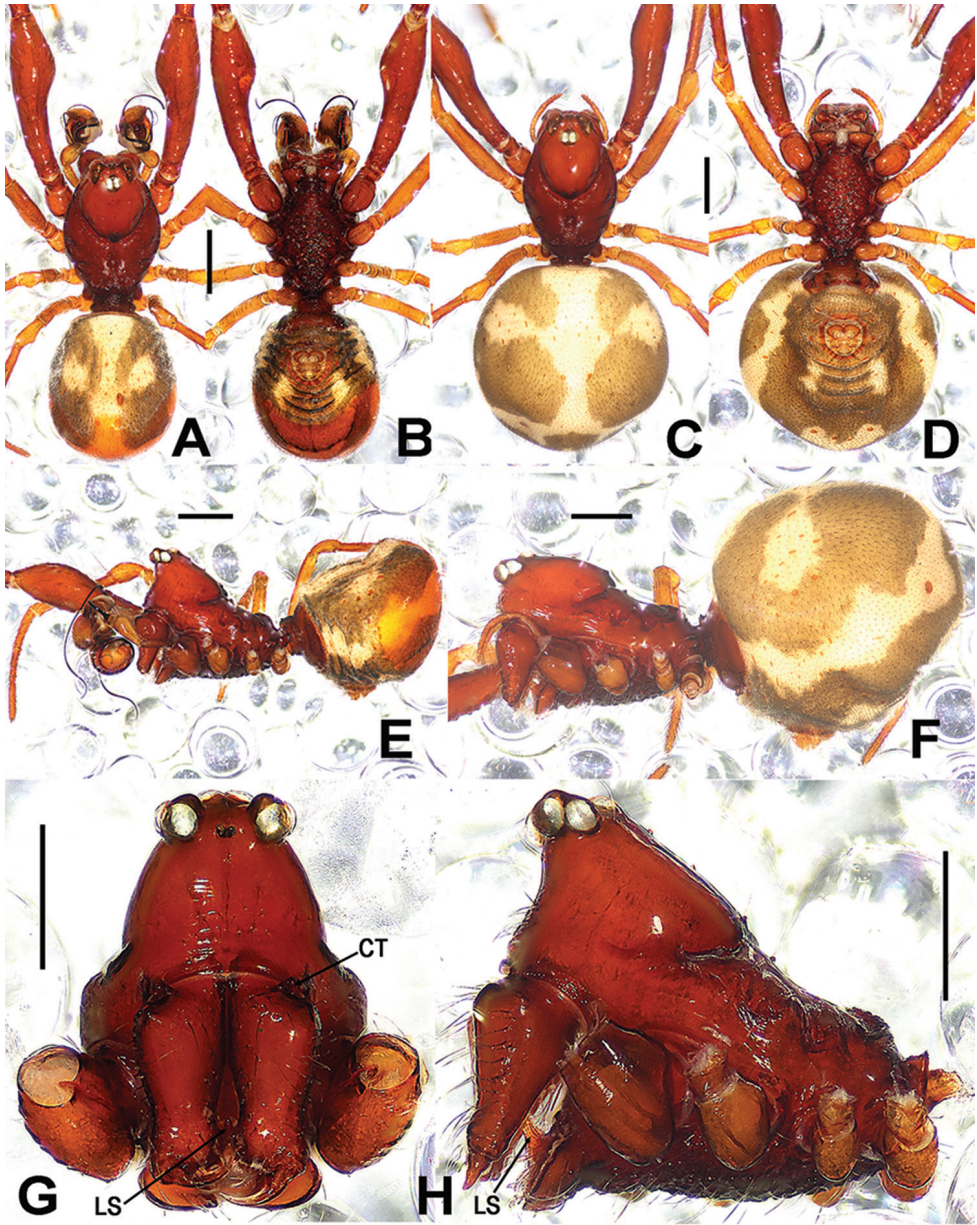


Figure 3. *Sinanapis longituba* Lin & Li, 2012, **A, B, E** Male habitus **C, D, F** Female habitus **G, H** Prosoma (appendages omitted) **A, C** dorsal **B, D** ventral **E, F, H** lateral **G** anterior. Abbreviations: CT cheliceral tubercle; LS labial spur. Scale bars: 0.50 (**A-F**); 0.20 (**G, H**).

Diagnosis. The male of *S. longituba* can be distinguished from *S. crassitarsa* and *S. medogensis* sp. n. by the presence of anterior median eyes (Figure 3G), lacking in two latter species (Figs 1D, 5G), and by the absence of a rasper-like dentigerous process (Figure 3A, B), whereas the dentigerous process is present in the other two species

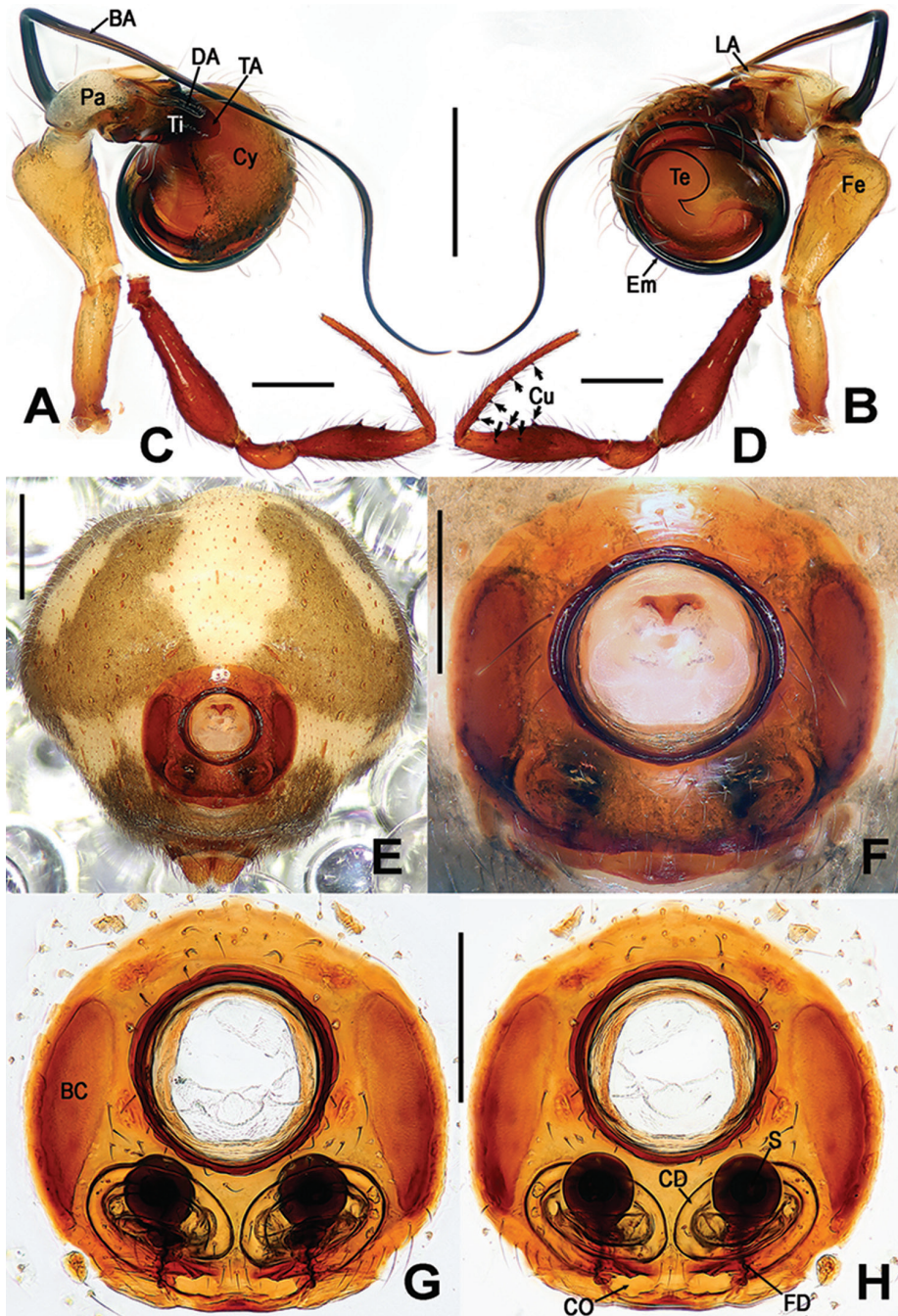


Figure 4. *Simanapis longituba* Lin & Li, 2012, **A, B** Male left palp **C, D** Male leg I **E** Female abdomen **F** Epigyne **G, H** Vulva **A, D** prolateral **B, C** reterolateral **E–G** ventral **H** dorsal. Abbreviations: **BA** basal patellar apophysis; **BC** booklung cover; **CD** copulatory ducts; **CO** copulatory opening; **Cy** cymbium; **Cu** cusps on leg I; **DA** dorsal patellar apophysis; **Em** embolus; **FD** fertilization ducts; **Fe** femur; **LA** lateral patellar apophysis; **Pa** patella; **S** spermathecae; **TA** tibial apophysis; **Te** tegulum; **Ti** tibia. Scale bars: 0.20 (**A, B, E–H**); 0.50 (**C, D**).

(Figs 2C, 6H). It differs from *S. wuyi* by the robust leg I in both sexes (Figs 3A–D, 4C, D), as against the normal leg I seen in *S. wuyi* (Figure 8A, B, D, E). It further differs from *S. wuyi* by having a very long basal patellar apophysis, 3 times longer than palpal femur (Figure 4A, B), while the basal patellar apophysis is shorter than the palpal femur in *S. wuyi* (Figure 9A, B). The female of *S. longituba* can be distinguished from that of the congeners by the larger copulatory openings and the longer copulatory ducts around the spermathecae (Figure 4G, H). On the other hand, the copulatory openings are smaller in *S. medogense* sp. n. (Figure 7G, I) and *S. wuyi* (Figure 9E, F) and their shorter copulatory ducts do not around the spermathecae.

Description. See Figs 3A–H, 4A–H and Lin and Li (2012).

Distribution. China (Hainan).

***Sinanapis medogense* sp. n.**

<http://zoobank.org/DD8E8CB0-CB1B-4100-AD16-FAD82BCDCC83>

Figs 5, 6, 7

Type material. *Holotype*: ♂ (NHMSU), CHINA: Tibet Autonomous Region, Nyingchi Prefecture, Medog County, Renqinbeng Mountain, 29°19.050'N, 95°19.998'E; 1314 m, 26.VIII.2015, J.L. Wu leg. *Paratypes*: 1♂, 2♀ (NHMSU), same data as holotype.

Etymology. The specific name derives from the type locality; adjective.

Diagnosis. The male of this new species can be distinguished from that of *S. longituba* and *S. wuyi* by the lack of anterior median eyes and having a rasper-like dentigerous process (Figs 5G, 6G, H). In the case of the two latter species, the anterior median eyes are present, and the rasper-like dentigerous patellar process is absent (Figs 3G, 4A, 9D; Yuan and Peng, 2014: figs 7, 9). It also differs from *S. crassitarsa* by having a tubular basal apophysis, and a smaller dentigerous process (Figure 6A, B, G–I). In *S. crassitarsus*, the basal apophysis is laminar, and the dentigerous process is larger (Figure 2A–D, F). The female of the new species differs from *S. longituba* by having shorter copulatory ducts, each coiling with less than two loops next to the spermatheca (Figure 7I). In *S. longituba*, each copulatory coil around the spermatheca in more than two loops (Figure 4H). *S. medogense* further differs from *S. wuyi* by the absence of anterior median eyes, and by having a white pattern on the abdomen (Figure 5C, F), whereas the anterior median eyes are present and the abdominal white pattern is absent in *S. wuyi* (Figure 8D, F; Yuan and Peng, 2014: figs 7, 9).

Description. Male (holotype): Somatic characters and coloration as in Figs 5A, B, E, G–I, 7A–C, E, F. *Measurements*: Total length 1.86. Carapace 0.96 long, 0.72 wide, 0.72 high. Clypeus 0.40 high. Sternum 0.52 long, 0.42 wide. Abdomen 0.90 long, 0.94 wide. Length of legs: I 3.76 (1.18, 0.40, 1.04, 0.42, 0.72); II 2.68 (0.82, 0.32, 0.62, 0.32, 0.60); III 2.02 (0.60, 0.22, 0.40, 0.28, 0.52); IV 2.52 (0.78, 0.24, 0.60, 0.34, 0.56).

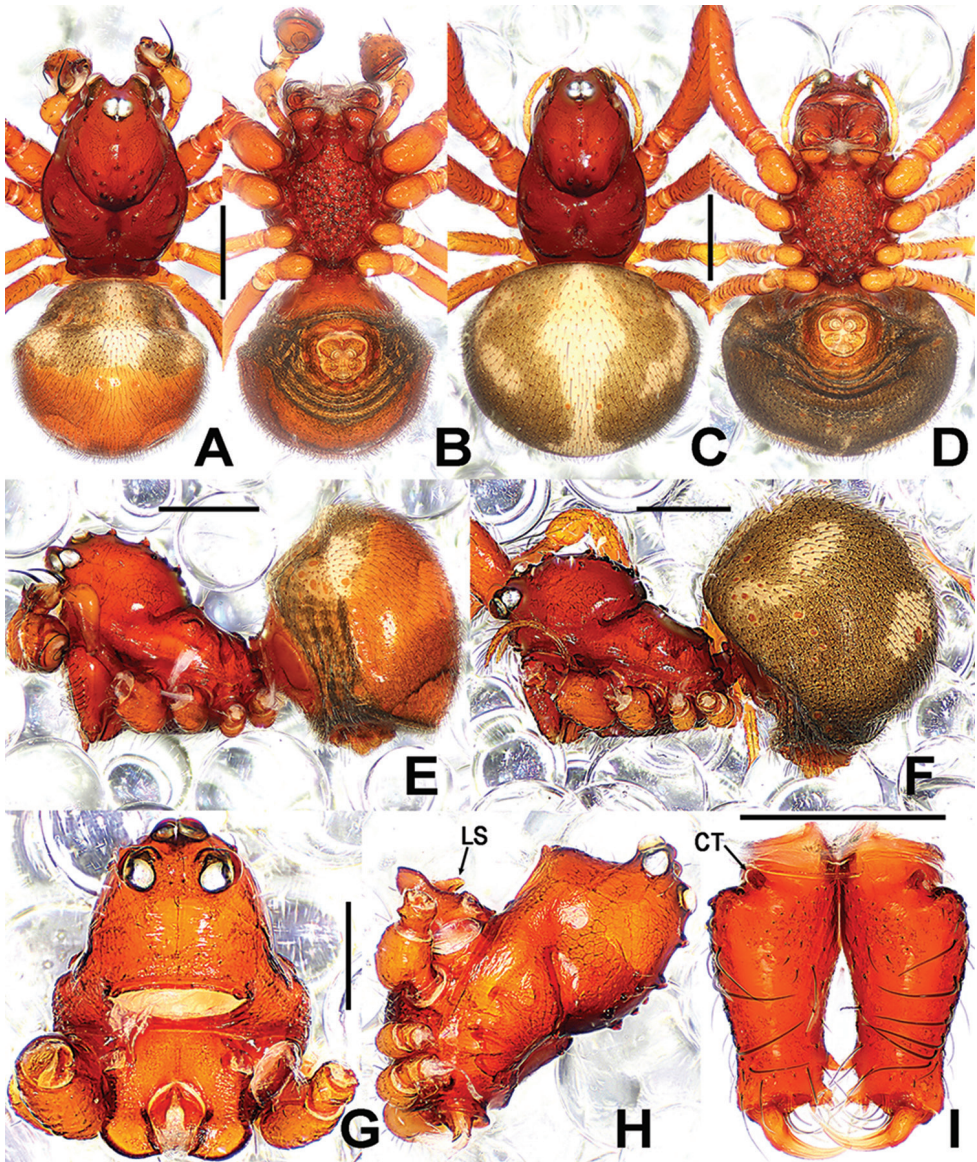


Figure 5. *Sinanapis medogense* sp. n., male holotype (A–B, E, G–I) and female paratype (C–D, F) from Xizang. A–F Habitus G, H Prosoma I Chelicerae A, C dorsal B, D ventral E–F, H lateral G, I frontal. Abbreviations: CT cheliceral tubercle; LS labial spur. Scale bars: 0.50 (A–F); 0.25 (G–I).

Palp (Figure 6A–I): Trochanter very long, subequal to 2/3 of femur length. Femur distally swollen approx. 2 times wider than proximally. Patella, complex, each modified with four apophyses (Figure 6H): basal apophysis long horned, almost as long as patella; two dorsal apophyses, one crooked and fingerlike, and another rasper-

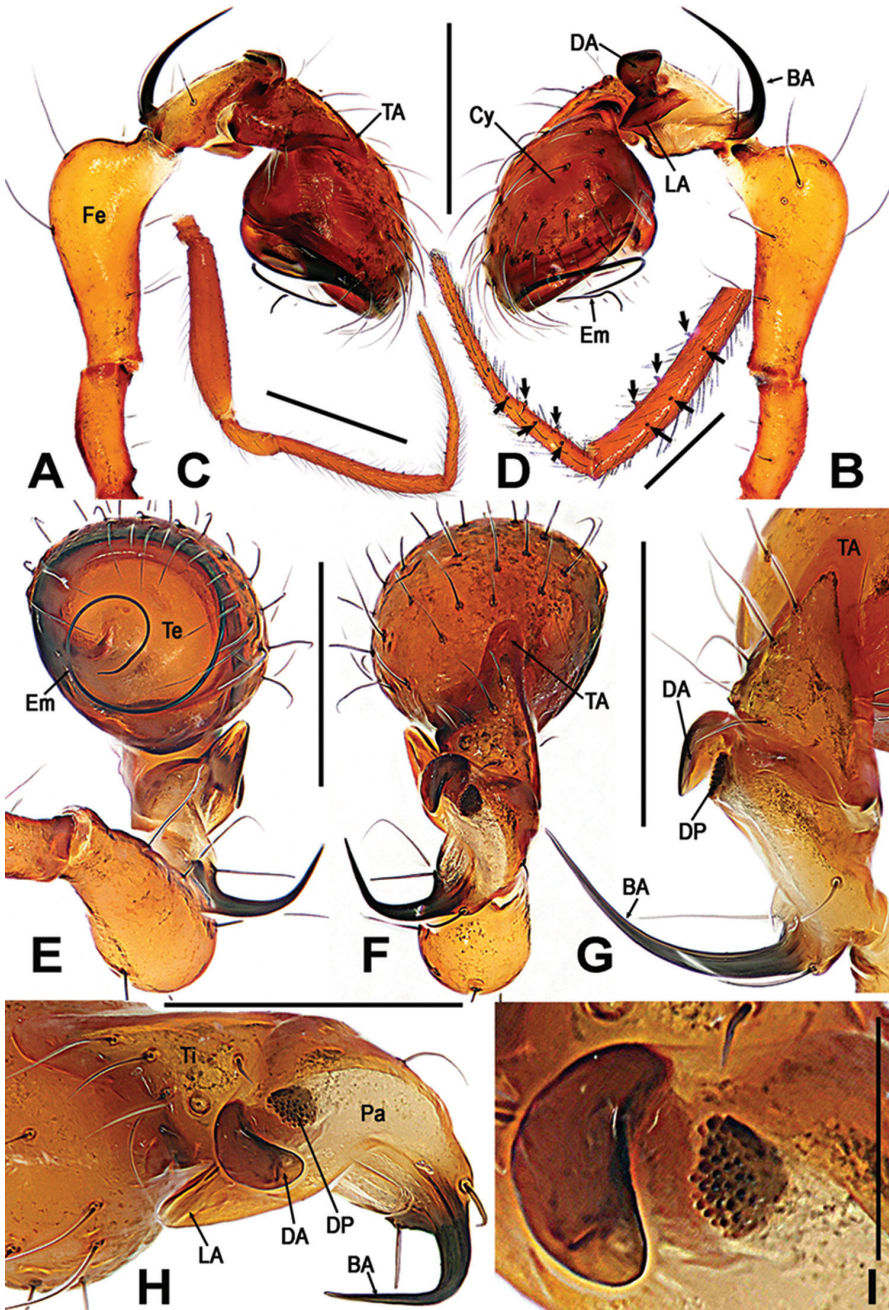


Figure 6. *Sinanapis medogensis* sp. n., male holotype from Xizang. **A, B, E, F** Left palp **C, D** Left leg I **G, H** Palpal patella and tibia **I** Patellar apophysis **A, D, G** prolateral **B, C** retrolateral **E** ventral **F, H, I** dorsal. Abbreviations: **BA** basal patellar apophysis; **Cu** cusps on leg I; **Cy** cymbium; **DA** dorsal patellar apophysis; **DP** dentigerous patellar process; **Em** embolus; **Fe** femur; **LA** lateral patellar apophysis; **Pa** patella; **TA** tibial apophysis; **Ti** tibia; **Te** tegulum. Scale bars: 0.25 (**A, B, E-H**); 1.00 (**C**); 0.50 (**D**); 0.05 (**I**).

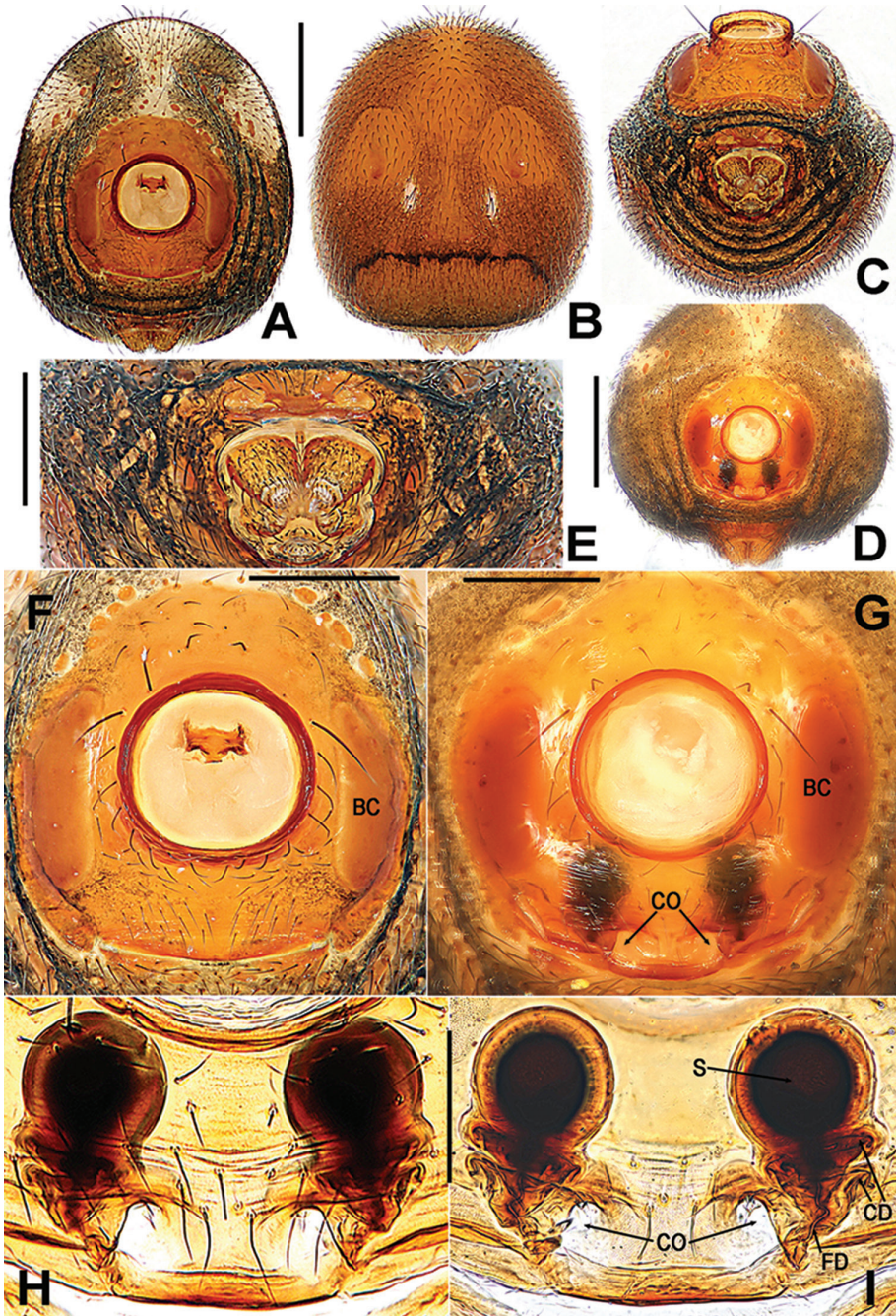


Figure 7. *Sinanapis medogense* sp. n., male holotype (**A–C, E, F**) and female paratype (**D, G–I**) from Xizang. **A–D** Abdomen **E** Spinnerets **F** Epigastric scutum **G** Epigyne **H, I** Vulva (lactic acid-treated) **A, D, F–H** ventral **B, I** dorsal **C, E** antapical. Abbreviations: **BC** booklung covers; **CD** copulatory duct; **CO** copulatory opening; **FD** fertilization duct; **S** spermatheca. Scale bars: 0.50 (**A–D**); 0.20 (**E–G**); 0.10 (**H, I**).

like dentigerous process (Figure 6I); a lateral apophysis straight, finger-shaped, protruded. Tibia with a dorsal apophysis and a dorsal trichobothrium (Figure 6F–H). Cymbium bowl-shaped, as wide as long, covered with sparse long setae. Bulb simple, cone-shaped, tegulum smooth and flat, without any apophysis. Embolus long, strongly sclerotized, started at the middle margin of bulb, and ends in the above of subcentral bulb, coiled almost into two loops, distally tapering (Figure 6A, E).

Female (paratype). Somatic characters and coloration as in Figs 5C, D, F, 7D. *Measurements*: Total length 1.96. Carapace 1.02 long, 0.64 wide, 0.80 high. Abdomen 0.94 long, 0.43 wide. Clypeus 0.46 high. Sternum 0.61 long, 0.43 wide. Length of leg: I 3.42 (1.12, 0.36, 0.90, 0.40, 0.64); II 2.48 (0.76, 0.30, 0.58, 0.28, 0.56); III 1.8 (0.54, 0.20, 0.38, 0.22, 0.46); IV 2.3 (0.72, 0.24, 0.56, 0.28, 0.50).

Epigyne (Figure 7G–I): Epigyne sclerotized, almost rectangular, about 2 times wider than booklung cover, vulva visible through the translucent integument; copulatory openings large, sub-rounded, closed to the epigynal posteromargin. Spermatheca globular, each with a width equal to 2/3 of the breadth of booklung cover, separated by a gap measuring around its own diameter; copulatory ducts coiled the base of spermathecae, starting near the rebordered epigynal posteromargin, and ended at the posterolateral margins of spermathecae; fertilization ducts short, and thin, connected with the bases of the spermathecae.

Distribution. Known only from the type locality.

Sinanapis wuyi Jin & Zhang, 2013

Figs 8, 9

Type material. *Holotype* ♂ (MHB), CHINA: Fujian Province, Wuyi Mountains, Nankeng, 27°56.000'N, 118°06.000'E, 6.VIII.2010, F. Zhang leg. (examined).

Other material examined. 3♂ 3♀ (HNU), CHINA: Hunan Province, Dawei Mountains, 28°14.598'N, 114°03.858'E; 1526 m, 1.V.2012, J.L. Wan leg.

Diagnosis. The male of *S. wuyi* can be distinguished from these of *S. crassitarsa* and *S. medogense* sp. n. by the lack of a rasper-like dentigerous patellar process on the palp, and by having anterior median eyes (Figure 9D; Yuan and Peng 2014: figs 7, 9). In the other two species, the dentigerous patellar process is present, and the anterior median eyes are absent (Figs 1D, 2C, 5G, 6H). It differs from *S. longituba* by having a shorter basal apophysis not exceeding the palpal femoral length, and the shorter copulatory ducts not coiled around the spermathecae (Figure 9A–F). On the other hand, in *S. longituba*, the very long basal apophysis exceed the at least 3 times the length of the palpal femur, and the lengthy copulatory ducts coil around the spermathecae (Figure 4A, B, G, H).

Description. See Figs 8A–H, 9A–F and Jin and Zhang (2013), and Yuan and Peng (2014).

Distribution. China (Hainan, Jiangxi, and Fujian).

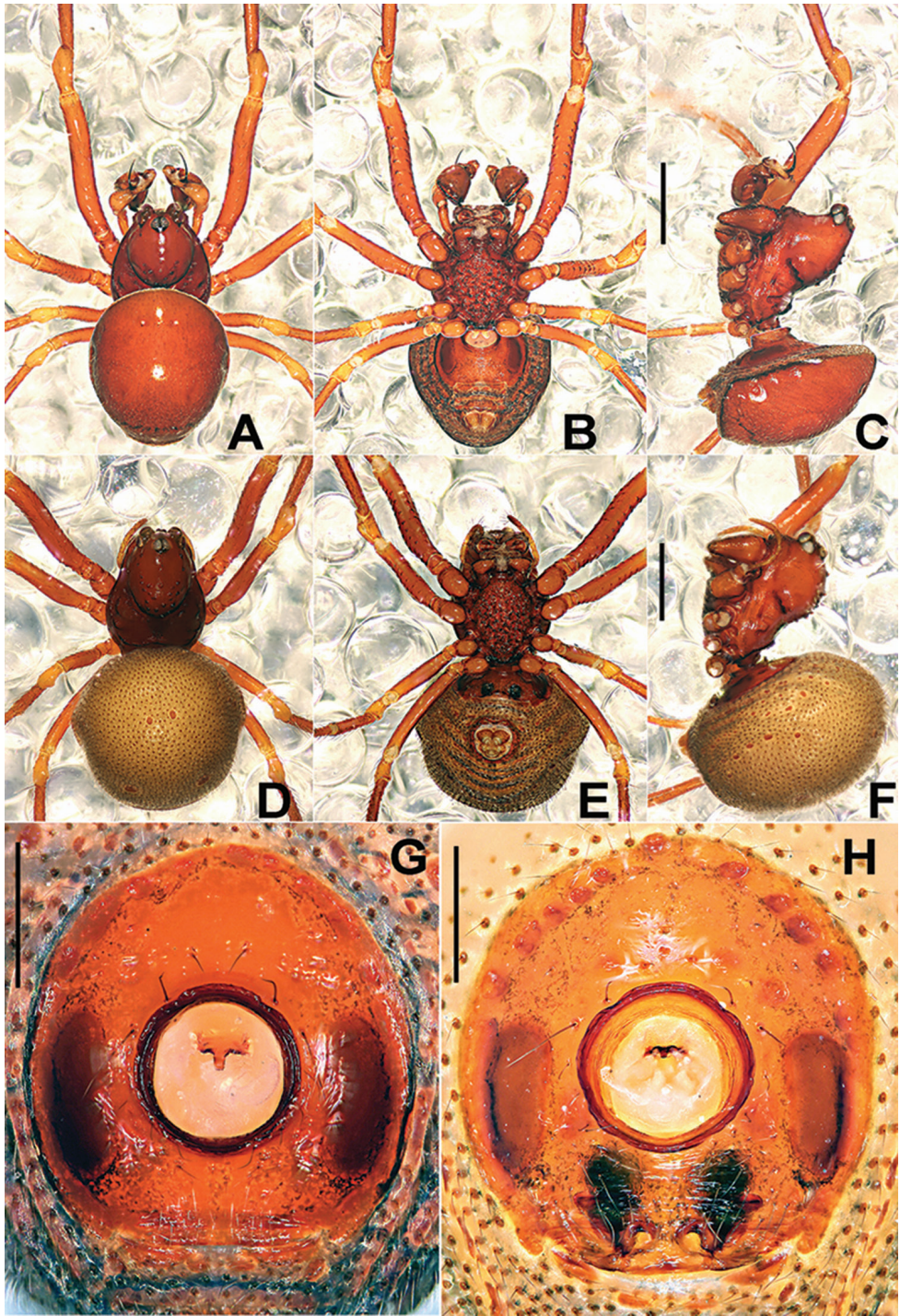


Figure 8. *Sinanapis wuyi* Jin & Zhang, 2013, male (A–C, G) and female (D–F, H) paratypes. A–F Habitus G Epigastric scutum H Epigyne A, D dorsal B, E, G, H ventral C, F lateral. Scale bars: 0.50 (A–F); 0.20 (G, H).

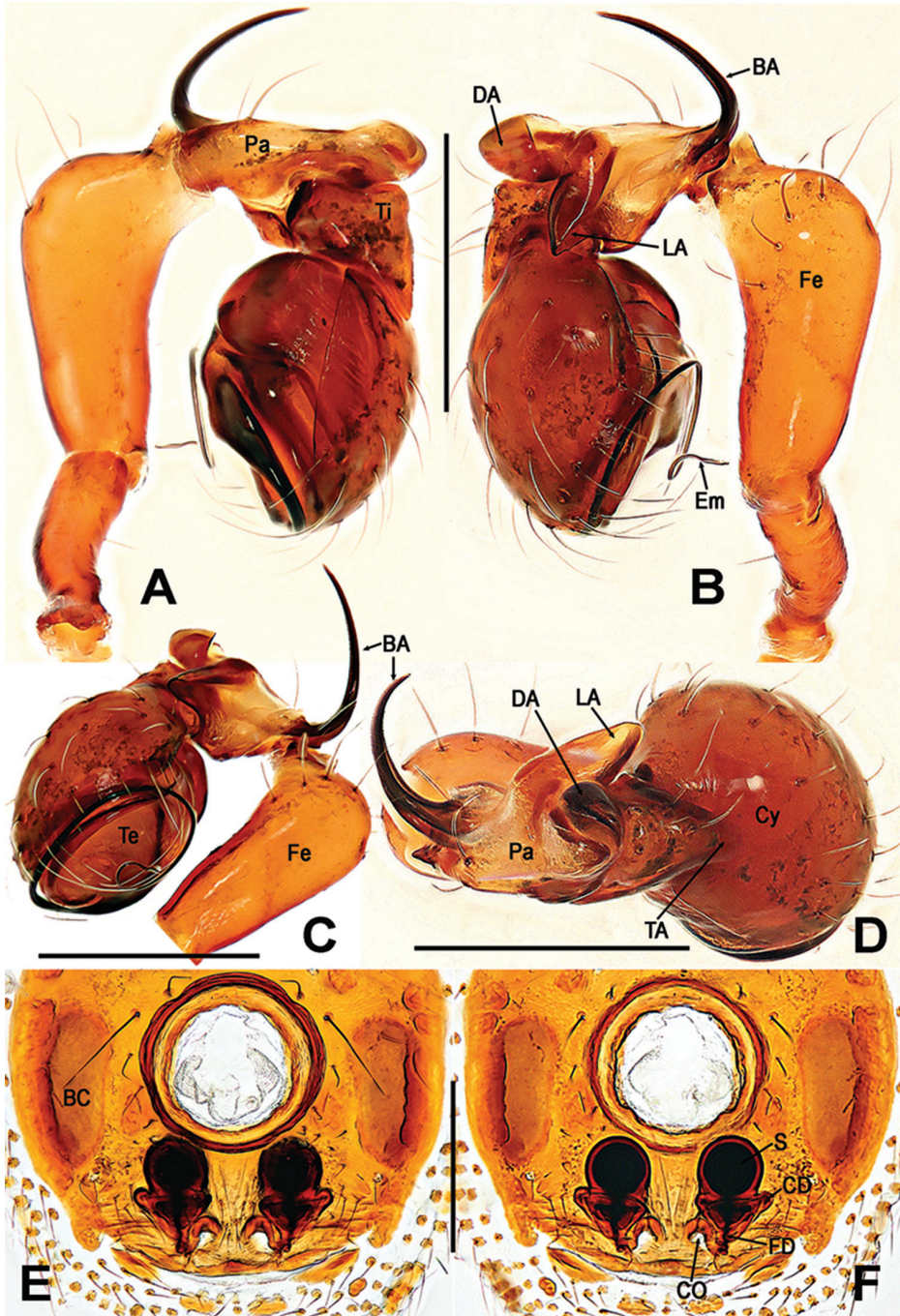


Figure 9. *Sinanapis wuyi* Jin & Zhang, 2013, male (A–D) and female (E, F) paratypes. A–D Left palp E, F Vulva A prolateral B retrolateral C retro-ventral D, F dorsal E ventral. Abbreviations: BA basal patellar apophysis; BC booklung cover; CD copulatory ducts; CO copulatory opening; Cy cymbium; DA dorsal patellar apophysis; Em embolus; FD fertilization ducts; Fe femur; LA lateral patellar apophysis; Pa patella; S spermathecae; TA tibial apophysis; Te tegulum; Ti tibia. Scale bars: 0.20 (A–D); 0.25 (E, F).

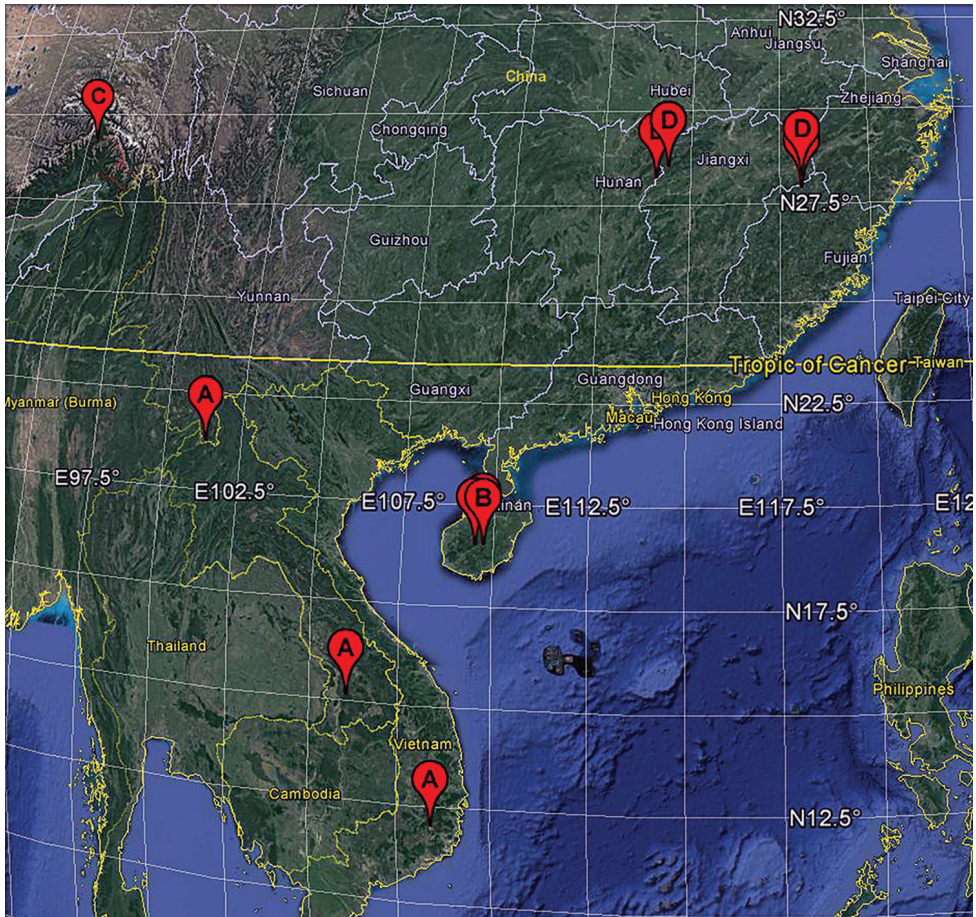


Figure 10. Distribution records of *Sinanapis* spp. in the world. **A** *S. crassitarsa* Wunderlich & Song, 1995 **B** *S. longituba* Lin & Li, 2012 **C** *S. medogensis* sp. n. **D** *S. wuyi* Jin & Zhang, 2013.

Acknowledgements

The manuscript benefitted greatly from comments by Jeremy A. Miller (Leiden, Netherlands) and Mikhail M. Omelko (Vladivostok, Russia). We are especially grateful to Yuri M. Marusik (Magadan, Russia), the subject editor of this manuscript for his editorial efforts. We would also like to thank Joseph K. H. Koh (National Praks Board, Singapore) helping us checked the English of the manuscript. This study was supported by the National Natural Science Foundation of China (NSFC-31772410, 31750002).

References

Jin C, Zhang F (2013) A new species of the genus *Sinanapis* Wunderlich & Song (Araneae, Anapidae) from China. *Zootaxa* 3681: 289–292. <https://doi.org/10.11646/zootaxa.3681.3.9>

- Khmelik VV, Kozub D, Glazunov A (2006) Helicon Focus 3.10.3. <http://helicon.com.ua/heliconfocus/> [accessed 25 May 2012]
- Lin Y, Li S (2012) Three new spider species of Anapidae (Araneae) from China. *Journal of Arachnology* 40: 159–166. <https://doi.org/10.1636/A08-99.1>
- Lin Y, Li S, Jäger P (2013) Anapidae (Arachnida: Araneae), a spider family newly recorded from Laos. *Zootaxa* 3608: 511–520. <https://doi.org/10.11646/zootaxa.3608.6.4>
- Ono H (2009) A new species of the genus *Sinanapis* (Araneae: Anapidae) from Lam Dong province, southern Vietnam. *Contributions to Natural History* 12: 1021–1028.
- World Spider Catalog (2018) World Spider Catalog. Natural History Museum Bern. <http://wsc.nmbe.ch>, version 19.0. [accessed on April 12, 2018]
- Wunderlich J, Song D (1995) Four new spider species of the families Anapidae, Linyphiidae and Nesticidae from a tropical rain forest area of SW-China. *Beiträge zur Araneologie* 4: 343–351.
- Yuan Z, Peng X (2014) Description on the female spider of *Sinanapis wuyi* Jin & Zhang (Araneae: Anapidae). *Zoological Systematics* 39(2): 236–247.

Bogidiella pingxiangensis, a new species of subterranean Amphipoda from southern China (Bogidiellidae)

Yami Zheng^{1,2}, Zhonghe Hou¹, Shuqiang Li¹

1 Key Laboratory of Zoological Systematics and Evolution, Institute of Zoology, Chinese Academy of Sciences, Beijing 100101, China **2** University of Chinese Academy of Sciences, Beijing 100049, China

Corresponding author: Zhonghe Hou (houze@ioz.ac.cn)

Academic editor: C.O. Coleman | Received 27 July 2018 | Accepted 12 September 2018 | Published 15 October 2018

<http://zoobank.org/252DCB31-B621-4ECD-82E2-E5EE334FD5CB>

Citation: Zheng Y, Hou Z, Li S (2018) *Bogidiella pingxiangensis*, a new species of subterranean Amphipoda from southern China (Bogidiellidae). ZooKeys 790: 63–75. <https://doi.org/10.3897/zookeys.790.28671>

Abstract

A new species of subterranean amphipod, *Bogidiella pingxiangensis* Hou & Li, **sp. n.**, is described from Xiongshizilong Cave in Pingxiang City, China. The new species is characterized by having the bases of pereopods III and V expanded; the inner ramus of pleopods I–III with one segment; the telson longer than wide and with the apical margin with a shallow U-shaped excavation. DNA barcode of the new species is documented as support of molecular differences between related species.

Keywords

Amphipod, barcode, cave, China, new species, taxonomy

Introduction

The genus *Bogidiella* Hertzog, 1933 contains more than 60 species that are widely distributed in subterranean freshwaters or marine interstitial habitats (Koenemann and Holsinger 1999, Coleman 2009). The genus exhibits typical subterranean adaptive

morphology in the loss of eyes and pigmentation, elongated pereopods, and reduced pleopods (Holsinger et al. 2006).

In China, only one species *Bogidiella sinica* Karaman & Sket, 1999 is known. It occurs in the lower storey of the cave system Qixinyan at Guilin, Guangxi Zhuang Autonomous Region. We have tried to get fresh specimens for *B. sinica*, but failed because of tourism in the locality. During a field survey of subterranean amphipods in southern China, a second new species of *Bogidiella* was found in a cave in Jiangxi Province, which is ca. 500 km away from the type locality of *B. sinica*. In this paper, *Bogidiella pingxiangensis* sp. n. is described and illustrated. The barcode sequence of the new species is presented and genetic distances between the new species and known species are calculated to confirm the species delimitation.

Materials and methods

Morphological observation

The specimens were collected by sweeping rotten wood with a fine-meshed hand net. Samples were preserved in 95% ethanol in the field, then deposited at -20 °C refrigerator for long-term preservation. The body length of the amphipod was recorded by holding the specimen straight and measuring the distance along the dorsal side of the body from the base of the first antenna to the base of the telson. All dissected appendages were mounted on slides according to the methods described by Holsinger (1967). Appendages were drawn using a Leica DM2500 compound microscope equipped with a drawing tube. Terminology and taxonomic descriptions follow the literature (Leijs et al. 2011), specially the terms “spines” and “setae” are used to distinguish between thin or fine and more robust setal structures. All types and other material are lodged in the Institute of Zoology, Chinese Academy of Sciences (IZCAS), Beijing.

Molecular methods

A partial fragment of the mitochondrial cytochrome oxidase subunit I (COI) was proposed as a crustacean barcode (Costa et al. 2007, Hou et al. 2009). The primers used are LCO1490 (5'-GGTCAACAAATCATAAAGATATTGG-3') and HCO2198 (5'-TAAACTTCAGGGTGACCAAAAAATCA-3') (Folmer et al. 1994). Genomic DNA extraction, amplification and sequencing procedures were performed as in Hou et al. (2007). Pairwise uncorrected sequence distances were calculated using PAUP* (Swofford 2001). The new sequence was deposited in GenBank (accession number MH880343).

Taxonomy

Infraorder Bogidiellida Hertzog, 1936

Family Bogidiellidae Hertzog, 1936

Genus *Bogidiella* Hertzog, 1933

Bogidiella pingxiangensis Hou & Li, sp. n.

<http://zoobank.org/7DE05148-BC5C-4CBD-8D58-B9936CDD0226>

Figs 1–7

Type species. *Bogidiella albertimagni* Hertzog, 1933.

Material examined. Holotype: male (IZCAS-I-A1316-1), 5.0 mm, Xiongshizilong Cave (113.76°E, 27.91°N), Changping Village, Futian Town, Shangli County, Pingxiang City, Jiangxi Province, May 9, 2013, collected by Yufa Luo and Jincheng Liu. Paratype: female (IZCAS-I-A1316-2), 4.0 mm, same data as holotype.

Etymology. The specific name refers to type locality; adjective.

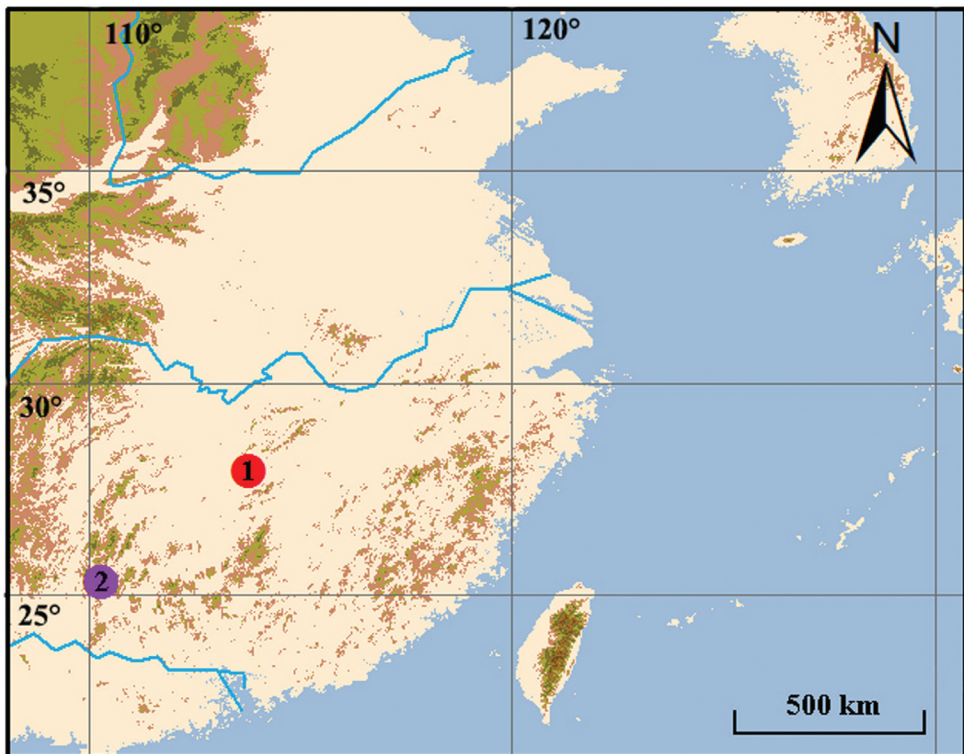


Figure 1. Type localities of *Bogidiella* species from China. 1 *Bogidiella pingxiangensis* sp. n. 2 *Bogidiella sinica* Karaman & Sket, 1990.



Figure 2. *Bogidiella pingxiangensis* sp. n., male holotype from Jiangxi, China.

Diagnosis. Antenna I longer than antenna II; palp of maxilla I with two apical setae; basis of gnathopod I expanded; bases of pereopods III–VI expanded, without spines and setae; coxal gills present on pereopods IV–VI; pleopod inner ramus with one segment, reduced; uropod II outer ramus shorter than inner ramus; telson 1.42 times longer than wide, apical margin with shallow U-shaped excavation, each lobe bearing one apical and two subapical stout spines.

Description of male holotype (IZCAS-I-A1316-1), 5.0 mm.

Head. (Figure 3A): eyes absent.

Antenna I (Figure 3B): longer than antenna II, peduncle articles I–III in length ratio 1.0: 0.7: 0.4, with distal spines; flagellum with 17 articles; accessory flagellum with two articles; both primary and accessory flagellum with short distal setae.

Antenna II (Figure 3C): peduncle articles III–V in length ratio 1.0: 2.6: 2.4, peduncle article III with two distal spines, articles IV–V nearly same length, article IV with three lateral spines, article V with stiff setae along anterior and posterior margins; flagellum with six articles, each article with distal setae; calceoli absent.

Upper lip (Figure 3D): ventral margin convex.

Mandible (Figure 3E, F): asymmetrical, left mandible incisor with five teeth; lacinia mobilis small; palp composed of three articles, second article with one distal seta,

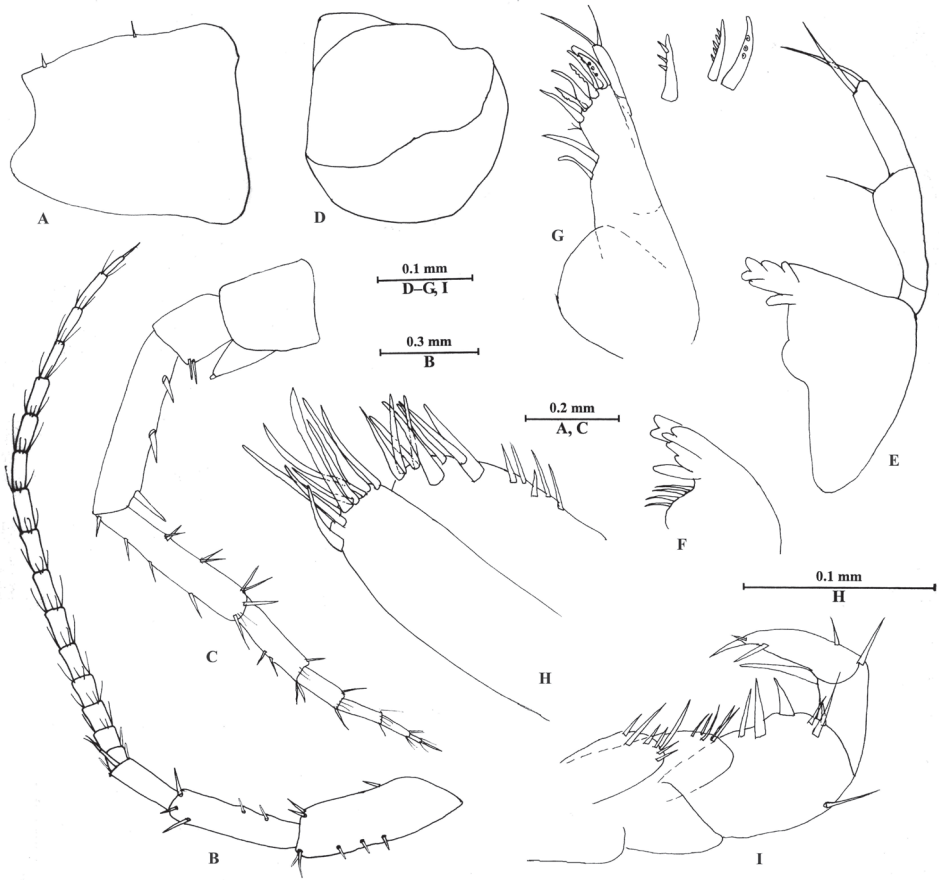


Figure 3. *Bogidiella pingxiangensis* sp. n. male holotype, from Jiangxi, China. **A** head **B** antenna I **C** antenna II **D** upper lip **E** left mandible **F** incisor of right mandible **G** maxilla I **H** maxilla II **I** maxilliped.

third article with two distal setae. Incisor of right mandible with four teeth, lacinia mobilis bifurcate, with small teeth.

Lower lip: destroyed.

Maxilla I (Figure 3G): inner plate with two setae; outer plate with seven apical spines, including simple (naked) spines, and spines bearing one, two or multiple denticles; palp with two articles, second article with two apical setae.

Maxilla II (Figure 3H): inner plate with five lateral setae, six apical setae, and two subapical spines; outer plate with nine setae.

Maxilliped (Figure 3I): inner plate with seven apical setae; outer plate with five setae; palp with four articles, second article with three spines on inner margin, one seta on outer margin, two setae on apical margin, third article with two spines apically, terminal article hooked, nail small.

Pereon. Gnathopod I (Figure 4A, B): coxal plate destroyed; basis expanded, with four spines on posterior margin, two spines on anterior margin; merus pubescent, with

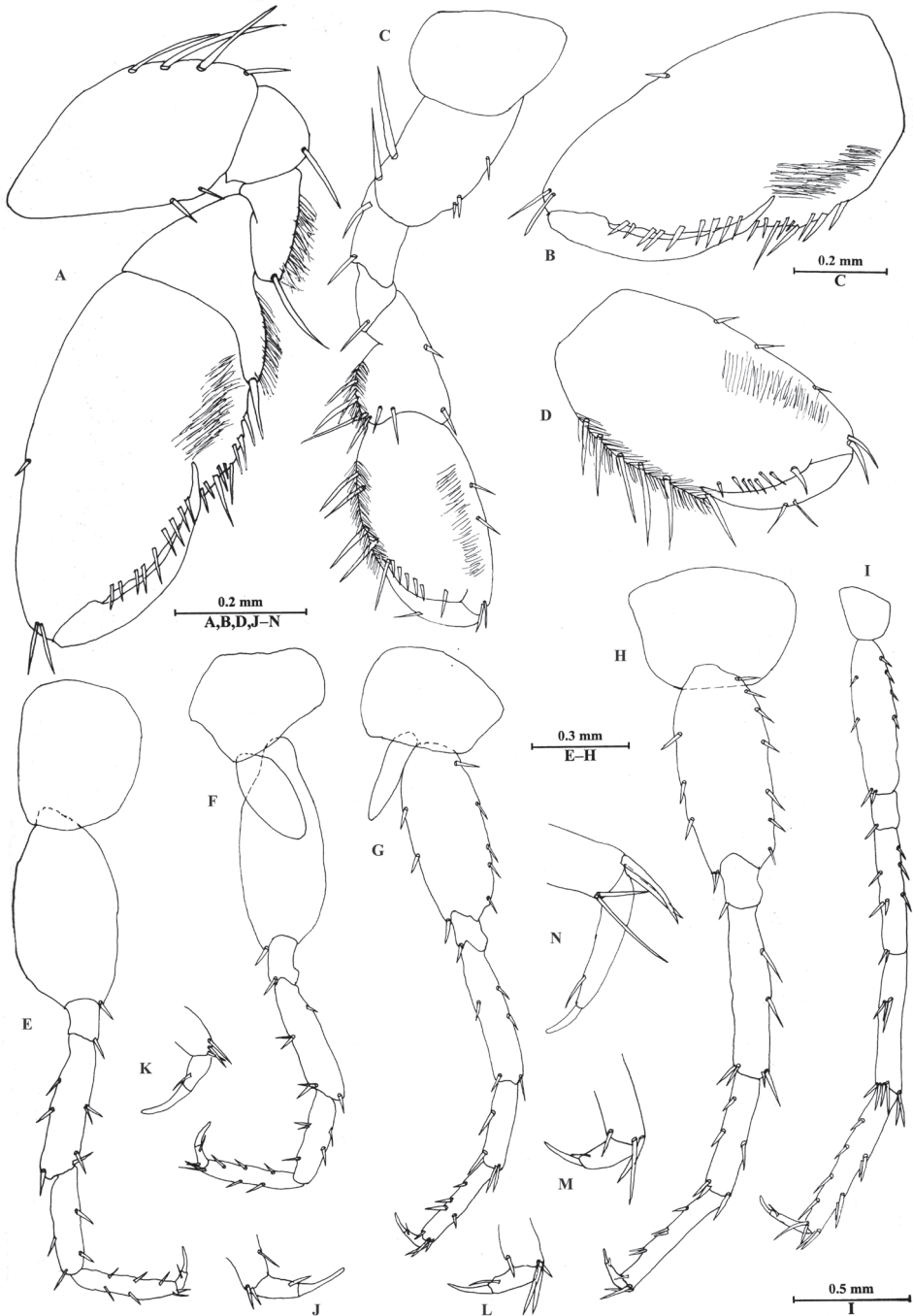


Figure 4. *Bogidiella pingxiangensis* sp. n., male holotype, from Jiangxi, China. **A** gnathopod I **B** propodus of gnathopod I **C** gnathopod II **D** propodus of gnathopod II **E** pereopod III **F** pereopod IV **G** pereopod V **H** pereopod VI **I** pereopod VII **J** dactylus of pereopod III **K** dactylus of pereopod IV **L** dactylus of pereopod V **M** dactylus of pereopod VI **N** dactylus of pereopod VII.

one long spine on posterior margin; carpus with pubescent, tapered distolateral lobe; propodus twice as long as wide, approx. 14% larger than propodus of gnathopod II, with pubescent face, palmar margin crenellated only in its proximal (angular) part, palmar margin with nine short spines, posterior margin with a row of spines extending on proximolateral margin; dactylus reaching approx. 60% length of propodus.

Gnathopod II (Figure 4C, D): slender than gnathopod I, coxal plate longer than wide, with no spines and setae; basis longer than that of gnathopod I, with three short spines on anterior margin and two long spines on posterior margin; merus short, without pubescence; carpus without tapered projection, posterior margin pubescent, with some spines on anterior margin and posterior margins; propodus 1.7 times as long as wide, subrectangular, with a row of very fine pubescent hairs on medial surface, palmar margin with a row of short spines, posterior margin with five long spines; dactylus reaching palmar corner, with two spines on posterior margin.

Pereopods III–IV (Figure 4E–F, J–K): similar to each other, coxal plate irregular, with no spines and setae; basis extremely expanded, without spines and setae, basis of pereopod III wider than those of pereopods IV–VII; merus to propodus with some spines along anterior and posterior margins; dactylus with one seta at hinge of unguis.

Pereopods V–VII (Figure 4G–I, L–N): similar in shape. Pereopod V (Figure 4G, L) coxal plate longer than wide, with no spines and seta; basis slightly dilated but linear, with two spines on anterior margin and five spines on posterior margin; merus to propodus slender, with spines on anterior and posterior margins; dactylus with one seta at hinge of unguis. Pereopod VI (Figure 4H, M) longer than pereopod V, basis wider than that of pereopod V, with four spines on anterior margin and seven spines on posterior margin; merus bare on anterior margin and with two spines on posterior margin; carpus shorter than merus and propodus, with two spines on anterior margin and one spine on posterior margin; propodus with three pairs of spines on anterior margin; dactylus with one seta at hinge of unguis. Pereopod VII (Figure 4I, N) nearly twice as long as pereopods V–VI, basis linear, with two short spines on anterior margin and four spines on posterior margin; carpus longer than merus, with a pair of spines on anterior margin; propodus with four long spines on anterior margin and two pairs of spines on posterior margin; dactylus elongate, with a seta at hinge of unguis.

Coxal gills present on pereopods IV–VI.

Pleon. Epimeral plates (Figure 5D–F): plate I ventrally rounded, with two setae on posterior margin; plate II posterior corner acute; plate III posterior corner blunt.

Pleopods I–III (Figure 5A–C): similar to each other, inner ramus short, with a long and plumose distal seta; outer ramus 3-articulate, each article with two long, plumose setae which are longer towards the tip of the ramus.

Urosome. Uropod I (Figure 5G) peduncle longer than rami, with one basofacial spine, one and four spines on inner and outer margins, respectively; inner ramus slightly longer than outer ramus, bearing one spine on inner margin; outer ramus with one spine on outer margin; both rami with three terminal spines. Uropod II (Figure 5H) peduncle longer than outer ramus but shorter than inner ramus, with one and two spines on inner and outer margins, respectively; inner ramus stronger than outer ramus,

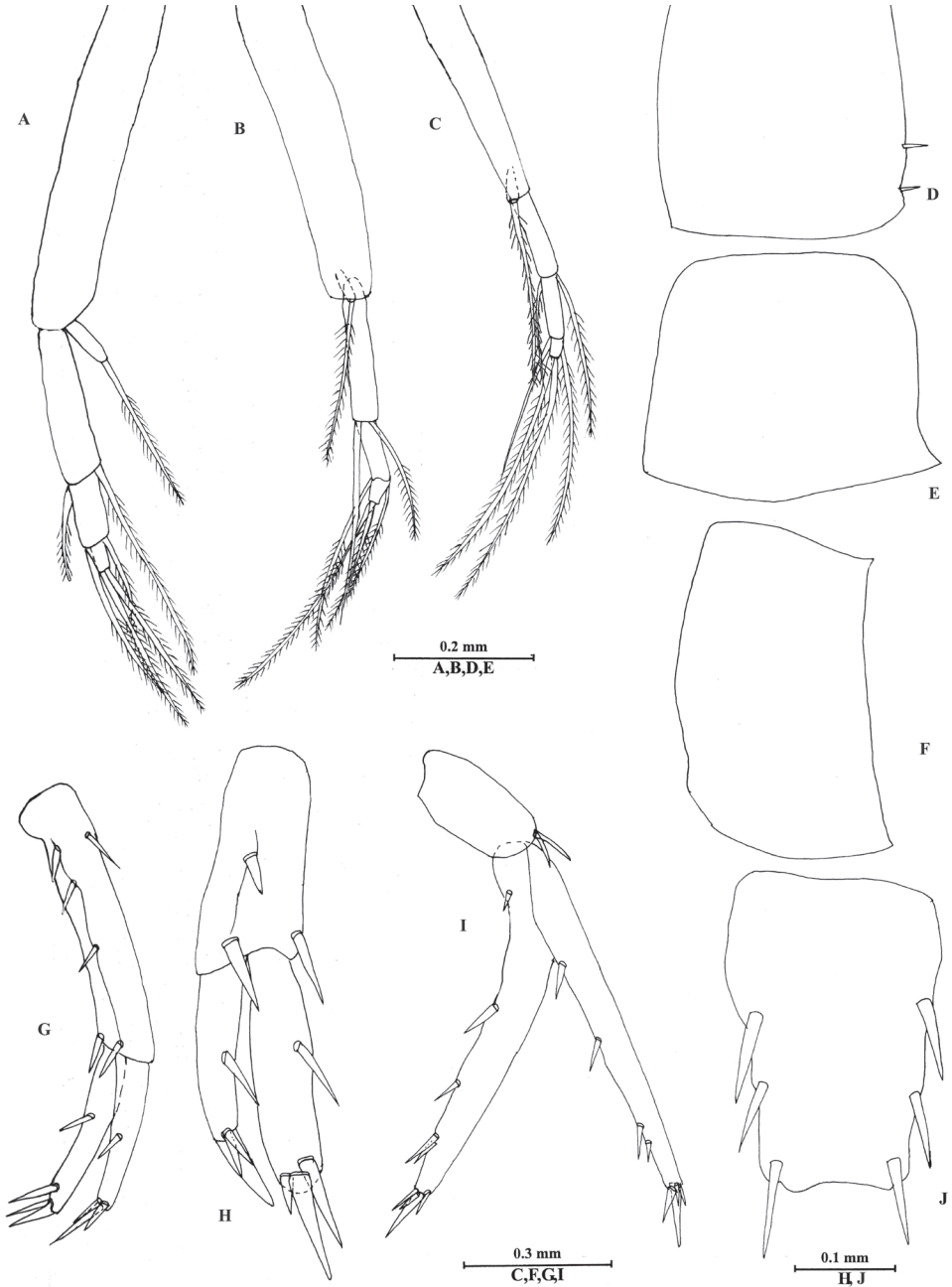


Figure 5. *Bogidiella pingxiangensis* sp. n., male holotype, from Jiangxi, China. **A** pleopod I **B** pleopod II **C** pleopod III **D** epimeral plate I **E** epimeral plate II **F** epimeral plate III **G** uropod I **H** uropod II **I** uropod III **J** telson.

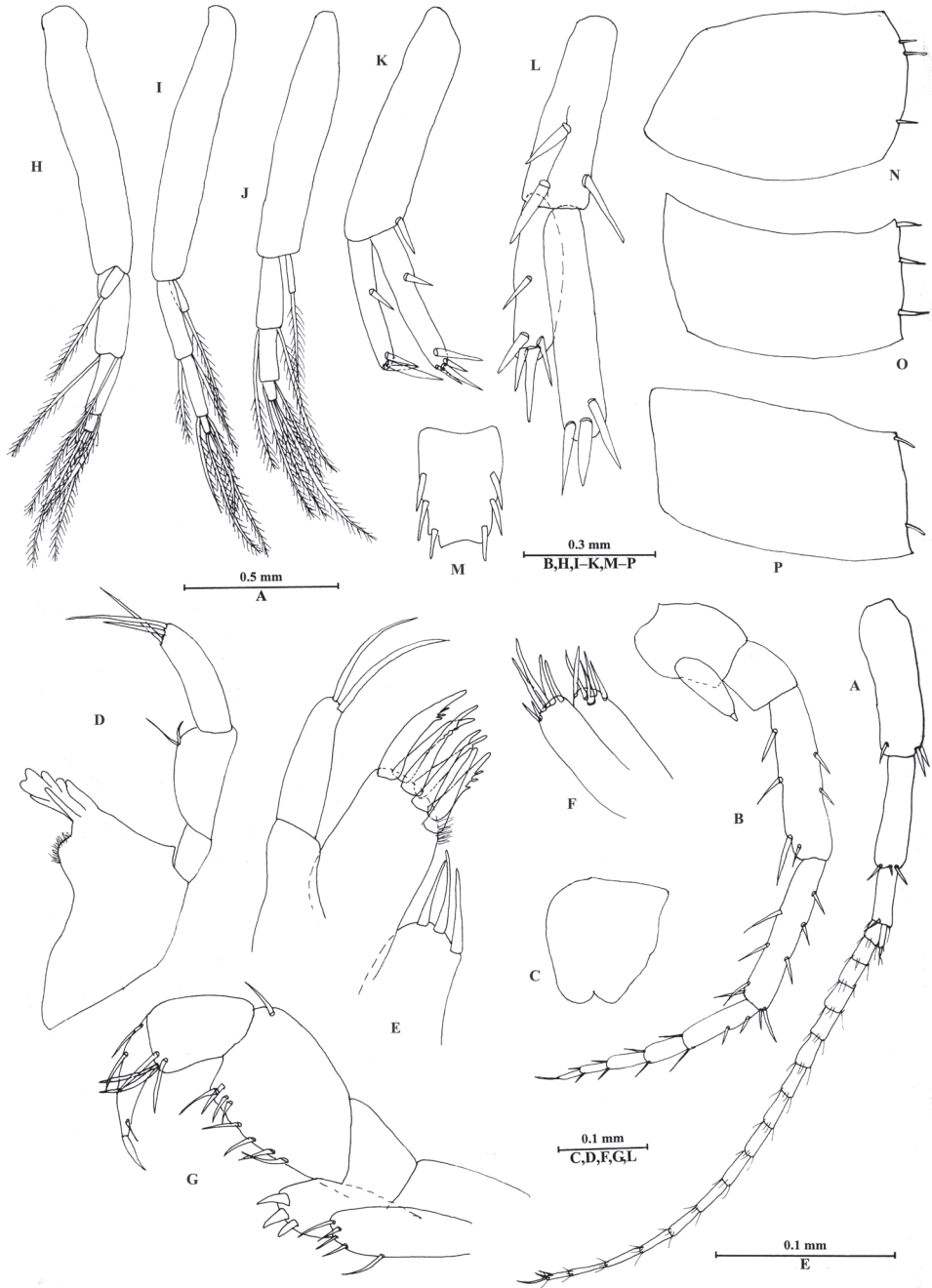


Figure 6. *Bogidiella pingxiangensis* sp. n., female paratype, from Jiangxi, China. **A** antenna I **B** antenna II **C** upper lip **D** left mandible **E** maxilla **F** maxilla II **G** maxilliped **H** pleopod I **I** pleopod II **J** pleopod III **K** uropod I **L** uropod II **M** telson **N** epimeral plate I **O** epimeral plate II **P** epimeral plate III.

with one spine on inner margin; outer ramus with one spine on inner margin, both rami with three terminal spines. Uropod III (Figure 5I) longer than uropods I–II, peduncle approx. $1/3$ the length of rami, with two spines on distal margin; inner and outer ramus rod-shaped, both with four to five marginal spines and four terminal spines.

Telson (Figure 5J): length 1.42 times as width, apical margin with shallow U-shaped excavation, each lobe bearing one apical and two lateral stout spines.

Description of paratype female (IZCAS-I-A1316-2), 4.0 mm.

Head. Antenna I (Figure 6A): peduncle articles with distal spines, flagellum with 16 articles, accessory flagellum with two articles.

Antenna II (Figure 6B): peduncle articles IV–V with three to four spines along anterior and posterior margins; flagellum with five articles, the first article twice as long as second article.

Upper lip convex (Figure 6C).

Mandible (Figure 6D): incisor with five teeth; lacinia mobilis small; palp with three articles, the second article expanded, with two setae, the third article with three distal setae.

Maxilla I (Figure 6E): inner plate with three distal setae; outer plate with seven serrated spines; second article of palp with two apical setae.

Maxilla II (Figure 6F): inner and outer plates with several setae.

Maxilliped (Figure 6G): inner plate with four setae; outer plate with three stout spines; second article of palp expanded, with eight marginal setae, third article short, fourth article claw-shaped.

Pereon. Gnathopod I (Figure 7A, B): similar to that of male. Basis expanded; carpus with tapered projection; propodus 2.7 times as long as that of gnathopod II, palmar margin with a row of 13 spines.

Gnathopod II (Figure 7C, D): slender, merus and carpus without pubescence; propodus twice as long as wide, with a row of very fine pubescent hairs on anterior side; posterior margin with a row of seven spines.

Pereopods III–VI (Figure 7E–L): similar to those of male, basis expanded.

Coxal gills present on pereopods IV–VI, with little bumps.

Oostegites present on gnathopod II and pereopods III–V.

Pleon. Epimeral plates I–III (Figure 6N–P): plate I–III with three, three and two setae on posterior margin respectively.

Pleopods I–III (Figure 6H–J) similar to those of male, inner ramus short.

Urosome. Uropod I (Figure 6K): peduncle without basofacial spine; both rami with three to four terminal spines. Uropod II (Figure 6I): outer ramus distinctly shorter than inner ramus. Uropod III missing.

Habitat. This species was collected from a cave, with rotten wood.

Remarks. The new species is assigned to the *Bogidiella-skopljensis* group (group B) according to inner ramus of pleopod with one segment (Koenemann and Holsinger 1999). *Bogidiella pingxiangensis* sp. n. is similar to *Bogidiella sinica* Karaman & Sket, 1990 in having antenna I longer than antenna II; gnathopod I distinctly larger than gnathopod II; and pleopods I–III inner ramus short. *Bogidiella pingxiangensis* sp. n.

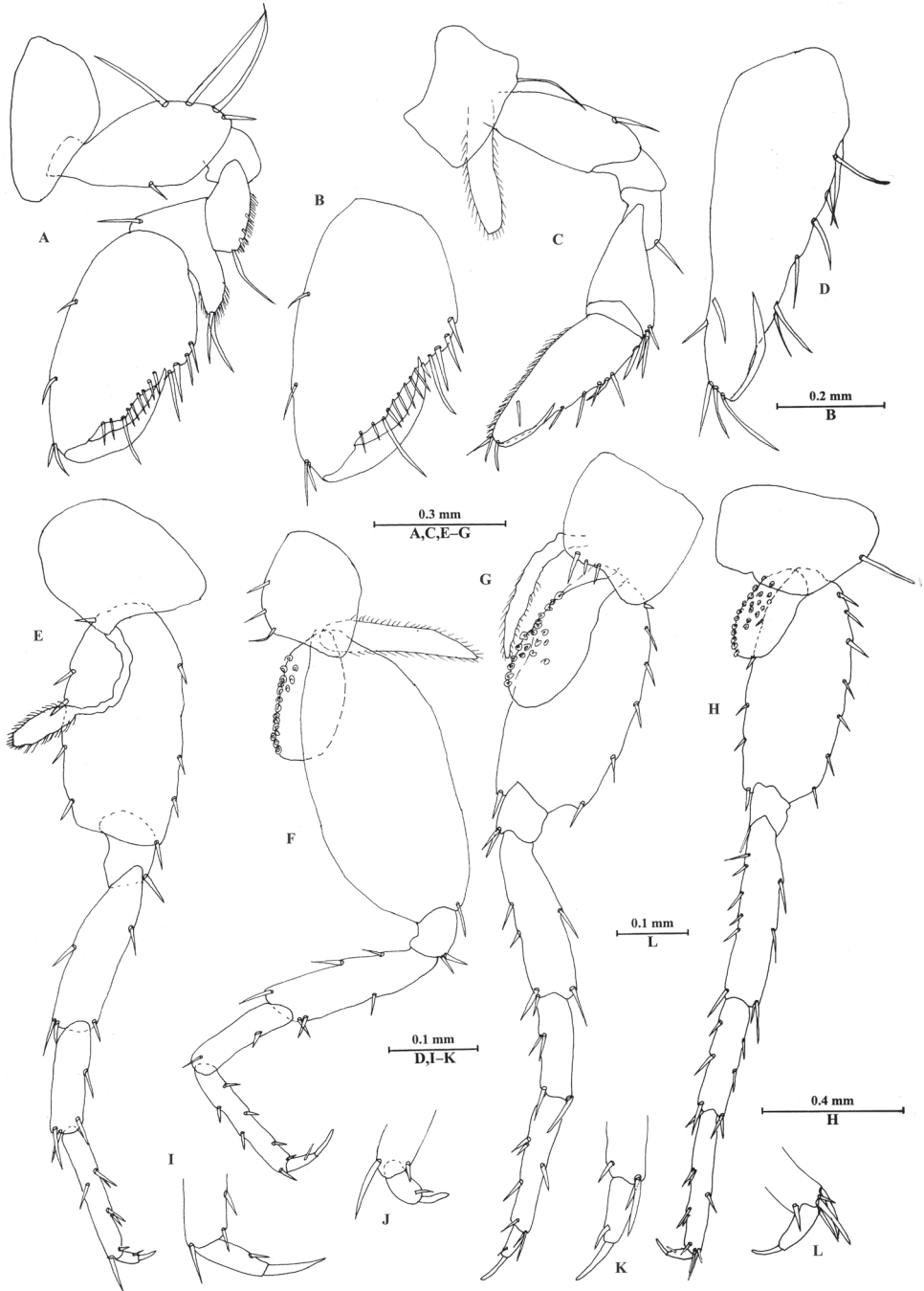


Figure 7. *Bogidiella pingxiangensis* sp. n., female paratype, from Jiangxi, China. **A** gnathopod I **B** propodus of gnathopod I **C** gnathopod II **D** propodus of gnathopod II **E** pereopod III **F** pereopod IV **G** pereopod V **H** pereopod VI **I** dactylus of pereopod III **J** dactylus of pereopod IV **K** dactylus of pereopod V **L** dactylus of pereopod VI.

differs from *B. sinica* (character states in parentheses) by gnathopod I basis expanded, rectangular (weakly expanded, elongate); pereopods III–IV bases expanded (slightly dilated but linear); telson 1.42 times longer than wide, apical margin with shallow U-shaped excavation, each lobe bearing one apical and two lateral stout spines (wider than long, with a straight distal margin bearing two disto-lateral spines which are longer than the telson itself, with three short plumose setae near each spine).

The new species is also similar to *Bogidiella veneris* Leijs, Bloechl & Koenemann, 2011 in having antenna I longer than antenna II; second article of palp in maxilla I with two apical setae; and in the shape of gnathopods I–II. *Bogidiella pingxiangensis* sp. n. differs from *B. veneris* (character states in parentheses) by articles III–IV of maxilliped without pubescent surfaces (with pubescent surfaces); bases of pereopods III–VII expanded (linear); propodus of pereopod VII with short spine (propodus with a cluster of long, posterodistal setae); inner ramus of pleopods I–III short (inner ramus absent); telson 1.42 times longer than wide, apical margin with shallow U-shaped excavation, each lobe bearing one apical and two subapical stout spines (small, as long as wide, with straight distal margin, equipped with two spines).

We downloaded all nine COI sequences of the genus *Bogidiella* from GenBank, including six for *B. albertimagni* Hertzog, 1933, two for *B. indica* Holsinger, Reddy & Messouli, 2006, and one for *B. veneris* Leijs, Bloechl & Koenemann, 2011. Molecular analyses showed high interspecific divergences. The uncorrected pairwise distance between *Bogidiella pingxiangensis* sp. n. and *B. albertimagni*, *B. indica*, *B. veneris* is 23.5–26.8% for COI. This value is larger than COI threshold (16%) for crustacean species delimitation (Lefébure et al. 2006). Therefore, morphological and molecular data support *B. pingxiangensis* sp. n. being a new species.

Acknowledgements

This study was supported by the Strategic Priority Research Program, Chinese Academy of Sciences (Category A, Tibet program XDA20050201), the National Natural Sciences Foundation of China (NSFC-31772417), and the National Science and Technology Basic Special (2014FY210700).

References

- Coleman CO (2009) Bogidiellidae. In: Lowry JK, Myers AA (Eds) Benthic Amphipoda (Crustacea: Pericarida) of the Great Barrier Reef, Australia. Zootaxa 2260: 279–284.
- Costa FO, DeWaard JR, Boutillier J, Ratnasingham S, Dooh RT, Hajibabaei M, Hebert PDN (2007) Biological identifications through DNA barcodes: the case of the Crustacea. Canadian Journal of Fisheries and Aquatic Sciences 64: 272–295. <https://doi.org/10.1139/f07-008>

- Folmer O, Black M, Hoeh W, Lutz R, Vrijenhoek R (1994) DNA primers for amplification of mitochondrial cytochrome *c* oxidase subunit I from diverse metazoan invertebrates. *Molecular Marine Biology & Biotechnology* 3: 294–299.
- Hertzog L (1933) *Bogidiella albertimagni* sp. nov., ein neuer Grundwasseramphipode aus der Rheinebene bei Strassburg. *Zoologischer Anzeiger* 102: 225–227.
- Hertzog L (1936) Crustacés des biotopes hypogés de la vallée du Rhin d’Alsace. *Bulletin de Société Zoologique de France* 61: 356–372.
- Holsinger JR (1967) Systematics, speciation, and distribution of the subterranean amphipod genus *Stygonectes* (Gammaridae). *Bulletin of United States National Museum* 259: 1–176. <https://doi.org/10.5479/si.03629236.259.1>
- Holsinger JR, Reddy YR, Messouli M (2006) *Bogidiella indica*, a new species of subterranean amphipod crustacean (Bogidiellidae) from wells in southeastern India, with remarks on the biogeographic importance of recently discovered Bogidiellids on the Indian subcontinent. *Subterranean Biology* 4: 45–54.
- Hou Z, Fu J, Li S (2007) A molecular phylogeny of the genus *Gammarus* (Crustacea: Amphipoda) based on mitochondrial and nuclear gene sequences. *Molecular Phylogenetics and Evolution* 45: 596–611. <https://doi.org/10.1016/j.ympev.2007.06.006>
- Hou Z, Li Z, Li S (2009) Identifying Chinese species of *Gammarus* (Crustacea: Amphipoda) using DNA barcoding. *Current Zoology* 55: 158–164.
- Karaman G, Sket B (1990) *Bogidiella sinica* sp. n. (Crustacea: Amphipoda) from southern China. *Bioloski Vestnik* 38: 35–47.
- Koenemann S, Holsinger JR (1999) Phylogenetic analysis of the amphipod family Bogidiellidae s. lat. and revision of taxa above the species level. *Crustaceana* 72: 781–816. <https://doi.org/10.1163/156854099503960>
- Lefébure T, Douady CJ, Gouy M, Gibert J (2006) Relationship between morphological taxonomy and molecular divergence within Crustacea: proposal of a molecular threshold to help species delimitation. *Molecular Phylogenetics and Evolution* 40: 435–447. <https://doi.org/10.1016/j.ympev.2006.03.014>
- Leijs R, Bloechl A, Koenemann S (2011) *Bogidiella veneris*, a new species of subterranean Amphipoda (Bogidiellidae) from Australia, with remarks on the systematics and biogeography. *Journal of Crustacean Biology* 31: 566–575. <https://doi.org/10.1651/11-3476.1>
- Swofford DL (2001) PAUP*: phylogenetic analysis using parsimony (* and other methods). Version 4.0b8. Sinauer, Sunderland, MA.

New records of *Tylokepon* with the description of a new species (Epicaridea, Bopyridae, Keponinae)

Jianmei An¹, Miao Zhang¹, Gustav Paulay²

1 School of Life Science, Shanxi Normal University, Linfen, 041000, PR China **2** Florida Museum of Natural History, University of Florida, Gainesville, FL, 32611-7800, USA

Corresponding author: Jianmei An (anjianmei@hotmail.com)

Academic editor: T. Horton | Received 3 July 2018 | Accepted 10 August 2018 | Published 15 October 2018

<http://zoobank.org/E0C03EB1-C423-4B6D-B19D-174A15BA888E>

Citation: An J, Zhang M, Paulay G (2018) New records of *Tylokepon* with the description of a new species (Epicaridea, Bopyridae, Keponinae). ZooKeys 790: 77–85. <https://doi.org/10.3897/zookeys.790.28134>

Abstract

The parasitic isopod genus *Tylokepon* is recorded for the first time from the Mariana Islands and Australia. *Tylokepon marianensis* **sp. n.** is described from the Mariana Islands, infesting *Thusaenys inami* (Laurie, 1906). The holotype female differs from other known *Tylokepon* females by the tri-lobed projection on pereopod 6, almost smooth lateral plates and pleopods, shape of oostegite 1, and widely opened brood pouch. The host is first recorded for bearing bopyrids. The new record of *T. bonnieri* Stebbing, 1904 from Australia on the type host extends the range of this species from China and India. A table of localities and hosts and a key to all species of *Tylokepon* are provided.

Keywords

Bopyridae, Epicaridea, new records, new species, *Tylokepon*

Introduction

Epicarid isopods remain greatly underdescribed, and Williams and Boyko (2012) predicted that the central Indian Ocean and east Asian seas hold a wealth of undescribed species. The keponine genus *Tylokepon* Stebbing, 1904 is a case in point. It currently contains four species (An 2009), three of which are known from single collections.

Here we add a fifth species and provide a new record for the only *Tylokepon* previously known from more than one record.

Boyko et al. (2013) recently erected the Keponinae for most genera previously attributed to Ioninae, restricting the latter to the type genus, *Ione* Latreille, 1818, and raising Ioninae to the family level. The keponine *Tylokepon* is readily differentiated from related genera by the prominent middorsal projections on the last two pereopods and the extremely swollen bilobed head. Stebbing (1904) erected the genus for *T. bonnieri* Stebbing, 1904 infesting the epialtid crab *Tylocarcinus styx* (Herbst, 1803) from the Maldives. An (2009) reported it from Beibu Gulf and South China Sea. Bonnier (1900) described *Cepon naxiae* infesting *Hyastenus diacanthus* (De Haan, 1839) from Hong Kong, based on a dried female specimen. After examining the type specimen, Markham (1982) transferred the species to *Tylokepon*. Shiino (1950) described a third species, *T. micippae*, infesting *Micippa philyra* (Herbst, 1803) from Japan, and compared *Tylokepon* with the related genera *Grapsicepon* Giard & Bonnier, 1887, *Merocepon* Richardson, 1910, *Cantricepon* Giard & Bonnier, 1887, *Paracepon* Nierstrasz & Brender à Brandis, 1931, and *Scyracepon* Tattersall, 1905. An (2009) added a fourth species, *T. biturus*, infesting *Menaethius monoceros* (Latreille, 1825) from Hainan, China. Recorded hosts of *Tylokepon* are crabs belonging to the majoid families Epialtidae and Majidae, with a single host record from a species of Parthenopidae (An 2009).

In the present paper, two epialtid crabs bearing bopyrids were examined and the parasites identified as *T. bonnieri* and a new species, *T. marianensis*. These are new records for the genus from Australia and Micronesia. A table (Table 1) and a key to the species of *Tylokepon* are provided.

Material and methods

The material reported here was found infesting host decapods in the collections of the Florida Museum of Natural History, University of Florida (UF). Animals were viewed and drawn using a Zeiss Stemi SV Apo.

Table 1. Localities and hosts of all species of genus *Tylokepon* Stebbing, 1904.

Species	Localities	Hosts
<i>Tylokepon biturus</i> An, 2009	China (Hainan)	<i>Menaethius Monoceros</i> (Latreille, 1825)
<i>Tylokepon bonnieri</i> Stebbing, 1904	Indian Ocean (Maldives);	<i>Tylocarcinus styx</i> (Herbst, 1803)
	China (Beibu Gulf and Hainan);	<i>Menaethius monoceros</i> (Latreille, 1825)
	Southwest India (Kovalam);	<i>Hyastenus diacanthus</i> (De Haan, 1839)
	Australia (Queensland, Lizard Island)	<i>Enoplolambrus validus</i> (De Haan, 1837)
<i>Tylokepon naxiae</i> (Bonnier, 1900)	Hong Kong	<i>Hyastenus diacanthus</i> (De Haan, 1839)
<i>Tylokepon micippae</i> Shiino, 1950	Japan	<i>Micippa philyra</i> (Herbst, 1803)
<i>Tylokepon marianensis</i> sp. n.	Mariana Islands, Guam Island	<i>Thusaenys irami</i> (Laurie, 1906)

Taxonomy

Family BOPYRIDAE Rafinesque-Schmaltz, 1815

Subfamily Keponinae Boyko, Moss, Williams & Shields, 2013

Genus *Tylokepon* Stebbing, 1904

Tylokepon marianensis sp. n.

<http://zoobank.org/4B1B0383-677A-4054-9230-60ECAC3462FF>

Figure 1

Material examined. UF 42220: holotype ♀ and allotype ♂, USA, Mariana Islands, Guam Island, Haputo, 13°34.74'N, 144°49.84'E, rubble, 8–10 m, 8 July 2003, Coll. G. Paulay, infesting the right branchial chamber of *Thusaenys irami* (Laurie, 1906) (host, UF 5935, identified by Dr. Amanda Windsor).

Diagnosis. Female: Head large, swollen, and bilobed. Without eyes. Pereon with seven segments, sixth pereomere with tri-lobed projection and seventh pereomere with a single, large median projection. Pleon of six segments, first five with uniramous lateral plates and biramous pleopods. Lateral plates tuberculated on both sides of first pleomeres, but smooth on remaining pleomeres. Sixth pleomere small with uniramous uropoda.

Male: Head semicircular, with black eyes. Seven pereomeres with truncate margins. Pereopods subequal in size and structure. First five pleomeres with tuberculate, uniramous pleopods. Sixth pleomere with a pair of round uropods covered in scales and each ramus with stout terminal setae.

Description of holotype female. Length 3.38 mm (excluding pleon and uropods), maximum width 1.9 mm across pereomere 4, head length 0.73 mm, head width 1.5 mm. All body regions and segments distinct; no pigmentation (Figure 1A, B).

Head large, covering pereomere 1, wider than long, bilobed, comprised of two ellipsoid structures separated by a deep median groove. Frontal lamina narrow and not extending to margin of head. Eyes absent (Figure 1A). First and second antennae rudimentary with two and three articles, respectively, terminally setose (Figure 1C). Barbula (Figure 1D) with two lateral digitate projections and a medial blunt projection on each side. Maxilliped (Figure 1E) with a smooth, curved palp and a sharp plectron; anterior article much larger than posterior one.

Pereon broadest across pereomere 3. Head covering much of pereomere 1, with only median part visible in dorsal view. Dorsolateral bosses distinct on first four pereomeres on both sides. Coxal plates absent. Tergal projections present on pereomeres 2–4. Last two pereomeres with middorsal projections: pereomere 6 with a tri-lobed projection; pereomere 7 with a single, large median projection (Figure 1A). Brood pouch widely open. Oostegite 1 (Figure 1F, G) composed of two equally-sized articles, internal ridge smooth, jagged posterior margin with sharp projections, without posterolateral point. Pereopod 1 much smaller than others, but all pereopods subequal in shape, all articles distinct, carpi and propodi with setae on ventral surface (Figure 1H, I).

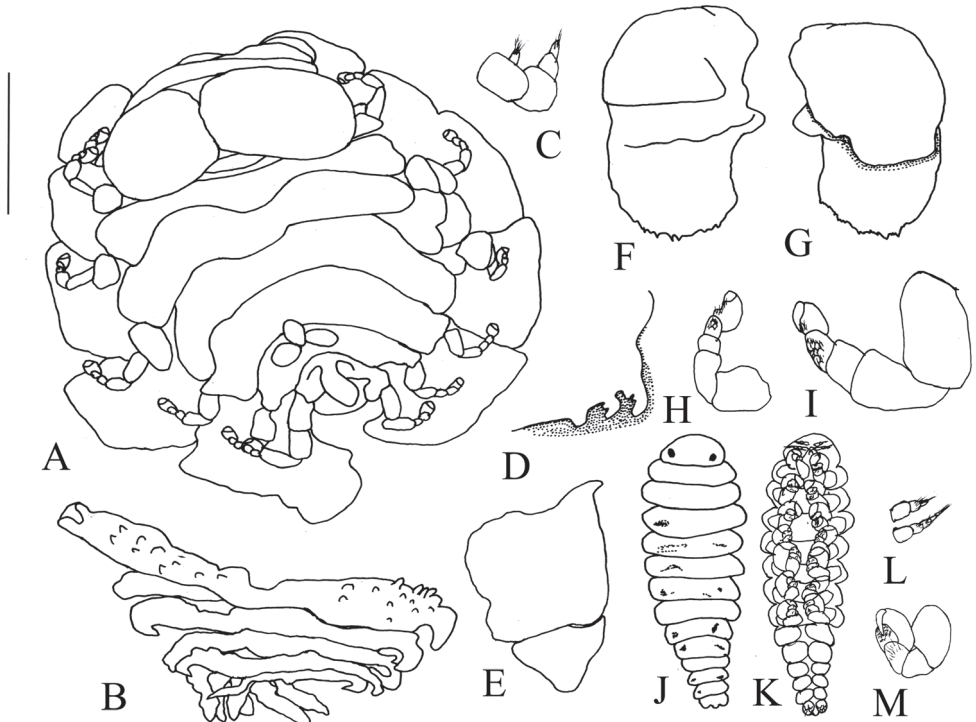


Figure 1. *Tylokepon marianensis* sp. n. Holotype female (UF 42220) (A–I). **A** Dorsal view **B** Pleon, dorsal view **C** Left antennae **D** Barbula, left side **E** Right maxilliped, external view **F** Left oostegite 1, external view **G** Left oostegite 1, internal view **H** Left pereopod 1 **I** Left pereopod 6. Allotype male (J–M) **J** Dorsal view **K** Ventral view **L** Left antenna **M** Left pereopod 4. Scale bars: 1.00 mm (A, B); 0.63 mm (D–G); 0.35 mm (H, I, L, M); 0.50 mm (J, K).

Pleon with six distinct pleomeres, first five with longer lateral plates and biramous pleopods (Figure 1B). Lateral plates tuberculated on both sides of first pleomeres, but smooth on remaining pleomeres. Terminal segment without lateral plates. All pleopods with slightly undulating to smooth margins, gradually shorter toward posterior. Pleomere 6 small. Uropods uniramous, lobose, with smooth surfaces and entire margins (Figure 1B).

Description of allotype male. Length 0.95 mm, maximal width 0.23 mm across pereon 3, head length 0.11 mm, head width 0.19 mm, pleonal length 0.31 mm. All body segments distinct with scattered pigmentation (Figure 1J, K).

Head semicircular, black eyes near posterior margin of head (Figure 1J). First and second antennae of three and four articles, respectively (Figure 1L), terminal articles fringed with setae. Third pereomere widest; all pereomeres with truncate margins. Pereopods subequal in size and structure (Figure 1M), meri and carpi with setae on ventral surfaces, each pointed dactylus retracts into groove formed between parallel series of tubercles on each propodus.

Pleon of six segments, first five pleomeres with tuberculate, uniramous pleopods. Sixth pleomere with a pair of round uropods covered in scales and each ramus with stout terminal setae; medial anal cone smooth.

Etymology. The specific epithet, *marianensis*, refers to the type locality in the Mariana Islands.

Remarks. Shiino (1950) and Markham (1982) summarized the distinguishing features of *Tylokepon* as follows: females have a large head formed by two semi-spherical structures separated by a deep median groove, and the last two pereomeres possess prominent middorsal projections. The present specimens are referred to *Tylokepon* on the basis of these characters. The new species is distinguished from the other four nominal species of *Tylokepon* by the tri-lobed middorsal projection on the sixth pereomere of females and the jagged posterior margin of oostegite 1. *Tylokepon marianensis* is most similar to *T. bonnieri*, which was recorded from Beibu Gulf in China on the related host *Hyastenus diacanthus* (An, 2009). Both have the middorsal projections on pereonite 6 consisting of three lobes and a single projection on pereonite 7. However, while the three lobes are separated at the base in *T. bonnieri*, they are united basally to form a tri-lobed structure in the new species (compare Figs. 1A and 2A). They also differ in the sculpture of the lateral plates on pleomeres 2–5 and pleopods: these are almost smooth in *T. marianensis* but tuberculate in *T. bonnieri*. *Tylokepon micippae* differs from *T. marianensis* in having a closed, rather than widely open brood pouch, tuberculate rather than nearly smooth pleopods and lateral plates on pleomeres 2–5, a sharp and pointed posterolateral point on oostegite 1 rather than an entire margin, and a cluster of three rather than a single mid-dorsal projection on the seventh pereomere. The poorly known *T. naxiae*, which also infests *H. diacanthus*, differs from the new species in the shape of the middorsal projections of the sixth pereomere, which are separated at the base as in *T. bonnieri*, and having digitate, rather than entire margins on the lateral plates of the second pleomeres. The new species also differs from *T. biturus* in having three rather than two mid-dorsal projections on the sixth pereomere, having the lobes of the head united into a dumbbell shape rather than separated by a groove, and smooth, rather than tuberculate, lateral plates on the first pleomeres.

Tylokepon bonnieri Stebbing, 1904

Figure 2

Tylokepon bonnieri Stebbing, 1904: 716–717, pl. LIII, B, C; Shiino 1950: 166; Pillai 1954: 19; Pillai 1964: 187–188, figs. 7–11; An 2009: 96–98.

Material examined. UF 42219: 1♀, 1♂, Australia, Queensland, Lizard Island, north side, at “Washing Machine, 14°39.02'S, 145°27.73'E, from dead *Pocillopora*, 21 February 2009, coll. Molly Timmers. Infesting right branchial chamber of *Tylocarcinus styx* (Herbst, 1803) (UF 18294).

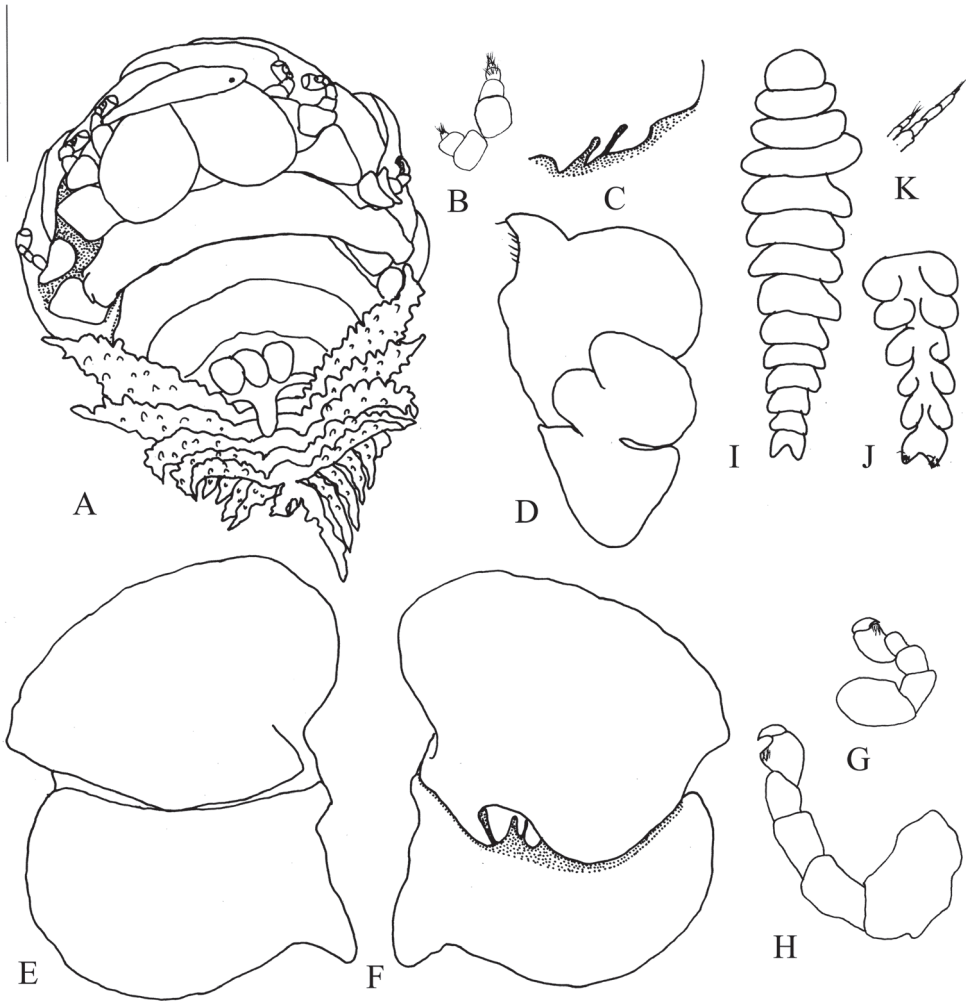


Figure 2. *Tylokepon bonnierii* Stebbing, 1904. Female (UF 42219) (A–H). **A** Dorsal view **B** Right antennae **C** Barbula, left side **D** Left maxilliped, external view **E** Left oostegite 1, external view **F** Left oostegite 1, internal view **G** Right pereopod 1 **H** Left pereopod 5. Male (UF 42219) (I–K). **I** Dorsal view **J** Left antenna **K** Pleon, ventral view. Scale bars: 1.00 mm (A); 0.65 mm (C); 0.42 mm (D–F); 0.31 mm (B, G, H, J); 0.42 mm (I, K).

Description of female. Length 3.58 mm (excluding uropods), maximum width 2.28 mm across pereomere 3, head length 0.66 mm, head width 1.26 mm. (Figure 2A).

Head large, covering pereomere 1, wider than long, completely bilobed, with two ellipsoid structures separated by a deep median groove. Frontal lamina narrow, visible in dorsal view. Small black eyes near frontal lamina (Figure 2A). First and second antennae rudimentary, with three and five articles, respectively, terminally setose (Figure 2B). Barbula (Figure 2C) with two large falcate projections and a mediad sharp

projection on each side. Anterior article of maxilliped (Figure 2D) much larger than posterior one, with prominent, inwardly-directed and setose palp, plectron short.

Pereon broadest across pereomere 3. Head covering much of pereomere 1. Distinct dorsolateral bosses on first four pereomeres on both sides. Coxal plates absent. Tergal projection present on pereomeres 2 and 3. Middorsal projections on last two pereomeres: three parallel projections on pereomere 6, one large and posteriorly extended projection on pereomere 7 (Figure 2A). Brood pouch incompletely covered by oostegites. Oostegite 1 (Figure 2E, F) composed of two subequal in size articles, with smooth internal ridge that bears three marginal projections; ending in extended posterolateral point. Pereopod 1 much smaller than others, all pereopods with short dactyli (Figure 2G, H).

Pleon of six distinct pleomeres, first five with well-developed, tuberculate lateral plates, and biramous, tuberculate pleopods. All lateral plates and exopodites of pleopods with digitate margins. Endopodites of pleopods 1–5 small and smooth (Figure 2A). Uniramous uropods similar to exopodites of pleopod 5.

Description of male. Length 1.08 mm, maximal width 0.32 mm, across pereomere 3, head length 0.11 mm, head width 0.16 mm, pleonal length 0.39 mm. Body gradually tapered posteriorly, all segments distinct (Figure 2I).

Head semicircular, broader than long; without eyes. First and second antennae of three and five articles, respectively (Figure 2J), basal articles greatly expanded, final articles fringed with setae. Pereon broadest across pereomere 3. Pleon of six segments, first five pleomeres with tuberculate uniramous pleopods. Pleomere 6 bilobed, with tuberculate projections and setae (Figure 2K).

Remarks. Stebbing (1904) erected *Tylokepon* for *T. bonnieri* infesting *Tylocarcinus styx* from the Indian Ocean. Pillai (1954, 1966) recorded the species from Kovalam, southwest India, infesting *Menaethius monoceros*. An (2009) reported it from Beibu Gulf and Hainan, China, infesting *Hyastenus diacanthus* and the parthenopid crab *Enoplolambrus validus* (De Haan, 1837). Although *Hyastenus diacanthus* was recorded to be infested by *Tylokepon naxiae* from Hong Kong, it is not impossible that a single host is found bearing two different species, such as the case of *Petrolisthes quadratus* Benedict, 1901 bearing *Aporobopyrus crutatus* (Richardson, 1910) and *A. bonairensis* Markham, 1988.

As for *T. naxiae*, Bonnier (1900) only gave a brief description, and Markham (1982) found that the holotype female is badly damaged, and only three useful characters can be defined. However, from the figure (Markham 1982: fig. 18), it can be seen that the species has an almost smooth surface to the pleopods and the lateral plates are not covered with tuberculate (while the pleopods and lateral plates of *T. bonnieri* are densely covered with tubercles). Therefore, *T. bonnieri* differs from *T. naxiae*.

The present specimens conform well to Stebbing's description (1904), except for some minor differences, such as the male specimen lacking eyes. There are slight differences between the present specimens and those from Beibu Gulf (An 2009) in the middorsal projections on pereopod 6 and frontal lamina of the head, but the key characters of the females, such as oostegite 1, maxilliped, barbula, lateral plates and pleopods, as well as of males, are similar.

Key to species of *Tylokepon*

- 1 Three middorsal projections on pereomere 6.....2
 – Two middorsal projections on pereomere 6..... *T. biturus* An, 2009
 2 Lateral plates of all pleomeres with digitate margins.....3
 – Lateral plates of pleomeres 2–5 nearly smooth *T. marianensis* sp. n.
 3 Two lobes of head separated by a shallow median groove
 *T. micippae* Shiino, 1950
 – Two lobes of head completely divided by deep median groove4
 4 Ventral surface of pleopods almost smooth *T. naxiae* (Bonnier, 1900)
 – Ventral surface of pleopods densely tuberculated
 *T. bonnieri* Stebbing, 1904

Acknowledgements

This work was supported by the National Natural Science Foundation of China (No. 31471970) and Fund Program for the Scientific Activities of Selected Returned Overseas Professionals in Shanxi Province (2016). We are indebted to all collectors of specimens in the Florida Museum of Natural History. We also wish to thank Mandy Bemis and John Slapcinsky of the Florida Museum of Natural History for all the help during the first author's visit. We thank Amanda Windsor for identifying the host of *Tylokepon marianensis*.

References

- An JM (2009) A review of bopyrid isopods infesting crabs from China. *Integrative and Comparative Biology* 49(2): 95–105. <https://doi.org/10.1093/icb/icp022>
 Benedict JE (1901) The anomuran collections made by the Fish Hawk Expedition to Porto Rico. *Bulletin of the United States Fisheries Commission* 20: 129–148.
 Bonnier J (1900) Contribution à l'étude des épicarides. Les Bopyridae. *Travaux de l'Institut Zoologique de Lille et du Laboratoire de Zoologie Maritime de Wimereux* 8: 1–478.
 Boyko CB, Moss J, Williams JD, Shields JD (2013) A molecular phylogeny of Bopyroidea and Cryptoniscoidea (Crustacea, Isopoda). *Systematics and Biodiversity* 11(4): 495–506. <https://doi.org/10.1080/14772000.2013.865679>
 De Haan W (1833–1849) Crustacea. In: von Siebold PhF (Ed.) *Fauna Japonica sive Descriptio Animalium, quae in Itinere per Japoniam, Jussu et Auspiciis Superiorum, qui Summum in India Batava Imperium Tenent, Suscepto, Annis 1823–1830 Collegit, Notis, Observationibus et Adumbrationibus Illustravit*: ix–xvi, i–xxi, vii–xvii, 1–243.
 Giard A, Bonnier J (1887) Contributions à l'étude des bopyriens. *Travaux de l'Institut Zoologique de Lille et du Laboratoire Marine de Wimereux* 5: 1–272.

- Herbst JFW (1803) Versuch einer Naturgeschichte der Krabben und Krebse, nebst einer systematischen Beschreibung ihrer verschiedenen Arten 3(3): 1–54. [pls 55–58]
- Latreille PA (1825) Encyclopédie Méthodique Entomologie, ou Histoire naturelle des Crustacés, des Arachnides et des Insectes. Encyclopédie méthodique. Histoire Naturelle 10: 1–344.
- Laurie RD (1906) Report on the Brachyura collected by Professor Herdman, at Ceylon, in 1902. In: Herdman WA (Ed.) Report to the Government of Ceylon on the Pearl Oyster Fisheries of the Gulf of Manaar with Supplementary Reports Upon the Marine Biology of Ceylon by Other Naturalists, Part 5, Suppl. Rep. 40: 349–432. [pls 1, 2]
- Markham JC (1982) Bopyrid isopods parasitic on decapod crustaceans in Hong Kong and southern China, vol 1. In: Morton BS, Tseng CK (Eds) Proceedings of the First International Marine Biological Workshop: The Marine Flora and Fauna of Hong Kong and Southern China. Hong Kong University Press, Hong Kong, 325–391.
- Nierstrasz HF, Brender à Brandis GA (1931) Papers from Dr. Th. Mortensen's Pacific Expedition 1914–16. 57. Epicaridea 2. Videnskabelige Meddelelser fra Dansk Naturhistorisk Forening i Kjøbenhavn 91: 147–225.
- Pillai NK (1954) A preliminary note on the Tanaidacea and Isopoda of Travancore. Bulletin of the Central Research Institute, University of Travancore, Trivandrum, Natural Sciences 3C(1): 1–21.
- Pillai NK (1966) Isopod parasites of south Indian crustaceans. Crustaceana 10: 183–191. <https://doi.org/10.1163/156854066X00702>
- Rafinesque-Schmaltz CS (1815) Analyse de la Nature, ou tableau de l'univers et des corps organisés. Palerme, 224 pp.
- Richardson H (1910) Marine isopods collected in the Philippines by the U.S. Fisheries steamer Albatross in 1907–8. Washington D.C. Department of Commerce Bureau of Fisheries Document No. 736.
- Shiino SM (1950) Notes on some new bopyrids from Japan. Mie Medical Journal 1(2): 151–167.
- Stebbing TRR (1904) Marine crustaceans. XII. Isopoda, with description of a new genus. In: Gardiner JS (Ed.) The fauna and geography of the Maldive and Laccadive Archipelagoes, being the account of the work carried on and of the collections made by an expedition during the years 1899 and 1900. University Press, Cambridge, 699–721. [pls 49–53]
- Tattersall WM (1905) The marine fauna of the coast of Ireland. Part V. Isopoda. Fisheries, Ireland, Scientific Investigations 1904(2): 1–90.
- Williams JD, Boyko CB (2012) The global diversity of parasitic isopods associated with crustacean hosts (Isopoda: Bopyroidea and Cryptoniscoidea). PLoS ONE 7(4): e35350. <https://doi.org/10.1371/journal.pone.0035350>

Description of a second South American species in the Malagasy earwig genus *Mesodiplatys* from a cave habitat, with notes on the definition of Haplodiplatyidae (Insecta, Dermaptera)

Yoshitaka Kamimura¹, Rodrigo L. Ferreira²

1 Department of Biology, Keio University, 4-1-1 Hiyoshi, Yokohama 223-8521, Japan **2** Center of Studies in Subterranean Biology, Biology Department, Federal University of Lavras, CEP 37200-000 Lavras (MG), Brazil

Corresponding author: Yoshitaka Kamimura (kamimura@fbc.keio.ac.jp)

Academic editor: Fabian Haas | Received 4 June 2018 | Accepted 4 September 2018 | Published 15 October 2018

<http://zoobank.org/6A4735FE-8FC3-4CBD-A1B5-9CE812ED752B>

Citation: Kamimura Y, Ferreira RL (2018) Description of a second South American species in the Malagasy earwig genus *Mesodiplatys* from a cave habitat, with notes on the definition of Haplodiplatyidae (Insecta, Dermaptera). ZooKeys 790: 87–100. <https://doi.org/10.3897/zookeys.790.27193>

Abstract

The genus *Mesodiplatys* (Dermaptera: Diplatyidae) comprises eight species from Madagascar and one species from Peru. Based on a sample collected from a cave in Brazil, a new species of this genus, *Mesodiplatys falcifer* Kamimura, **sp. n.**, is described as the second species from South America. Based on a reexamination of the holotype of *Mesodiplatys insularis*, a revised key to *Mesodiplatys* species is provided. The definitions of the genera *Mesodiplatys* and *Haplodiplatys* and the family Haplodiplatyidae are also reconsidered.

Keywords

Brazil, cave insects, *Haplodiplatys*, Madagascar, *Mesodiplatys falcifer* sp. n.

Introduction

Diplatyidae (*sensu* Sakai 1996, including *Haplodiplatys* and *Cylindrogastrinae*) is an earwig family comprising approximately 150 described species. This family shows typical Gondwanan distribution (Popham 2000), possessing many plesiomorphic characteristics (Haas 1995; Haas and Kukalová-Peck 2001; Haas and Klass 2003; Klass

2003). Among diplatyids, the members of the genus *Haplodiplatys* Hincks, 1955 (type species; *Haplodiplatys niger* Hincks, 1955) are considered to be among the earliest offshoots in the suborder Neodermaptera (i.e., extant earwigs: Haas 1995; Popham 2000; Haas and Kukalová-Peck 2001; Haas and Klass 2003). Recently, Engel et al. (2017) treated *Haplodiplatys* as the sole genus of the family Haplodiplatyidae, and we follow this approach in the present study.

The genus *Mesodiplatys* was originally proposed as a subgenus of *Haplodiplatys* with the type species *Diplatys nana* Burr, 1914 (Steinmann 1986b). Although the parameres (= external parameres or metaparameres) are relatively simple (lacking teeth, projections, and branching) as in other *Haplodiplatys* spp., Anisyutkin (2014) treated *Mesodiplatys* as a separate Diplatyidae genus based on many differences in external morphology, including the differentiation of the head into frontal and occipital regions.

The distribution of this genus is enigmatic: eight species are known from Madagascar and one species from Peru. Anisyutkin (2014) proposed three hypotheses to explain this disjunct distribution. First, the observed similarities in genital morphology between Malagasy and South American *Mesodiplatys* species evolved in parallel. Second, this genus displays Gondwanan distribution and African species remain undiscovered or have gone extinct. Third, the common ancestor of *Mesodiplatys* originated in Madagascar and then expanded its distribution to South America (or vice versa). Case (2002) proposed a land bridge (the Gunnerus Ridge) between Madagascar and Antarctica in the middle to late Cretaceous. Although recent estimates based on geological and geophysical data do not support the presence of such a causeway (Ali and Krause 2011), similar disjunct distributions in Madagascar and South America are known for several animal groups, including some boid snakes (Noonan and Chippindale 2006a), iguanids (pleurodont iguanians: Noonan and Chippindale 2006b), and podocnemidid turtles (Noonan and Chippindale 2006b), suggesting past direct bioconnections between these regions.

To explore these possibilities, extensive taxonomic surveys in South American and African regions are needed. In the current study, we report and describe in detail the second *Mesodiplatys* species from South America based on a male sample collected from a Brazilian cave. For comparison, the external morphology is re-described based on the *M. insularis* (Borelli, 1932) type specimens. A contemporary key is provided for males of *Mesodiplatys* spp. Based on our results, we briefly discuss the definitions of the genera, *Mesodiplatys* (Diplatyidae) and *Haplodiplatys* (Haplodiplatyidae).

Materials and methods

The material examined in this study was collected from a cave in Brazil in 2017, and preserved in 70% ethanol. After removal of the genitalia, the specimen was mounted on cardboard using fish glue and allowed to dry. The genitalia were examined under a BX53 differential interference contrast (DIC) microscope (Olympus, Tokyo, Japan), mounted in Euparal (Waldeck GmbH and Co. KG, Münster, Germany) between two

coverslips, and attached to the pin of the specimen. Based on photographs taken under the DIC microscope and a S8-APO stereo microscope (Leica, Wetzlar, Germany), we created a digital composition of selected in-focus parts of each image using the Combine ZM image-stacking software (Hadley 2008).

For comparison, external morphologies of the holotype (male) and a paratype (female) of *M. insularis* deposited in the Zoological Museum (ZMH), part of the Centrum für Naturkunde (CeNak) at the Universität Hamburg, were examined based on photographs provided by CeNak staff.

The type of the newly described species was deposited in the Subterranean Invertebrate Collection of Lavras (ISLA), at the Universidade Federal de Lavras (UFLA), Lavras, Brazil.

We followed Kamimura and Ferreira (2017) in the suprageneric classification of the infraorder Protodermaptera. The terminology of Kamimura (2014) was used to describe male genital structures.

Taxonomy

Order DERMAPTERA de Geer, 1773

Infraorder PROTODERMAPTERA Zacher, 1910

Family DIPLATYIDAE Verhoeff, 1902

Genus *Mesodiplatys* Steinmann, 1986

***Mesodiplatys falcifer* Kamimura, sp. n.**

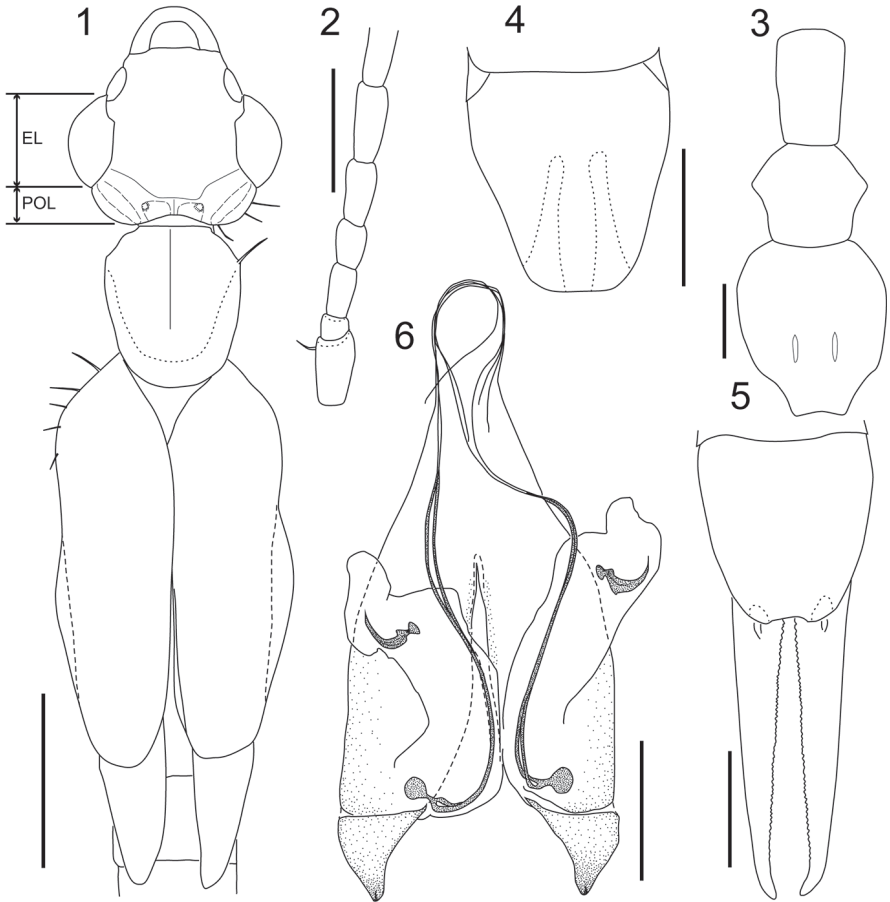
<http://zoobank.org/2BE92C3E-D821-4593-BF57-11D44A027CE5>

Figs 1–14

Material examined. Holotype ♂, ‘Lapa dos Peixes II | (UTM 612750, 8971635) | Carinhanha municipality,| Bahia, Brasil’, ‘ISLA 46682’, ‘15.x.2017 | Coleta Geral (general sampling), Ferreira R.L. leg.’, ‘HOLOTYPE (male) | *Mesodiplatys falcifer* | sp. nov. | Det. Y. Kamimura 2018’.

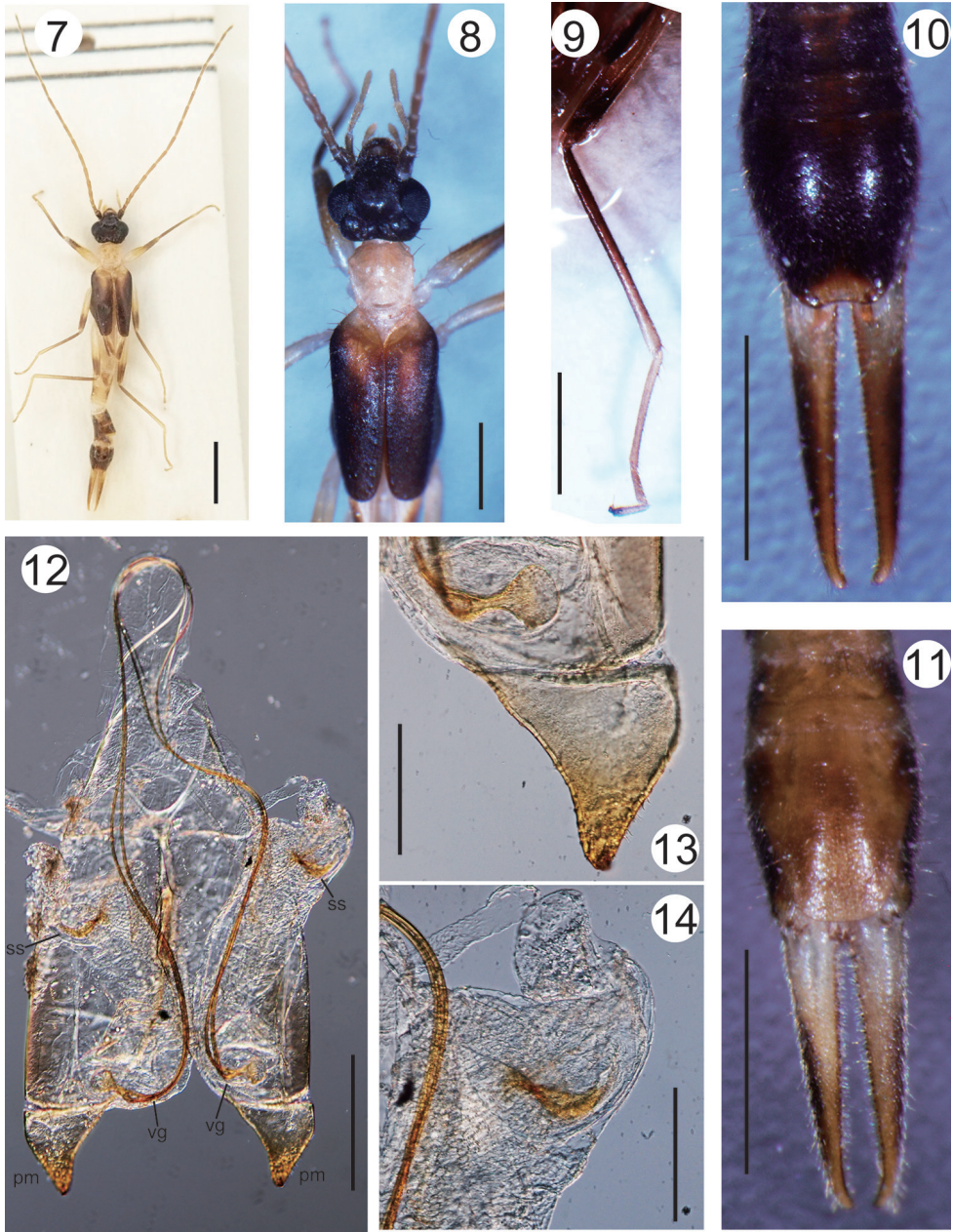
Diagnosis. *Mesodiplatys falcifer* sp. n. is a small-sized species with a slender abdomen and simple forceps. This species differs all other species of *Mesodiplatys* with the combination of the following characters: the sickle-shaped sclerite in the penis lobe; notably short parameres lacking dentiform curvature near base on inner margin and its articulation with main body of genitalia perpendicular to its anterior-posterior axis; notably large eyes; and uniformly pale pronotum and darker tegmina.

Description. Male (holotype, Figure 7). Measurements are shown in Table 1. Body color generally amber except for 3rd antennal segment and beyond, distal third of femur, basal half of tibia, tegmina (except for region around scutellum), fustis of wings, dorsal side of 7th abdominal segments and beyond, and lateral sides of 6th abdominal segment dark brown. Head and 1st and 2nd antennal segments black. Forceps reddish brown. Abdomen and forceps densely pubescent.



Figures 1–6. *Mesodiplatys falcifer* sp. n. (male, holotype): **1** head, thorax, and proximal part of abdomen **2** proximal part of left antenna **3** thoracic sternites **4** penultimate abdominal sternite **5** ultimate abdominal tergite and forceps **6** genitalia. Abbreviations: EL, eye length; POL, post-ocular length. Scale bars: 1 mm (**1**); 0.5 mm (**2–5**); 250 μ m (**6**).

Head (Figs 1, 8) slightly longer than width, widest in eye region; frons tumid but weakly depressed at apex; occiput strongly and widely depressed; transverse and median sutures visible but not conspicuous; posterior margin strongly emarginated in middle with a pair of semi-oval tubercles lateral to median suture, of which outer-anterior angle protrudes dorsally as small papilla; post-ocular carina conspicuous as oblong swelling; lateral margins of post-ocular region bordered by strong bristles. Eyes conspicuously prominent, eye length 2.5 times the post-ocular length (EL/POL, measured along anterior-posterior axis as shown in Figure 1; Table 2). Antennae (Figs 2, 8) comprise 19 segments: segment I stout, expanded apically, length almost half of distance between antennal bases; segment II shorter than width; segment III twice as long as width; segment IV 1.5 times longer than width; segment V almost as long as III;



Figures 7–14. *Mesodiplatys falcifer* sp. n. (male, holotype): **7** habitus **8** head, thorax, and tegmina **9** right hind leg **10** tergites of post-abdomen and forceps **11** sternites of post-abdomen and forceps **12** general view of genitalia **13** right parameres and basal part of virga **14** sickle-shaped sclerite in right penis lobe (Fig. 14). Abbreviations: pm, paramere; ss, sickle-shaped sclerite; vg, virga. Scale bars: 2 mm (**7**); 1 mm (**8–11**); 250 μ m (**12**); 100 μ m (**13, 14**).

Table 1. Measurements of the male holotype of *Mesodiplatys falcifer* sp. n. (mm) in comparison with those of the South American congener *M. venado* (Anisytukin, 2014).

	<i>M. falcifer</i> sp. n. (A)	<i>M. venado</i> (B)	Ratio (A/B)
Length			
Body without forceps	8	-	-
Head	1.1	1.5	0.73
Pronotum	0.87	1.0	0.87
Tegmen	2.3	2.9	0.79
Fore/mid/hind femur	1.5/1.8/2.2	1.6/2.0/2.2	0.94/0.90/1.0
Fore/mid/hind tibia	1.5/1.5/2.0	1.7/1.8/2.2	0.88/0.83/0.90
Forceps	1.3	1.8	0.72
Width			
Head	1.2	1.7	0.71
Pronorum	0.76	1.1	0.69
Tegmen	0.66	0.9	0.73
Ultimate tergite	0.80	1.2	0.67

Table 2. Eye length (EL) relative to post-ocular length (POL) in male *Mesodiplatys* species. Measurements are as shown in Figure 1.

	Ratio (EL/POL)	Source image used for measurement
South American species		
<i>M. venado</i>	2.07	Fig. 1 (Anisytukin 2014)
<i>M. falcifer</i> sp. n.	2.50	Fig. 1 (this study)
Malagasy species		
<i>M. nanus</i>	1.99	Fig. 7 (Brindle 1966)
<i>M. insularis</i>	1.61	Fig. 16 (this study)
<i>M. olsufiewi</i>	0.69	Fig. 1 (Brindle 1967)
<i>M. longicornis</i>	1.35	Fig. 16 (Hincks 1955)
<i>M. gracillimus</i>	1.75	Fig. 4 (Brindle 1966)
<i>M. mucronatus</i>	1.35	Fig. 4 (Brindle 1969)
<i>M. major</i>	1.27	Fig. 1 (Brindle 1966)
<i>M. raharizoninai</i>	1.90	Fig. 5 (Brindle 1969)

remaining segments gradually lengthening. Pronotum (Figs 1, 8) slightly longer than broad; anterior margin almost straight; humeral angles strong; sides weakly narrow posteriorly; posterior margin broadly rounded; median sulcus visible but not distinct; prozona weakly raised. Tegmina (Figs 1, 8) well developed, approx. twice as wide as pronotum, 2.5 times as long as pronotum, broad triangular scutellum visible. Mesonotum with well-developed spiny ridge (a component of tegmina locking device sensu Haas 1995). Wings (Figure 1) well developed. Legs slender, notably long (Table 1); hind tarsi with segments I and II 3–3.5 times as long as III, claw with small arolium. Prosternum elongated, semi-rectangular, not constricted at middle; mesosternum hexagonal; metasternum semi-oval, narrowing posteriorly, posterior margin emarginated (Figure 3). Abdomen long, cylindrical, segments VIII and IX slightly expanded. Penul-

ultimate sternite (= sternite IX) elongated (Figs 4, 11), posterior margin almost truncate with rounded angles, regions at base of forceps weakly raised. Ultimate tergite (= tergite X) moderately inflated (Figs 5, 10), semi-oval, narrowing and sloping posteriorly. Forceps (cerci; Figs 5, 10, 11) slender, almost straight, densely pubescent especially on inner margins, tapering and weakly curving inward apically, inner margin with small tooth. Genitalia (Figs 6, 12–14), virga consists of bifurcated thin tubes, approx. three times as long as penis lobe, and 1.2 times as long as main part of genitalia (from base to distal end of paramere), spherical vesicle at base followed by short common duct; penis lobe also encloses sickle-shaped sclerite in characteristic swelling; parameres short, simple, triangular, distal part curving dorsally with many short spines near apex.

Female. Unknown.

Remarks. *Mesodiplatys falcifer* sp. n. is apparently allied to *M. venado* Anisyutkin, 2014 recorded from Peru. However, in addition to the characteristic sickle-shaped sclerite in the penis lobe, the former species is distinguished from the latter by possession of triangular parameres, penultimate sternite with truncated posterior margin, and pale coloration of the pronotum. This new species is also differentiated from all Malagasy members of the genus with the combination of the following characters: sickle-shaped, distinct sclerite in penis lobe; notably short parameres lacking dentiform curvature near base on inner margin and its articulation with main body of genitalia perpendicular to its anterior-posterior axis; eyes notably longer than POL (Table 2); and uniformly pale pronotum with darker tegmina.

Previous authors have noted that the male of the Malagasy species *M. insularis* (Borelli, 1932) has conspicuously large eyes, twice the POL in length (Hincks 1955; Brindle 1966, 1969). However, our reexamination of the holotype (male: Figure 15) at ZMH revealed that its eye length is only 1.6 times the POL (Figure 16), shorter than those of the two South American species (2.07–2.50) and some Malagasy species including *M. nanus* (Burr, 1914) and *M. raharizoninai* (Brindle, 1966) (Table 2). The genitalia of this species have not been illustrated. Although Borelli (1932) briefly described their characteristics including simple parameres and very long virga branches, the holotype does not include genitalia, which were likely removed from the main body. We were unable to locate any other slide-mounted materials derived from this specimen within the ZMH collection.

Thoracic traits, other than the shapes of the pronotum and tegmen, have not been described in detail for any Malagasy members of *Mesodiplatys* (Burr 1904, 1911, 1914; Borelli 1932a,b; Hincks 1953, 1955, 1957; Brindle 1966, 1967, 1969; Steinmann 1974, 1986a,b). In the single paratype female of this species (Figs. 17, 19), which has been preserved in ethanol, well-developed spiny ridges are visible through the tegmina (Figure 18). The morphologies of the thoracic sternites of this paratype are essentially similar to those of *M. falcifer* sp. n., including conspicuous emargination at the middle of the posterior margin of the metasternum (Figure 20). As another candidate member of *Mesodiplatys*, *Diplatys viator* Burr, 1904 has been reported from Madagascar. However, this species was described based only on a broken and discolored female specimen. Hincks (1955) treated *Diplatys hova* Burr, 1914, which was also described



Figures 15–20. **15, 16** *Mesodiplatys insularis* (Borelli, 1932) (male, holotype): **15** habitus **16** head, thorax, and proximal part of abdomen. **17–20** *Mesodiplatys insularis* (female, paratype): **17** habitus from above **18** thorax and proximal part of tegmina **19** habitus from below **20** metasternum. Blue arrowheads in **18** indicate spiny ridges. Broken line in **20** indicates the posterior margin of the metasternum. Scale bar: 2 mm.

from a single male collected in Madagascar, as a junior synonym of *D. viator*. Although Hincks found a possible female specimen of this species in Burr’s collection, he failed to trace the male holotype, leaving the position of this species doubtful.

Key to known *Mesodiplatys* species (males only)

- 1 Both pronotum and tegmina uniformly yellow or yellowish brown..... **2**
- Pronotum and/or tegmina uniformly blackish or dark brown, or pale brown with darker markings **6**
- 2 Small species, 9 mm or smaller in total length (including forceps) **3**
- Large species, 14 mm or larger in total length (including forceps)..... **4**
- 3 Virga short, not exceeding base of genitalia when in repose. Mucro at distal apex of parameres. No conspicuous denticulated sclerite in the penis lobe
..... *Mesodiplatys mucronatus* (Hincks, 1957)
- Virga relatively long, apparently exceeding base of genitalia. No mucro at distal apex of parameres. Rectangular denticulated sclerite in the penis lobe..
..... *Mesodiplatys nanus* (Burr, 1914)

- 4 Penultimate sternite truncate, not sinuated or notched at the middle of the posterior margin *Mesodiplatys raharizoninai* (Brindle, 1966)
- Posterior margin of penultimate sternite weakly sinuated at the middle, or with conspicuous emargination..... 5
- 5 Pronotum more than 1.5 times as long as broad
..... *Mesodiplatys longicornis* (Hincks, 1955)
- Pronotum almost quadrate, slightly longer than broad (Fig. 16)
..... *Mesodiplatys insularis* (Borelli, 1932)
- 6 Eyes very small, shorter than post-ocular length. Body shiny and black.....
..... *Mesodiplatys olsufewi* (Borelli, 1932)
- Eyes large, longer than post-ocular length. Body not shiny and black.....7
- 7 Tegmina blackish, with conspicuous yellow marking at center
..... *Mesodiplatys gracillimus* (Hincks, 1957)
- Tegmina not blackish. If blackish, then without conspicuous yellow marking at center..... 8
- 8 Minute dentiform curvature near base on inner margin of parameres. Forceps macrolabial, asymmetrical, with left branch more strongly curved than right.
..... *Mesodiplatys major* (Brindle, 1966)
- Inner margin of parameres uniformly rounded without dentiform curvature. Forceps symmetrical..... 9
- 9 Penis lobe lacks accessory sclerites. Posterior margin of penultimate sternite with conspicuous emargination at the middle. Pronotum, dark brownish. Paramere obtuse, thumb-shaped *Mesodiplatys venado* Anisyutkin, 2014
- Sickle-shaped sclerite in penis lobe. Penultimate sternite truncate, not sinuated at the middle of posterior margin. Pronotum pale. Parameres subtriangular *Mesodiplatys falcifer* Kamimura, sp. n.

Etymology. The species epithet refers to the sickle- or falx-shaped sclerite in the penis lobe, which is characteristic to this new species among the species of the genus *Mesodiplatys* known to date.

Distribution. Bahia, Brazil.

Discussion

Association with caves

This is the first report of a *Mesodiplatys* species from a cave habitat. The *Mesodiplatys falcifer* sp. n. specimen was collected in a cave (Lapa dos Peixes II) located in a region known as Serra do Ramalho, which is characterized by extensive limestone outcrops extending for dozens of kilometers. Lapa dos Peixes II is the cave furthest downstream among a four-cave system comprising more than 23 km of galleries. This cave represents a horizontal length of 2,100 m, and its main conduit contains some submerged

areas (lakes). The adult specimen was found freely walking on the surface of a speleothem, located around 700 m from the entrance and approximately 50 m deep from the ground surface. The speleothem contained guano spots, with associated troglobitic springtails and isopods. Three nymphs, possibly *Mesodiplatys falcifer* sp. n., were also found near the holotype collection site.

Two aspects of the position of this specimen within the cave are noteworthy. First, most earwigs observed in Brazilian caves have been found near the entrances, with rare exceptions such as *Euborellia janeirensis* (Dohrn, 1864), which was observed near guano piles in the aphotic zone of a sandstone cave (Kamimura and Ferreira 2017). Thus, it is uncommon for this group to occur in deeper zones of caves in Brazil. Second, the presence of possible nymphs of this species indicates an established population rather than occasional use of the cave.

Organisms that live in subterranean environments are frequently classified into three categories (e.g., Souza-Silva et al. 2011): i) troglonexes, which are occasionally found in caves or use caves as night-time or daytime shelters, ii) troglophiles, which can complete their entire life cycle inside or outside caves, and iii) troglobites, which do not occur in epigeal habitats. Troglobites, especially those recently adapted to cave life, do not necessarily possess highly modified morphology (troglomorphy) for their exclusively hypogean life. For example, the troglobitic stonefly species *Protonemoura gevi* Tierno de Figueroa et López-Rodríguez, 2010 (Plecoptera: Nemouridae) has smaller eyes and longer antennae than related congeners. Nevertheless, its general appearance resembles that of related species on the surface (Tierno de Figueroa and López-Rodríguez 2010). Although *Mesodiplatys falcifer* sp. n. possesses well-developed eyes, its appendages are relatively long considering its smaller body size than that of *M. venado*, which is putatively the most closely related species (Table 1). Furthermore, pigmentation is reduced in some body parts. Similar conditions have been reported in *Haplodiplatys milloti* (Chopard, 1940) (Haplodiplatyidae), which has been exclusively reported from an entirely dark part of an African cave (Chopard 1940). In *Mesodiplatys falcifer* sp. n., the developed eyes could be used to sense light, allowing it to avoid entrance zones or external environments, as has been observed in some troglobitic beetles (Bartkowiak et al. 1991; Pellegrini and Ferreira 2011). Given the extremely dry external environment in the collection area, as well as the intense deforestation that increased in the last decades, these caves represent a suitable but isolated habitat, providing more stable temperatures and higher humidity than the surrounding epigeal habitats. Hence, this new species might be a troglophile like *E. janeirensis* or a troglobite endemic to caves of the region. Further samples and studies of the ecology of this new species are necessary to determine the status of this species.

Distribution of *Mesodiplatys* species

Mesodiplatys falcifer sp. n. is the first diplatyid species described from Brazil except for *Cylindrogaster* spp. (Cylindrogastrinae), which are characterized by simple, non-bifurcated virgae (Haas 2012; Kamimura and Ferreira 2017). In both *M. venado* and

M. falcifer sp. n., the parameres are much shorter than the entire length of the male genitalia, and are articulated with the main body perpendicular to its anterior-posterior axis. These similarities in genital morphology strongly support the view that these two South American species form a monophyletic clade. As suggested by Anisyutkin (2014), the monophyly of the genus as a whole is also supported by multiple genital characteristics: the relatively simple structure of the parameres, which lack branching and/or accessory structures (epimeres), and the whip-like bifurcated virgae, which have very short, undivided parts. However, parallel evolution of genital structures has been reported in several insect groups (e.g., Yoshizawa et al. 2016). Molecular studies are needed to confirm the phylogenetic relationships between Malagasy and South American *Mesodiplatys* species.

Under the assumption that *Mesodiplatys* is monophyletic, the present study provides further evidence of their enigmatic disjunct distribution. From South America (Republic of Colombia and southward), only approximately 20 species belonging to Diplatyidae or Haplodiplatyidae have been reported to date (Popham 2000). Nevertheless, recent successive discoveries of *Mesodiplatys* spp. (Anisyutkin 2014; this study) strongly indicate that this region has not been sufficiently surveyed. Although far more Diplatyidae + Haplodiplatyidae species (> 35) have been reported from Africa (Popham 2000), only one cavernicolous species, *Haplodiplatys milloti*, has been reported (Chopard 1940). Further exploratory studies of cave earwig fauna are required before it can be concluded that *Mesodiplatys* spp. are extinct in Africa or have expanded their distribution between Madagascar and South America.

Definitions of the genus *Haplodiplatys* and the family Haplodiplatyidae

Although the phylogenetic relationships between dermapteran taxa remain largely unsettled, detailed studies on their morphology suggest paraphyly of Diplatyidae *sensu lato* (including Haplodiplatyidae), among which *Haplodiplatys* is one of the earliest offshoots of Neodermaptera (Haas 1995; Haas and Kukalová-Peck 2001; Haas and Klass 2003; Klass 2003). Many species of the genus *Haplodiplatys* are characterized by multiple features presumed to be plesiomorphic, including laterally symmetrical tegmina, the absence of a spiny ridge on the dorsal side of the mesothorax, and poor differentiation of the head into frontal and occipital regions (Hincks 1955; Haas 1995; Haas and Kukalová-Peck 2001). According to this view, Engel removed this genus from Diplatyidae and placed it in the monogeneric family Haplodiplatyidae (Engel et al. 2017). Engel et al. (2017) also noted that the posterior margin of the metasternum is straight in *Haplodiplatys*, but frequently concave in Diplatyidae. *Mesodiplatys falcifer* sp. n., however, possesses well-developed spiny ridges together with laterally asymmetrical tegmina (Figs. 1, 8), as do *M. venado* (Anisyutkin 2014) and *M. insularis* (Figs. 16, 18). In these species, the posterior margin of the metasternum is emarginated, as is common in Diplatyidae. Thus, aside from the relatively simple structure of the parameres, which may be homoplasious, there is no reason to move *Mesodiplatys* from Diplatyidae to Haplodiplatyidae.

Steinmann (1974; 1986b) revised the taxonomy of Diplatyidae sensu lato (as Diplatyinae in Pygidicranidae) mainly based on parameres shape, a trait which is usually described and illustrated in contemporary taxonomic studies of Dermaptera. In contrast, the spiny ridges and metasternum have seldom been described in detail in previous studies. These structures should be carefully observed in future studies to stabilize the taxonomy of this group.

Acknowledgments

We are grateful to the team at the Center of Studies in Subterranean Biology at the Federal University of Lavras (CEBS/UFLA) for their efforts during sampling. We also thank Martin Husemann and Thure Dalsgaard for their help in taking photographs of the specimens at ZMH, and Petr Kočárek, Leonid N. Anisyutkin, and Masaru Nishikawa for useful comments on a previous version of the manuscript. This study was partly supported by Japan Society for the Promotion of Science (JSPS) research grants (Kakenhi Nos. 15H04409 [head, Kazunori Yoshizawa] and 15K07133) to YK and a CNPq grant (n.304682/2014-4 from the Conselho Nacional de Desenvolvimento Científico e Tecnológico) to RLF.

References

- Ali JR, Krause DW (2011) Late Cretaceous bioconnections between Indo-Madagascar and Antarctica: refutation of the Gunnerus Ridge causeway hypothesis. *Journal of Biogeography* 38: 1855–1872. <https://doi.org/10.1111/j.1365-2699.2011.02546.x>
- Anisyutkin LN (2014) *Mesodiplatys venado* sp. nov. (Dermaptera: Diplatyidae), probable evidence of contact between Neotropical and Malagasy faunas. *Zookeys* 3794: 593–599. <https://doi.org/10.11646/zootaxa.3794.4.11>
- Bartkowiak D, Tschardt T, Weber F (1991) Effects of stabilizing selection in the regressive evolution of compound eyes in hypogean carabid beetles. *Mémoires de Biospéologie* 18: 19–24.
- Borelli A (1932a) Dermaptères nouveaux du Muséum zoologique de Hamburg. *Konowia* 11: 87–97.
- Borelli A (1932b) Dermaptères de Madagascar. *Bulletin de la Société des naturalistes luxembourgeois (N Série)* 26: 56–58.
- Brindle A (1966) The Dermaptera of Madagascar. *Transactions of the Royal Entomological Society of London* 118: 221–259. <https://doi.org/10.1111/j.1365-2311.1966.tb02305.x>
- Brindle A (1967) A designation of a neo-type for *Diplatys osofewi* Borelli (Dermaptera, Diplatyidae), with a redescription of the species. *Entomologist's Monthly Magazine* 103: 73–76.
- Brindle A (1969) Dermaptera. *Fauna de Madagascar, Paris* 30: 1–112.
- Burr M (1904) Observations on the Dermaptera, including revisions of several genera and descriptions of New Genera and Species. *Transactions of the Entomological Society of London* 1904: 277–322. <https://doi.org/10.1111/j.1365-2311.1904.tb02747.x>

- Burr M (1911) A revision of the genus *Diplatys* Serville (Dermaptera). Transactions of the Entomological Society of London 1911: 21–47.
- Burr M (1914) Notes on the Forficularia. XXIII. More new Species. Annals and Magazine of Natural History 8: 420–428. <https://doi.org/10.1080/00222931408693597>
- Case JA (2002) A new biogeographical model for dispersal of late Cretaceous vertebrates into Madagascar and India. Journal of Vertebrate Paleontology 22 (3, supplement): 42A.
- Chopard L (1940) Un remarquable Dermaptera cavernicole de l'Afrique occidentale, *Diplatys milloti* sp. n. Bulletin de la Société Zoologique de France 65: 75–79.
- Engel MS, Huang D, Thomas JC, Cai C (2017) A new genus and species of pygidicranid earwigs from the Upper Cretaceous of southern Asia (Dermaptera: Pygidicranidae). Cretaceous Research 69: 178–183. <https://doi.org/10.1016/j.cretres.2016.09.009>
- Haas F (1995) The phylogeny of the Forficulina, a suborder of the Dermaptera. Systematic Entomology 20: 85–98. <https://doi.org/10.1111/j.1365-3113.1995.tb00085.x>
- Haas F (2012) A Ordem Dermaptera. In: Rafael JA, Melo ARG, Carvalho CJB, Casari SA, Constantino R (Eds) Insetos do Brasil: diversidade e taxonomia. Holos Editora, Sao Paulo, Brazil, 297–305.
- Haas F, Klass K-D (2003) The basal phylogenetic relationships in the Dermaptera. In: Klass K-D (Ed.) Proceedings of the 1st Dresden meeting on insect phylogeny: Phylogenetic Relationships within the Insect Orders (Dresden, September 19–21, 2003). Entomologische Abhandlungen 61: 138–142. http://www.senckenberg.de/files/content/forschung/publikationen/arthropodsystematics/ea_61_2/ea_61_2-119-172_klass.pdf
- Haas F, Kukalová-Peck J (2001) Dermaptera hindwing structure and folding: New evidence for familial, ordinal and superordinal relationships within Neoptera (Insecta). European Journal of Entomology 98: 445–509. <https://doi.org/10.14411/eje.2001.065>
- Hadley A (2008) *Combine ZM imaging software*. Available from: <https://combinezm.en.lo4d.com/details> [Accessed 10 February 2018]
- Hincks WD (1953) Liste préliminaire des Dermapteres de Madagascar. Mémoires de l'Institut Scientifique de Madagascar (E)4: 361–382.
- Hincks WD (1955) A Systematic Monograph of the Dermaptera of the World. Part I. Pygidicranidae. Subfamily Diplatyinae. British Museum (Natural History), London, 132 pp.
- Hincks WD (1957) New species of the genus *Diplatys* Serville (Dermaptera: Pygidicranidae). Proceedings of the Royal Entomological Society of London B 26: 149–154.
- Kamimura Y (2014) Pre- and postcopulatory sexual selection and the evolution of sexually dimorphic traits in earwigs (Dermaptera). Entomological Science 17: 139–166. <https://doi.org/10.1111/ens.12058>
- Kamimura Y, Ferreira RL (2017) Earwigs from Brazilian caves, with notes on the taxonomic and nomenclatural problems of the Dermaptera (Insecta). ZooKeys 713: 25–52. <https://doi.org/10.3897/zookeys.713.15118>
- Klass K-D (2003) The female genitalic region in basal earwigs (Insecta: Dermaptera: Pygidicranidae s.l.). Entomologische Abhandlungen 61: 173–225. http://www.senckenberg.de/files/content/forschung/publikationen/arthropodsystematics/ea_61_2/ea_61_2-173-225_klass.pdf
- Noonan BP, Chippindale PT (2006a) Dispersal and vicariance: The complex evolutionary history of boid snakes. Molecular Phylogenetics and Evolution 40: 347–358. <https://doi.org/10.1016/j.ympev.2006.03.010>

- Noonan BP, Chippindale PT (2006b) Vicariant origin of Malagasy reptiles supports Late Cretaceous Antarctic land bridge. *The American Naturalist* 168: 730–741. <https://doi.org/10.1086/509052>
- Pellegrini TG, Ferreira RL (2011) *Coarazuphium tapiaguassu* (Coleoptera: Carabidae: Zuphiini), a new Brazilian troglobitic beetle, with ultrastructural analysis and ecological considerations. *Zootaxa* 3116: 47–58.
- Popham EJ (2000) The geographical distribution of the Dermaptera (Insecta) with reference to continental drift. *Journal of Natural History* 34: 2007–2027. <https://doi.org/10.1080/00222930050144837>
- Sakai S (1996) *Dermapterorum Catalogus XXXI: Notes on contemporary classification of Dermaptera and recent references of Dermaptera*. Daito Bunka University, Tokyo, 588 pp.
- Souza-Silva M, Martins RP, Ferreira RL (2011) Cave lithology determining the structure of the invertebrate communities in the Brazilian Atlantic Rain Forest. *Biodiversity and Conservation* 20: 1713–1729. <https://doi.org/10.1007/s10531-011-0057-5>
- Steinmann H (1974) A new generic classification of the species group of *Diplatys* Serville (Dermaptera: Pygidicranidae). *Acta Zoologica Academiae Scientiarum Hungaricae* 20: 187–205.
- Steinmann H (1986a) Dermaptera. Catadermaptera I. *Das Tierreich* 102: 1–343.
- Steinmann H (1986b) A new generic classification for the *Diplatys* species-groups (Dermaptera: Pygidicranidae). *Acta Zoologica Hungarica* 32: 169–179.
- Tierno de Figueroa JM, López-Rodríguez MJ (2010) *Protonemura gevi* sp. n., a cavernicolous new species of stonefly (Insecta: Plecoptera). *Zootaxa* 2365: 48–54.
- Yoshizawa K, Yao I, Lienhard C (2016) Molecular phylogeny reveals genital convergences and reversals in the barklouse genus *Trichadenotecnum* (Insecta: Psocodea: 'Psocoptera': Psocidae). *Molecular Phylogenetics and Evolution* 94: 358–364.

Review of the bamboo-feeding leafhopper genus *Neomohunia*, with descriptions of two new species from China (Hemiptera, Cicadellidae, Deltocephalinae, Mukariini)

Qiang Luo^{1,2}, Lin Yang^{1,2}, Xiang-Sheng Chen^{1,2,3}

1 Institute of Entomology, Guizhou University, Guiyang, Guizhou, 550025, PR China **2** The Provincial Special Key Laboratory for Development and Utilization of Insect Resources of Guizhou, Guizhou University, Guiyang, Guizhou, 550025, PR China **3** Guizhou Key Laboratory for Plant Pest Management of Mountainous Region, Guizhou University, Guiyang, Guizhou, 550025, PR China

Corresponding author: Xiang-Sheng Chen (chenxs3218@163.com)

Academic editor: M. Webb | Received 24 April 2018 | Accepted 30 August 2018 | Published 15 October 2018

<http://zoobank.org/8901CF56-1F16-4BAA-BB58-B8AA37AF7CDA>

Citation: Luo Q, Yang L, Chen X-S (2018) Review of the bamboo-feeding leafhopper genus *Neomohunia*, with descriptions of two new species from China (Hemiptera, Cicadellidae, Deltocephalinae, Mukariini). ZooKeys 790: 101–113. <https://doi.org/10.3897/zookeys.790.26130>

Abstract

The bamboo-feeding leafhopper genus *Neomohunia* Chen & Li, 2007, is reviewed to include three species: *N. longispina* **sp. n.**, *N. pyramida* (Li & Chen, 1999), and *N. sinuatipenis* **sp. n.** The generic characteristics are redefined and the new species are described and illustrated. A key to species based on male genitalia is also provided.

Keywords

Homoptera, morphology, Oriental region, taxonomy

Introduction

Chen and Li (2007) established the Chinese bamboo-feeding leafhopper genus *Neomohunia* (Cicadellidae: Deltocephalinae: Mukariini) for *Mohunia pyramida* Li & Chen, 1999 (type species). The genus belongs to the tribe Mukariini based on body medium sized, with orange, brown and reddish orange markings dorsally; head

moderately produced; ocelli distant from eyes; frontoclypeus strongly convex basally, depressed apico-medially, without median carina. Forewing venation obscure except near apex, with four apical cells and appendix well developed.

In this paper, two new species: *N. longispina* sp. n. and *N. sinuatipennis* sp. n., from China are described and illustrated. A key based on male genitalia to distinguish males of all three included species is given.

Materials and methods

Terminology used for morphological and genital characters follow Li et al. (2011) and Zahniser and Dietrich (2013). Leg chaetotaxy follows Dietrich (2005). All specimens were collected by sweep net, dry male specimens were used for the description and illustration. External morphology was observed under a stereoscopic microscope and characters were measured with an ocular micrometer. Measurements are given in millimeters; body length is measured from the apex of the head to the apex of the forewing in repose. Habitus photographs were taken using a KEYENCE VHX-1000 system. The genital segments of the specimens examined were macerated in 10% NaOH and drawn from preparations in glycerin jelly using a Leica MZ 12.5 stereomicroscope. The photographs and the illustrations were scanned with Canon CanoScan LiDE 100 and imported into Adobe Photoshop CS5 for plate composition and labeling.

The type specimens examined are deposited in the Institute of Entomology, Guizhou University, Guiyang, Guizhou Province, China (IEGU) and the Natural History Museum, UK (NHMUK).

Taxonomy

Genus *Neomobunia* Chen & Li, 2007

Type species. *Mobunia pyramida* Li & Chen, 1999, by original designation.

Diagnosis. The genus is separated from other similar genera of Mukariini by crown rounded to face, without apical transverse marginal carina; frontoclypeus strongly convex dorsally, depressed ventro-medially; male pygofer with one or two processes at caudal apex; subgenital plate with numerous macrosetae laterally; aedeagus with pair of spinous processes arising from base, with or without a single ventral basal medial process.

Description. Medium-sized, delicate leafhoppers; with orange, brown and reddish orange markings dorsally including reddish medial longitudinal stripe on head and pronotum.

Head and thorax. Head moderately produced, apex in profile truncate (Figs 4, 17, 29). Crown slightly convex and rounded to face, without anterior marginal carina, median length subequal to width between eyes (Figs 3–4, 16–17, 28–29); coronal

suture short; ocelli near crown margin, equidistant from eyes to crown apex (Figs 4, 17, 29). Face with frontoclypeus strongly convex basally, depressed apico-medially, without median carina; clypellus with lateral margins parallel; lorum broad (Figs 5, 18, 30). Pronotum broad, wider than head including eyes, with lateral margins divergent posteriorly, anterior margin strongly convex between eyes, posterior margin weakly concave (Figs 1, 3, 14, 16, 26, 28). Mesoscutum and scutellum together wider than long, transverse suture slightly curved and depressed, not reaching lateral margin (Figs 3, 16, 28). Forewing elongate, considerably longer than abdomen, with four apical cells, venation obscure except near apex, vein M_{3+4} originating from inner antepical cell, converging toward middle of appendix; appendix well developed (Figs 1–2, 14–15, 26–27). Hind wing with four closed apical cells. Profemur with AM1 and AV1 present, intercalary row with 10 or more slender setae. Protibia with macrosetal formula 7+1 and approximately 14 macrosetae of equal length in row AV (Figure 23). Hind femur macrosetal formula 2+2+1.

Male genitalia. Male pygofer broad at base in lateral aspect, tapering caudally with one or two processes at caudal apex; with macrosetae ventrocaudally (Figs 8–9, 21–22, 33–34). Valve triangular (Figs 10, 20, 32). Subgenital plate nearly triangular, with numerous macrosetae laterally (Figs 10, 20, 32). Connective Y-shaped, with stem longer than arms, apex broad (Figs 11, 24, 35). Aedeagus with pair of spinous processes arising either dorsobasally on shaft or from preatrium, with or without a single ventral basal medial process; gonopore apical or subapical on dorsal surface (Figs 11–13, 24–25, 35–36). Style with articulating arm moderately long and robust, apophysis digitate, slightly laterally curved (Figs 6, 19, 31).

Female genitalia. Sternite VII (Figs 37, 40, 43) with posterior margin strongly or slightly convex, with or without acute median tooth. First valvula (Figs 38, 41, 44) weakly curved, tapering apically with strigate sculpture extended to dorsal margin. Second valvula (Figs 39, 42, 45) broad, widest at distal two thirds, thereafter gradually tapered to acute apex; dorsal margin with numerous triangular, distinct and regular teeth; with dorsal sclerotized and hyaline region and dorsal prominence (in *N. sinuatipenis*).

Host plants. Bamboo.

Distribution. China (Guizhou).

Key to species of the genus *Neomohunia* (males)

- 1 Aedeagal shaft with a ventral medial process arising from basal one-third of shaft (Figs 24–25) *N. pyramida* (Li & Chen)
- Aedeagal shaft without a medial ventral process 2
- 2 Aedeagal shaft sinuate in lateral view, with two dorsal processes arising from base (Figs 35–36) *N. sinuatipenis* sp. n.
- Aedeagal shaft evenly curved in lateral view; three spinous processes arising from base of preatrium of aedeagus (Figs 11–13) *N. longispina* sp. n.

***Neomobunia longispina* sp. n.**

<http://zoobank.org/3E6AADA6-89B0-4A03-B305-6417F4F36832>

Figs 1–13, 37–39, 48

Diagnosis. The salient characteristics of the new species include the pygofer in profile with pair of small unequal spines arising directly from posteroventral margin (Figs 8–9), and the aedeagus with its shaft slightly laterally compressed, with three spinous processes arising from base of long preatrium (Figs 11–13).

Description. *Measurements.* Body length (including forewing): male 5.11–5.67 mm (7 specimens); female 5.92–5.98 mm (4 specimens).

Coloration. Crown and pronotum pale yellow to white, with a longitudinal medial bright red band widening from apex of head to base of pronotum (Figs 1, 3). Eyes yellowish brown to brown (Figs 2, 4). Face yellow, anteclypeus, and lorum yellowish white (Figure 5). Mesoscutum and scutellum brown (Figs 1, 3). Forewing orange red to red, clavus with a longitudinal broad brown stripe along lateral margin (Figs 1, 2, 7); brachial cell with a bright red stripe along inner margin (Figs 1, 2, 7); brachial cell at apex, inner antepical cells near m-cu₃, costal margin near middle, outer apical cell near R₂₊₃ with dark brown markings (Figs 1, 2, 7); outer and central antepical cells with a pellucid spot at apex, inner apical cell slightly brown (Figs 1, 2).

Head and thorax. External features as in generic description with following proportions. Crown slightly shorter medially than width between eyes (0.68:1) (Figs 1, 3); coronal suture shorter than half of length of crown in median line (0.35:1) (Figs 1, 3). Pronotum slightly wider than head including eyes (1.19:1) and about 2 times longer than head (1.85:1) (Figs 1, 3). Mesoscutum and scutellum together distinctly shorter than pronotum (0.70:1) (Figure 3). Forewing about 3 times longer than widest part (2.75:1) (Figs 1, 2).

Male genitalia. Pygofer in profile with pair of small unequal spines arising directly from posteroventral margin (Figs 8–9). Aedeagus with shaft slightly laterally compressed, gonopore subapical on dorsal surface; with three spinous processes arising from base of long preatrium, two shorter lateral processes directed obliquely outwards and a longer medial process curving ventrally from base at its articulation with connective then curved dorsally and tapered to acute apex (Figs 11–13).

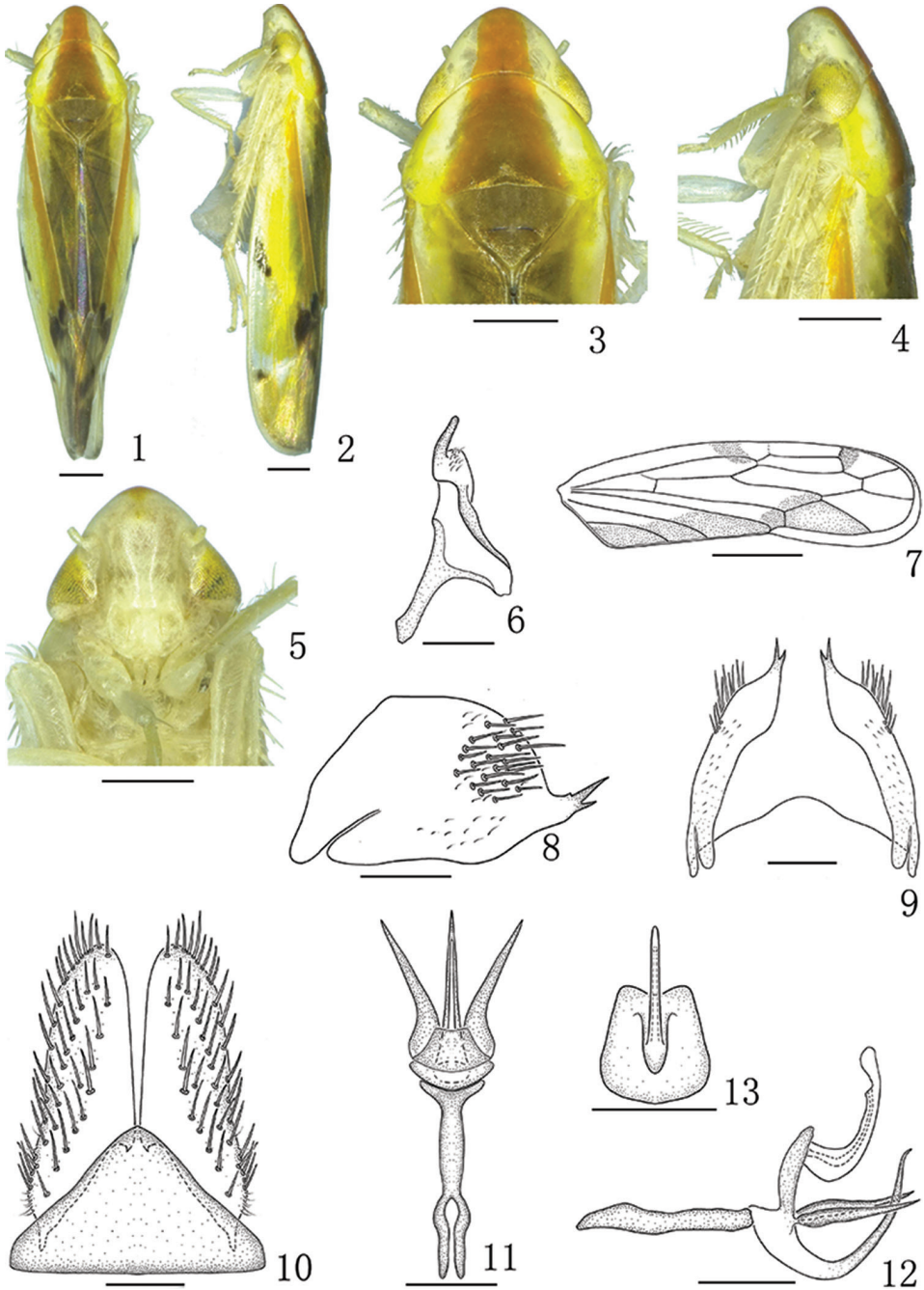
Female genitalia. Sternite VII (Figure 37) with anterior margin slightly concave; lateral margin slightly expanded at basal 1/3; posterior margin strongly convex and with acute median tooth. Ovipositor as in generic description.

Material examined. Holotype: ♂, **China:** Guizhou Province, Xishui County, Sanba Nature Reserve (28°20'N, 106°12'E), 27 September 2017, Bin Yan and Nian Gong (IEGU); paratypes: 4♂♂3♀♀, same data as holotype (IEGU); 2♂♂1♀, same data as holotype (NHMUK).

Host plant. Bamboo (Figure 48).

Distribution. China (Guizhou Province).

Remarks. This species can be distinguished from other species mainly by the unusual position of the aedeagal processes at the base of the preatrium (Figs 11–13).



Figures 1–13. *Neomohunia longispina* sp. n., male **1** Male habitus, dorsal view **2** Male habitus, lateral view **3** Head and thorax, dorsal view **4** Head and thorax, lateral view **5** Face **6** Style, dorsal view **7** Forewing **8** Male pygofer, lateral view **9** Male pygofer, ventral view **10** Valve and subgenital plate, ventral view **11** Connective and aedeagus, dorsal view **12** Connective and aedeagus, lateral view **13** Shaft and preatrium, caudal view. Scale bars: 0.5 mm (**1–5, 7**); 0.2 mm (**6, 8–13**).

Etymology. The name is derived from prefix *longi* and the Latin word *spina*, which refers to the long medial process of the aedeagus.

***Neomohunia pyramida* (Li & Chen, 1999)**

Figs 14–25, 40–42, 46–47

Mohunia pyramida Li & Chen, 1999: 123, figs 1–10.

Neomohunia pyramida: Chen, Li and Yang 2007: 373, figs 36–46.

Diagnosis. This species has a pygofer which, in profile, is more triangular with its apex tapering into a single stout spinous process, the dorsal margin sinuate (Figs 21–22), the aedeagal shaft (Figs 24–25) curved dorsally, tubular with apex blunt, and with a ventral medial process arising from basal one-third and two processes arising dorsobasally (Figs 24–25).

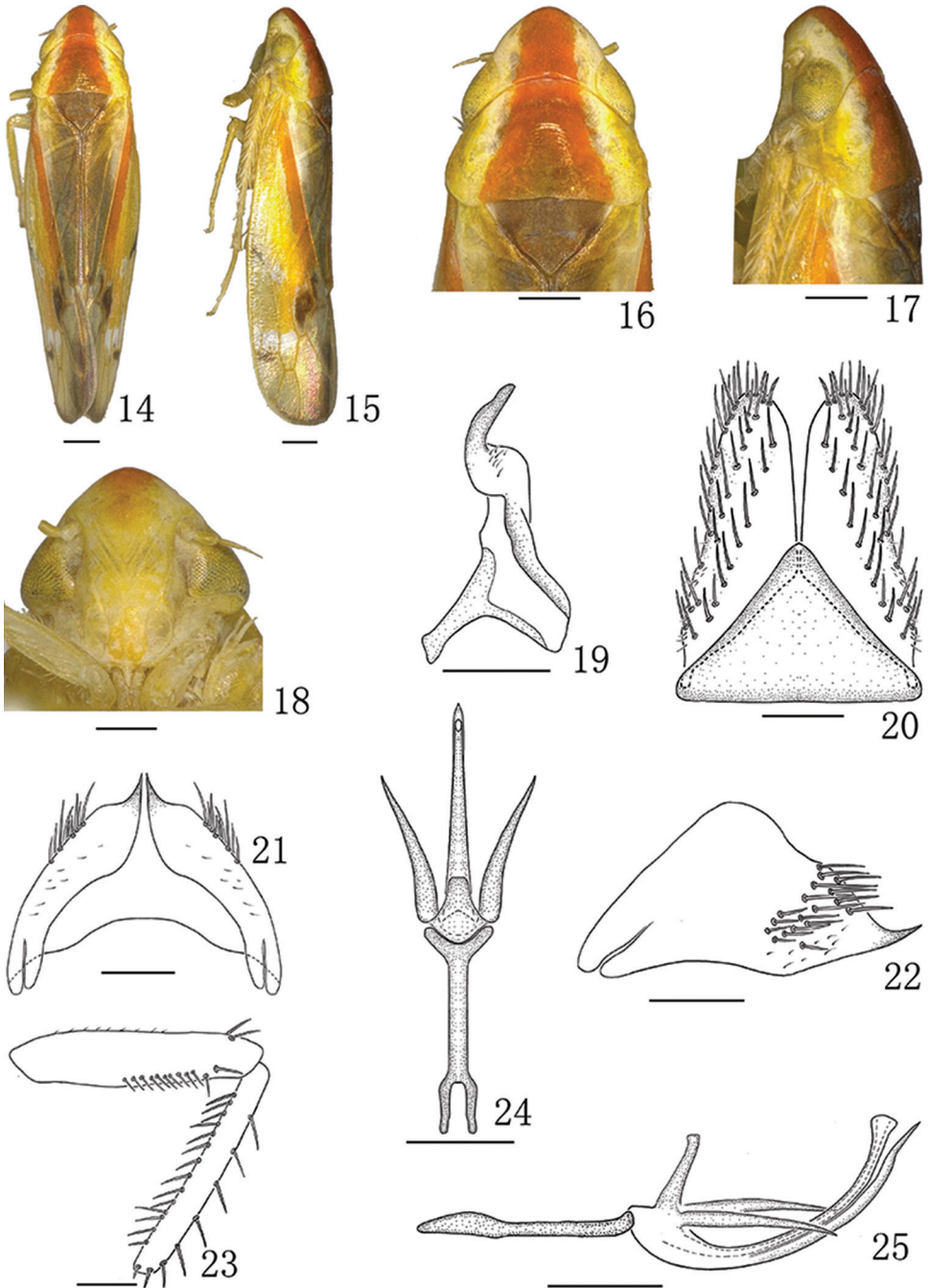
Description. *Measurement.* Body length (including forewing): male 5.12–5.46 mm (37 specimens), female 5.81–6.07 mm (48 specimens).

External features as in *N. longispina*.

Male genitalia. Male genitalia as in previous species but pygofer in profile more triangular with apex tapering into a single stout spinous process, dorsal margin sinuate (Figs 21, 22). Aedeagal shaft (Figs 24, 25) curved dorsally, tubular with apex blunt, one spinous process arising ventrally from basal one-third thereafter closely appressed to shaft and then diverging at distal one-third; another processes arising on each side dorsobasally, directed caudally; gonopore apical.

Female genitalia. Sternite VII (Figure 40) with both anterior margin and posterior margin slightly concave. Ovipositor as in generic description.

Material examined. 1♂ (holotype), **China:** Guizhou Province, Suiyang County, Kuankuoshui Nature Reserve (27°58'N, 107°11'E), 28 July 1984, Zi-Zhong Li (IEGU); 5♂♂11♀♀ (paratypes), same data as holotype (IEGU); 1♂1♀ (paratypes), same data as holotype (NHMUK). 1♂4♀♀ (paratypes), Guizhou Province, Jiangkou County, Fanjingshan National Nature Reserve (27°55'N, 108°41'E), 11 August 1984, Xiang-Sheng Chen and Mao-Fa Yang (IEGU); 2♂♂3♀♀, Guizhou Province, Suiyang County, Kuankuoshui Nature Reserve, 1 August 1984, Zi-Zhong Li (IEGU); 1♀, Guizhou Province, Guiyang City, Forest Park (26°35'N, 106°42'E), 12 June 2002, De-Yan Ge (IEGU); 1♂, Guizhou Province, Jiangkou County, Fanjingshan National Nature Reserve, 28 July 2002, Zi-Zhong Li (IEGU); 6♂♂9♀♀, Guizhou Province, Daozhen County, Dashahe Nature Reserve (28°53'N, 107°36'E), 22–23 May 2004, Xiang-Sheng Chen (IEGU); 15♂♂15♀♀, same locality, 17–24 August 2004, Xiang-Sheng Chen, Bin Zhang and Mao-Fa Yang (IEGU); 5♂♂ 4♀♀, Guizhou Province, Fanjingshan National Nature Reserve, 31 June 2004, Xiang-Sheng Chen (IEGU); 9♀♀, Guizhou Province, Suiyang County, Kuankuoshui Nature Reserve, 28 July 2014, Yan-Li Zheng (IEGU); 3♂♂2♀♀, Guizhou Province, Suiyang County, Kuankuoshui Nature Reserve, 12 July 2017, Nian Gong (IEGU).



Figures 14–25. *Neomohunia pyramida* (Li & Chen, 1999), male **14** Male habitus, dorsal view **15** Male habitus, lateral view **16** Head and thorax, dorsal view **17** Head and thorax, lateral view **18** Face **19** Style, dorsal view **20** Valve and subgenital plate, ventral view **21** Male pygofer, ventral view **22** Male pygofer, lateral view **23** Fore femur and tibia, anterior surface **24** Connective and aedeagus, dorsal view **25** Connective and aedeagus, lateral view. Scale bars: 0.5 mm (14–18); 0.2 mm (19–25).

Host plant. Bamboo (*Qiongzhusia communis* and *Fargesia spathacea*) (Figs 46, 47).

Distribution. China (Guizhou Province).

Remarks. We re-examined the type specimens of this species and found that there were some inaccuracies in original figures in Chen et al. (2007), e.g., the style was damaged. Hence, we have redrawn the species and provide digital images of the male adult. The species resembles *N. sinuatipenis* sp. n. but differs from the later by the aedeagal shaft being tubular with a blunt apex and with a ventral medial process arising from the basal one-third of shaft. Additionally, the gonopore is apical (Figs 24, 25).

***Neomohunia sinuatipenis* sp. n.**

<http://zoobank.org/709ECD56-9397-4B5F-80B7-A5915E1CDDFF6>

Figs 26–36, 43–45, 49–51

Diagnosis. The characteristics of the new species include the following: pygofer with ventro-posterior angle produced into one short and a long process arising directly from posteroventral margin (Figs 33, 34); aedeagus with shaft laterally compressed, sinuate in lateral view, with a pair of long spinous processes arising dorsobasally, curved caudoventrally (Figs 35, 36).

Description. *Measurements.* Body length (including forewing): male 4.87–5.30 mm (10 specimens); female 5.51–5.84 mm (8 specimens).

External features as in *N. longispina* but body slightly smaller.

Male genitalia. Male pygofer as in *N. longispina* but pygofer with ventroposterior angle produced into one short and a long process arising directly from posteroventral margin, the shorter process directed posteriorly and the longer one directed dorsally (Figs 33–34). Aedeagus simple, with shaft laterally compressed, sinuate in lateral view, with a pair of long spinous processes arising dorsobasally, curved caudoventrally; gonopore subapical on dorsal surface (Figs 35–36).

Female genitalia. Sternite VII (Figure 43) as in *N. pyramida*. Ovipositor as in generic description.

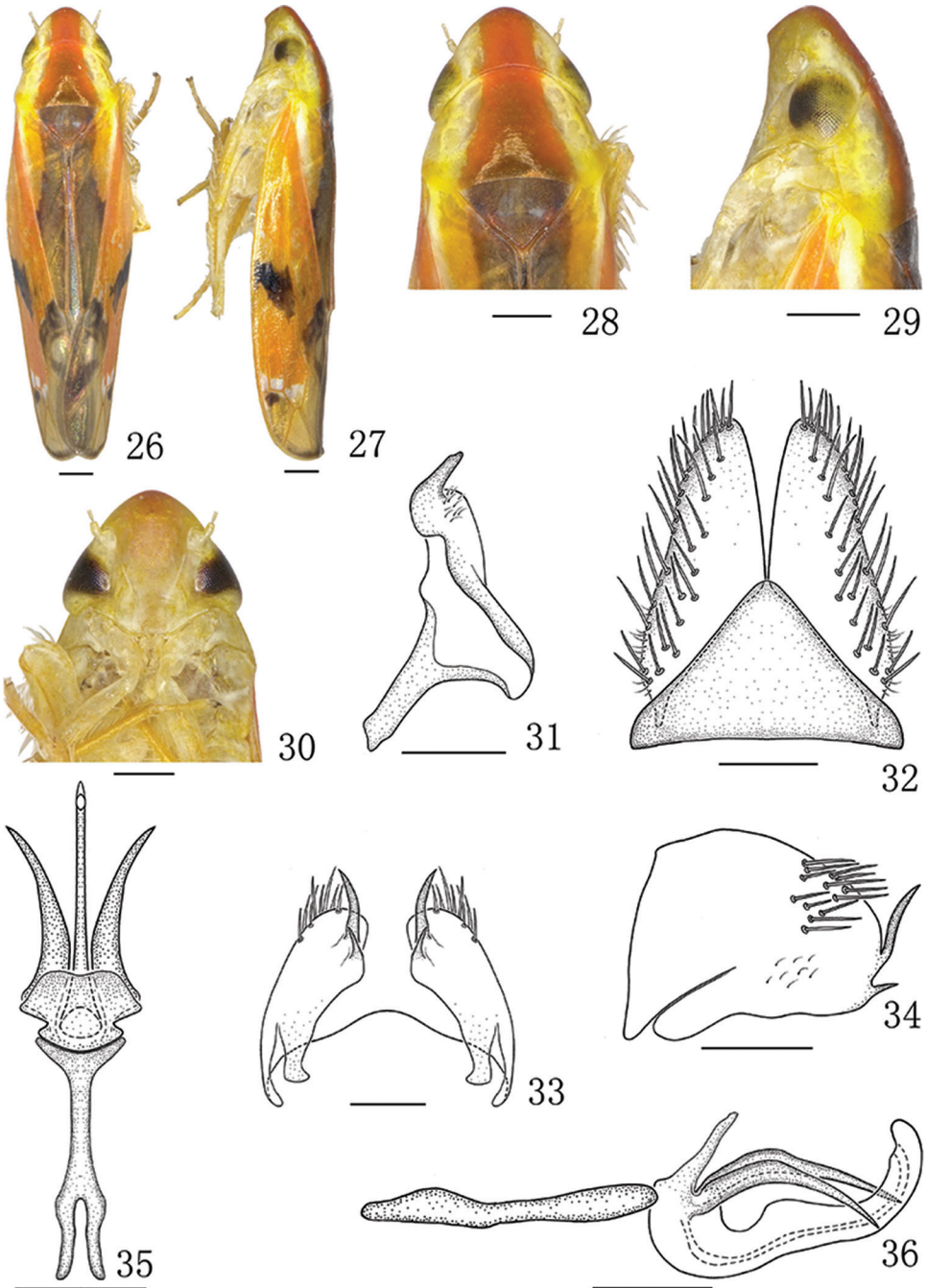
Material examined. Holotype: ♂, **China:** Guizhou Province, Duyun City, Doupengshan (26°22'N, 107°23'E), 18 August 2016, Jian-Kun Long (IEGU); paratypes: 1♂4♀♀, same locality, 24 September 2016, Qiang Luo and Ya-Lin Yao (IEGU); 1♂, Guizhou Province, Leishan County, Leigong Mountain (26°22'N, 108°10'E), 7 September 2014, Xiang-Sheng Chen (NHMUK); 7♂♂4♀♀, Guizhou Province, Anlong County, Xianheping (24°59'N, 105°37'E), 28 August 2012, Jian-Kun Long (IEGU).

Host plant. Bamboo (Figs 49–51).

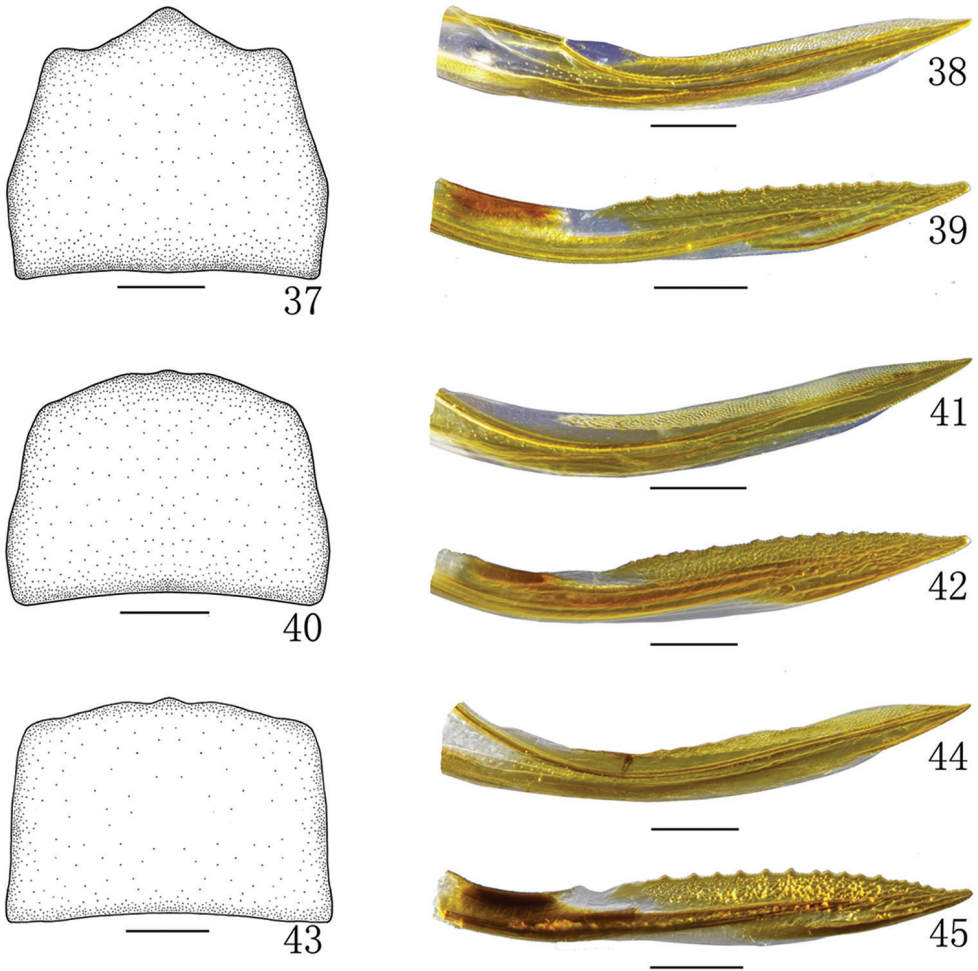
Distribution. China (Guizhou Province).

Remarks. The new species is similar to *N. pyramida* (Li & Chen, 1999), but differs in the aedeagal shaft being sinuate in lateral view, with two dorsal processes arising from base; the gonopore is subapical (Figs 35, 36).

Etymology. The name is derived from the Latin words *sinuosus* and *penis*, which refers to the sinuate aedeagal shaft in lateral view (Figure 36).



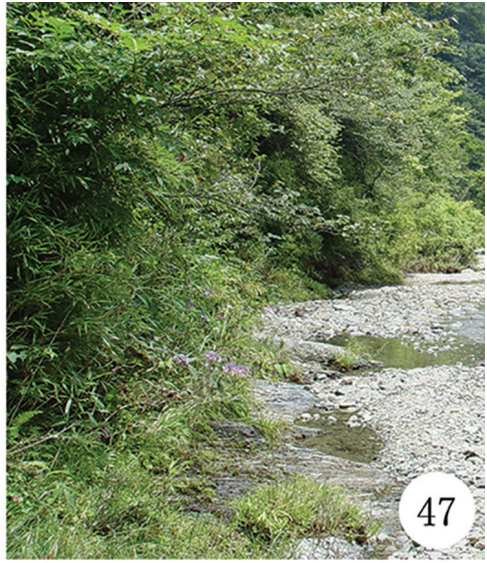
Figures 26–36. *Neomohunia sinuatipenis* sp. n., male **26** Male habitus, dorsal view **27** Male habitus, lateral view **28** Head and thorax, dorsal view **29** Head and thorax, lateral view **30** Face **31** Style, dorsal view **32** Valve and subgenital plate, ventral view **33** Male pygofer, ventral view **34** Male pygofer, lateral view **35** Connective and aedeagus, dorsal view **36** Connective and aedeagus, lateral view. Scale bars: 0.5 mm (**26–30**); 0.2 mm (**31–36**).



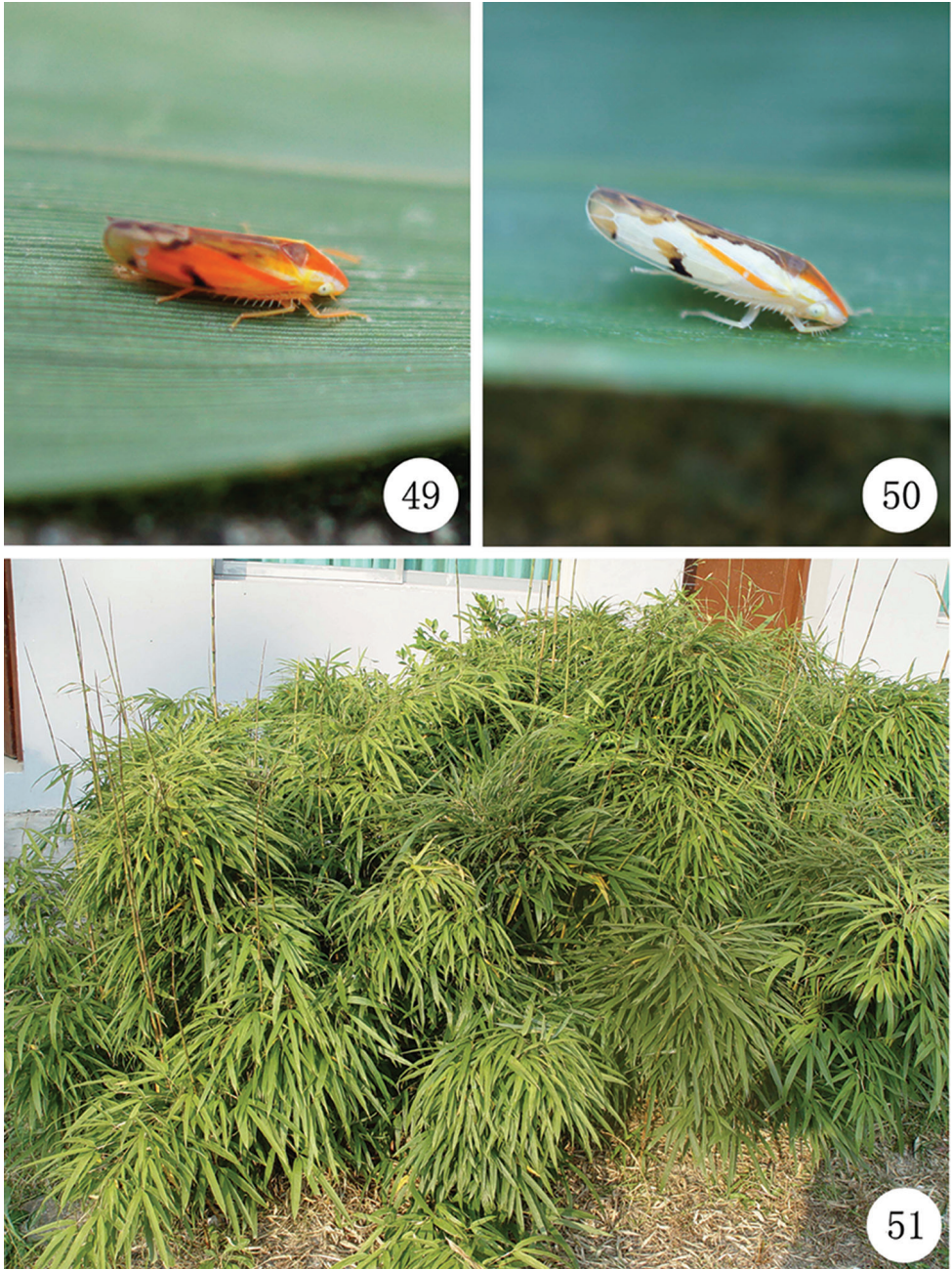
Figures 37–45. **37–39** *Neomohunia longispina* sp. n., female **37** Female sternite VII, ventral view **38** First valvula, lateral view **39** Second valvula, lateral view **40–42** *Neomohunia pyramida* (Li & Chen, 1999), female **40** Female sternite VII, ventral view **41** First valvula, lateral view **42** Second valvula, lateral view **43–45** *Neomohunia sinuatipennis* sp. n., female **43** Female sternite VII, ventral view **44** First valvula, lateral view **45** Second valvula, lateral view. Scale bars: 0.2 mm (**37–45**).

Discussion

Species of *Neomohunia* are distinctly marked leafhoppers, mainly with orange, brown and reddish orange markings dorsally including a reddish medial longitudinal stripe on the head and pronotum. In the male genitalia they can be distinguished by the aedeagus with pair of spinous processes arising from base. All are very similar in coloration



Figures 46–48. **46** *Neomohunia pyramida* (Li & Chen, 1999) resting on a leaf of host plant (bamboo) **47** The habitat photo of *N. pyramida* (Li & Chen, 1999) (Guizhou Province, Daozhen County, Dashahe, 19 August 2004, photography by Xiang-Sheng Chen) **48** The habitat photo of *Neomohunia longispina* sp. n. (Guizhou Province, Xishui County, Sanba Nature Reserve, 27 September 2017, photography by Nian Gong).



Figures 49–51. *Neomohunia sinuatipenis* sp. n. **49** *N. sinuatipenis* sp. n. resting on a leaf of host plant (bamboo)(male) **50** *N. sinuatipenis* sp. n. resting on a leaf of host plant (bamboo)(female) **51** The habitat photo of *N. sinuatipenis* sp. n. (Guizhou Province, Leishan County, Leigong Mountain, 7 September 2014, photography by Xiang-Sheng Chen).

and difficult to distinguish externally, but can be easily separated from other species by the structure of male genitalia: (1) aedeagal shaft evenly curved in lateral view; three spinous processes arising from base of preatrium of aedeagus in *N. longispina* sp. n.; (2) aedeagal shaft with a ventral medial process arising from basal one-third of shaft in *N. pyramida*; (3) aedeagal shaft sinuate in lateral view in *N. sinuatipennis* sp. n.

As a result of our investigation in the field, members of *Neomohunia* were found feeding exclusively on some native bamboos, with many specimens collected from the beginning of May to the end of September in Guizhou province. So far, there are no collection records in other zoogeographic regions or on other plants in China, which may suggest that the distribution and host of *Neomohunia* species are very limited. More precise ecological records are needed.

Acknowledgements

We are grateful to the specimen collectors for their hard work in the field collections, and also grateful to anonymous referees for their valuable comments. This work was supported by the National Natural Science Foundation of China (No. 31660209, 31860209), the Program of Excellent Innovation Talents, Guizhou Province (No. 20154021), the Program of Science and Technology Innovation Talents Team, Guizhou Province (No. 20144001) and the International Cooperation Base for Insect Evolutionary Biology and Pest Control (No. 20165802).

References

- Chen XS, Li ZZ, Yang L (2007) Oriental Bamboo leafhoppers: revision of Chinese Species of *Mohunia* (Hemiptera: Cicadellidae: Mukariinae) with descriptions of new genera and new species. *Annals of the Entomological Society of America* 100(3): 366–374.
- Dietrich CH (2005) Keys to the families of Cicadomorpha and subfamilies and tribes of Cicadellidae (Hemiptera: Auchenorrhyncha). *Florida Entomologist* 88(4): 502–517.
- Li ZZ, Dai RH, Xing JC (2011) Deltocephalinae from China (Hemiptera: Cicadellidae). *Popular Science Press*, Beijing, 336 pp.
- Zahniser JN, Dietrich CH (2013) A review of the tribes of Deltocephalinae (Hemiptera: Auchenorrhyncha: Cicadellidae). *European Journal of Taxonomy* 45: 1–211.

Revision of the lacewing genus *Laccosmylus* with two new species from the Middle Jurassic of China (Insecta, Neuroptera, Saucrosmylidae)

Hui Fang¹, Dong Ren¹, Jiayi Liu¹, Yongjie Wang¹

¹ College of Life Sciences, Capital Normal University, Beijing 100048, China

Corresponding author: Yongjie Wang (wangyjosmy@foxmail.com)

Academic editor: Shaun Winterton | Received 11 July 2018 | Accepted 5 September 2018 | Published 15 October 2018

<http://zoobank.org/B355C74B-7225-48F5-8DAF-B2FA02136331>

Citation: Fang H, Ren D, Liu J, Wang Y (2018) Revision of the lacewing genus *Laccosmylus* with two new species from the Middle Jurassic of China (Insecta, Neuroptera, Saucrosmylidae). ZooKeys 790: 115–126. <https://doi.org/10.3897/zookeys.790.28286>

Abstract

The genus *Laccosmylus* Ren & Yin, 2003 belonging to Saucrosmylidae was erected by using a single hind wing only. Based on new fossil material and re-examination of the type specimen, the diagnosis of the genus is emended with supplementary forewing characters, reported for the first time. In addition, two new species *Laccosmylus cicatricatus* **sp. n.** and *Laccosmylus latizonus* **sp. n.** are described.

Keywords

Daohugou, Inner Mongolia, Jiulongshan Formation, Mesozoic, Ningcheng

Introduction

The family Saucrosmylidae is an enigmatic lineage of Neuroptera, characterised by the typically large body size, extensively expanded RA-RP area and complicated venation (Ren and Yin 2003, Fang et al. 2015). It was originally considered to be related to Osmylidae (Ren and Yin 2003, Winterton et al. 2017). However, a phylogenetic analysis conducted by Yang et al. assigned it within Myrmeleontiformia (Yang et al. 2012).

Engel et al. (2018) pointed out the family was possibly a stem group of Osmylidae or Osmyloidae. Therefore, the phylogenetic position of the family is still not resolved.

Notably, the saucrosmylids are restricted to two Middle Jurassic localities, i.e., the Jiulongshan Formation of China and the Kubekovo locality of Russia. To date, eight genera with nine species have been formally described (Ren and Yin 2003, Wang et al. 2010, Liu et al. 2013, Liu et al. 2014, Fang et al. 2015, Khramov 2017). Despite the relatively low specific diversity, saucrosmylids show distinctive morphological diversity, especially various wing markings, e.g., *Saucrosmylus* with transverse bands, *Bellinympa* with distinct pinnate leaf-like markings, which were possibly related to their specialised adaptations to the Mesozoic environments (Wang et al. 2010). Among the known saucrosmylids, the genus *Laccosmylus* Ren & Yin, 2003 was erected based on a single hind wing (Ren and Yin 2003), with characteristic irregular dark and light patches.

This type of taxonomic treatment, i.e., establishing a new taxon based on a single hind wing, is common among Saucrosmylidae and other large neuropterans (Fang et al. 2015). For example, *Rudiosmylus* Ren & Yin, 2003, *Laccosmylus* Ren & Yin, 2003 and *Daohugosmylus* Liu et al., 2014 (Ren and Yin 2003, Liu et al. 2014) were established based on the hind wing only. Although single hind wing could provide some informative characters, the absence of forewing of the genus might result in incomplete information for the overall comparison with other saucrosmylid genera. Herein, we provide an emended diagnosis of *Laccosmylus* with additional forewing characters, re-describe the type species *Laccosmylus calophlebius* Ren & Yin, 2003 based on the re-examination of the type specimen and additional material, and describe two new species *Laccosmylus cicatricatus* sp. n. and *Laccosmylus latizonus* sp. n.

Materials and methods

All the specimens reported here were collected from the Middle Jurassic Jiulongshan Formation at Daohugou Village, Ningcheng County, Inner Mongolia, northeastern China (Ren et al. 2010; Gu et al. 2012; Wang et al. 2012; Meng et al. 2017). All photographs were taken using Canon 70D digital camera, and modified by Photoshop CC. The line drawings were prepared on photographs using the image-editing software CorelDRAW X7. The venation terminology follows Kukalová-Peck and Lawrence (2004) as interpreted by Yang et al. (2012, 2014) and Breitkreuz et al. (2017). Abbreviations of wing veins are as follows (those used in the traditional terminology in parentheses):

ScP (= Sc, subcosta)	subcostal posterior;
R	radius;
RA (= R1, first branch of radius)	radius anterior;
RP (= Rs, radial sector)	radius posterior;
RP1 (= Rs1)	proximal-most branch of RP;
RP2 (= Rs2)	branch of RP distal to RP1;
M	media;
MA	media anterior;

MP	media posterior;
Cu	cubitus;
CuA	cubitus anterior;
CuP	cubitus posterior;
AA1-AA3 (= 1A-3A)	first to third anal veins.

Systematic palaeontology

Class Insecta Linnaeus, 1758

Order Neuroptera Linnaeus, 1758

Family Saucrosmylidae Ren & Yin, 2003

Genus *Laccosmylus* Ren & Yin, 2003

Type species. *Laccosmylus calophlebius* Ren & Yin, 2003.

Species included. *Laccosmylus calophlebius* Ren & Yin, 2003; *Laccosmylus cicatricatus* sp. n.; *Laccosmylus latizonus* sp. n.

Emended diagnosis. Large body size, body length more than 35 mm, forewing length approx. 60–80 mm, hind wing length approx. 55–76 mm. Forewing elongated, with undulant outer margin. Hind wing broader and shorter than forewing, with slightly undulant outer margin. Forewing and hind wing with similar venation, i.e., presence of 6–7 rows of smaller veinlets between costal veinlets; RA-RP area expanded, with 4 to 7 rows of irregular cells; RP sharply bent towards RA anteriorly, forming an angle of approx. 45°; space between other longitudinal veins producing 1 to 4 rows of cells.

Remarks. *Laccosmylus* Ren & Yin, 2003 was assigned to Saucrosmylidae according to its expanded RA area and complicated wing venation of hind wing (Ren & Yin, 2003). Nevertheless, this remarkable genus was established without forewing information which prevent to conduct full comparisons with other saucrosmylids. Herein, the newly collected fossil specimen related to the genus provides significant forewing information to address the issue. The new specimen CNU-NEU-NN2018007P/C of *L. cicatricatus* sp. n. clearly belongs to *Laccosmylus* because of the similar characters of hind wing (Figs. 1, 2, 3), i.e. the same broad wing shape with undulant outer margin, the similar patches and spots markings in hind wing, the same expanded RA area with seven rows of irregular cells, the same longitudinal veins and similar cross-veins.

This new species of *L. cicatricatus* sp. n. and *L. latizonus* sp. n. together with a new specimen of *L. calophlebius* Ren & Yin, 2003 provide significant information, especially the supplement of forewing features, to corroborate the status of *Laccosmylus*. *Laccosmylus* is definitely different from *Rudiosmylus* Ren & Yin, 2003, *Ulrikezza* Fang, Ren & Wang, 2015 and *Huiyingosmylus* Liu et al., 2013 by its sharply bent RP at terminal of the wing and unique patch-like and stripe-like wing markings, in contrast to the three genera bearing slightly bent RP and spot-like wing markings (Ren and Yin 2003, Liu et al. 2013, Fang et al. 2015). *Laccosmylus* is different from *Saucrosmylus* Ren & Yin, 2003 by its deeply un-

dulant outer margin of forewing and broad hind wing, while *Saucrosmylus* only has slightly undulant outer margin in both wings and slender hind wing (Ren and Yin 2003). Comparing to *Daohugosmylus* Liu et al., 2014 that was established by an incomplete hind wing, *Laccosmylus* possesses the undulant outer margin of hind wing, pigmented wing marking at the basal part of hind wing and more rows of smaller veinlets between costal veinlets in hind wing, which are absent in *Daohugosmylus* (Liu et al. 2014). Interestingly, *Laccosmylus* possesses similar forewing shape with *Bellinympa*, however, both of the two species of *Bellinympa* have pinnate-like markings on forewings and three continuous markings on hind wings, and bearing slender hind wings (Wang et al. 2010), while *Laccosmylus* develops patch-like or stripe-like wing markings on both wings and bears broad hind wings.

Laccosmylus calophlebius Ren & Yin, 2003

Figure 1

Emended diagnosis. Hind wing with many hyaline patch-like markings and mottled with some irregular pigmented patch-like markings, and the costal region with intermittent marking; outer margin undulant. RA-RP area expanded with 6–7 rows of irregular cells. One or two rows of cells present among RP branches and MA-CuA area.

Re-description of holotype and description of new material. Hind wing length approx. 70 mm, width approx. 35 mm. Costal veinlets distally forked, interlinked by 6–7 rows of smaller veinlets. ScP fused with RA apically. RP with 5 main branches before RP sharply bent towards RA anteriorly. MA forked at 1/3 part of hind wing or forked terminally (Figure 1). The first branch of MP forming several dichotomous branches terminally, the second branch of MP with multiple pectinate branches terminally. CuA forming a large triangular area, with numerous oblique pectinate branches. CuP much shorter than CuA, with approx. 8 branches. AA1 and AA2 with several pectinate branches, AA3 short and simple.

Material examined. Holotype: CNU-NEU-NN99003, only hind wing preserved. New material: CNU-NEU-NN2018006P/C, only hind wing preserved. These specimens are deposited in the Key Laboratory of Insect Evolution and Environmental Changes, College of Life Sciences, Capital Normal University, Beijing, China.

Type locality and horizon. Jiulongshan Formation, Daohugou locality (41°18.5'N, 119°13'E (DDM)), Shantou Township, Ningcheng County, Chifeng City, Inner Mongolia, China; Middle Jurassic, Bathonian-Callovian boundary.

Remarks. The new material CNU-NEU-NN2018006P/C evidently belongs to the *L. calophlebius* Ren & Yin, 2003 according to the same hind wing shape, marking and venation. This species was first erected based on only one specimen with a hind wing. Moreover, at that time, this species was the representative with generic diagnosis for the *Laccosmylus*, which led some unilateral diagnosis of the genus and species. Here, the MA in the new specimen shows the previous diagnosis of *L. calophlebius* with MA early branching needs to be changed. In addition, individual differences might have happened frequently in Saucrosmylidae, which has multiple venation.

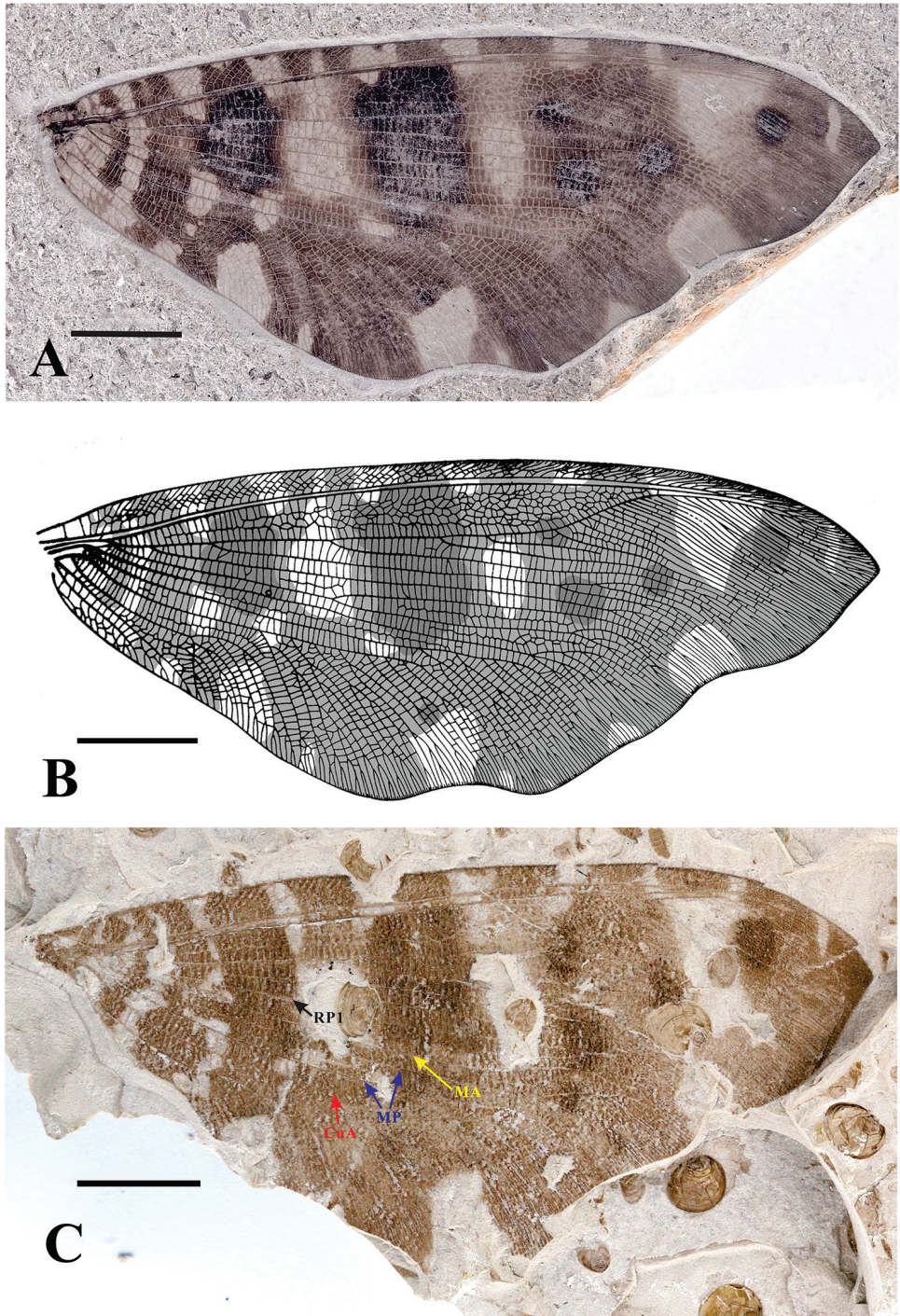


Figure 1. *Laccosmylus calophlebius* Ren & Yin, 2003. **A** Holotype: CNU-NEU-NN99003, a well-preserved hind wing **B** line drawing of holotype CNU-NEU-NN99003 (modified from Ren and Yin 2003) **C** part of new material CNU-NEU-NN2018006P/C, a well-preserved hind wing. Scale bar: 10 mm.

***Laccosmylus cicatricatus* sp. n.**

<http://zoobank.org/59608202-1E21-4AEA-A975-9863806D7391>

Figures 2, 3

Diagnosis. Large body size, body length more than 37.8 mm, forewing length approx. 60–80 mm, hind wing length approx. 55–76 mm. Forewing distinctly painted with three irregular pigmented marking, outer margin deeply undulant. Hind wing with many hyaline patch-like markings and mottled with some irregular pigmented patch-like markings, and the entire dark costal region. The venation of fore- and hind wings: RA-RP area expanded with 6–7 rows of irregular cells; 1–4 rows of cells present among RP branches and MA-CuA area.

Description. Forewing elongated, with irregularly undulant outer margin. Forewings most heavily pigmented, with two irregular hyaline stripes and a patch-like marking near the outer margin. Trichosors present along distal half of wing margin. Costal veinlets distally forked, interlinked by 6–7 rows of smaller veinlets. ScP fused with RA apically. RA-RP area expanded, with 6–7 rows of irregular cells. RP with five main branches before RP sharply bent towards RA anteriorly. One to three rows of crossveins existing between main longitudinal veins from radius area to anal area. MA forked terminally. The first branch of MP forming several dichotomous branches terminally, the second branch of MP with multiple pectinate branches terminally. CuA forming a large triangular area, with numerous oblique pectinate branches. CuP much shorter and simpler than CuA, with only two main branches. AA1 with approx. eight pectinate branches, while AA2 and AA3 almost invisible.

Hind wing broader and shorter than forewing, with outer margin slightly undulant. The membrane of hind wing covered with numerous dark and hyaline patch-like markings. Trichosors preserved along distal half of wing margin. Venation of hind wing similar to forewing from costal section to media area. CuP in hind wing with approx. eight branches, more complicated than those in forewing. AA1 partially preserved. AA2 and AA3 invisible.

Material examined. Holotype: CNU-NEU-NN2018007P/C, sex unknown, body, and four wings preserved. This specimen is deposited in Inner Mongolia Ningcheng Daohugou Paleontological Protection Museum, Chifeng City, Inner Mongolia, China.

Type locality and horizon. Jiulongshan Formation, Daohugou locality (41°18.5'N, 119°13'E (DDM)), Shantou Township, Ningcheng County, Chifeng City, Inner Mongolia, China; Middle Jurassic, Bathonian-Callovian boundary.

Etymology. The Latin *cicatricatus* is derived from mottles and patches on pigmented wings of this species.

Remarks. The new species belongs to the *Laccosmylus* according to the features of hind wing, i.e. the broad hind wing shape, undulate outer margin, similar venation, and similar distinct colour markings. *L. cicatricatus* sp. n. can be distinguished from the type species *L. calophlebius* by the following characters in hind wing, e.g., the entire dark costal region vs. the costal region with intermittent marking on *L. calophlebius*, and more rows of cells present among RP branches and MA-CuA area than in *L. calophlebius*. In addition, a hyaline spot on the hind wing apex presents in the *L. calophlebius* but absent in *L. cicatricatus* sp. n.

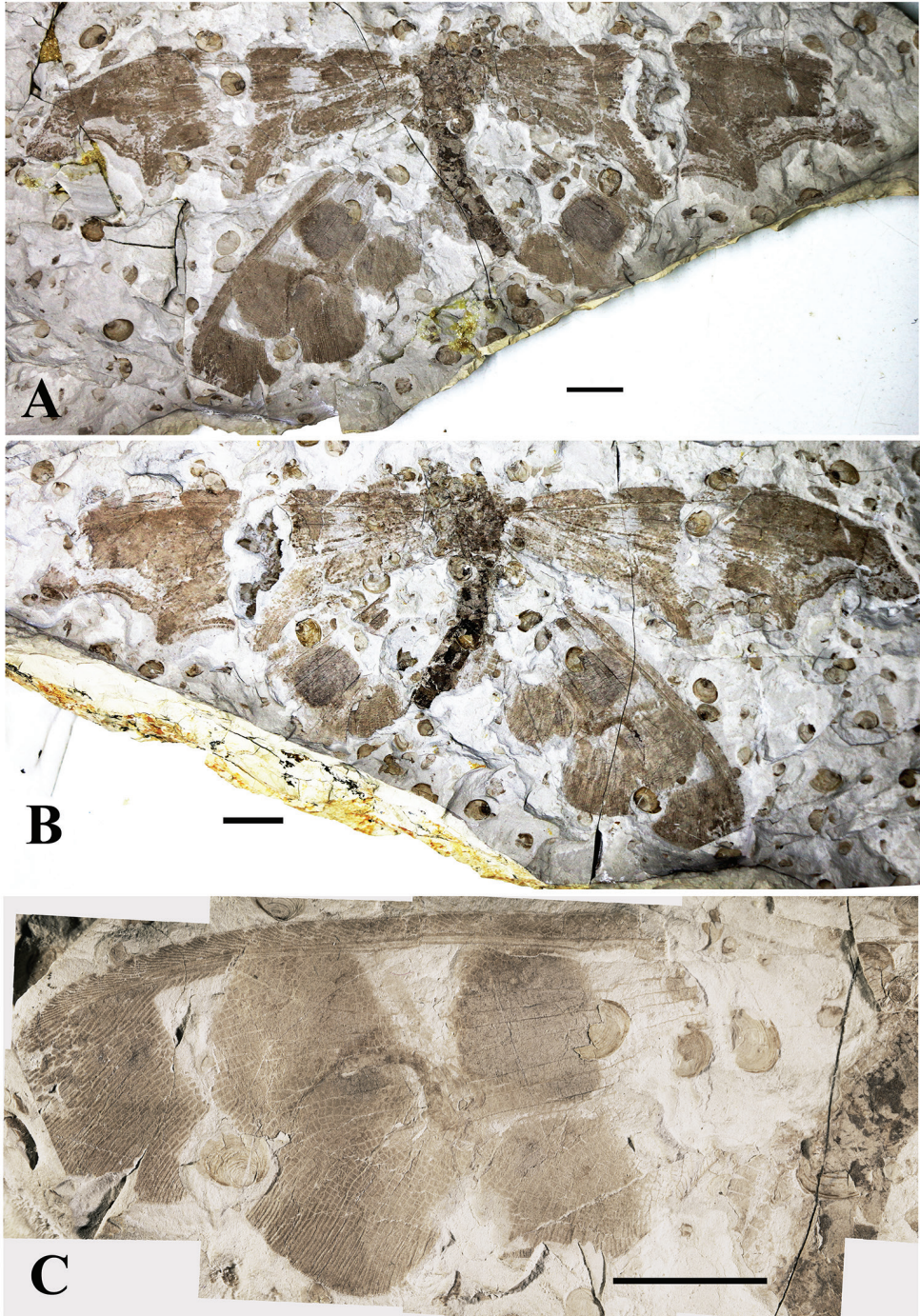


Figure 2. *Laccosmylus cicatricatus* sp. n., Holotype: CNU-NEU-NN2018007P/C. **A** part **B** counterpart **C** hind wing of part. Scale bar: 10 mm.

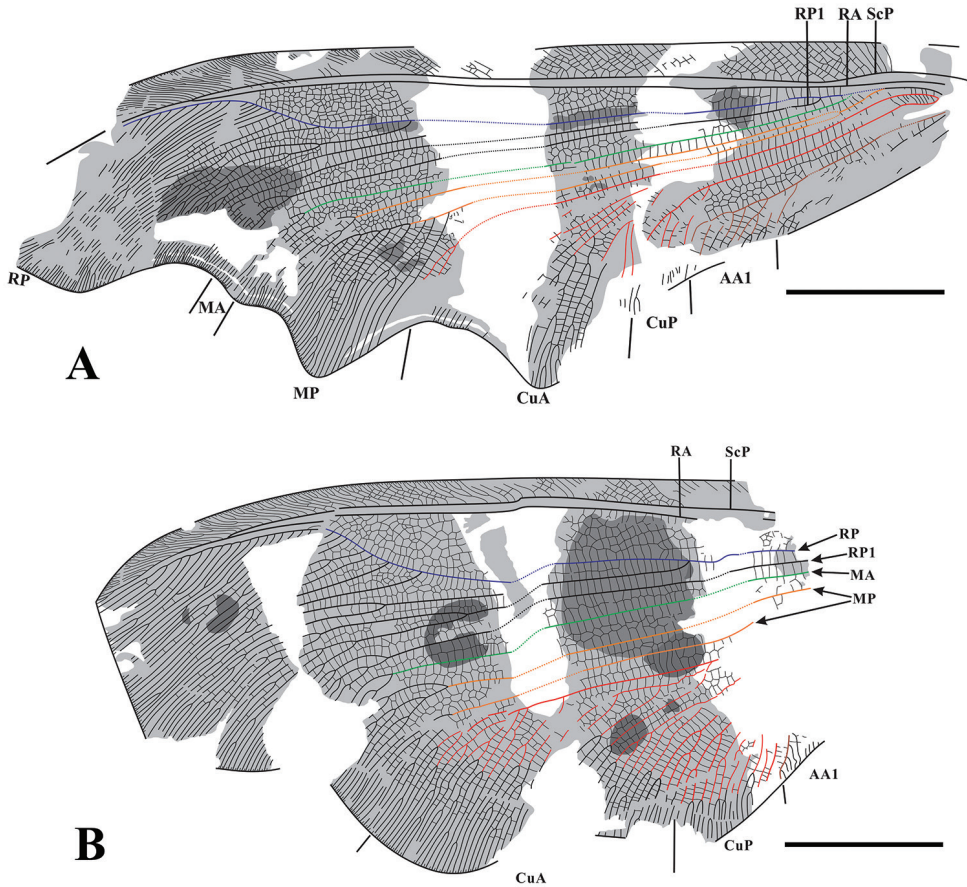


Figure 3. *Laccosmylus cicatricatus* sp. n., Holotype. **A** Line drawing of forewing **B** Line drawing of hind wing. Scale bar: 10 mm.

***Laccosmylus latizonus* sp. n.**

<http://zoobank.org/E65B109E-D091-4C8A-B58D-40FB2156CF52>

Figures 4, 5

Diagnosis. Forewing with four pigmented patch-like markings. Hind wing with three pigmented stripes, and the third stripe interlinked with a fuscous patch covering wing apex. The venation of fore- and hind wing: RA area forming 4–5 rows of irregular cells; 1 to 2 rows of cells between longitudinal veins from radius area to anal area.

Description. Forewing more than 54.4 mm long, partially preserved, outer margin unknown (Figure 4A, B). Four pigmented patch-like markings present. Costal veinlets forked twice distally, interlinked by 5–7 rows of smaller veinlets. ScP fused with RA apically. RA-RP area broad, forming 4–5 rows of irregular cells. RP sharply bent towards RA terminally, forming an angle of approx. 45°. Single row of cells between main longitudinal veins from radius area to anal area. MA and MP partially preserved. CuA forming a large triangular area.

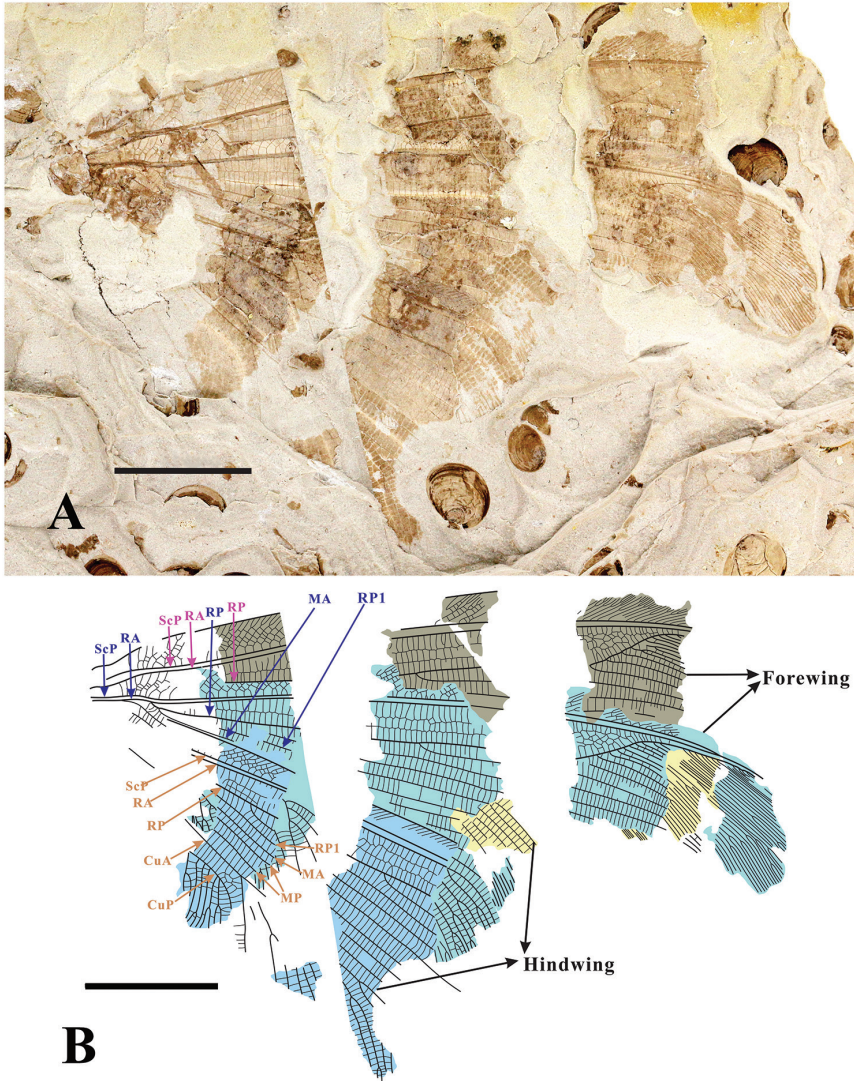


Figure 4. *Laccosmylus latizonus* sp. n. **A** Paratype: CNU-NEU-NN2018009 with four wings overlapped **B** Line drawing of CNU-NEU-NN2018009. Scale bar: 10 mm.

Hind wing length 56–59 mm, width 22–26 mm. Hind wing broad, with outer margin slightly undulant, same shape as the type species *L. calophlebius* (Figures 1A, 5A), covered with 3 pigmented stripes, and the third stripe interlinked with a fuscous patch covering wing apex. (Figure 5A, C). Trichosors present along distal half of wing margin. Hind wing showing similar vein pattern as forewing from costal area to media area (Figures 4, 5A, B). In addition, RPI deeply branched at the base or not (Figure 4A, B, D); MA forming three main branches distally; MP forked before the separation of MA from RP; MP forming several pectinate branches distally; CuP with several pectinate branches. AA1 and AA2 simple, partially preserved.

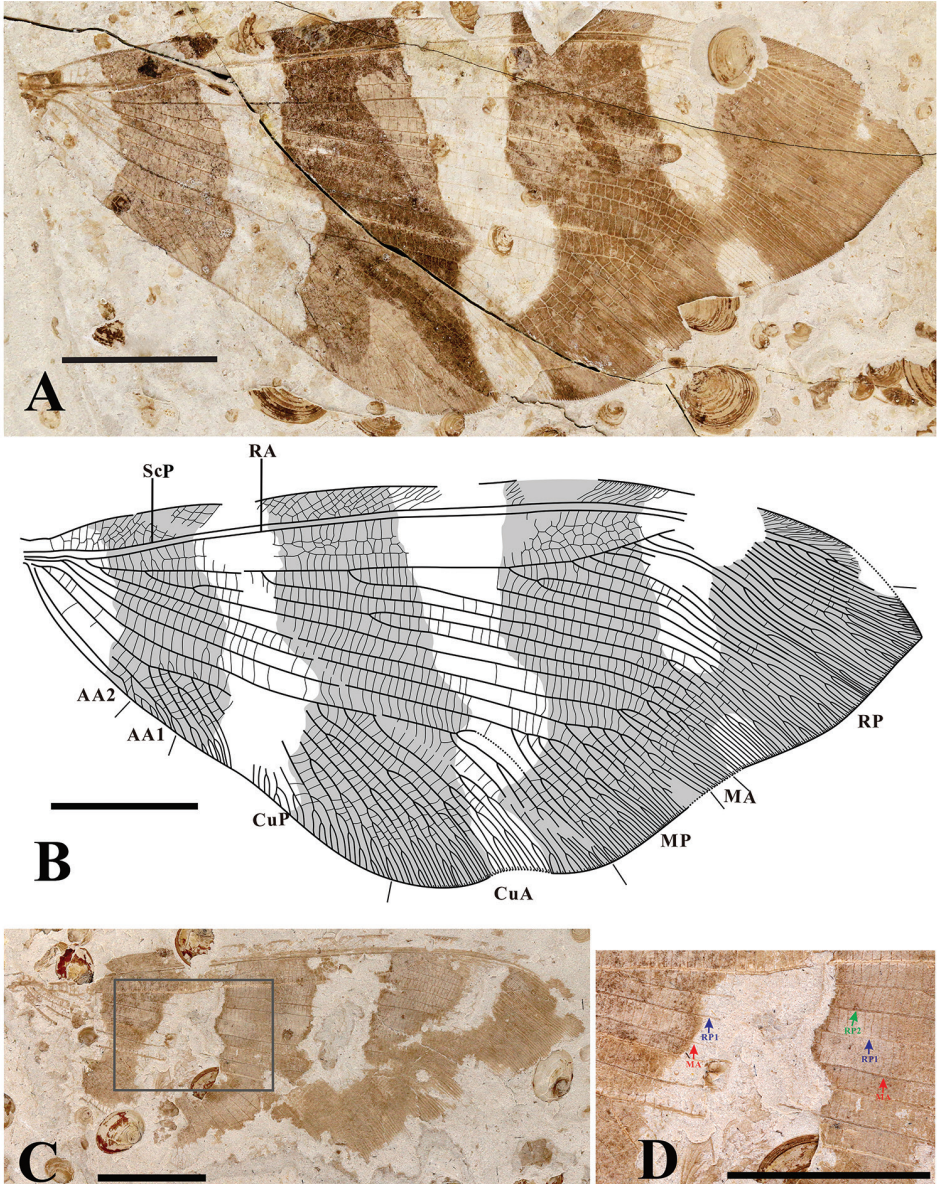


Figure 5. *Laccosmylus latizonus* sp. n. **A** Part of holotype CNU-NEU-NN2018008P/C, a well-preserved right hind wing **B** Line drawing of hind wing of Holotype **C** Part of paratype CNU-NEU-NN2018010P/C, a well-preserved hind wing **D** Amplification of the rectangle part of C. Scale bar: 10 mm.

Type material. Holotype: CNU-NEU-NN2018008P/C, only hind wing preserved; **Paratypes:** CNU-NEU-NN2018009, four wings partially preserved and joined together; CNU-NEU-NN2018010P/C, only hind wing partially preserved. These specimens are deposited in the Key Laboratory of Insect Evolution and Environmental Changes, College of Life Sciences, Capital Normal University, Beijing, China.

Type locality and horizon. Jiulongshan Formation, Daohugou locality (41°18.5'N, 119°13'E (DDM)), Shantou Township, Ningcheng County, Chifeng City, Inner Mongolia, China; Middle Jurassic, Bathonian-Callovian boundary.

Etymology. The Latin *latizonus* is derived from the stripe-like wing markings of this species.

Remarks. The new species evidently belongs to *Laccosmylus* according to the emended diagnosis of the genus, i.e., the same broad hind wing shape, undulate outer margin and similar venation, and even the arrangement of wing markings. *Laccosmylus latizonus* sp. n. can be easily distinguished from *L. calophlebius* and *L. cicatricatus* sp. n. by the following characters of the hind wing markings, i.e. three distinct pigmented stripes in the *L. latizonus* vs. scattered patch-like markings on the other two species. In addition, the venation of these species are also distinctively different, e.g., *L. latizonus* sp. n. with 4–5 rows of irregular cells between RA and RP vs. 6–7 rows of irregular cells in the other two species; relatively simpler cross-veins in *L. latizonus* sp. n. in radial sector than in the other two species.

Acknowledgments

We sincerely thank Dr. Xingyue Liu, Alexander Khramov, Vladimir Makarkin, Sonja Wedmann, and an anonymous reviewer's critical comments to improve this paper. We also thank Dr. Chungkun Shih (Capital Normal University and Department of Paleobiology, National Museum of Natural History, Smithsonian Institution, Washington, DC) for the copy-editing to improve this paper. Moreover, we thank the Inner Mongolia Ningcheng Daohugou Paleontological Protection Museum (Chifeng City, Inner Mongolia, China) for providing the important specimen CNU-NEU-NN2018007P/C. This work is supported by National Science Foundation of China (grants 31672323, 31730087, 41372013 and 41688103), Youth Innovative Research Team of Capital Normal University, and Program for Changjiang Scholars and Innovative Research Team in University (IRT-17R75) and Project of High-level Teachers in Beijing Municipal Universities (IDHT20180518).

References

- Breitkreuz LCV, Winterton SL, Engel MS (2017) Wing tracheation in Chrysopidae and other Neuropterida (Insecta): A resolution of confusion about vein fusion. *American Museum Novitates* 3890: 1–44. <http://digitallibrary.amnh.org/handle/2246/6819>
- Engel MS, Winterton SL, Breitkreuz L (2018) Phylogeny and evolution of Neuropterida: Where have wings of lace taken us? *Annual Review of Entomology* 63: 531–551. <https://doi.org/10.1146/annurev-ento-020117-043127>
- Fang H, Ren D, Wang YJ (2015) Familial clarification of Saucrosmylidae stat. nov. and new saucrosmylids from Daohugou, China (Insecta, Neuroptera). *PLoS ONE* 10: e0141048. <https://doi.org/10.1371/journal.pone.0141048>

- Gu JJ, Montealegre-Z F, Robert D, Engel MS, Qiao GX, Ren Dong (2012) Wing stridulation in a Jurassic katydid (Insecta, Orthoptera) produced low-pitched musical calls to attract females. *Proceedings of the National Academy of Sciences of the United States of America* 109: 3868–3873. <https://doi.org/10.1073/pnas.1118372109>
- Khramov AV (2017) Jurassic lacewings (Insecta: Neuroptera) of western Siberia. *Paleontological Journal* 51: 59–68. <https://doi.org/10.1134/S0031030117010063>
- Kukalová-Peck J, Lawrence JF (2004) Relationships among coleopteran suborders and major endoneopteran lineages: Evidence from hind wings characters. *European Journal of Entomology* 101: 95–144. <https://doi.org/10.14411/eje.2004.018>
- Liu Q, Zhang HC, Wang B, Fang Y, Zheng DR, Zhang Q, Jarzembowski AE (2013) A new genus of Saucrosmylinae (Insecta, Neuroptera) from the Middle Jurassic of Daohugou. *Zootaxa* 3736: 387–391. <https://doi.org/10.11646/zootaxa.3736.4.6>
- Liu Q, Zhang HC, Wang B, Fang Y, Zheng DR, Zhang Q, Jarzembowski AE (2014) A new saucrosmylid lacewing (Insecta, Neuroptera) from the Middle Jurassic of Daohugou, Inner Mongolia, China. *Alcheringa* 38: 301–304. <https://doi.org/10.1080/03115518.2014.886849>
- Meng QM, Labandeira CC, Ding QL, Ren D (2017) The natural history of oviposition on a ginkgophyte fruit from the Middle Jurassic of northeastern China. *Insect Science* 2017: 1–9. <https://doi.org/10.1111/1744-7917.12506>
- Ren D, Shih CK, Gao TP, Yao YZ, Zhao YY (2010) *Silent Stories – Insect Fossil Treasures from Dinosaur Era of the Northeastern China*. Science Press, Beijing, 332 pp.
- Ren D, Yin JC (2003) New ‘osmylid-like’ fossil Neuroptera from the Middle Jurassic of Inner Mongolia, China. *Journal of New York Entomological Society* 111: 1–11. [https://doi.org/10.1664/0028-7199\(2003\)111\[0001:NOFNFT\]2.0.CO;2](https://doi.org/10.1664/0028-7199(2003)111[0001:NOFNFT]2.0.CO;2)
- Wang YJ, Labandeira CC, Shih CK, Ding QL, Wang C, Zhao YY, Ren D (2012) Jurassic mimicry between a hangingfly and a ginkgo from China. *Proceedings of the National Academy of Sciences of the United States of America* 109: 20514–20519. <https://doi.org/10.1073/pnas.1205517109>
- Wang YJ, Liu ZQ, Wang X, Shih CK, Zhao YY, Engel SM, Ren D (2010) Ancient pinnate leaf mimesis among lacewings. *Proceeding of the National Academy Sciences of the United States of America* 107: 16212–16215. <https://doi.org/10.1073/pnas.1006460107>
- Winterton SL, Zhao J, Garzón-orduña IJ, Wang YJ, Liu ZQ (2017) The phylogeny of lance lacewings (Neuroptera: Osmylidae). *Systematic Entomology* 42: 555–574. <https://doi.org/10.1111/syen.12231>
- Yang Q, Makarkin VN, Ren D (2013) A new genus of the family Panfiloviidae (Insecta, Neuroptera) from the Middle Jurassic of China. *Palaeontology* 56: 49–59. <https://doi.org/10.1111/j.1475-4983.2012.01157.x>
- Yang Q, Makarkin VN, Winterton SL, Khramov AV, Ren D (2012) A remarkable new family of Jurassic insects (Neuroptera) with primitive wing venation and its phylogenetic position in Neuropterida. *PLoS ONE* 7: e44762. <https://doi.org/10.1371/journal.pone.0044762>
- Yang Q, Makarkin VN, Ren D (2014) Two new species of *Kalligramma* Walther (Neuroptera: Kalligrammatidae) from the Middle Jurassic of China. *Annals of the Entomological Society of America* 107: 917–925. <https://doi.org/10.1603/AN14032>

The complete mitochondrial genome of *Orancistrocerus aterrimus aterrimus* and comparative analysis in the family Vespidae (Hymenoptera, Vespidae, Eumeninae)

Qiao-Hua Zhang¹, Pan Huang¹, Bin Chen¹, Ting-Jing Li¹

¹ Institute of Entomology & Molecular Biology, College of Life Sciences, Chongqing Normal University, Chongqing 401331, China

Corresponding author: Ting-Jing Li (ltjing1979@hotmail.com)

Academic editor: A. Köhler | Received 28 March 2018 | Accepted 25 September 2018 | Published 15 October 2018

<http://zoobank.org/89EBDEC5-A83E-4034-8DC6-EB880183F306>

Citation: Zhang Q-H, Huang P, Chen B, Li T-J (2018) The complete mitochondrial genome of *Orancistrocerus aterrimus aterrimus* and comparative analysis in the family Vespidae (Hymenoptera, Vespidae, Eumeninae). ZooKeys 790: 127–144. <https://doi.org/10.3897/zookeys.790.25356>

Abstract

To date, only one mitochondrial genome (mitogenome) in the Eumeninae has been reported in the world and this is the first report in China. The mitogenome of *O. a. aterrimus* is 17 972 bp long, and contains 38 genes, including 13 protein coding genes (PCGs), 23 tRNA genes, two rRNA genes, a long non-coding region (NCR), and a control region (CR). The mitogenome has 79.43% A + T content, its 13 PCGs use ATN as the initiation codon except for *cox1* using TTG, and nine genes used complete translation termination TAA and four genes have incomplete stop codon T (*cox2*, *cox3*, *nad4*, and *cytb*). Twenty-two of 23 tRNAs can form the typical cloverleaf secondary structure except for *trnS1*. The CR is 1 078 bp long with 84.69% A+T content, comprising 28 bp tandem repeat sequences and 13 bp T-strech. There are two gene rearrangements which are an extra *trnM2* located between *trnQ* and *nad2* and the *trnL2* in the upstream of *nad1*. Within all rearrangements of these mitogenomes reported in the family Vespidae, the translocation between *trnS1* and *trnE* genes only appears in Vespinae, and the translocation of *trnY* in Polistinae and Vespinae. The absent codons of 13 PCGs in Polistinae are more than those both in Vespinae and Eumeninae in the family Vespidae. The study reports the complete mitogenome of *O. a. aterrimus*, compares the characteristics and construct phylogenetic relationships of the mitogenomes in the family Vespidae.

Keywords

Eumeninae, mitochondrial genomes, *Orancistrocerus aterrimus aterrimus*, phylogenetic analysis, Vespidae

Introduction

Animal mitochondrial genomes (mitogenomes) have been widely used in studies of molecular evolution, population genetic structure, and phylogeny because of their stable gene content, rapid evolutionary rate, relatively conserved gene arrangement, maternal inheritance, and infrequent recombination (Wolstenholme 1992; Saccone et al. 1999; Oliveira et al. 2008; Li et al. 2017). The family Vespidae has more than 5000 known species worldwide, which are divided into six subfamilies, Euparagiinae, Masarinae, Eumeninae, Stenogastrinae, Polistinae, and Vespinae (Carpenter 1993), but their phylogenetics have not been settled. There have been ten mitogenomes sequences reported in the Vespidae (seven in the subfamily Vespinae, three in Polistinae, and one in Eumeninae) (Table 1). Among these six subfamilies, there are more than 3600 species in the subfamily Eumeninae worldwide, more than half of the known species of Vespidae. The species in Eumeninae, also known as potter wasps, are solitary, and mostly catch caterpillars as food for their next generation in the environment of farmlands, forests, and orchards, which can directly control caterpillar pests. To date, there is only one species (*Abispa ephippium*) with its mitogenome published (Cameron et al. 2008). *Orancistrocerus aterrimus aterrimus*, the species under study in this work, belongs to the Eumeninae, and is widely distributed in China (Jiangsu, Anhui, Fujian, Jiangxi, Hunan, Guangxi, Chongqing, Sichuan, Yunnan provinces), and Laos, Vietnam (Li 1985; Selis 2018).

In the present study, the complete mitogenome of *O. a. aterrimus* was sequenced using Illumina sequencing technique, and its characteristics analyzed, including gene rearrangements, nucleotide composition, codon usage, etc. More importantly, the phylogenetic relationships of 12 species of mitogenomes in Vespidae are constructed and discussed based on nucleotide sequences of 13 PCGs using both Maximum Likelihood (ML) and Bayesian Inference (BI) methods. The study updates phylogenetic research based on the mitogenomes, and provides basic information framework of mitogenomes in Vespidae for further research on the phylogenetic relationships of both genera and subfamilies in this family.

Materials and methods

Sample collection and DNA preparation

The specimens of *O. a. aterrimus* were collected from Yangshuo county of Guangxi province, preserved in the 100% ethanol, and stored at -20 °C. Total DNA of a single adult specimen was extracted from the muscle tissues using the DNeasy DNA Extraction Kit (QIAGEN) in accordance with the manufacturer's instructions. The concentration of genomic DNA in extraction product was assayed on a Qubit fluorometer using a dsDNA High-sensitivity Kit (Invitrogen).

Table 1. The information of Vespidae mitogenomes used in the phylogenetic analysis in the present study.

Subfamily	Species	Migenome size (bp)	Gene number	GenBank Accession	Reference
Ingroup (Vespidae)					
Eumeninae	<i>Orancistrocerus aterrimus aterrimus</i>	17972	38	KY941926	This study
Eumeninae	<i>Abispa ephippium</i>	16953	41	EU302588	Cameron et al. (2008)
Polistinae	<i>Polistes jokahamae</i>	16616	34	KR052468	Song et al. (2016)
Polistinae	<i>Polistes humilis synoecus</i>	14741	34	EU024653	Cameron et al. (2008)
Polistinae	<i>Parapolybia crocea</i>	16619	37	KY679828	Peng et al. (2017)
Vespinae	<i>Vespula germanica</i>	16342	33	KR703583	Zhou et al. (2016)
Vespinae	<i>Vespa ducalis</i>	15779	37	KX950825	Kim et al. (2017a)
Vespinae	<i>Vespa mandarina</i>	15902	37	KR059904	Chen et al. (2015)
Vespinae	<i>Vespa bicolor</i>	16937	35	KJ735511	Wei et al. (2014)
Vespinae	<i>Vespa velutina nigrithorax</i>	16475	37	KY091645	Kim et al. (2017b)
Vespinae	<i>Vespa orientalis</i>	16101	37	KY563657	Nizar et al (2017)
Vespinae	<i>Dolichovespula panda</i>	17137	37	KY293679	Fan et al (2017)
Outgroup (Formicidae)					
Formicinae	<i>Formica selysi</i>	16752	37	KP670862	Yang et al. (2015)

Mitogenomes sequencing and assembling

The Illumina TruSeq library was constructed from the gDNA with the average length of the inserted fragment of 480 bp. The library was sequenced on a full run of Illumina HiSeq 2500 with 500 cycles and paired-end sequencing (250 bp reads). High-quality reads were used in *de novo* assembly with IDBA-UD after removing adapters, unpaired, short and low quality reads (Peng et al. 2012). With IDBA-UD, these parameters have a similarity threshold of 98% and minimum and maximum k values of 80 and 240 bp, respectively. To identify the mitogenome assemblies from the pooled sequencing files, two different fragments of mtDNA (*cox1* and *rrnS*) were amplified as bait sequences by standard PCR reactions using primers designed with reference of Simon et al. (2006). Using BLASTN search against the reference of bait sequences, matching rate of 100% was confirmed as the mitogenome of *O. a. aterrimus*. The identical or near-identical overlapping terminal regions of mitogenome sequences were examined and circularized by Geneious (<http://www.geneious.com/>).

Sequence annotations and analysis

PCGs and rRNA genes were aligned with other published Vespidae insect mitogenomes by Clustal X (Thompson et al. 1997). The majority of the tRNA gene locations and secondary structures were identified by tRNAscan-SE Search Server v.1.21 (Lowe and Eddy 1997), and the remaining tRNA were identified in comparison with other known species of tRNAs in Vespidae (Cameron et al. 2008; Song et al. 2016). The CR

and the tandem repeat sequence were analyzed with Tandem Repeats Finder (<http://tandem.bu.edu/trf/trf.html>) (Benson 1999). Base composition and codon usage in all 12 mitogenomes of Vespidae were calculated by MEGA v 6. 0 (Tamura et al. 2013). In addition, the AT skew = $[A - T] / [A + T]$ and GC skew = $[G - C] / [G + C]$ were computed (Perna and Kocher 1995).

Phylogenetic analysis

Eleven known mitogenome sequences in the family Vespidae and the mitogenome sequence of *Formica selysi* (KP670862) in the family Formicidae were downloaded from GeneBank, and that of *O. a. aterrimus* was produced in the present study (Table 1). The phylogenetic tree of 12 mitogenomes sequences in the family Vespidae was constructed using ML and BI methods with MEGA 6.0 (Tamura et al. 2013) and MrBayes 3.1.1 (Huelsenbeck and Ronquist 2001), and the *Formica selysi* (KP670862) was used as outgroup. The nucleotide sequences of 13 PCGs were applied in the phylogenetic inference, and the best fitting substitution model was detected using Mrmodeltest 2.3 (Nylander 2004). The bootstrap values were calculated based on 1000 replications, and the confidence values of the topology is high.

Results and discussion

Genomic organization

The complete mitogenome of *O. a. aterrimus* is a double-strand of circular molecular DNA and 17,972 bp. It contains 38 genes: 13 PCGs, 23 tRNAs, two rRNAs, a control region (CR), and a long non-coding region (NCR) (Figure 1), of which 24 genes are situated in the majority strand (J-strand) and the other 14 genes are located in the minority strand (N-strand) (Table 2). An extra *trnM2* and a long NCR were found in the mitogenome. The gene *trnM2* is 67 bp and located in 2 142-2 208 between *trnQ* and *nad2*. The NCR is 1 946 bp long, located in 128-2 073 between *trnM1* and *trnQ*. With the exception of the NCR (1 946 bp), 14 intergenic spacers exist and sum to 174 bp, of which the longest spacer is 48 bp long, located between *nad4l* and *trnT*. In addition, a total of 24 bp overlaps was identified in 12 genes, with the overlap length of each gene ranging from 1 to 8 bp.

Gene rearrangements

The gene order of 13 PCGs and two rRNAs in *O. a. aterrimus* mitogenome is consistent with the putative hymenopteran ancestor: the sawfly *Perga condei* (Hymenoptera: Symphyta: Pergidae:) (Castro and Dowton 2005). However, there are two rearrange-

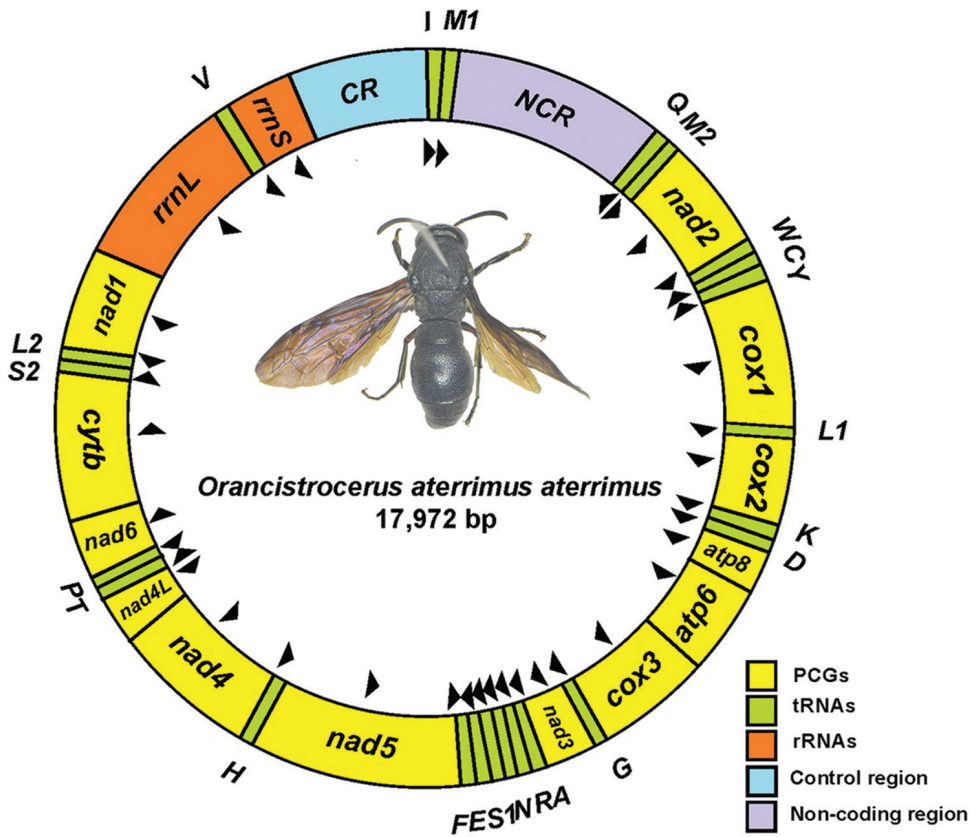


Figure 1. The mitochondrial genome of *O. a. aterrimus*. Arrows indicate the direction of genes. Abbreviations of the gene name are as follows: *nad1-4* and *nad4L* act as nicotinamide adenine dinucleotide hydrogen dehydrogenase subunits 1-6 and 4L; *cox1*, *cox2*, and *cox3* act as the cytochrome C oxidase subunits; *cytb* act as cytochrome b; *atp8* and *atp6* act as adenosine triphosphate synthase subunits 6 and 8; *rrnL* and *rrnS* act as large and small rRNA subunits; In addition, *CR* indicates control region and *NCR* indicates non-coding region.

ments of tRNAs in the mitogenome (Figure 2), namely, an extra *trnM2* and *trnL2* in the upstream of *nad1*, contributing to the novel gene order: *trnL2* - *nad1* - *rrnL* - *trnV* - *rrnS* - *CR* - *trnI* - *trnM1* - *trnQ* - *trnM2* - *nad2* (Figure 2). In the mitogenome of *Abispa ephippium*, another species in the subfamily Eumeninae, the gene order of rearrangements is *trnL2* - *trnM1* - *trnQ* - *trnM2* - *trnI*, *trnL1* - *trnL1* - *trnL1* - *trnL1* and *trnS2* - *nad1* (Figure 2) (Cameron et al. 2008). In the subfamily Polistinae, the translocation between *nad1* and *trnL1* is present in three reported species. In addition, the translocation of *trnY* in *Parapolybia crocea* occurs, *trnQ*, *trnM* and *trnY* genes are lost in *Polistes humilis* mitogenome, and in *Polistes jokahamae* mitogenome, not only *trnD* is in the upstream of *trnK* but also *trnI*, *trnQ* and *trnY* are missing (Figure 2) (Cameron et al. 2008; Song et al. 2016; Peng et al. 2017). In the subfamily Vespinae, except for the incomplete mitogenomes of *Vespula germanica* and *Vespa bicolor*, there is the

Table 2. Mitochondrial genome annotation of *O. a. aterrimus*.

Gene	Direction	Location	Size (bp)	Anticodon	Codon		Intergenic nucleotides
					Start	Stop	
<i>trnI</i>	F	1–63	63	30–32 GAT			
<i>trnM1</i>	F	63–127	65	93–95 CAT			-1
non-coding region							1946
<i>trnQ</i>	R	2074–2138	65	2108–2110 TTG			0
<i>trnM2</i>	F	2142–2208	67	2173–2175 CAT			3
<i>nad2</i>	F	2209–3234	1026		ATC	TAA	0
<i>trnW</i>	F	3249–3315	67	3280–3282 TCA			14
<i>trnC</i>	R	3308–3374	67	3342–3344 GCA			-8
<i>trnY</i>	R	3383–3447	65	3416–3418 GTA			8
<i>cox1</i>	F	3446–4981	1536		TTG	TAA	-2
<i>trnL1</i>	F	5006–5073	68	5035–5037 TAA			24
<i>cox2</i>	F	5074–5752	679		ATC	T-	0
<i>trnK</i>	F	5753–5824	72	5785–5787 CTT			0
<i>trnD</i>	F	5824–5893	70	5858–5860 GTC			-1
<i>atp8</i>	F	5894–6049	156		ATC	TAA	0
<i>atp6</i>	F	6049–6720	672		ATG	TAA	-1
<i>cox3</i>	F	6742–7525	784		ATG	T-	21
<i>trnG</i>	F	7526–7593	68	7556–7558 TCC			0
<i>nad3</i>	F	7594–7947	354		ATT	TAA	0
<i>trnA</i>	F	7947–8011	65	7977–7979 TGC			-1
<i>trnR</i>	F	8011–8074	64	8038–8040 TCG			-1
<i>trnN</i>	F	8078–8147	70	8108–8110 GTT			3
<i>trnS1</i>	F	8147–8206	60	8168–8170TCT			-1
<i>trnE</i>	F	8214–8277	64	8244–8246 TTC			7
<i>trnF</i>	R	8277–8342	66	8307–8309 GAA			-1
<i>nad5</i>	R	8344–10032	1689		ATT	TAA	1
<i>trnH</i>	R	10033–10096	64	10065–10067 GTG			0
<i>nad4</i>	R	10097–11402	1306		ATA	T-	0
<i>nad4l</i>	R	11399–11677	279		ATT	TAA	-4
<i>trnT</i>	F	11726–11789	64	11756–11758 TGT			48
<i>trnP</i>	R	11789–11858	70	11823–11825 TGG			-1
<i>nad6</i>	F	11860–12399	540		ATG	TAA	1
<i>cytb</i>	F	12403–13534	1132		ATG	T-	3
<i>trnS2</i>	F	13544–13612	69	13572–13574 TGA			9
<i>trnL2</i>	R	13640–13707	68	13676–13678 TAG			27
<i>nad1</i>	R	13708–14676	969		ATA	TAA	0
<i>rrnL</i>	R	14682–16044	1363				5
<i>trnV</i>	R	16043–16106	64	16074–16076 TAC			-2
<i>rrnS</i>	R	16107–16894	788				0
Control region		16895–17972	1078				0

same rearrangements in other four reported species, such as the translocation of *trnY*, the translocation between *trnQ* and *trnM* genes, between *trnS1* and *trnE* genes, and between *nad1* and *trnL2^(CUN)* genes, respectively and *Dolichovespula panda* is different from other four species: the translocation between *trnS1* and *trnE* genes in exchange

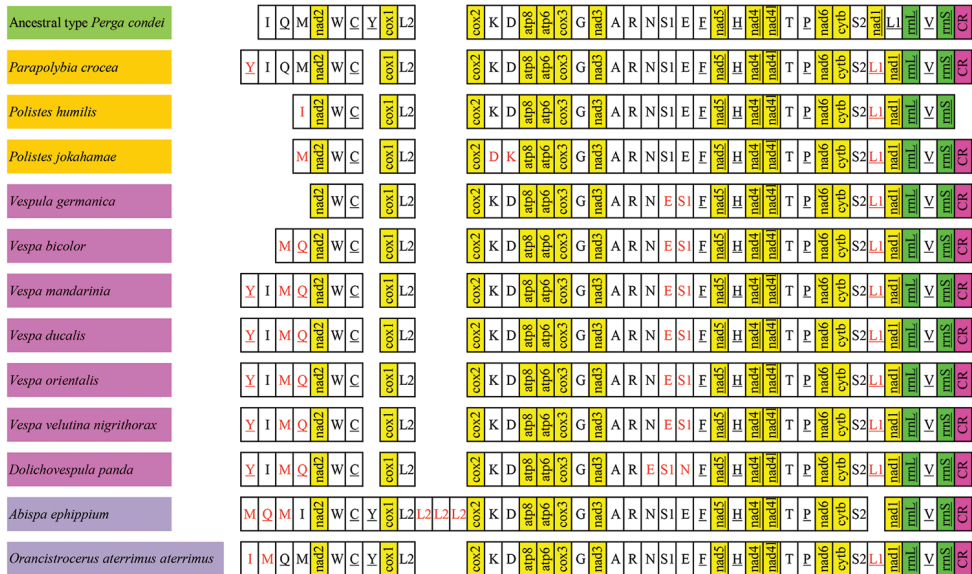


Figure 2. Mitochondrial gene arrangement of 12 species of Vespidae. The red fonts indicate the rearrangement of the genes.

for shuffling of *trnN* and *trnE* (Figure 2) (Chen et al. 2016; Fan et al. 2017; Kim et al. 2017a; Kim et al. 2017b; Nizar et al. 2017). In general, the rearrangement frequency in Eumeninae is lower than those of both Vespinae and Polistinae. The rearrangement of *tRNAs* is a typical event in the mitogenomes of Hymenoptera (Dowton and Austin 1999; Dowton et al. 2009; Chen et al. 2016).

Nucleotide composition

To date, the nucleotide compositions of ten complete mitogenomes have been reported in the family Vespidae. In the subfamily Eumeninae, the overall A + T content of *O. a. aterrimus* and *Abispa ephippium* mitogenomes is 79.43% and 80.61%, respectively (Table 3). Among all Vespidae mitogenomes, there are no significant differences of the A + T content of Polistinae, i.e., *P. humilis* being 84.73%, *P. jokahamae* 83.41%, and *Parapolybia crocea* 82.94%, respectively. In the subfamily Vespinae, there are a little differences of the A + T content from *Vespa mandarina* 79.39% to *Dolichovespula panda* being 84.61%. Generally speaking, the A + T content of Eumeninae is lower than those of both Vespinae and Polistinae. According to these different regions of *O. a. aterrimus* mitogenome, the A + T content of 13 PCGs is 78.27% near to *A. ephippium* (78.67%). In *tRNAs*, *rRNAs*, and CR, the A + T content is 83.41%, 84.29% and 84.69%, respectively. From the A + T content of all known Vespidae complete mitogenomes (Table 3), a universal feature is presumed that A + T content of *tRNAs* and *rRNAs* higher than that of PCGs.

Table 3. Nucleotide composition of different regions in all complete Vespidae mitogenomes.

Species	Regions	Size(bp)	A%	T%	G%	C%	(A+T)%	AT-skew	GC-skew
<i>Orancistrocerus aterrimus</i>	Whole genome	17972	39.53	39.9	8.06	12.51	79.43	-0.005	-0.216
	Protein coding genes	11122	33.15	45.12	10.02	11.72	78.27	-0.153	-0.078
	tRNA genes	1525	42.69	40.72	9.25	7.34	83.41	0.024	0.115
	rRNA genes	2151	41.89	42.4	10.79	4.93	84.29	-0.006	0.373
	Control region	1078	39.8	44.9	6.49	8.81	84.69	-0.06	-0.152
<i>Abispa ephippium</i>	Whole genome	16953	39.55	41.05	6.02	13.38	80.61	-0.019	-0.38
	Protein coding genes	11305	35.2	43.48	10.12	11.21	78.67	-0.105	-0.051
	tRNA genes	1787	44.66	38.84	8.95	7.55	83.49	0.07	0.085
	rRNA genes	2180	43.62	38.35	5.14	12.89	81.97	0.064	0.43
	Control region	308	43.83	46.1	1.3	8.77	89.94	-0.025	-0.742
<i>Polistes jokahamae</i>	Whole genome	16616	41.97	41.45	5.8	10.79	83.41	0.006	-0.301
	Protein coding genes	10852	36.77	46.61	8.11	8.51	83.38	-0.118	-0.024
	tRNA genes	1318	44.76	42.64	6.98	5.61	87.4	0.024	0.108
	rRNA genes	2257	43.95	41.25	4.3	10.5	85.2	0.032	0.419
	Control region	1096	39.05	46.53	6.84	7.57	85.58	-0.087	-0.051
<i>Polistes humilis</i>	Whole genome	14741	43.09	41.65	5.32	9.95	84.73	0.017	-0.303
	Protein coding genes	10852	36.77	46.61	8.11	8.51	83.38	-0.118	-0.024
	tRNA genes	1258	47.22	41.02	6.52	5.25	88.24	0.07	0.108
	rRNA genes	1932	43.27	43.22	9.16	4.35	86.49	0.001	0.356
	Control region	*	*	*	*	*	*	*	*
<i>Parapolybia crocea</i>	Whole genome	16619	43.39	39.55	5.91	11.15	82.94	0.046	-0.307
	Protein coding genes	11022	35.48	45.16	9.54	9.82	80.65	-0.12	-0.015
	tRNA genes	1486	44.01	42.13	7.67	6.19	86.14	0.022	0.107
	rRNA genes	2176	40.3	45.96	9.38	4.37	86.26	-0.066	0.365
	Control region	1316	42.25	46.05	5.17	6.53	88.3	-0.043	-0.117
<i>Vespa ducalis</i>	Whole genome	15779	40.32	39.8	5.8	14.08	80.12	0.006	-0.417
	Protein coding genes	11159	34.32	43.46	10.36	11.86	77.78	-0.118	-0.067
	tRNA genes	1487	45.46	40.15	8.14	6.25	85.61	0.062	0.131
	rRNA genes	2299	44.58	39.58	11.44	4.39	84.17	0.059	0.445
	Control region	166	46.99	45.78	0	7.23	92.77	0.013	-1
<i>Vespa mandarinia</i>	Whole genome	15902	38.88	40.51	6.07	14.53	79.39	-0.021	-0.41
	Protein coding genes	11119	33.73	43.37	10.56	12.35	77.09	-0.125	-0.078
	tRNA genes	1505	45.12	40.47	8.37	6.05	85.58	0.054	0.161
	rRNA genes	1569	43.91	39.64	12.11	4.33	83.56	0.051	0.473
	Control region	200	49	39.5	0.5	11	88.5	0.107	-0.913
<i>Vespa velutina nigrithorax</i>	Whole genome	16475	40.3	41.44	5.43	12.83	81.74	-0.014	-0.406
	Protein coding genes	11197	34.99	44.75	9.42	10.83	79.74	-0.122	-0.07
	tRNA genes	1514	44.58	41.35	8.12	5.94	85.93	0.038	0.155
	rRNA genes	2319	45.11	40.06	10.52	4.31	85.17	0.059	0.419
	Control region	132	50.76	41.67	0	7.58	92.42	0.098	-1
<i>Vespa orientalis</i>	Whole genome	16101	40.65	40.3	5.86	13.19	80.95	0.004	-0.384
	Protein coding genes	10653	34.5	44.08	9.74	11.68	78.58	-0.122	-0.09
	tRNA genes	1481	45.51	40.51	7.97	6.01	86.02	0.058	0.14
	rRNA genes	2079	43.67	39.15	11.5	5.68	82.83	0.055	0.339
	Control region	60	48.33	41.67	8.33	1.67	90	0.074	0.667
<i>Dolichovespula panda</i>	Whole genome	17136	42.8	41.81	5.39	10	84.61	0.012	-0.3
	Protein coding genes	11276	35.82	46.78	8.78	8.62	82.6	-0.133	0.009
	tRNA genes	1506	45.88	40.44	7.9	5.78	86.32	0.063	0.155
	rRNA genes	2126	43.7	40.87	10.68	4.75	84.57	0.033	0.384
	Control region	586	67.24	32.42	0	0.34	99.66	0.349	-1

* *P. humilis* (EU024653), not sequenced for the control region

Two other parameters, AT-skew and GC-skew, have been widely used to measure the nucleotide compositional behaviors of mitogenome in addition to the A + T content (Enrico et al. 2011). The AT skew of *O. a. aterrimus* mitogenome is -0.005 near to 0, and the GC skew (-0.216) is negative. The base composition bias plays an important role in researching the mechanism of replication and transcription of mitogenomes (Wei et al. 2010).

Among the PCGs of 12 Vespidae species (containing two incomplete mitogenomes), the A + T content of *cox1* is the lowest in 13 PCGs, ranging from 70.18% (*Vespa mandarinia*) to 75.29% (*P. humilis*) (Figure 3). The A + T content of *atp8*, *nad2*, and *nad4L* is highest (Figure 3). This result ascertains *cox1* is conserved relatively again, which is the reason for former abundant phylogenetic analysis in other insects (Rivera and Currie 2009; Santos et al. 2015). In addition, it is a common phenomenon that T content is more than A, and C content is slightly more than G (Figure 3).

Protein coding genes

In the 13 PCGs of the *O. a. aterrimus* mitogenome, nine PCGs are encoded in the J-strand, and the other four PCGs are located in the N-strand. The total length of PCGs is 11 122 bp. All PCGs use the conventional start codons ATN except for *cox1* using TTG which was also employed as the initiation codon in other insects (Sheffield et al. 2008; Li et al. 2012a). The termination codons of nine PCGs in *O. a. aterrimus* mitogenome use complete TAA (*nad2*, *cox1*, *atp8*, *atp6*, *nad3*, *nad5*, *nad4L*, *nad6* and *nad1*), and other four genes have incomplete stop codons T (*cox2*, *cox3*, *nad4* and *cytb*). In general, the termination codons of insect mitogenomes PCGs were the TAA or incomplete T (Ojala et al. 1981; Li et al. 2012a).

There is a total of 3697 codons in *O. a. aterrimus* mitogenome, excluding termination codons, which is within the range of the common insect mitogenomes codon number (3585-3746) (Cha et al. 2007). According to the relative synonymous codon usage (RSCU), all of these 12 Vespidae species frequently used UUU, UUA, AUU and AUA (Figure 4), leading to the high A + T content in the PCGs of the family Vespidae mitogenomes. CUG is absent in *O. a. aterrimus* mitogenome and CGC and AGC are absent in *A. ephippium*. Some codons are also lacking in other species of Vespidae. For example, CGC and AGC in *Vespa orientalis*, CUG, GCG, CGC in *V. bicolor* and CCG, ACC, ACG, GCG, UGC, and CGC in *Dolichovespula panda* are absent, respectively. There are several codons missing in *Polistes jokahamae*, namely, CUG, GUC, ACG, GCG, CGC, CGG, AGC; and CUG, GUC, GCG, CGC, and GGC are also lacked in *P. humilis* (Figure 4). Thus, the amount of absent codons in Vespinae and Polistinae is more than in Eumeninae.

Transfer RNA and ribosomal RNA genes

There are 23 tRNAs found in *O. a. aterrimus* mitogenome and their lengths range from 60 bp (*trnS1*) to 72 bp (*trnK*) including an extra *trnM2*, whereas usually there

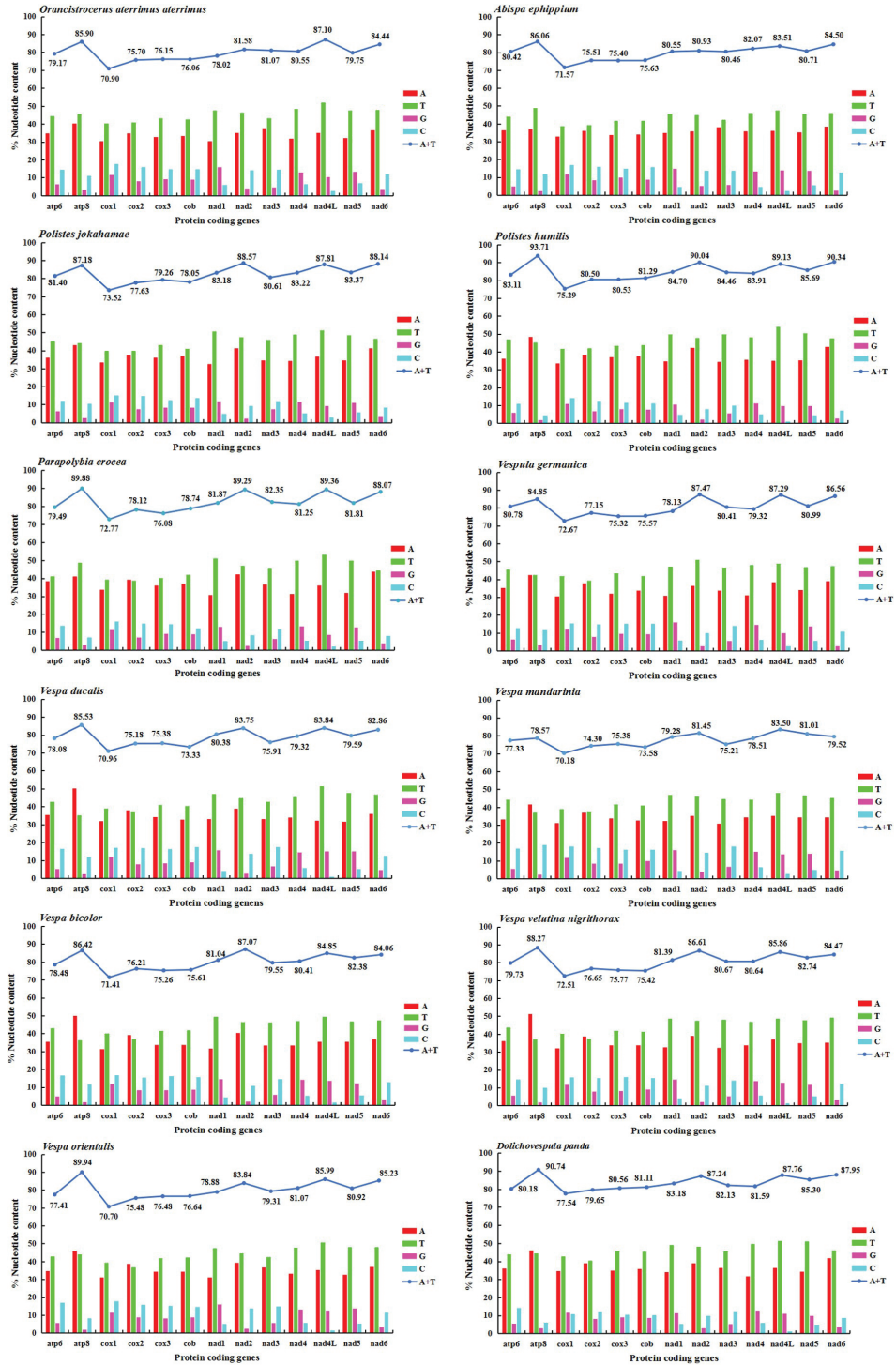


Figure 3. Nucleotide composition of all 13 PCGs of eleven species of Vespidae.

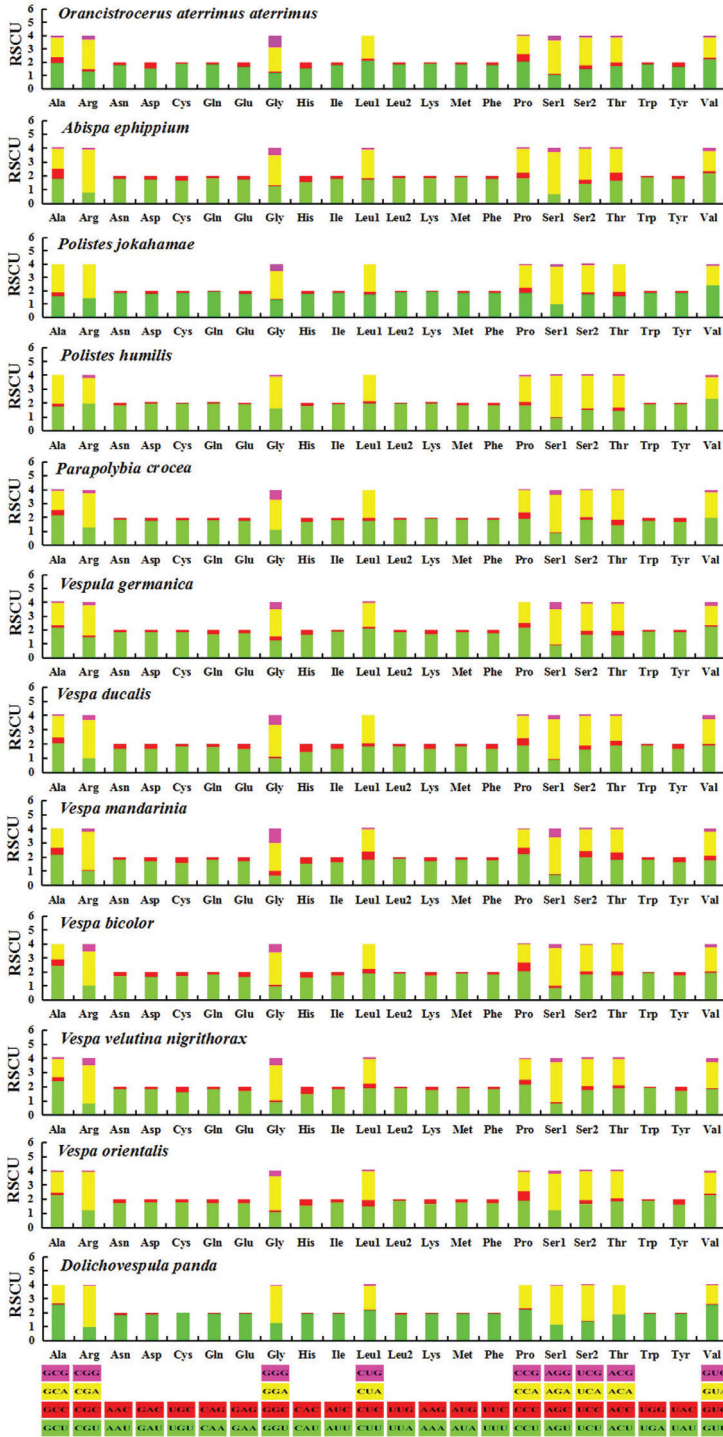


Figure 4. Relative synonymous codon usage (RSCU) in Vespidae. Codon families are displayed along the x-axis.

are 22 tRNAs in other insects (Boore 1999; Chen et al. 2015). Among 23 anticodons of these tRNAs, 21 are coincident with the majority of insects mitogenomes (Lee et al. 2008; Hua et al. 2016), but *trnI* and *trnS1* change from CCT to GAT, and GCT to TCT, respectively. Except for *trnS1*, the other 22 tRNAs have the capability of folding into typical clover-leaf secondary structures. The secondary structure of *trnS1* lacks the dihydrouridine DHU arm and reduces its shape to a simple loop (Figure 5), which is a common phenomenon in metazoan mitogenomes (Wolstenholme 1992; Li et al. 2012b). There are 20 mismatches in 13 tRNAs, including 18 unmatched GU base pairs, an unmatched AG, and an unmatched UU (Figure 5).

The length of *rrnL* is 1 363 bp long, located between *nad1* and *trnV*, and *rrnS* 788 bp long in minority strand between *trnV* and CR. The A + T content of two genes is 84.29% (*rrnL* and *rrnS*) (Table 3).

A control region and a non-coding region

The CR plays an important role in regulating of replication and transcription of mitogenomes (Taanman 1999; Saito et al. 2005). The CR of *O. a. aterrimus* mitogenome is 1078 bp long, located between *rrnS* and *trnI*. The A + T content of this region (84.69%) is higher than other region of the *O. a. aterrimus* mitogenome. There is a tandem repeat model of 28 bp (TATTCCATTTAAGTTCGTAAAACTAAT) which occurs more than eight times in the *O. a. aterrimus* mitogenome. Tandem repeat structures in the CR are different in different species (Peng et al. 2017). There is also a poly-T stretch of 13 bp, which may be as recognition site for the initiation of replication in the mitogenomes (Andrews et al. 1999). In the *O. a. aterrimus* mitogenome, a NCR is situated in position 128 - 2 073 (1 946 bp) between *trnM1* and *trnQ*, which is reported in most insect mitogenomes (Saito et al. 2005; Cameron et al. 2008; Jiang et al. 2016). The A + T content of NCR is 73.69%, among which there is 97 bp (close to *trnQ* gene) with obviously high A + T content 90.72%. In addition, two tandem repetitive sequences are found in the NCR, which repeated 17 and 18 times, respectively.

Phylogenetic relationships

The best fitting model GTR + G + I was selected for ML analysis. The phylogeny of mitogenomes in Vespidae was constructed based on the nucleotide sequences of 13 PCGs of 13 species using ML and BI methods (Figure 6). The phylogenetic relationships between 12 species in the family Vespidae are ((((*Vespa bicolor* + *Vespa velutina nigrithorax*) + *Vespa orientalis*) + (*Vespa mandarinia* + *Vespa ducalis*) + *Vespula germanica* + *Dolichovespula panda*) + (*Parapolybia crocea* + (*Polistes humilis synoecus* + *Polistes jokahamae*))) + (*Orancistrocerus aterrimus aterrimus* + *Abispa ephippium*) (Figure 6). *O. a. aterrimus* and *A. ephippium* belong to the subfamily Eumeninae, which is concordant with morphological classification. In the present

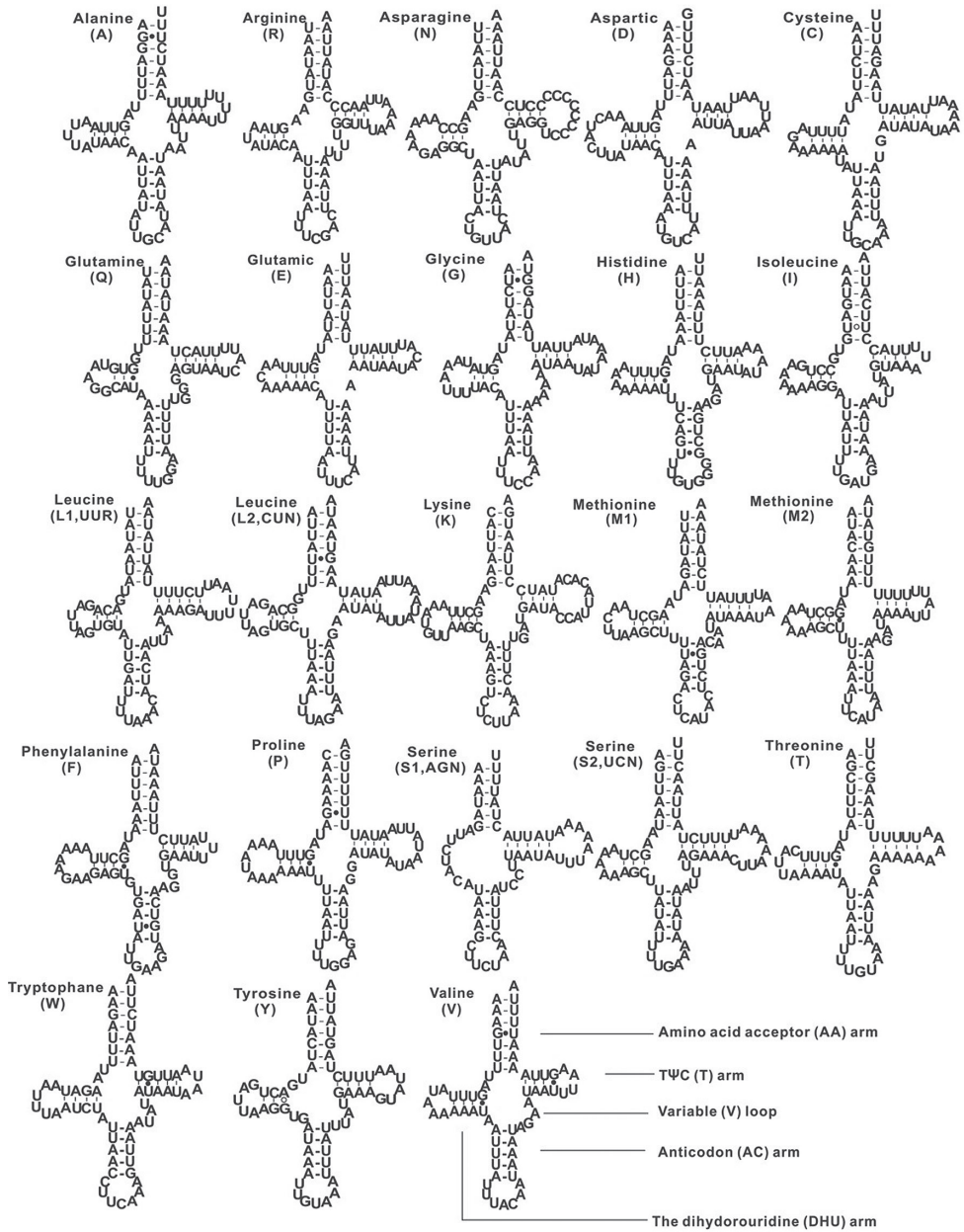


Figure 5. Secondary structures of 23 tRNAs of *O. a. aterrimus* mitochondrial genome. Watson-Crick bonds are shown by dashes, GU pairs by filled dots, and AG and UU by open dots.

study, Eumeninae is the sister group with (Polistinae + Vespinae), which is different from morphological classification “(Eumeninae + (Stenogastrinae + (Vespinae + Polistinae)))” (Carpenter 1982, 2003). So far, there is no reported mitogenome in the subfamily Stenogastrinae, so the relationships among the four subfamilies

Acknowledgements

We are very grateful to James M. Carpenter and Rogério Lopes for their critical comments. This study was funded by the National Natural Science Foundation of China (Nos: 31772490, 31372247, 31000976, 31372265), Young Talent Incubation Program of Chongqing Normal University (14CSDG07), and the Par-Eu Scholars Program.

References

- Andrews RM, Kubacka I, Chinnery PF, Lightowlers RN, Turnbull DM, Howell N (1999) Reanalysis and revision of Cambridge reference sequence for human mitochondrial DNA. *Nature Genetics* 23(2): 147. <https://doi.org/10.1038/13779>
- Benson G (1999) Tandem repeats finder: a program to analyze DNA sequences. *Nucleic Acids Research* 27: 573–580. <https://doi.org/10.1093/nar/27.2.573>
- Boore JL (1999) Animal mitochondrial genomes. *Nucleic Acids Research* 27(8): 1767–1780. <https://doi.org/10.1093/nar/27.8.1767>
- Cameron SL, Downton M, Castro LR, Ruberu K, Whiting MF, Austin AD, Diement K, Stevens J (2008) Mitochondrial genome organization and phylogeny of two vespid wasps. *Genome* 51(10): 800–808. <https://doi.org/10.1139/G08-066>
- Carpenter JM (1982) The phylogenetic relationships and natural classification of the Vespoidea (Hymenoptera). *Systematic Entomology* 7: 11–38. <https://doi.org/10.1111/j.1365-3113.1982.tb00124.x>
- Carpenter JM (1993) Biogeographic patterns in the Vespidae (Hymenoptera): Two views of Africa and South America. *Biological relationships between Africa and South America*. Yale University Press, New Haven, 139–155. <https://doi.org/10.2307/j.ctt22726mc.11>
- Carpenter JM (2003) On “Molecular phylogeny of Vespidae (Hymenoptera) and the evolution of sociality in wasps”. *American Museum Novitates* 3389: 1–20. [https://doi.org/10.1206/0003-0082\(2003\)389<0001:OMPOVH>2.0.CO;2](https://doi.org/10.1206/0003-0082(2003)389<0001:OMPOVH>2.0.CO;2)
- Castro LR, Downton M (2005) The position of the Hymenoptera within the Holometabola as inferred from the mitochondrial genome of *Perga condei* (Hymenoptera: Symphyta: Pergidae). *Molecular Phylogenetics & Evolution* 34(3): 469–479. <https://doi.org/10.1016/j.ympev.2004.11.005>
- Cha SY, Yoon HJ, Lee EM, Yoon MH, Hwang JS, Jin BR, Han YS, Kim I (2007) The complete nucleotide sequence and gene organization of the mitochondrial genome of the bumblebee, *Bombus ignitus* (Hymenoptera: Apidae). *Gene* 392(1–2): 206–220. <https://doi.org/10.1016/j.gene.2006.12.031>
- Chen PY, Wei SJ, Liu JX (2015) The mitochondrial genome of the *Vespa mandarinia* Smith (Hymenoptera: Vespidae: Vespinae) and a phylogenetic analysis of the Vespoidea. *Mitochondrial DNA* 27(6): 4414–4415. <https://doi.org/10.3109/19401736.2015.1089550>
- Chen PY, Zheng BY, Liu JX, Wei SJ (2016) Next-Generation sequencing of two mitochondrial genomes, from Family Pompilidae (Hymenoptera: Vespoidea) Reveal Novel Patterns

- of Gene Arrangement. *International Journal of Molecular Sciences* 17: 1641. <https://doi.org/10.3390/ijms17101641>
- Dowton M, Austin AD (1999) Evolutionary dynamics of a mitochondrial rearrangement “hot spot” in the Hymenoptera. *Molecular Biology and Evolution* 16(2): 298–309. <https://doi.org/10.1093/oxfordjournals.molbev.a026111>
- Dowton M, Cameron SL, Dowavic JI, Austin AD, Whiting MF (2009) Characterization of 67 mitochondrial tRNA gene rearrangements in the Hymenoptera suggests that mitochondrial tRNA gene position is selectively neutral. *Molecular Biology and Evolution* 26: 1607–1617. <https://doi.org/10.1093/molbev/msp072>
- Enrico N, Massimiliano B, and Tomaso P (2011) The mitochondrial genome of the ascalaphid owlfly *Libelloides macaronius* and comparative evolutionary mitochondriomics of neuropterid insects. *BMC Genomics* 12(5): 221.
- Fan XL, Gong YJ, Chen PY, Tan QQ, Tan JL, Wei SJ (2017) Next-generation sequencing of the mitochondrial genome of *Dolichovespula panda* (Hymenoptera: Vespidae) with a phylogenetic analysis of Vespidae. *Journal of Asia-Pacific Entomology* 20(3): 971–976. <https://doi.org/10.1016/j.aspen.2017.07.009>
- Hua YQ, Din YR, Yan ZT, Si FL, Luo QC, Chen B (2016) The complete mitochondrial genome of *Anopheles minimus* (Diptera: Culicidae) and the phylogenetics of known Anopheles mitogenomes. *Insect Science* 23(3): 353–365. <https://doi.org/10.1111/1744-7917.12326>
- Huelsenbeck JP, Ronquist F (2001) MRBAYES: Bayesian inference of phylogenetic trees. *Bioinformatics* 17: 754–755. <https://doi.org/10.1093/bioinformatics/17.8.754>
- Jiang P, Li H, Song F, Cai Y, Wang JY, Liu JP, Cai WZ (2016) Duplication and remodeling of tRNA genes in the mitochondrial genome of *Reduvius tenebrosus* (Hemiptera: Reduviidae). *International Journal of Molecular Sciences* 17(6): 951. <https://doi.org/10.3390/ijms17060951>
- Kim JS, Jeong JS, Jeong SY, Kim MJ, Kim I (2017a) Complete mitochondrial genome of the black-tailed hornet, *Vespa ducalis* (Hymenoptera: Vespidae): Genomic comparisons in Vespoidea. *Entomological Research* 47: 129–136. <https://doi.org/10.1111/1748-5967.12218>
- Kim JS, Jeong JS, Kim I (2017b) Complete mitochondrial genome of the yellow-legged Asian hornet, *Vespa velutina nigrithorax* (Hymenoptera: Vespidae). *Mitochondrial DNA Part B: Resources* 2(1): 82–84. <https://doi.org/10.1080/23802359.2017.1285211>
- Lee YS, Oh J, Kim YU, Kim N, Yang S, Hwang UW (2008) Mitome: dynamic and interactive database for comparative mitochondrial genomics in metazoan animals. *Nucleic Acids Research* 36: 938–942. <https://doi.org/10.1093/nar/gkm763>
- Li H, Leavengood Jr JM, Chapman EG, Burkhardt D, Song F, Jiang P, Liu JP, Zhou XG, Cai WZ (2017) Mitochondrial phylogenomics of Hemiptera reveals adaptive innovations driving the diversification of true bugs. *Proceedings of the Royal Society B: Biological Sciences* 284: 1–10. <https://doi.org/10.1098/rspb.2017.1223>
- Li H, Liu H, Shi AM, Štys P, Zhou XG, Cai WZ (2012a) The complete mitochondrial genome and novel gene arrangement of the unique-headed bug *Stenopirates sp.* (Hemiptera: Enicocephalidae). *PLoS ONE* 7: e29419. <https://doi.org/10.1371/journal.pone.0029419>

- Li H, Liu HY, Song F, Shi AM, Zhou XG, Cai WZ (2012b) Comparative mitogenomic analysis of damselfly bugs representing three tribes in the family Nabidae (Insecta: Hemiptera). *PLoS ONE* 7: e45925. <https://doi.org/10.1371/journal.pone.0045925>
- Li TS (1985) Economic insect fauna of China, Hymenoptera: Vespoidea. Science Press, Beijing, 120–121.
- Lowe TM, Eddy SR (1997) tRNAscan-SE: a program for improved detection of transfer RNA genes in genomic sequence. *Nucleic Acids Research* 25: 955–964.
- Nizar JH, Kosai AN, Bent P, Love D, Nikolaj B, Thomas SP (2017) Complete mitochondrial genome of the Oriental hornet, *Vespa orientalis* F. (Hymenoptera: Vespidae). *Mitochondrial DNA Part B: Resources* 2(1): 139–140. <https://doi.org/10.1080/23802359.2017.1292480>
- Nylander JAA (2004) MrModeltest v2. Program distributed by the author. Uppsala University: Evolutionary Biology Centre.
- Ojala D, Montoya J, Attardi G (1981) tRNA punctuation model of RNA processing in human mitochondria. *Nature* 290: 470–474. <https://doi.org/10.1038/290470a0>
- Oliveira DCSG, Rhitoban R, Lavrov DV, Werren JH (2008) Rapidly evolving mitochondrial genome and directional selection in mitochondrial genes in the parasitic wasp *Nasonia* (Hymenoptera: Pteromalidae). *Molecular Biology and Evolution* 25: 2167–2180. <https://doi.org/10.1093/molbev/msn159>
- Peng Y, Chen B, Li TJ (2017) Complete sequence and analysis of *Parapolybia crocea* mitochondrial genome (Hymenoptera: Vespidae). *Acta Entomologica Sinica* 60(4): 464–474.
- Peng Y, Leung HCM, Yiu SM, Chin FYL (2012) IBDA-UD: a de novo assembler for single-cell and metagenomic sequencing data with highly uneven depth. *Bioinformatics* 28: 1420–1428. <https://doi.org/10.1093/bioinformatics/bts174>
- Perna NT, Kocher TD (1995) Patterns of nucleotide composition at fourfold degenerate sites of animal mitochondrial genomes. *Journal of Molecular Evolution* 41: 353–358. <https://doi.org/10.1007/BF01215182>
- Rivera J, Currie DC (2009) Identification of Nearctic black flies using DNA barcodes (Diptera: Simuliidae). *Molecular Ecology Resources* 9: 224–236. <https://doi.org/10.1111/j.1755-0998.2009.02648.x>
- Saccone C, De Giorgi C, Gissi C, Pesole G, Reyes A (1999) Evolutionary genomics in Metazoa: the mitochondrial DNA as a model system. *Gene* 238: 195–209. [https://doi.org/10.1016/S0378-1119\(99\)00270-X](https://doi.org/10.1016/S0378-1119(99)00270-X)
- Saito S, Tamura K, Aotsuka T (2005) Replication origin of mitochondrial DNA in insects. *Genetics* 171(4): 1695–1705. <https://doi.org/10.1534/genetics.105.046243>
- Santos BF, Payne A, Pickett KM, Carpenter JM (2015) Phylogeny and historical biogeography of the paper wasp genus *Polistes* (Hymenoptera: Vespidae): implications for the overwintering hypothesis of social evolution. *Cladistics* 2015 31(5): 535–549. <https://doi.org/10.1111/cla.12103>
- Selis M (2018) Additions to the knowledge of solitary wasps (Hymenoptera: Vespidae: Eumeninae), with description of eight new species. *Zootaxa* 4403(3):441–468. <https://doi.org/10.11646/zootaxa.4403.3.2>

- Sheffield NC, Song H, Cameron SL, Whiting MF (2008) A comparative analysis of mitochondrial genomes in Coleoptera (Arthropoda: Insecta) and genome descriptions of six new beetles. *Molecular Biology and Evolution* 25: 2499–2509. <https://doi.org/10.1093/molbev/msn198>
- Simon C, Buckley TR, Frati F, Stewart JB, Beckenbach AT (2006) Incorporating Molecular Evolution into Phylogenetic Analysis, and a New Compilation of Conserved Polymerase Chain Reaction Primers for Animal Mitochondrial DNA. *Annual Review of Ecology Evolution & Systematics* 37(1–2): 545–579. <https://doi.org/10.1146/annurev.ecolsys.37.091305.110018>
- Song SN, Chen PY, Wei SJ, Chen XX (2016) The mitochondrial genome of *Polistes jokahamae* and a phylogenetic analysis of the Vespoidea (Insecta: Hymenoptera). *Mitochondrial DNA* 27(4): 1–2.
- Taanman JW (1999) The mitochondrial: structure, transcription, translation and replication. *Biochimica et Biophysica Acta* 1410(2): 103–123. [https://doi.org/10.1016/S0005-2728\(98\)00161-3](https://doi.org/10.1016/S0005-2728(98)00161-3)
- Tamura K, Stecher G, Peterson D, Filipiński A, Kumar S (2013) MEGA6: molecular evolutionary genetics analysis version 6. 0. *Molecular Biology and Evolution* 30(12): 2725–2729. <https://doi.org/10.1093/molbev/mst197>
- Thompson JD, Gibson TJ, Plewniak F, Jeanmougin F, Higgins DG (1997) The CLUSTAL_X windows interface: flexible strategies for multiple sequence alignment aided by quality analysis tools. *Nucleic Acids Research* 25: 4876–4882. <https://doi.org/10.1093/nar/25.24.4876>
- Wei SJ, Niu FF, Tan JL (2014) The mitochondrial genome of the *Vespa bicolor* Fabricius (Hymenoptera: Vespidae: Vespinae). *Mitochondrial DNA* 27(2): 1–2.
- Wei SJ, Shi M, Chen XX, Sharkey MJ, Achterberg C van, Ye GY, He JH (2010) New views on strand asymmetry in insect mitochondrial genomes. *PLoS ONE* 5(9): e12708. <https://doi.org/10.1371/journal.pone.0012708>
- Wolstenholme DR (1992) Animal mitochondrial DNA: structure and evolution. *International Review of Cytology* 141(6): 173–216. [https://doi.org/10.1016/S0074-7696\(08\)62066-5](https://doi.org/10.1016/S0074-7696(08)62066-5)
- Yang S, Li X, Cai LG, Qian ZQ (2015) Characterization of the complete mitochondrial genome of *Formica sebsyi* (Insecta: Hymenoptera: Formicidae: Formicinae). *Mitochondrial DNA* 27: 3378–3380.
- Zhou Y, Hu YL, Xu ZF, Wei SJ (2016) The mitochondrial genome of the German wasp *Vespula germanica* (Fabricius, 1793) (Hymenoptera: Vespoidea: Vespidae). *Mitochondrial DNA* 27(4): 1–2.

